THE UNIVERSITY *of* EDINBURGH

Saccadic Vector Optokinetic Perimetry - A Technique and System for Automated Static Perimetry in Children Using Eye Tracking

Ian C. Murray

Thesis submitted for the degree of Doctor of Philosophy
The University of Edinburgh
2011

Declaration

This thesis is submitted to the University of Edinburgh in accordance with the requirements for the degree of Doctor of Philosophy in the College of Medicine and Veterinary Medicine. It has not been submitted for any other degree or diploma of any examining body. Except where specifically acknowledged, it is the work of the author.

Signed ..... Date .....

Ian C. Murray

Acknowledgements

I would like to express immense gratitude to my three supervisors. Robert Minns, Brian Fleck and Harry Brash complemented each other wonderfully well and I thank them for enabling me to undertake this doctorate and for their assistance with writing funding proposals which have enabled the continuation of this research. I have found the many clinical and technological discussions I have had with each of them invaluable.

I am grateful to ophthalmologists Mary MacRae and Alan Mulvihill for their clinical expertise and help with patient recruitment. Special thanks also goes to the nursing staff within the Clinical Research Facility at the Royal Hospital for Sick Children. In particular I would like to thank Kay Riding, Debbie Miller and Michelle Heron who were extremely helpful assisting with the child participants in this research.

This visual fields research has received funding from several sources. Initial funding provided by The Mackay Trust enabled the research to initiate and grow in a manner which made it an attractive project to receive further funding from Action Medical Research (including support from The R S Macdonald Charitable Trust).

Spelling and punctuation are not among my greatest strengths. However, with help from my wife (who read and re-read this thesis) my grammar is hopefully improving. I would like to express special thanks to Jacqui for all her time, effort and support throughout. Special thanks also goes to my parents, particularly for the persistent “encouragement” they have provided.

Abstract

Perimetry is essential to identify visual field defects in disorders of the visual pathways. In compliant adults, automated static perimetry (ASP) is the preferred method of visual field assessment. However, children under 10 years have difficulty with the visuo-motor task and constant fixation required. Manual kinetic perimetry is often used for children as it can be adapted to a child's age. However, it suffers from many of the problems inherent to ASP. In infants perimetry is limited to the "confrontation" technique which can be imprecise and does not generate quantitative data. The lack of reliable ASP in children and quantitative perimetry in infants is a longstanding clinical problem. The aims of this research were to (i) develop, and (ii) clinically evaluate, a technique for ASP in children which utilises "eye tracking".

The first part of this research was concerned with the development of the technique, termed "Saccadic Vector Optokinetic Perimetry" (SVOP). The system comprises a personal computer, display screen, and an X50 eye tracker (Tobii Technology, Sweden). The eye tracker is non-contact and provides data on (i) eye position in 3D space, and (ii) the point of gaze. This allows the screen position of "test stimuli" to be calculated, and eye gaze responses to the "test stimuli" to be assessed in "real time". A software algorithm was developed to determine if "test stimuli" have been perceived based on the direction, amplitude and latency of a subject's gaze response.

A feasibility study was conducted with 29 subjects comprising 4 groups: (i) healthy adults, (ii) healthy children, (iii) adult patients with visual field defects, and (iv) child patients with visual field defects. Subjects performed SVOP tests which replicated the Humphrey Field Analyser (HFA) C-40 screening test with a stimulus size of Goldmann III and intensity of 14dB. Subjects able to do so also performed equivalent HFA C-40 tests for comparison. In healthy subjects 99.1% of SVOP test points were in agreement with a healthy visual field. In patients with visual field defects, 89.8% of test points were in agreement with HFA equivalent tests. The visual field defects identified using SVOP in the child patients were consistent with their clinical findings.

A clinical evaluation of SVOP was undertaken in the second stage of this research with 122 subjects comprising the same four subject groups as in the feasibility trial. An "ideal" test protocol resulted in 8 uniocular visual field tests for each subject comprising 4 SVOP tests

and 4 HFA tests. In children where uniocular testing was not tolerable, two binocular SVOP tests were performed. The sensitivity and specificity of the SVOP tests were computed using a direct comparison with reliable HFA tests, and repeatability of SVOP and HFA tests were assessed using Cohen's kappa coefficient. In child patients unable to provide a reliable HFA test, their clinical history, other clinical findings and the repeatability of their SVOP tests were used to assess the SVOP results. The overall sensitivity and specificity of the SVOP testing was 72.7% and 96.8% respectively. The sensitivity had a greater variation than the specificity amongst the different subject groups. The repeatability of SVOP tests was slightly reduced as compared to the HFA tests across all groups with kappa coefficient's of 0.65 and 0.74 for SVOP and HFA respectively. In child patients without reliable HFA equivalent tests the SVOP results could commonly be associated with other clinical findings and repeatable testing added to the confidence in the reliability of these cases.

The developed SVOP technique performs well with accurate eye tracking data and an attentive child. It has proved extremely useful in identifying and monitoring visual field defects in several child patients who required regular visual field assessment.

Contents

List of Figures

List of Tables

List of Abbreviations

ASP	Automated Static Perimetry
CAMEC	Computer Assisted Moving Eye Campimeter
CLIP	Continuous Light Increment Perimetry
CVI	Cerebral Visual Impairment
EEG	Electroencephalography
EOG	Electrooculography
FDT	Frequency Doubling Technology
FOV	Field of View
FT	Fast Threshold
FTT	Full Threshold Test
GKP	Goldmann Kinetic Perimetry
HFA	Humphrey Field Analyser
HPR	High Pass Resolution
IOP	Intraocular Pressure
LCD	Liquid Crystal Display
LGN	Lateral Geniculate Nucleus
MD	Mean Deviation
MHT	Magnetic Head Tracking
PC	Personal Computer
PSD	Pattern Standard Deviation
PVL	Periventricular Leucomalasia
SDK	Software Development Kit
SIOP	Societé Internationale pour Oncolgie Paediatrique
SITA	Swedish Interactive Thresholding Algorithm
SVOP	Saccadic Vector Optokinetic Perimetry
TOP	Tendency-Oriented Perimetry
VEP	Visual Evoked Potentials
VOG	Video-Oculography
VOR	Vestibulo-Ocular Reflex
WHO	World Health Organization

Chapter 1

Introduction

1.1 The clinical problem

Visual field measurement (known as perimetry) is crucial in the diagnosis and management of children with certain brain tumours, raised intracranial pressure and cerebral visual impairment (CVI) which can be caused, for example, by the following:[1–6]

- developmental brain defects,
- asphyxia,
- infections of the central nervous system, and
- head trauma.

In many regions of the world the prevalence of childhood visual impairment is not known. However, it is thought that complete blindness accounts for approximately one-third of all visual impairment. In industrialised countries the prevalence of childhood visual impairment, severe visual impairment and blindness combined has been approximated to be between 10 and 22 per 10,000, while in developing countries it may be as high as 30 to 40 per 10,000.[7] Excluding children who have complete blindness, this means that visual impairment affects approximately 7 to 16 per 10,000 in industrialised countries and 20 to 27 per 10,000 in developing countries.

There is also call for a reliable and sensitive method to monitor visual field changes in children who are on the drug Vigabatrin for epilepsy due to a potential visual field constriction side effect,[8–10] and in paediatric glaucoma.[11,12] However, the preferred visual field assessment method, known as automated static perimetry (ASP), is only used in adults as it is not suitable for use in children.

ASP requires the patient to fixate on a central target and indicate, by pressing a button, when they observe light stimuli at various locations in their visual field, so building up a plot of the patient's visual field as further stimuli are shown. The test requires a conscious effort by the patient to inhibit their natural reaction to fixate on the light stimuli. It is very difficult for children, particularly children below the age of 5 years, to inhibit this natural response [13,14] and maintain stable fixation on a central target. [15,16] Also, children have a reduced ability to learn the task required of them and hence to provide appropriate responses. [17] Children are less likely to cooperate due to their lack of understanding of the test methods and their short attention span. [18–20] Additionally, many children may not tolerate the restrictions of head movement imposed on them during the test which requires the use of a chin rest. All these factors vastly reduce the reliability of performing ASP in children and as a result it is not routinely performed in those younger than approximately 10 years of age.

Alternative methods of perimetry are used to assess the visual fields of children aged between 5 and 10 years. A popular method for this age group, known as Goldmann Kinetic Perimetry (GKP), [21,22] uses light stimuli which are moved manually by the examiner from a blind area (for example the periphery of the visual field or known blind spot) towards an area where they can be seen. The patient indicates when they first see the stimuli by pressing a buzzer and this position is marked by the examiner. This process is repeated at different locations and with different intensities or sizes of light stimuli to build up a contour map of the patient's visual field. GKP gives more control and freedom to the examiner, allowing adaptability to the child's age and maturity. However, the child's cooperation in maintaining a continuous fixation on a central target during the test is still required. Results are dependent upon the examiner's skills and knowledge, and examiner bias is easily introduced. [23] In addition, GKP does not provide the level of detail possible with ASP.

Visual field assessment in children younger than 5 years is currently limited to the technique of confrontation. The attention of the child is gained using an object such as a small toy while another object is moved in from the periphery of the child's vision. The examiner waits to see if the child orients themselves to view the object and if this does not happen a visual field defect is suspected. This method of assessment is a very gross technique as it does not generate any real quantitative data.

The inability of children to accurately perform the more comprehensive adult perimetry technique of ASP and the lack of any well defined quantitative perimetry in infants is a major problem in clinical practice. Children born prematurely are known to be at risk of brain abnormalities within the visual processing regions. [24] As a result it is thought that the number of children with cerebral visual impairment is rising due the increase in survivors of prematurity. The early detection of these defects is of great importance in understanding the visual function of the affected child, and thereby allowing practical advice, to be given if the defect cannot be

reversed. For example, a child with defective inferior visual field may have impaired mobility and difficulties with school work which may be helped by the use of mobility strategies and tilted work desks. Children with brain tumours can also have visual field defects. The ability to measure these defects would allow early detection and more reliable monitoring of treatment responses in these patients. Visual field defects occur in children with raised intracranial pressure, where detection of visual field defect would aid decisions on medical and surgical treatment. Also, visual field defects can occur as a side effect of taking Vigabatrin, an anti-epilepsy drug. The drug is used in adults alongside visual field monitoring. However such monitoring cannot be performed in children and the drug is therefore either used in a way which risks visual damage, or is not used in children who would have otherwise benefited from the improved epilepsy control it would have provided.

1.2 Purpose of this research

Recognising that ASP is the preferred method of perimetry, in an effort to overcome the difficulties associated with performing ASP in children under 10 years, researchers have concentrated on finding ways of improving children's test reliability. The development of algorithms designed to provide faster testing time for ASP such as Swedish Interactive Thresholding Algorithm (SITA) Fast[25,26] and Tendency-Oriented Perimetry[27] (TOP) have been investigated with child subjects. However the youngest aged child capable of producing reliable results remains approximately 7-8 years.[20,28,29] Training and familiarisation strategies for particular techniques have also been investigated as a way of improving reliability.[18,30] These research efforts do not address the fundamental problems inherent in performing ASP on children and it is a new, child friendly technique which is required. The development and assessment of a novel technique and system for assessment of visual fields in children is therefore the focus of this research. The system makes use of relatively new advances in eye tracking technology and should be more suitable for use with children. The Technique and system, named Saccadic Vector Optokinetic Perimetry (SVOP)[31], uses a personal computer, display screen and an eye tracker to detect a child's eye movement when a stimulus is presented in their visual field. The only task required of the child is to follow their natural reaction to fixate on the stimulus of interest when they see it, rather than having to maintain continuous fixation on a central target while stimuli are presented in their peripheral vision. The proposed visual field assessment test should not require any understanding from the child subject as they are not required to learn any task or to give subjective responses. The purpose of this research is to:

- develop the technique and system of SVOP, and
- assess the validity of SVOP in children.

1.3 Summary of thesis structure

This research uses relatively recent advances in eye tracking technology in an effort to solve a clinical problem within ophthalmology, and so involves two different (although related) topics: (i) eye movement and eye tracking technology, and (ii) the clinical problem of paediatric perimetry. These two topics will be discussed independently in two initial background chapters to provide readers with sufficient knowledge in both subject areas.

Following the background material, a detailed literature review on methods of perimetry in children and research efforts, to date, to achieve reliable perimetry in children is presented, and the specific aims of this research project are also outlined.

There are two main stages to this research: (i) the development of the technique and system of SVOP for assessment of visual fields in children, and (ii) an assessment of the validity of the developed system as a diagnostic tool for visual field assessment. These two aspects of the research make up the contents of the two main chapters (Chapters 5 and 6, "System Development" and "Clinical Validation Trial") respectively. Chapter 5 details the aspects of the system development including theory of operation, the assessment of equipment used, the physiological data collected and how it is used, and limitations of the system. In addition, a feasibility study of the technique is undertaken. Within this chapter are several methods and results sections for each of the individual aspects of the development. Chapter 6 presents the methods and results for a full clinical validation trial in which the developed system is assessed as a diagnostic tool by comparison with an established form of adult ASP and as a suitable form of perimetry for children. Ethical and NHS management approval was gained for both the development and validation studies presented in this thesis (details of these are given in Appendix A).

Chapter 2

Background - The human visual field and its measurement

2.1 The normal human visual field

The visual field is the total area which a person can see when fixating on one location. The visual field is described in relation to the individual in free space, a normal human visual field extends approximately 100° temporally, 60° nasally and superiorly, and 70° inferiorly from the point of fixation for each eye individually. Visual sensitivity is greatest at the point of fixation, corresponding to the fovea, and decreases towards the periphery in all directions. The visual field of each eye has previously been described as a hill or island of vision, the peak of which corresponds to the point of fixation (Figure 2.1).

The shape and height of the hill of vision varies and is dependent upon factors such as patient age, facial features (for example the nose and eyebrows) and methods of visual field testing (for example ambient light and the size and duration of visual stimuli used). A visual field defect is defined as any statistically or clinically significant departure from the expected normal hill of vision for a particular patient. Specific visual field defects will be discussed in more detail in section 2.3.1 “Clinical Importance”. However, at this point it is useful to state that visual field defects (also termed scotomas), are described in terms of size and depth and how much they depart from the expected normal visual sensitivity. A reduction in, but not total loss of, visual sensitivity in an area is termed a relative scotoma, whereas total loss of vision in an area is termed an absolute scotoma. The normal blind spot is an example of a physiological absolute scotoma due to an absence of photo-receptors at the optic disc.

Considering both the left and right eyes together, there is extensive overlapping of the visual fields from each eye creating a combined binocular visual field extending approximately 190°

laterally, and consisting of a single central binocular region and two peripheral monocular regions. The visual field of each eye is described in terms of four quadrants laterally and vertically with the point at which they all meet being the point of fixation.

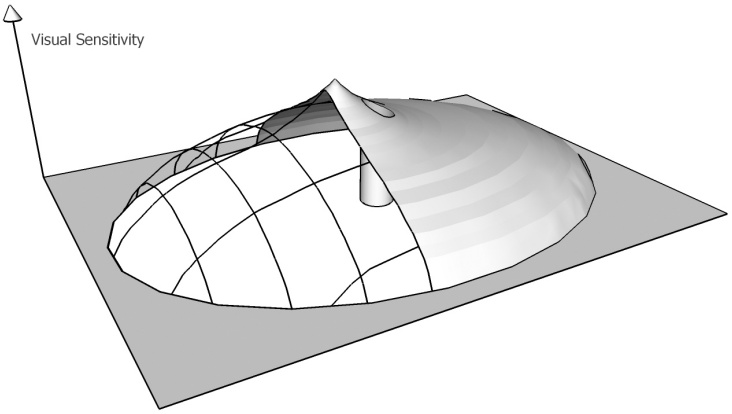

(a)

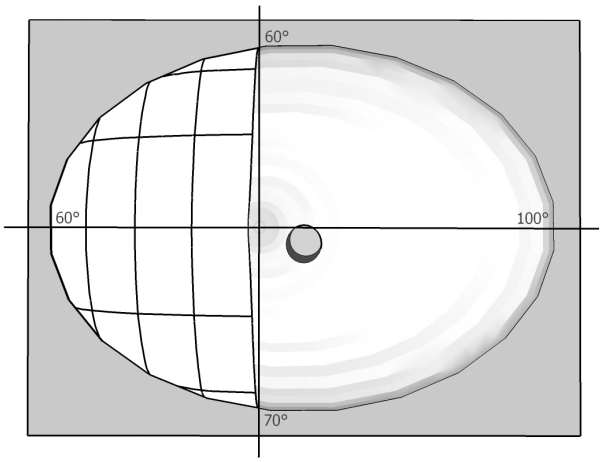

(b)

Figure 2.1: The normal right eye hill of vision. (a) The peak corresponds to the point of fixation where sensitivity is greatest. Sections are cut out to show the sensitivity drop at the natural blind spot. (b) View from above demonstrating field of view and blind spot location.

2.2 The human visual system

The human visual system, in particular the anatomy of the visual pathways, is important when understanding the causes of many visual field defects. Problems with the visual system can lead to very specific changes to the normal visual field, hence by association, assessment of a patient's visual field provides a form of diagnosis. This will be discussed in further detail with particular reference to specific visual field defects in section 2.3.1 "Clinical Importance". Here, the anatomy of the human visual system will be discussed so as to provide sufficient information

to understand the reasons behind specific visual field defects.

The retina comprises three sets of neurones: (i) photoreceptor neurones which exist in the well-known forms of rod and cone neurons, their function being to commence the visual cycle by converting light into an electrical signal through photo-transduction. These synapse onto; (ii) intermediate or bipolar neurones which in turn synapse onto; (iii) retinal ganglion cells. The retinal ganglion cells conduct action potentials along the visual pathways. A small quantity of ganglion cells (approximately 10%) are additionally photo-receptive and are involved in relaying information to the superior colliculus, responsible for controlling eye movements, the pretectum, which manages the pupillary light reflex and the hypothalamus which regulates the circadian rhythms. The vast majority (approximately 90%) of ganglion cells project to the lateral geniculate nucleus (via the optic nerve, optic chiasm and optic tracts) which relays visual information to the primary visual cortex. There are no synapses between the ganglion cells and the lateral geniculate body so visual field defects and optic atrophy are caused by damage along this section of the visual pathways. The visual pathways traverse the optic nerve, the optic chiasm and an optic tract to end at the appropriate lateral geniculate body in the thalamus. The thalamus is the major subcortical centre which relays visual information to the primary visual cortex via the optic radiation.

These visual pathways are shown in figure 2.2. The four quadrants of the visual field for each eye are colour coded in the figure, along with the individual pathways for each quadrant and each eye to show the way in which the visual pathways are rigidly structured according to these sections of the visual field. The pathways are additionally described in the following paragraphs, each paragraph corresponding to the various sections of the visual pathways after exiting the eyeballs.

The optic nerves

The physiological blind spot is attributed to the area where the optic nerve leaves the eye at the optic disc where there are no photo-receptors. The optic nerve is rounded and carries approximately 1.2 million axons towards the optic chiasm. Initially nerve fibres with visual information from the macula region are situated temporally within the optic nerve. At approximately 1cm behind the eyeball, the retinal artery (heading towards the eyeball) enters the optic nerve, and at this same point, the nerve fibre bundles carrying visual information from the various parts of the visual field move so that the macular bundle now occupies the centre of the optic nerve and peripheral retinal fibres are situated peripherally, heading towards the optic chiasm.

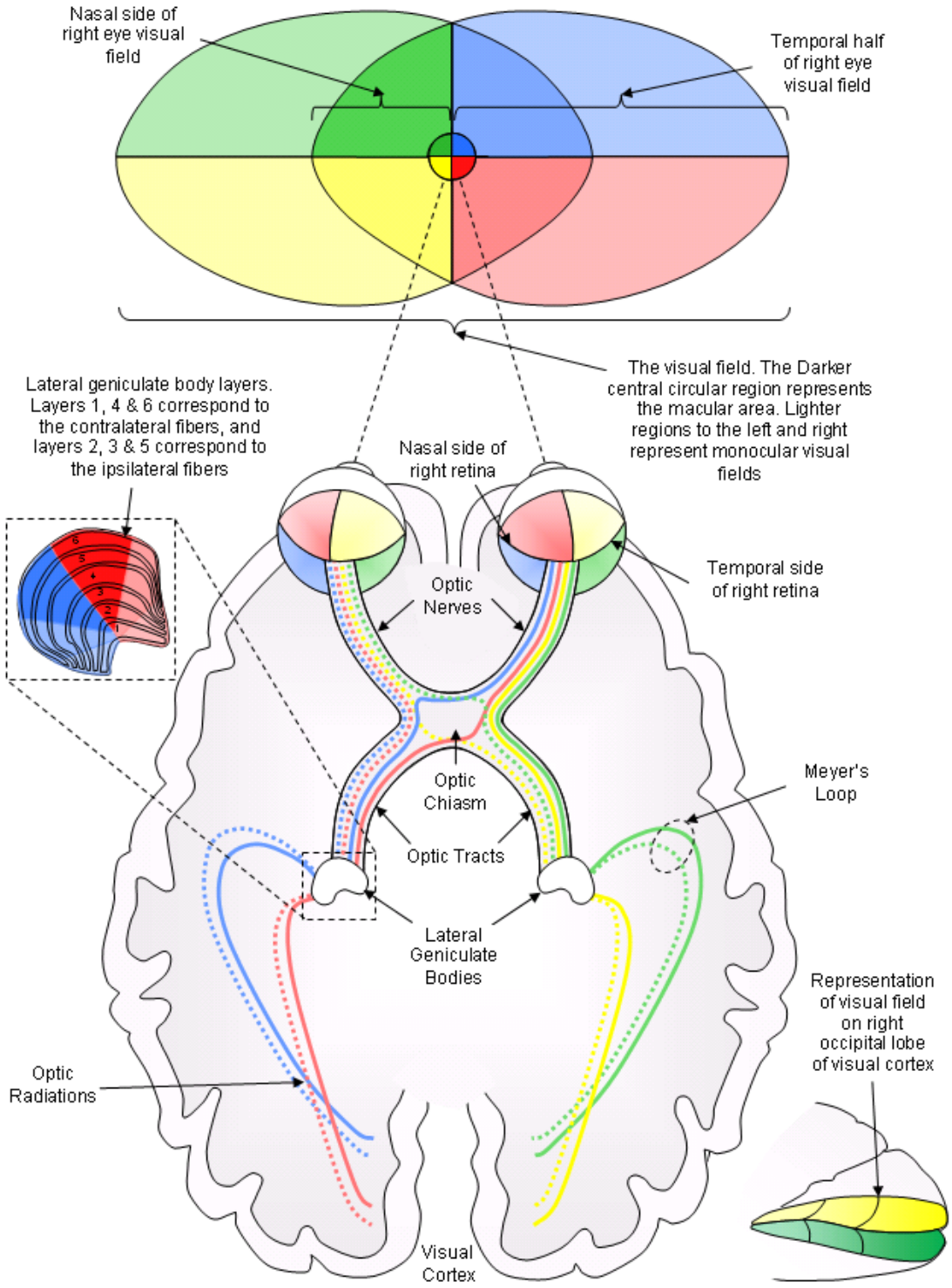

Figure 2.2: The human visual field and corresponding visual pathways. The four visual field quadrants of each eye are colour coded to enable depiction of the various pathways carrying visual information from each quadrant. Additionally, the pathways of the left nerve fibre bundles are shown with dashed lines while those from the right eye are displayed with full lines.

The optic chiasm and optic tracts

At the optic chiasm the optic nerves from the left and right eyes meet and approximately 50% of the axons cross over to the opposite pathway and 50% continue on the same side. Vision in the nasal visual field stimulates the retina on the temporal side of the fovea and the fibres carrying these impulses pass through the chiasm without decussating. Vision in the temporal field causes stimulation in the retina on the nasal side of the fovea and these fibres cross to the opposite optic tract. Information about the right side of the visual field now passes along the left optic tract, and conversely, information about the left side of the visual field is located on the right side of the brain along the right optic tract. All the nerve fibres concerned with vision pass along the optic tracts from two posterior corners of the optic chiasm to the lateral geniculate bodies.

The lateral geniculate bodies

The nerve fibres from each of the optic tracts end at the Lateral Geniculate Nucleus (LGN) in the thalamus where they synapse with nerve cells. Fibres arising from upper quadrants of the retina (relating to the inferior quadrants of the visual field) end in the medial portion of the body. Those arising from the lower quadrants of each retina are represented laterally. The LGN is composed of six layers of cells (figure 2.2). The layers are numbered 1 to 6. Layers 1, 4 and 6 correspond to information from the contralateral (crossed) fibres of the nasal visual field. Layers 2, 3 and 5 correspond to information from the ipsilateral (uncrossed) fibres of the temporal visual field. Additionally, specific LGN layers are concerned with visual functions such as the processing of colour and fine detail (the parvocellular layers 3 to 6), and the detection of depth and motion (the magnocellular layers 1 and 2).

The optic radiation

From the lateral geniculate body, fibres of the optic radiation fan out as they pass to the primary visual cortex. Specifically, fibres representing the superior visual field pass through the temporal lobe of the brain (known as Meyer's loop) and fibres representing the lower visual field pass through the parietal lobe of the brain in the retrolenticular limb of the internal capsule.

The primary visual cortex

The primary visual cortex has a representation of the contralateral visual hemifield. The foveal region is mapped in the most posterior part of the visual cortex, whereas more peripheral parts of the visual field are mapped in progressively more anterior parts. The upper visual field is mapped on the lower bank of the calcarine sulcus, the lower visual field on the upper bank.

2.3 Visual field measurement - perimetry

2.3.1 Clinical importance

Due to the well defined nature of the visual pathways, lesions involving the pathways can have a very well defined effect on the visual field. Characteristic visual field defects can be observed when lesions are present at different locations along the visual pathways meaning visual field assessment can be a highly useful form of diagnosis. Most visual field defects resulting from CVI respect (do not cross over) the horizontal and/or vertical midlines of the visual field (which intersect at the point of fixation).

Figure 2.3 shows the types of visual field defects that would develop due to lesions at various sites along the visual pathways. It is possible to determine which defect corresponds to each site due to the structured anatomy of the visual pathways bearing in mind the following points relating to the anatomy of the visual pathways:

- The retinal image is reversed and inverted with respect to the visual field such that the temporal visual field is projected to the nasal part of the retinas and the nasal visual field is projected to the temporal side of the retinas. Similarly, the superior and inferior visual fields are projected to the inferior and superior parts of the retinas respectively.
- Nerve fibres resulting from the temporal half of the visual field from each eye cross over in the optic chiasm resulting in fibres carrying information about the left visual field passing along the right optic tract and those carrying information about the right side of the visual field passing along the left optic tract.
- Posterior to the optic tract, nerve fibres carrying information about the lower and upper visual field separate. Those carrying information about the inferior visual field are found in the superior optic radiation, those with information relating to the superior visual field are located in the inferior radiation (Meyer's loop) passing through the temporal lobe.

Loss of half of the visual field is called a hemianopia. Loss of half of the visual field on the same side of each eye is termed a homonymous hemianopia, for example a lesion in the left optic tract causes a right homonymous hemianopia. If visual field loss is in the temporal fields of each eye it is termed a bitemporal hemianopia, and if it is in the nasal fields it is termed a binasal hemianopia. A quadrantanopia is the term for loss of vision in a quadrant of the visual field and additionally may be termed superior or inferior depending on whether the upper or lower visual field is affected. Similarly these types of defect can also be homonymous and bitemporal/binasal.

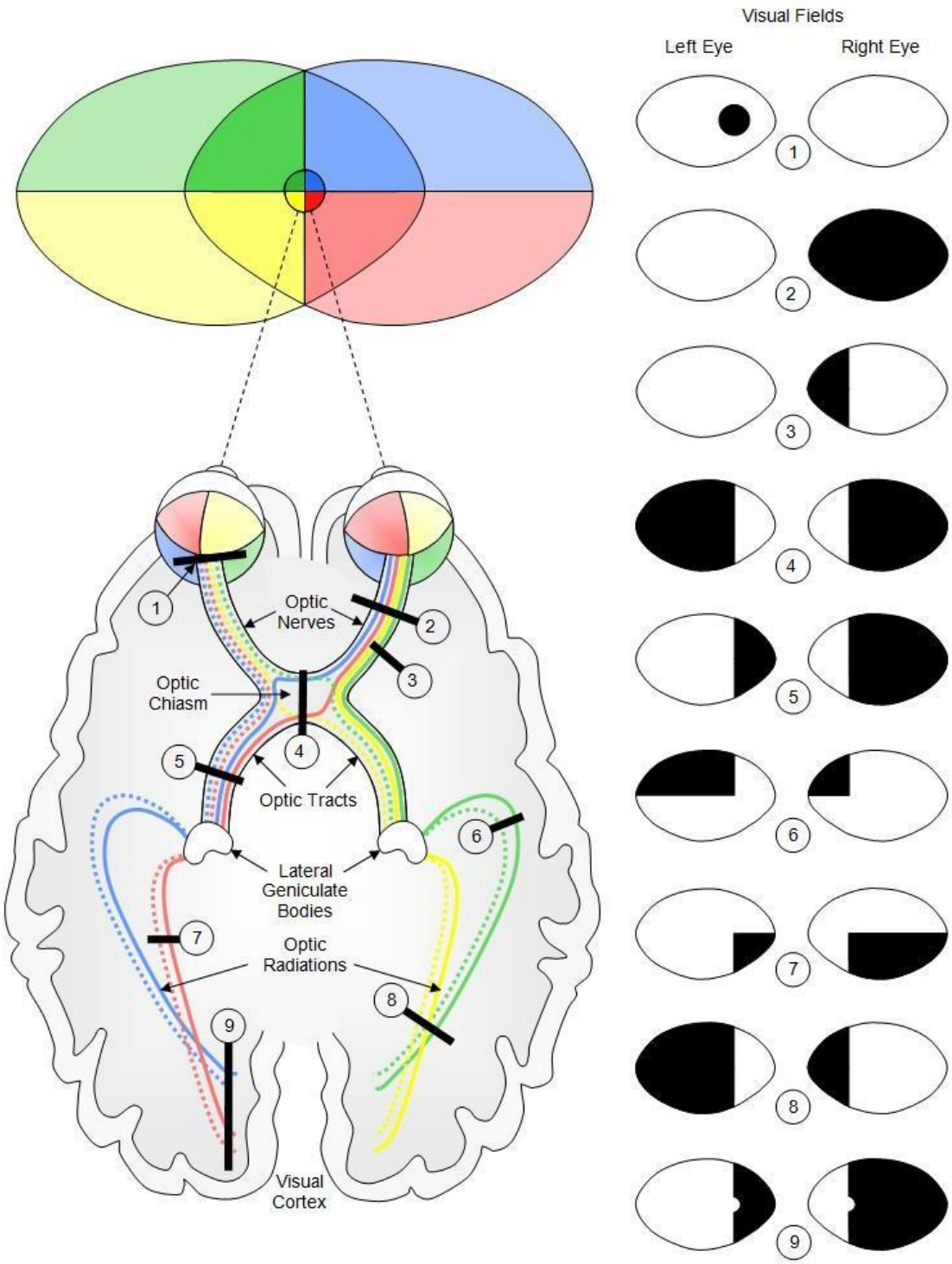

Figure 2.3: The human visual pathways, potential lesion sites and resultant visual field defects. The resultant visual field defects (coloured black) are shown on the right and correspond to the 9 lesion sites shown along the visual pathways.

Types of field defects are discussed in further detail, with reference to the various areas within the visual pathways, in the following paragraphs.

The optic nerves

Lesions in the area behind the eye and anterior to the chiasma (termed retrobulbar lesions), whether due to inflammation or compression, usually give rise to central scotoma (figure 2.3, lesion site 1). The scotoma in these cases typically occupies both sides of the central midline. If a field defect is limited to one eye then the site of the lesion must be anterior to the chiasma. If there is a complete lesion of an optic nerve then this results in total blindness in one eye (figure 2.3, lesion site 2).

The optic chiasm

Assessment of visual field defects is extremely important in the diagnosis of chiasmal lesions. A pituitary tumour will cause bitemporal field defects if the tumour is in the midline as it will compress the crossed nasal fibres first (figure 2.3, lesion site 4). The uncrossed temporal fibres may still remain undamaged due to their wider position. Pressure on an optic nerve at its junction with the chiasma interferes with the anterior knee of Wilbrand and the inferior peripheral retinal nasal fibres from the other eye may be impaired resulting in an upper temporal quadrantic defect in that eye's visual field. An inferior temporal quadrantic defect would result from interference with the posterior knee of Wilbrand. However, this is less commonly seen. Pressure on the chiasma in the midline posteriorly by an expanding pituitary tumour hinders conduction in the macular crossing fibres and tends to cause bitemporal central defects.

The optic tracts

A complete lesion of an optic tract will cause a total contralateral homonymous hemianopic defect, for example a right homonymous hemianopia is caused by a complete lesion of the left optic tract (figure 2.3, lesion site 5). However, partial lesions of the optic tract are more common. These will also cause contralateral homonymous defects, but due to the position of the retinal nerve fibres which relate to the various areas of the visual field, incongruity often results, with different patterns of visual field loss in the two eyes. As such, marked incongruity in partial hemianopia indicates a tract lesion, since lesions of the optic radiations cause only mild incongruity, and striate lesions are highly congruous. A lesion of any part of the visual pathway anterior to the lateral geniculate bodies causes optic atrophy in addition to visual field defect. The nearer the lesion to the eyeball, the earlier the atrophy occurs. Atrophy can be seen in a retinal image as pallor of the optic disc and may take months to appear due to an optic tract lesion. This is one reason why visual field assessment is essential in tract lesions.

The lateral geniculate bodies

Lesions of the LGN are relatively uncommon due to their small size and secluded location. Tumours of the temporal lobe are those which most frequently affect this area. By the time they are large enough to damage the visual pathway they distort the adjacent structures so much that it is often difficult to be sure whether the interference is in the posterior end of the optic tract, the LGN, or beginning of the optic radiation. All three structures may be involved. The main defect seen with LGN lesions is an incongruous hemianopia, much like that seen with optic tract lesions, reflecting the continued segregation of ocular inputs in the LGN.

The optic radiation

The optic radiations can potentially be affected anywhere along their paths and the type of field defect is still related to the site of the damage. Damage close to the visual cortex usually causes a complete homonymous hemianopia (figure 2.3, lesion site 8). A quadrantanopia results from interruption of either the superior or inferior optic radiation (clinically this usually involves a lesion in either the parietal or temporal cortex) or alternatively from a partial lesion of the visual cortex. Lesions of the ventral fibres in the anterior temporal lobe cause a contralateral superior quadrantanopic visual defect (figure 2.3, lesion site 6). Lesions of the dorsal fibres in the parietal lobe cause an inferior quadrantanopic defect (figure 2.3, lesion site 7). Because there is no sharp demarcation of the dorsal fibres from the ventral fibres in these portions of the posterior pathway, the defects do not always conform to the horizontal midline.

The primary visual cortex

Lesions of the visual cortex produce homonymous contralateral hemianopic field defects. However, unlike the defects from lesions of the optic radiations and the optic tracts, the hemianopic defects from visual cortex lesions are highly congruent, with virtually identical defects in the two eyes. Complete destruction of visual cortex causes a complete homonymous hemianopic visual field defect, but because this involves not only peripheral vision but also the contralateral half of the foveal region, it is called a macular-sparing homonymous hemianopia (figure 2.3, lesion site 9). Most cortical lesions are not large enough to affect the whole extensive cortical area representing the macular, thus leaving some of the area unaffected. Macular splitting hemianopias can occur with complete lesions anywhere along the post-chiasmal visual pathways, and can thus lack localising value. In these cases other signs may help in localisation, such as optic atrophy and the relative afferent pupillary defect with optic tract lesions.

Of course, neuroimaging can provide highly detailed images which are used to confirm diagnosis and monitor disease, but due to the characteristic visual field defects which can arise as a result

of many neurological disorders, quantitative visual field testing is also of immense value in diagnosing and managing the causes of CVI. In addition to simple and quick diagnosis visual field testing also provides an effective way of monitoring response to treatment over time.

Retina

Whilst the main cause of visual impairment in children is attributed to CVI, in addition to these it is also useful to mention retinal diseases which cause visual field defects and in particular glaucoma. Visual field testing has a role in diagnosing and treating many retinal diseases. However, direct observation of the retina through ophthalmoscopy is also of great value in retinal disease diagnosis as defects will often correspond to inflammatory or degenerative disease which can be seen with the ophthalmoscope. Perimetry becomes one of many supplementary examinations. Retinal lesions cause field defects that correspond to the path of the retinal nerve fibres or to the area of supply of the retinal blood vessels and they can cross the vertical midline through the fovea. For example, arcuate defects which commonly occur with glaucoma conform to the course of the retinal nerve fibres and also cross the midline. Although glaucoma is the most well-known and most commonly occurring retinal disease, arcuate scotoma can also occur in other retinal conditions.

Glaucoma refers to a group of diseases that affect the retina and which cause damage to retinal ganglion cells resulting in visual field loss presenting in a characteristic pattern. Raised intraocular pressure (IOP) is the main significant risk factor for developing glaucoma. IOP is related to the production of liquid aqueous humour by the ciliary processes of the eye and its drainage through the trabecular meshwork. Aqueous fluid flows from the ciliary processes into the posterior chamber. It then flows through the pupil of the iris into the anterior chamber, bounded posteriorly by the iris and anteriorly by the cornea. From here the fluid is released into general blood circulation through drainage channels in the trabecular meshwork. In the normal eye, the fluid produced is equalled by the fluid draining out. However, a pressure increase will result if it cannot drain away properly or too much is produced. If the eye is under increased pressure damage can occur which is dependent on the increased level of pressure and how long it has existed and additionally whether there is a good blood supply or any other weakness to the optic nerve.

Glaucomatous visual field loss usually occurs first in the so-called Bjerrum areas of the upper and lower hemifields. These two areas curve around the macula, extending upward and downward from the blind spot toward the nasal field in two arcs. Early glaucomatous field defects often take the form of relative scotomas, or small regions of decreased sensitivity. Defects in the nasal field are particularly common, and sensitivity differences across the horizontal meridian are often used diagnostically, particularly in the nasal hemifield. Perimetric testing of glaucoma patients

is rarely done outside the central 30° field because only a small percentage of glaucomatous defects occurs in the peripheral field alone. Types of glaucoma are listed in the following paragraphs.

Primary open angle glaucoma is the most common form of glaucoma, occurring over time it is often referred to as chronic glaucoma. There is reduced flow through the trabecular meshwork with IOP rising very slowly. Initially there are no symptoms and if it is not diagnosed and treated, it will cause a gradual loss of vision without noticeable sight loss for many years. It will usually respond well to medication particularly if diagnosed and treated early. However, sight loss sustained is irreversible.

Angle closure glaucoma (also known as acute or narrow angle glaucoma) differs from open angle glaucoma in that there is a sudden and more rapid increase in IOP due to the iris being pushed forward against the trabecular meshwork, blocking fluid from escaping. Treatment of angle closure glaucoma usually involves surgery to create a small hole in the peripheral iris (a procedure known as "laser iridotomy"). This allows aqueous fluid to flow through the hole in the iris and bypass the resistance flow at the pupil. With equalisation of pressure between the anterior and posterior chambers, the iris is no longer pushed forward and settles into its normal position allowing IOP to return to normal. Symptoms of angle closure glaucoma may include headaches, eye pain, nausea, rainbows around lights at night, and very blurred vision.

Normal tension glaucoma (also known as low-tension or normal pressure glaucoma) causes damage to the optic nerve and resultant visual field loss despite a normal IOP level. The reason for this is not well-known. However those at higher risk for this form of glaucoma are those with a family history of normal tension glaucoma and people with a history of systemic heart disease. It is treated with medication or surgery which will maintain a low IOP.

Secondary glaucoma is caused when a rise in eye pressure is caused by an additional eye condition for example as the result of an eye injury, inflammation, tumour or by certain drugs such as steroids. This form of glaucoma may be mild or severe. The type of treatment will depend on whether it is open angle or angle closure glaucoma.

Paediatric glaucomas consist of congenital glaucoma (present at birth), infantile glaucoma (appears during the first year) which by convention is also often referred to as congenital, and juvenile glaucoma (above infancy through the teenage years), and all the secondary glaucomas occurring in the paediatric age group. Congenital glaucoma is present at birth. However sometimes symptoms are not recognised until later in infancy or early childhood. It is very important to catch paediatric glaucoma early in order to prevent blindness.

2.3.2 Methods of perimetry

Visual field testing (known as perimetry) is the method by which the extent and the sensitivity of the visual field is measured. Perimetry may be kinetic or static and manual or automated. Methods of perimetry are described in this section with reference to some common instruments and strategies used for visual field measurement.

2.3.2.1 Visual threshold

An important concept in perimetry is visual threshold. Each point within the visual field has a visual threshold level. The threshold level at a location within the visual field is defined as the weakest stimulus that is visible in that visual field location, such that at that location all visual stimuli that are larger or brighter than the threshold stimulus can be seen and those smaller or less bright cannot be seen. A stimulus that is stronger than the threshold stimulus is described as a suprathreshold stimulus.

A threshold visual field test seeks to identify the visual threshold levels within the visual field area that is tested, while a suprathreshold test is used to identify defects but not identify the depth of these defects.

2.3.2.2 Static & kinetic perimetry

There are two main techniques used for presenting visual stimuli – static and kinetic perimetry. Static perimetry involves presenting stimuli at specific locations and recording whether or not the stimuli are seen at each location, while kinetic perimetry involves the presentation of a stimulus which is moved from an area where it is unseen towards an area where it is expected to be seen (this is usually in a direction towards the fixation point), and this point is recorded. Static perimetry asks, "What is the visual sensitivity for a specific location?", while kinetic perimetry asks, "Where is the threshold for a specific stimulus?" In general, kinetic methods are used in manual perimetry and static methods are used in automated perimetry. However, kinetic perimetry can make use of static methods, and kinetic perimetry can be performed by some automated perimeters.

Static perimetry

In static threshold perimetry, the patient is instructed to look at a fixation target which is located in a central position. Once fixation has been achieved, a visual stimulus (usually in the form of a spot of light) is presented at a location within the visual field and the patient indicates whether they have seen it. The visual stimulus presented is of a specific size and

brightness intensity and is presented on a screen with known background intensity. The size of the stimulus and the background illumination are kept the same throughout the test and the dimmest stimulus that can be seen (the threshold level stimulus) at specific predetermined locations of interest in the visual field is determined by trial and error using stimuli of varying brightness. The method is termed static perimetry as specific locations are chosen and the stimuli are presented at these locations without being moved.

Static threshold perimetry is useful in that it determines the sensitivity of locations in the visual field. However, it can be time consuming and is not a good method for determining the boundaries of a visual field as this requires a large number of visual field locations to be tested. Automated perimeters now include strategies which shorten the testing time and this technique is the most widely used method of perimetry.

Similarly static perimetry can be suprathreshold, where the threshold is not specifically determined at locations within the visual field, but it is determined whether or not the patient can see stimuli presented at a specific brightness level in a static fashion. A suprathreshold test is useful as a fast screening test to quickly identify visual field defects of a certain level but not quantify the specific threshold level.

Kinetic perimetry

A continuous line connecting common threshold levels within the visual field is termed an isopter. Visual stimuli greater than the threshold cannot be seen outside the region surrounded by an isopter line but can generally be seen everywhere inside the isopter region. The isopter line is in effect a boundary between "not seeing" and "seeing" a stimulus of a certain intensity. Because of this fact the location of the isopter for a given stimulus can be determined by moving the stimulus from an area where it is not seen towards an area where it is expected to be seen. This is usually from the periphery toward the point of fixation.

In kinetic perimetry the patient is instructed to look at a fixation target which is located in a central position and a stimulus of a specific brightness and size is moved from an area where it is not seen toward an area where it is expected to be seen. When the patient first sees the stimulus they communicate this to the examiner and the location is recorded. This process is repeated from several directions toward the central fixation point until the isopter can be drawn by connecting the points recorded. Several different isopters can be drawn by repeating the process with visual stimuli of differing intensity or size. When several isopters are plotted together on a chart, they give a picture of the overall extent of the visual field and a measure of the sensitivity of the visual field, depending on how far the isopters extend for a particular size and intensity of stimulus.

It should not always be assumed that all areas inside an isopter boundary line will respond

to the isopter level or brighter stimulus. An area of visual field defect (scotoma) could be contained within the boundaries of an isopter. These can be found kinetically by moving the stimulus around inside the isopter boundary and having the patient indicate if the stimulus dims or disappears at any point. A scotoma found could then be mapped by presenting the stimulus in a non-seeing area and moving outward until seen. The determined location of the isopters depends on the rate of movement of the stimulus and the reactions of the patient.

2.3.2.3 Non-quantitative perimetry: the confrontation technique

Not all methods of visual field testing quantify the visual threshold at representative locations in the field. For certain diagnostic purposes, quantified threshold determination may not be necessary or possible (e.g. in young children).

The confrontation visual field test is a quick screening test that can determine the limits of the visual field and can also detect large visual field defects.[32,33]In adults the test involves a comparison of the patient's visual field with the examiner's visual field. The patient sits facing the examiner and is instructed to look at the examiners face (a specific feature such as the nose or one eye is often used) with one eye covered. The examiner also covers their eye (corresponding to the same eye as the patient) so that the visual fields of the examiner and patient will correspond. The examiner holds up some fingers in each of the visual field quadrants in turn and the patient must identify how many fingers are presented at each location. If the patient is unable to confirm the presence of the examiners fingers or is unable to identify the number of fingers a visual field defect can be suspected. A problem with the procedure described above is that the limits of the visual field are not tested, and an alternative method whereby the examiner moves their fingers slowly in from the periphery of vision until the patient sees them can be used.

Monocular confrontation testing in adults and older children (which depends on congruence between the visual field of the examiner and patient) is routine. However, in infants, younger children and older patients unable to participate in monocular testing, binocular testing will often be performed. The child's gaze is attracted to an interesting (but not too captivating) central stimulus. For example, a toy or face is an appropriate central stimulus if the child is less than 6 months old. Then a dynamic stimulus is presented peripherally while observing the orienting eye and head movement of the child towards the peripheral stimulus if it is seen. This dynamic peripheral stimulus will often take the form of another toy or graded white balls (known as Stycar balls) which are also commonly used for assessing visual acuity in young children.[34]

The confrontation method is simple to perform and does not require a great deal of equipment. However, it is only useful for detecting large field defects such as hemianopia and quadrantanopia

and results are imprecise and not quantifiable. In children, its usefulness is limited by the attention and concentration of the child and the technique is dependent on examiner experience.

The confrontation method is widely used and is currently very important in visual field assessment in children because, despite its lack of quantitative data, it is often the only form of perimetry possible in these patients.

2.3.2.4 Perimetry devices & strategies

There are two main types of equipment in regular use for testing the visual field. These are manual projection devices and automated perimeters. This section provides an overview on each type of device with specific reference to two of the main perimeters used for the manual projection and automated techniques (The Goldmann Perimeter and the Humphrey Field Analyser).

Manual projection perimetry: the Goldmann perimeter

Manual projection perimeters require the examiner to control the stimulus selection and presentation. A commonly used example of the manual perimeter is the Goldmann perimeter which is a device employing the kinetic perimetry method.

The Goldmann perimeter standardised many of the variables in perimetry testing. The background light level was standardised by using an evenly illuminated bowl into which the patient looks and the "test stimuli" were standardised by enabling them to be varied by known specific increments of brightness and size.

Testing is performed with one eye covered so as to perform uniocular testing. The patient is instructed to maintain fixation on a central target at all times and light stimuli are moved manually by an examiner through the use of a mechanical projection system. The patient indicates when they first see the stimuli by pressing a buzzer. This process is repeated to build up a contour map of the patient's visual field (as described in the section 2.3.2.2). Figure 2.4 shows the Goldmann manual projection perimeter.

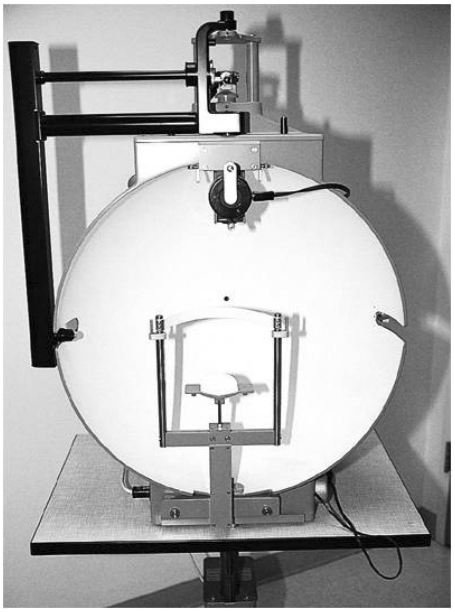

Figure 2.4: The Goldmann manual projection perimeter.

The Goldmann standard - stimulus intensity

Brightness intensity, also termed luminance, is measured in the SI units of Candelas per meter squared (cd/m^2). However, another unit also used for luminance is the apostilb (asb) where:

$1\,cd/m^2 = 1\,asb/\pi$

The Goldmann perimeter can project a spot light stimulus with a maximum luminance of 1000 asb onto a bowl illuminated with a background luminance of 31.6 asb. Light stimuli at different intensity (luminance) levels are created by the use of filters which attenuate the light intensity by specified amounts.

The attenuation of light is expressed in decibels (dB) on a logarithmic scale related to the maximum stimulus luminance such that a ratio between the maximum luminance and a level of stimulus luminance can be expressed in dB by:

$L_{dB} = 10\,log_{10}\left(\frac{L_{Max}}{L_{Stim}}\right)$

Where L_{dB} is the stimulus luminance measured in dB, L_{Max} is the maximum luminance for that device and L_{Stim} is a luminance value corresponding to a specific stimulus luminance (so long as L_{Max} and L_{Stim} are in the same units).

$\therefore\ L_{Stim} = \frac{L_{Max}}{10^{L_{dB}/10}}$

As these logarithmic values relate to the maximum stimulus luminance available for a given perimeter, 1 dB on one device may not be equivalent to 1 dB on another unless they have the

same dynamic range (and other test conditions such as background luminance). For example, the maximum stimulus on Goldmann perimeter is 1000 asb while on the Humphrey Field Analyser (a device discussed in the next section) it is 10,000 asb, so 1dB represents a luminance of 794.3 asb on the Goldmann perimeter, but 7943 asb on the Humphrey Field Analyser.

The units of dB rather than absolute luminance values are often used because visual perception relates well to ratios between light intensities rather than differences between them. For example, the sensation related to doubling the intensity from 50 to 100 asb is equivalent to the sensation of doubling the intensity from 500 to 1000 asb, even though the latter involves an increase of 500 asb. An additional advantage of using logarithmic units is that visual threshold can be examined over a wide range.

The Goldmann perimeter standardised this method of presenting varying levels of stimulus luminance. In order to provide this wide luminance range the Goldmann perimeter is equipped with three sets of filters designed to attenuate light from the maximum luminance level. The first set of filters (with notation 1 to 4) attenuate light in steps of 5 dB such that filter 4 produces no attenuation, filter 3 produces a 5dB attenuation, filter 2 produces a 10dB attenuation and so on. A second set of filters (with notation a to e) attenuates the light in steps of 1dB such that filter e provides no attenuation, filter d provides attenuation of 1dB, filter c provides attenuation of 2dB and so on. One filter from each set is used in combination to provide varying levels of light attenuation from the maximum, and the notation used to describe the attenuation is simply the number-letter combination. Additionally, a third set of filters can be used which allow a 20 dB or 40 dB attenuation. The notation for when either of these two filters are used is to place a single or a double bar above the previously described number letter combination (for the 20 dB and 40 dB filter respectively). For the Goldmann Perimeter (with maximum luminance of 1000 asb) several decibel, luminance and Goldmann notation values are shown in table 2.1

dB	Apostilbs (asb)	Goldmann notation
0	1000	4e
1	794	4d
5	316	3e
7	200	3c
10	100	2e
13	50.1	2b
15	31.6	1e
19	12.6	1a
20	10	$\overline{4e}$
30	1	$\overline{2e}$
40	0.1	$\overline{\overline{4e}}$

Table 2.1: Stimuli dB, luminance and Goldmann notation for the Goldmann Perimeter.

The Goldmann standard - stimulus size

The projected stimulus light spot is described in terms of area (with a known distance between the eye and the screen) or in terms of the angular diameter of the stimulus (i.e. the angle subtended by the stimulus to the eye). The Goldmann perimeter has the patient's eye located at a distance of 30cm from the screen and uses notation in Roman numerals to define five standard sizes (Table 2.2).

Goldmann size	Area at distance of 30 cm (mm^2)	Angle subtended (Degrees)
I	0.25	0.11
II	1	0.22
III	4	0.43
IV	16	0.86
V	64	1.72

Table 2.2: The Goldmann standard stimulus sizes.

The Goldmann perimeter - advantages and disadvantages

The Goldmann perimeter is best suited for kinetic perimetry. It enables the examiner to test both central and peripheral fields with one instrument, it is relatively inexpensive and can provide basic visual field information in a relatively fast and efficient manner. When it was introduced it standardised many of the variables associated with perimetry. However, the main disadvantage of the instrument is that the movements of the stimuli are controlled by the operator, limiting the reliability of serial visual field results. It cannot perform static perimetry efficiently and so is rarely used for this purpose meaning that it can be difficult to detect and investigate smaller scotomas.

There are significant disadvantages with using this system in children, in addition to examiner dependence and skill, a child has to maintain a fixed head position in front of a hemispheric bowl. This requires prolonged cooperation by the child who will need teaching and encouragement to reinforce good central fixation, because it is harder for children to suppress the natural orienting eye movements. Furthermore, "reaction time" may be delayed in very young children, and in older children with developmental difficulties, and the speed of the kinetic scan must be set slower than with adults, at 2-3 degrees per second for example.

Automated perimetry - the Humphrey Field Analyser

Due to the fact that it is difficult to standardise and reproduce results with manual kinetic perimetry methods, the automated perimeter has now become the standard (in adults). Automated perimetry predominantly uses static perimetry as its technique, although some automated devices also offer the capability of kinetic perimetry (despite it not being routinely

used). Most automated devices are also capable of both static threshold and suprathreshold (screening) tests. There are many devices from various manufacturers capable of automated static perimetry. However, the Humphrey Field Analyser (HFA), from Carl Zeiss Meditec, is the most commonly used computer assisted static perimeter and as such has virtually become a standard in its own right. The HFA is shown in figure 2.5.

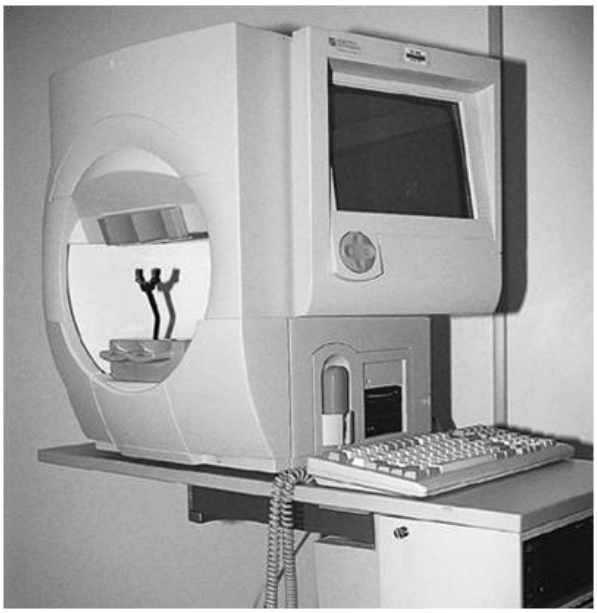

Figure 2.5: The Humphrey field analyser.

To accomplish full threshold testing, the HFA presents stimuli of variable intensity randomly at different retinal coordinates within a bowl with constant photopic background illumination. Fixation is maintained on a central "fixation" point and the patient indicates that the stimuli are seen by pressing a button for the computer to record which stimuli are seen and which are not. The intensity of a stimulus presented at a given location is decreased from a previous presentation if the patient saw the previous stimulus at that location, and vice versa. This requires a computer decision based on the accumulated responses of the patient. The process is repeated until threshold levels for each location have been reached.

For static suprathreshold testing, stimuli of a selected intensity are presented in predetermined locations, and the perimeter simply records for each location whether the stimulus was seen or not. Some important aspects of automated static perimetry devices, and of particular relevance to the HFA, are discussed below.

Stimulus size

While in kinetic perimetry both the size and the intensity of a stimulus may be adjusted to achieve a range of isopters, in static threshold perimetry the size of the stimulus is kept fixed

during a test and only the intensity is changed. A common stimulus size used by automated perimeters is a size equivalent to Goldmann size III (table 2.2), because the smaller size I at maximum intensity is not a strong enough stimulus to quantify the full depth of some defects.

Stimulus intensity

In static perimeters that use uncovered LEDs the stimulus intensity is simply the intensity of light produced by the LED. In projection perimeters the total luminous intensity in the spot of light is the intensity of the background plus the additional light projected as a stimulus. However, the stimulus intensity is still usually expressed simply as the amount of light (in apostilbs) projected onto the existing background or the corresponding dB level despite the fact that it is not the absolute intensity but the difference between the spot and the surrounding "background" that is relevant to the visual perception tested in perimetry.

Static threshold strategies

In automated perimetry a bracketing or "staircase" strategy is used to determine threshold levels. At each visual field location, stimulus brightness is first changed in large steps until the boundary from invisibility to visibility (or vice versa) is crossed. This brackets the general range of luminance that contains the threshold value. Then going back and forth with smaller increments of luminance, the threshold is more accurately determined. The various automated strategies differ with regard to how it is determined when the end point has been reached and with regard to the interval of luminance used in the final steps. The threshold is not necessarily determined at one location before moving on to another. These details affect how long the test takes as well as the precision of the threshold value obtained and its reproducibility on retesting. The strategy used is beyond the control of the examiner and they must depend on the manufacturer for a reasonable compromise between accuracy and the time required to perform the test.

Several methods are used to reduce the time required for the visual field test by anticipating the threshold at each location. One estimate is the normal expected threshold value for the age of that person. This method provides a good estimate for nearly normal fields, but not so good for those with more severe defects. Another estimate is the threshold determined on the previous visual field examination in that individual. This method is particularly useful for abnormal fields but depends on the instruments having the capability of storing and retrieving the previous test results. Another method (called prethresholding), effective for both normal and abnormal fields, is to determine threshold completely at one point in each quadrant and then use the value obtained at each spot as a starting point for determining threshold at the several immediately adjacent points, the values at those locations are then used as starting

points for the next series of surrounding points, and so on. This method uses the fact that an abnormal visual field point is likely to be surrounded by other abnormal points while normal points are likely to have other normal points adjacent to them.

Printouts

When static perimetry is performed at numerous locations, as is typically done in full thresholding programs of automated perimeters, the results may be reported as threshold values printed on a map of the visual field. To aid in perceiving a diagnostic pattern at a glance, a greyscale is often also provided. Each grey level represents a certain small range of threshold values. The boundary between the grey levels is equivalent to an isopter. In some printouts not all the locations with a greyscale symbol are tested. Untested locations may be assigned a presumed threshold value (calculated by interpolation from neighbouring points that were tested) to shade in the greyscale plot and make the contour of the isopters easier to appreciate. As with kinetic perimetry, the threshold is known only at the points tested and the threshold at other locations is either estimated or assumed.

Additional features

Automated programs may also (routinely or as an option) perform "catch trials". To catch false-positive responses (in which the patient responds to a light they did not see), the device may make all the mechanical sounds of presenting a stimulus but not actually do so. Doing this several times during a test allows calculation of the proportion of times the patient responds to a non presentation. To catch false-negative responses, a bright stimulus is presented in a known seeing region of the field and the number of times the patient fails to respond to it is recorded.

Various methods are used to monitor the steadiness with which the patient maintains visual fixation on the central target. The Heijl-Krakau methods consist of presenting a "test stimulus" in the known position of the physiologic blind spot.[35,36] The patient can see it only if the eye has wandered from the central position of gaze. In other instruments fixation is monitored by the image of the pupil or a corneal reflection. This method is continuous whereas the Heijl-Krakau method is an intermittent sampling of fixation steadiness. Neither of these automatic methods is totally satisfactory for fixation monitoring. The best method is direct observation by the perimetrist, either through a telescope or on a video monitor.

One advantage of static fields is that it produces numerical data at pre-determined points which can be handled statistically. Despite these there are limitations for its use in children and only children above 8 to 10 years are capable of the vigilant rapid response and good fixation required so it is rarely used in this patient group.

Chapter 3

Background - Eye movements and eye tracking technology

3.1 Human Eye Movements

For any application of eye movement instrumentation the type of eye movements to be observed must be understood. There are three main categories of eye movements which are related to the situations in which they occur:

- fixational eye movements,
- gaze shifting movements, and
- image stabilising movements.

The following three sections (3.1.1, 3.1.2 and 3.1.3) describe the specific eye movements within each of the three categories listed above which are relevant to this research. By way of example, prior to the detailed descriptions in the following three sections, several types of eye gaze movements are shown in figure 3.1. The figure shows horizontal and vertical eye gaze position on a computer screen and demonstrates fixation, saccadic eye movement and smooth pursuit. Screen position is measured in pixels and the location (0,0) refers to the top left corner of the screen. Initially fixation is maintained at a screen location of (800,800) before a saccadic fixation change to an area in the top right of the screen where fixation is again maintained prior to a smooth pursuit eye movement back to the original screen location. The data within this figure was collected using a Tobii x50 eye tracker (*Tobii Technology, Danderyd, Sweden*) at a sample rate of 50Hz.

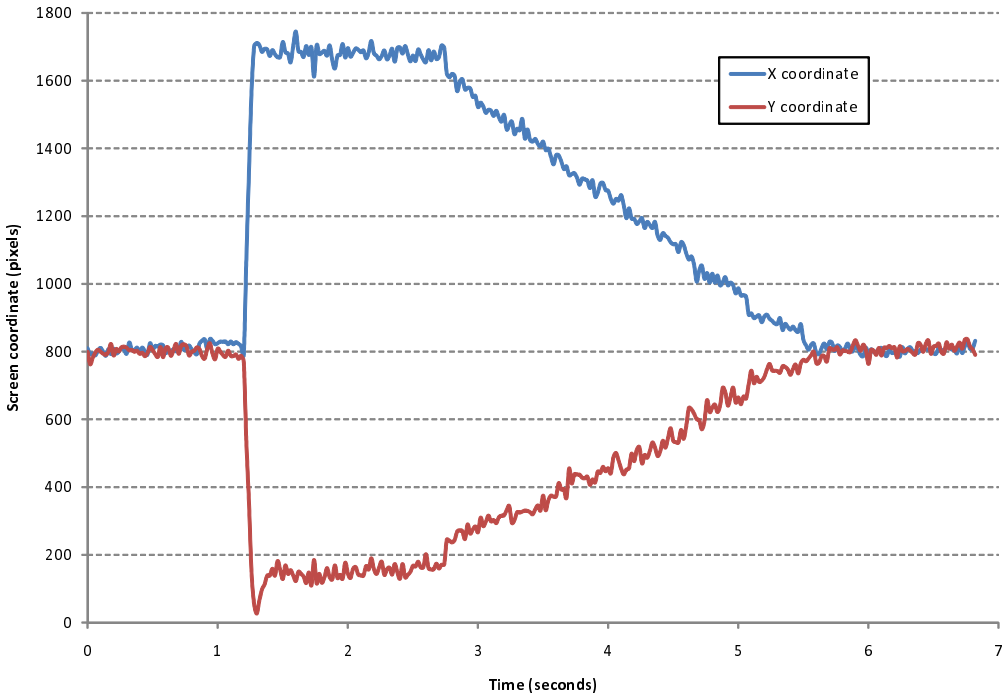

Figure 3.1: Horizontal and vertical gaze position on a computer screen demonstrating fixation, saccadic eye movement and smooth pursuit. Screen position is measured in pixels and the location (0,0) refers to the top left corner of the screen. Initially fixation is maintained at a screen location of (800,800) before a saccadic fixation change to an area in the top right of the screen where fixation is again maintained before a smooth pursuit movement back to the original screen location.

3.1.1 Fixation movements

Fixation movements include a variety of motions which are generally less that 1° in amplitude and occur during fixation on a target. Drift is the slow random motion of the eye away from a fixation point at velocities of only a few minutes of arc per second. Flicks, or microsaccades, are small rapid eye movements which have been shown to be dynamically of the same nature as large voluntary saccades, of magnitudes as large as 1°, occurring at intervals separated by as little as 30ms and which generally redirect the eye towards the position necessary for fixation on the target. Both flicks and drifts tend to occur along a single preferred axis in any individual. There is currently no general agreement on the error-correcting nature of the flicks or drifts. In addition normal individuals fixating on targets exhibit a high frequency tremor in the range 30 to 150Hz with peak amplitudes of approximately 30 arc seconds in the region of 70Hz. Because of the presence of these fixation movements, accuracy of 0.5 to 1° is often sufficient in eye-monitoring tasks designed to show what part of the visual field is being fixated.

The role of microsaccades in visual perception has been a debated topic which is still largely

unresolved. It has been proposed that microsaccades correct displacements in eye position produced by drifts, although non-corrective microsaccades also occur. Microsaccades were also believed to prevent the retinal image from fading, but they do not occur often enough for that purpose, considering that perfectly stabilised images can disappear from perception in a few seconds or less. The current consensus is that all fixational eye movements are important for the maintenance of visibility.

Some of the errors in eye gaze data produced by eye trackers can be eliminated because microsaccades of equal magnitude and direction will typically occur in both eyes at the same time, whereas errors due to the eye tracking technique will seemingly occur randomly without correlation between the left and right eye (as can be seen in figure 3.1).

3.1.2 Gaze shifting movements

Of the three gaze shifting mechanisms detailed below, the saccadic eye movement is of most importance in this research as it is saccadic movement which is to be detected and measured as part of the automated perimetry test developed. Smooth pursuit and vergence movements are described briefly for completeness.

3.1.2.1 Saccades

Saccadic eye movements are the fast, conjugate movements by which fixation is changed from one point to another voluntarily with the purpose of fixating an image of a target of interest on the fovea. They are characterised by very high initial acceleration and a peak velocity during the motion which varies with the amplitude of the saccade and may be as high as approximately $600°/s$.[37] The duration of a saccadic eye movement also varies depending on its magnitude, with saccades larger than 5° lasting approximately 20-30ms plus 2ms for each additional degree of amplitude.[38,39] Head movement is often involved when the target motion exceeds 30°. In response to a visual stimulus saccadic eye movements exhibit a variable latency from 120-350ms or more which is dependent on several factors such as the task being undertaken or the brightness of the stimulus which triggered the saccadic eye movement.[37,40]

3.1.2.2 Smooth pursuit

Pursuit movement is the ability of the eyes to smoothly follow a moving object. These slow tracking conjugate eye movements are used to track slowly moving visual targets (less than approximately $30°/s$) and the pursuit of targets moving with velocities larger than this usually require catch-up saccades.[41] The purpose of smooth pursuit movements are again to stabilise

the image of a moving target or background on the fovea, independent of the saccadic eye-movement system. Smooth pursuit movements are not generally under voluntary control and usually require the existence of a moving visual target for their execution.

3.1.2.3 Vergence

Vergence eye movements are movements of the two eyes in opposite directions in order to combine the image of near or far objects. These movements are considerably slower and smoother than the fast conjugate saccadic eye movements and are normally performed unconsciously in response to visual objects which are closer or further away from the eyes, being stimulated by focusing error as well as binocular disparity.[37]

3.1.3 Image stabilising movements

The understanding of these types of eye movements is useful so as to enable comprehension of some limitations of the developed perimetry device and additionally for understanding some patient eye movement disorders. So for these reasons, and for completeness, several types of image stabilising eye movements are briefly described below.

3.1.3.1 Optokinetic reflex

The optokinetic reflex allows the eye to follow repeating pattern targets while the head remains static. It demonstrates a characteristic sawtooth pattern of eye motion occurring as a result of a moving visual field containing repeated patterns. Optokinetic reflex consists of a slow phase, where the eye fixates on and follows a particular moving target with pursuit motion, and then a fast phase or return saccadic "jump" where the eye fixates on a new location, reversing the previous pursuit motion. The minimum time between fast phases is approximately 0.2s, resulting in a maximum frequency of 5Hz, although the reflex frequency may be less for slow field motions. The amplitude of the optokinetic reflex is variable, generally from 1 to 10°.[42]

3.1.3.2 Vestibulo-ocular reflex

The vestibulo-ocular reflex (VOR) is an eye movement which stabilises images on the fovea during head movements. It is primarily attributable to stimulation of the semi-circular canals and the otoliths in the inner ear. The vestibulo-ocular reflex has both rotational and translational aspects. When the head rotates about any axis, be that horizontal (head rotation up and down), vertical (head rotation left and right) and torsional (head rotation along line of sight, often called "counter-rolling"), images are stabilised on the retina by rotating the eyes about the

same axis but in the opposite direction. When the head translates, during walking for example, visual fixation is maintained on a target by rotation of the eye by an amount that is dependent on the distance to the target.

The "gain" of the VOR is defined as the change in the eye rotation angle divided by the change in the head rotation angle such that equivalence between the two angles would result in a gain of 1.0. The gain of horizontal and vertical VOR is usually close to 1.0, but the gain of the torsional VOR (rotation around the line of sight) is generally lower and varies depending on several factors including the amount of head tilt. [43,44]

3.2 Eye tracking

Eye tracking is the method of measuring the point of fixation usually by measuring the motion of an eye relative to the head. An eye tracker is a device for measuring eye movement and computing point of gaze.

3.2.1 Eye tracking uses

Measurement of the direction of gaze has long been of interest. It can provide information of clinical importance for example in oculomotor disorders such as nystagmus and neurological disorders where eye movement characteristics are important in diagnosis. In psychology, reading specialists have understood the importance of measuring gaze for assessing good reading practice and its importance for child development. Additionally much research has been conducted looking into visual searching behaviour and the patterns of perceiving and processing visual information. Human factors engineers, concerned with the design of systems and the placement of controls and displays (for example in the design of helicopter cockpits) are interested in gaze patterns while looking at instruments, controls, and the world scene. Research engineers interested in biological control systems and bionics have found eye movement control systems particularly challenging. However there are now assistive technology systems which are able to aid with communication by using eye movements in people with certain disabilities such as cerebral palsy. In more commercially orientated research, such as advertising and marketing, the evaluation of the effectiveness of visual stimuli are of interest and can be made using measurements of gaze and also pupil size as indicators of levels of interest. More recently web site usability has become a subject of great interest and ability to monitor gaze is highly useful in these studies.

The wide range of possible interest and applications involving assessment of eye movement and gaze position has resulted in a wide variety of measurement techniques. [42]

3.2.2 Eye tracking methods and technologies

3.2.2.1 Historical techniques

Direct observation would have been the first technique for determining the nature of human eye movement and is still the basis for fast clinical tests employed today to diagnose nystagmus or gross disorders of the saccadic or pursuit tracking systems. Direct observation obviously suffers from the shortcomings of no quantitative data and the lack of any record.

Early researchers were particularly imaginative in developing mechanical methods to detect and record eye movements. For example, a light rod fixed directly to the cornea of an anaesthetised eye by means of a plaster-of-paris ring. The mechanical motion of the rod, passing through a number of levers to amplify its motion, was recorded directly on a rotation drum kymograph.[45] A later development took advantage of the shape of the cornea to detect the movement of the corneal bulge through a closed eyelid. All these direct mechanical techniques, of course, interfered with the normal eye movements, but set the standard later surpassed by photographic and photoelectric techniques.

In the early 1900's photographic records of eye movements were made. Horizontal eye position could be tracked by the displacement of the light-dark boundary between the sclera and the iris. Use of continuous constant speed film later extended the method. A number of researchers improved the photographic technique by attaching some bright foreign object to the eye.[46–48] The use of direct high-speed motion-picture photography for recording torsional eye movements later became one of the most reliable and simple techniques for measurement about that axis. In all direct photographic techniques, each frame is compared with master calibration photographs to determine the angle of eye movement. These methods were expensive and required excessive time during post-processing of individual frames to determine the history of eye movements.

The contact lens has also been used as a method of direct contact eye tracking. Eye movement could be measured using a magnetic sensor or mirror embedded in the lens providing accurate measurements with tight fitting lenses.[49–51] The main issue with these techniques is the comfort of the subject. For example many earlier systems were painful, had to be performed under anaesthetic, did not allow the subject to blink and could not be used over very long periods.

3.2.2.2 Current techniques

The techniques currently in use for measuring eye movements can be grouped into two main categories:

- methods using the electrical characteristics of the eye (electrooculography), and
- methods using the optical properties of the eye (video-oculography).

Electrooculography (EOG)

The position of the eye can be measured by placing skin electrodes around the eye and recording potential differences. The source of the electrical energy is the corneoretinal potential which changes with respect to the rotation of the eye. The cornea remains approximately 1mV positive with respect to the retina, attributable to the higher metabolic rate at the retina. Usually, pairs of electrodes are placed either above and below the eye or to the left and right of the eye. As the eye rotates, the electrostatic dipole rotates with it. Consequently, a potential difference occurs between the electrodes and assuming that the resting potential is constant, the recorded potential difference is a measure for the eye position. This is not constant though which causes the method to be unsuitable for measuring slower eye movements and fixations, and is better for measuring the fast saccadic eye movements. It is most commonly used to measure rapid eye movements during sleep.

The recorded potentials are small, in the range of 15 to 200μV, with nominal sensitivities of the order of 4μV per degree of eye movement. These signals are at times difficult to detect in the presence of large muscle-action-potential artifacts, which can also be picked up as potential differences by the skin electrodes. EOG accuracy is 0.5 to 1.5° with sufficient care in preparation, and has an advantage in that is works well with large eye movements (up to ±90°).

Video-oculography (VOG)

VOG uses optical techniques which generally do not have any contact with the head by analysing light reflections (often infrared) from the eye. One or more characteristic reflections are detected and measured for changes in position. The reflection from the cornea and the location of the pupil are features often used. Optical methods, particularly those based on video recording, are widely used for gaze tracking and are favoured for being non-invasive and unobtrusive. There are different types of VOG setups, they may be head mounted, non-contact but requiring fixed head position (e.g. using a chin and forehead rest), and more recently non-contact devices allowing head movement. Those which are non-contact and also allow head movement must also track the location of the eyes by computing eye position optically or magnetically (which requires a head mounted transmitter and an additional receiver somewhere nearby).

Methods of VOG

Limbus tracking. The limbus is the boundary between the white sclera and the dark iris of the eye. Due to the fact that the sclera is (normally) white and the iris is darker, this boundary can easily be optically detected and tracked. This technique is based on the position and shape of the limbus relative to the head, so either the head must be held quite still or the apparatus

must be fixed to the user's head. Due to the more or less occasional covering of the top and bottom of the limbus by the eyelids, limbus tracking is more suitable for precise horizontal tracking only.

Pupil tracking. Tracking the direction of gaze by the pupil tracking technique is similar to limbus tracking, only here the smaller boundary between the pupil and the iris is used instead. Once again, the apparatus must be held completely still in relation to the head. An advantage of this technique over limbus tracking is that the pupil is far less covered by the eyelids than the limbus, and thus enables additional vertical gaze tracking. The disadvantage is that the difference in contrast is lower between the pupil and iris than between the iris and sclera-thus making the border detection more difficult.

Corneal and pupil reflection relationship. The most widely used current designs are video-based eye trackers. A camera focuses on one or both eyes and records their movement as the viewer looks at some kind of stimulus. Most modern eye-trackers use infrared and near-infrared non-collimated light to create a corneal reflection and also to locate the centre of the pupil. The vector between these two features can be used to compute gaze intersection with a surface after a simple calibration for an individual.

When (infrared) light is shone into the user's eye, reflections occur from the boundaries of the lens and cornea (known as the four Purkinje images). The first Purkinje image from the front of the cornea, called the glint, is the brightest and this, together with the reflection of light off the retina (the so-called bright-eye corresponding to the pupil) can be video-recorded using an infrared sensitive camera as a very bright spot and a less bright disc, respectively. When the eye gaze changes, the relative positioning of the glint and the centre of the bright pupil change accordingly, and the direction of gaze can be calculated from these relative positions. Additionally head movements can be compensated for, so long as eye position is known so as to allow computation of gaze angle and target intersection, as head movement does not significantly change the position of the bright "glint" on the eye. Figure 3.2 shows images of a subject's eye taken using a simple computer camera with a white LED mounted above it. Images were then taken with the subject's eye staring straight ahead but in different locations (a and b), and also gazing in different directions (c - f) to demonstrate the principle of the corneal-pupil reflection technique.

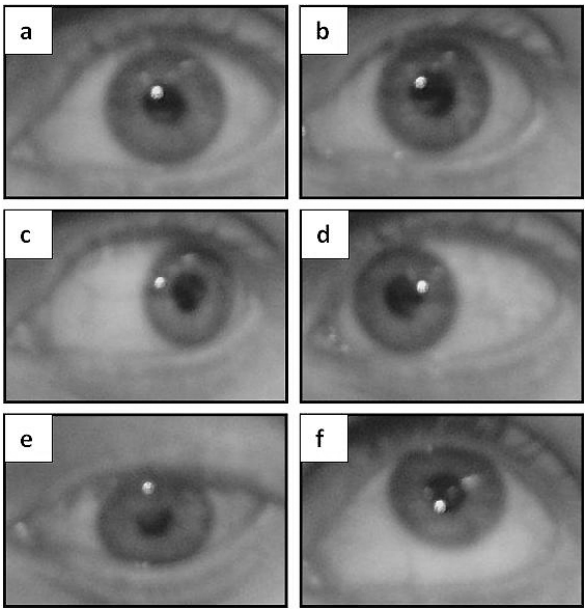

Figure 3.2: The pupil-corneal reflection eye tracking technique. The figure shows a left eye and how the relative positions of the bright "glint" and pupil change under different gaze and head positions. a) gaze straight forward. b) gaze straight forward after head translation left. c) gaze left. d) gaze right. e) gaze down. f) gaze up.

Two general types of eye tracking techniques are used: bright pupil and dark pupil. Their difference is based on the location of the illumination source with respect to the optics. If the illumination is coaxial with the optical path, then the eye acts as a retroreflector as the light reflects off the retina creating a bright pupil effect similar to "red eye". If the illumination source is offset from the optical path, then the pupil appears dark because the retroreflection from the retina is directed away from the camera.

Bright Pupil tracking creates greater iris/pupil contrast allowing for more robust eye tracking and greatly reduces interference caused by eyelashes and other obscuring features. It also allows for tracking in lighting conditions ranging from total darkness to very bright. But bright pupil techniques are not effective for tracking outdoors as extraneous IR sources interfere with monitoring.

Eye tracking setups vary greatly; some are head-mounted, some require the head to be stable (for example, with a chin rest), and some function remotely and automatically track the head during motion. A sampling rate of approximately 50/60 Hz is most common as this is sufficient to monitor eye movements for most applications. Larger sample rates (>200Hz) are available for applications which are interested in studying the detail of fixational eye movements for example.

The problems associated with this technique are primarily those of getting a good view of the eye. Lateral head movement can put the video image of the eye out of focus, or even make the

image of the eye fall out of view of the camera. The range over which the direction of gaze can be tracked by simple software algorithms is $\pm 12^\circ$ to 15° due to the fact that further eye movement may render the glint outside the spherical part of the cornea. More complex algorithms are required to perform the necessary geometrical corrections for gaze tracking beyond the range of $\pm 15^\circ$.

Chapter 4

Literature review and research aims

4.1 Literature review - perimetry in children

Existing "gold standard" techniques for visual field assessment, namely devices utilising ASP, are not routinely used in children and remain a "gold standard" only in the adult population. Many researchers have documented the problems which prevent accurate ASP testing in children. Difficulties in learning the task required to perform the test [17], maintaining a stable fixation on a central target [15,16] and sustaining attention and concentration [18–20] are some of the major contributing factors which lead to poor test reliability with young children. Additionally, for children below the age of approximately 5 years it is difficult to inhibit the natural saccadic response that is normally triggered by the sudden appearance of light stimuli in the visual field [13,14,52] also leading to poor test performance. Some children may also not tolerate the restrictions of head movement imposed on them during the test as they are required to place their head on a chin and forehead rest facing an immersive bowl shaped screen.

As discussed in previous chapters, the methods of visual field assessment in children are highly dependent upon their age. For example ASP is not routinely performed in those younger than approximately 10 years of age, [53] and visual field assessment in children younger than 5 years is limited to the technique of confrontation which provides only very limited detail. [54] However, visual field assessment is still crucial in the diagnosis and management of children with certain brain tumours, raised intracranial pressure and cerebral visual impairment, caused by developmental brain defects, asphyxia, infections of the central nervous system and head trauma [2–6]. There is also call for a reliable and sensitive method to monitor visual field changes in children who are on the drug Vigabatrin for epilepsy due to a potential visual field constriction side effect, [8–10] and in paediatric glaucoma. [11]

Recognising the difficulties associated with performing perimetry in children, previous research

has largely concentrated on using various current perimetry techniques (used normally in the adult population) on children, and investigating the lower limits of age that can be tested. This review reports on these studies. The two main traditionally used methods of perimetry can be divided into kinetic and static perimetry. Studies involving these main types of perimetry will be discussed first. In addition, there are also a number of more recently developed "computer graphics" perimetry techniques and the use of these techniques in children is also reviewed.

4.1.1 Automated static perimetry and kinetic perimetry

4.1.1.1 Automated static perimetry

As stated, the majority of studies have focused on how to use current adult ASP techniques with children. These studies have all involved using testing strategies which have become available as standard on ASP devices (designed mostly to reduce test time), and also by introducing new strategies not routinely used, for example training and familiarisation procedures.

Tschopp et al. (1995)[55] recognised the difficulties of performing computerised static perimetry on children due to the problems of fixation stability, concentration, and reliability of results, and so investigated using a familiarisation strategy for children aged between 5 and 8 years before performing a one-level screening test (where one bright light is presented at each location) with a 12 point visual field test pattern. It was found that this form of ASP examination could provide reliable results (based on an analysis of false-positive catch-trials) in children as young as five years old once a familiarisation procedure had been conducted and so long as the duration of the familiarisation phase and test phase did not exceed the child's capacity to remain task focused.

A year later the same group extended this initial investigation with increased numbers of patients.[30] The study involved 42 subjects aged 5 - 8 years with unremarkable ophthalmic history. They used an Octopus 2000R perimeter, which uses the automated static perimetry technique with central fixation and a button to press when light stimuli are seen within the visual field, with a custom made test pattern consisting of 12 test locations within the central 15° of the visual field and using a two level strategy, meaning that at each location both a bright and a dim stimulus was shown during the test. A preliminary familiarisation phase specifically adapted to the age group was introduced which demonstrated how to perform the test by showing the light stimuli presented while the subject fixated centrally and how and when to press the buzzer. False positive and false negative catch trials were used to evaluate the subjects' reliability. The familiarisation phase was found to be mandatory for the children to perform well with regard to the duration of the examination and the reliability of the answers. The detection of stimuli improved with age, but the difference between the age groups when considering the catch trials

was not significant, allowing the group to conclude that children as young as 5 years were able to give reliable answers to the two-level screening test.

Encouraged by these preliminary results, the same group conducted a study to first validate a testing procedure involving a familiarisation phase, and to obtain normative visual field threshold values in children 5-8 years old. This has been reported in the literature in two parts. [18,56]

In part 1 the approach of the familiarisation procedure was introduced. To perform the tests, the child was sat in a specially designed chair able to adjust and tilt appropriately to enable each child to sit with their chin rested against a specially adapted support. The task was introduced as a tale where an image of a little bear was used as a fixation target and the light stimuli were described as stars. The children were instructed to press the button in response to seeing the stars and were told that the bear was happy when the child looked at him, but very sad when they looked at the stars. The familiarisation procedure consisted of 4 phases gradually introducing different aspects of the test and using custom made field tests on the Octopus 2000R perimeter. Phase 1: subject introduced to the task using bright stimuli. Phase 2: as phase 1 but using supra-threshold stimuli. Phase 3: bright stimuli with the addition of catch trials. Phase 4: as phase 3 but using supra-threshold stimuli. The examination phase used a test consisting of 12 supra-threshold stimuli, 12 false-positive catch trials and 3 false-negative catch trials. This test was repeated up to a maximum of 15 times but the trial was stopped if the child showed any signs of fatigue. The average total duration for familiarisation and examination was about 30 minutes. Age had a marked effect on reliability where, with the exception of the 5-year-olds and one six-year-old, false positive rates were less than 20%. Endurance increased significantly as age increased with a large increase in the number of tests that could be performed. It was concluded that most children as young as five could undergo an examination by ASP. However there are several factors which mean that reliability and endurance is a significant issue when testing these younger subjects. Maintaining fixation on the central target while paying attention to the peripheral stimuli was the most taxing requirement and high rates of no-response and false-negatives demonstrated signs of fatigue. However, the amount of testing (although not all done in a single test) which could be performed was impressive, and it was this which lead the research group to perform a similar trial in order to obtain normative threshold values for children within this age group.

In part 2 the children underwent a familiarisation which was the same as that described above with the addition of one phase consisting of 12 supra-threshold stimuli, 12 false-positive catch trials and 3 false-negative catch trials. A week later quantitative examination was performed according to a specially designed schedule divided into three phases to build up a 76-point threshold visual field test for the right eye. The three phases were designed in such a way that a meaningful test pattern could still be produced should the participant not complete phase 2

or 3. Normative threshold values were obtained for all the age groups. However, there were less data for the younger subjects due to no 5-year-olds being able to complete phase 2 and no 6-year-olds able to complete phase 3. It was suggested that 5- and 6-year olds had higher threshold levels but these could have been inflated by non physiological factors.

It is impressive that this group were able to perform threshold testing on such a young age group. However the testing procedure required lengthy familiarisation phases using custom tests and multiple examination phases which would not be practical in a busy clinical setting. There also was a clear worsening of reliability and endurance with the younger children in these studies.

Several groups have investigated using ASP in children because of advances made to the algorithms which control the way a test is conducted in order to shorten testing times without sacrificing accuracy. The Swedish Interactive Thresholding Algorithm (SITA) is one such algorithm.[25,26,57] The SITA strategy was developed specifically for threshold ASP (on the Humphrey Field Analyser) and uses a combination of the usual stair-case strategy with the introduction of probability procedures. The principles are as follows. For each location the initial stimulus is presented at an estimated sensitivity and subsequent presentations are determined using a 4dB/2dB staircase (such that the presented stimuli are shown initially in 4dB steps then once sensitivity threshold is crossed this changes to a 2dB change). In addition, with the presentation of each stimulus and subsequent patient response, two probability functions describing the likelihood of threshold levels at that location are created. One probability function gives the probability for each threshold value assuming the location is normal, the other describes the probability for each threshold value assuming the location is abnormal. The location threshold is determined if either one of the probability functions has a small enough variance between two subsequent responses or if two reversals are achieved in the staircase.

Another accelerated thresholding algorithm used to reduce test time (developed for the Octopus 2000R) is Tendency-oriented perimetry (TOP). Each test location is assessed such that the subject's response at that location is used to assess not only sensitivity at that location but also to modify the current sensitivity estimate of neighbouring locations within the visual field. This results in each threshold estimate being based on one direct response and three indirect responses from neighbours.

Donahue et al. (2001)[28] investigated using the SITA algorithm as a means of visual field assessment on children by performing a retrospective review of all automated visual field assessments performed on children (17 years and younger) over a period of 16 months. The patient age range was from 73 to 227 months). In their ophthalmology department they originally used the Humphrey Field Analyser with the full threshold test (FTT), (i.e. no time saving algorithm used) and then converted to using SITA in 1999. They then also began using it on children as well as adults based on their experiences with the adults. They performed the 24-2 field test

which tests visual field sensitivity in 56 locations within the central 30° field. It was found that SITA reduced the test time by over 50% to an average of slightly over 6.5 minutes when compared with FTT. This study was focused on comparing experiences using SITA and FTT and was not designed to look at reliability in the younger aged children. However, it is interesting that this group have used ASP in children in the clinical setting, though it is clear that it is not performed on children below 6 years and there were few results from 6- to 8-year olds.

Another group looked at using an improved version of SITA (the SITA Fast algorithm) in children with prepubertal idiopathic intracranial hypertension.[58] 26 patients were included in the study ranging from 2 to 11 years. The youngest age patient able to perform the SITA Fast test was 4 years and it was reported that two patients (aged 4 and 5 years) were unable to perform the test. They found that the reliability of the tests was not dependent on age although stated that the small sample size could impact the results. It is not clear what test pattern was employed or how many of each age group performed the testing, and although it was concluded that SITA Fast testing can be performed from 4 years of age, it is clear that not every young child has the ability to perform this type of testing.

Two groups have looked at using TOP in children. Morales et al (2001)[20] performed visual field testing using the Octopus TOP-32 program on 50 normal children aged 6 to 12 years. They did not use any form of adaptations or familiarisation strategies and testing was performed in the normal clinical setting. All subjects successfully completed all tests leading them to conclude that TOP programs can be successfully performed on children as young as 6 years. However, in children aged 6 and 7 years there was significant inter-individual variability and testing success was more dependent on the child's maturity and ability to communicate. Morales et al. concluded that training and familiarisation to the test is needed before a real test is performed on children.

Brown et al. (2005)[29] performed visual field testing on 142 healthy children aged 6 to 13 years of age. The study was designed to gain normative threshold values in children of this age group and concluded that comparison against the programmed normal mean sensitivity values for 20-year-olds is appropriate but additionally found that both learning and fatigue effects were evident across the subject group and that the false positive response rate was high irrespective of the child's age. Additionally, the 6-year-old children showed high inter-subject variability and so were excluded.

Also recently, Wabbels et al. (2005)[59] reviewed the use of two new test strategies, Continuous Light Increment Perimetry (CLIP) and Fast Threshold (FT), in children in the standard clinical setting. CLIP is performed on a Twinfield perimeter. Stimulus intensity is increased incrementally (at a rate of 1 dB per patient reaction time) starting from a stimulus brightness 5 dB below the expected (age corrected) threshold value until the patient responds. The Fast threshold technique is a full threshold technique staircase strategy which uses threshold values

that have already been determined during the test to adjust the initial presentation brightness for neighbouring points which are yet to be tested. In this study 28 children aged 5 to 14 years were examined using these two techniques with a short teaching phase where a few stimuli were presented under test conditions. Testing reliability was highly dependent on age, maturity and ability to concentrate and reliable results could be obtained from many children upwards of 8 years of age. It was also found that testing using CLIP was easier than with the FT strategy as it can be quicker and produces less false-positive errors. However, many of their results were still found to be unreliable and further research was called for.

Akar et al (2008)[60] investigated which visual field testing strategies on the HFA were most appropriate for the paediatric population by assessment of false-positive, false-negative and fixation loss scores when using Fast-Pac (another form of time saving algorithm which uses a staircase strategy with 3dB steps and crosses threshold only once) and SITA Fast. Of 68 participants (aged 6-13 years) all but 8 participants successfully completed the tests. The children older than 8 years produced significantly higher test reliability scores, but SITA Fast seemed to be the more reliable method of visual field assessment and could be a promising strategy for visual field assessment in the paediatric population.

The key points and conclusions of the literature involving children and ASP are summarised in table 4.1. The use of familiarisation strategies can improve how well children are able to perform ASP and the introduction of new faster thresholding algorithms has no doubt pushed the boundary of the lower age limit for visual field testing. However, the introduction of familiarisation phases introduces longer testing sessions increasing the chances of fatigue which is also a reported problem when performing ASP in children. Despite the success of some of the research groups in performing threshold and suprathreshold ASP, the technique has not found its way to being used routinely for children in the clinic and is highly unlikely to be used in the younger children (younger than 6 years) because of the widely reported problems of compliance and variability. The normal drawbacks of ASP such as the need for continuous fixation on a central target is still the main problem with these ASP methods.

4.1.1.2 Kinetic perimetry

Manual kinetic perimetry such as Goldmann and double-arc perimetry (a form of kinetic perimetry with LEDs located on arcs which can be rotated) are among the methods which have been more popular techniques used to assess visual fields in children. This is because manual kinetic perimetry gives more control and freedom to the examiner. The examiner can provide a greater level of guidance and encouragement while continuously monitoring fixation, and tailor the test to the child's level of attention and comprehension. However, more recently these types of perimetry devices are being used less and less because the manual technique can introduce

Study	Subject details		Tests performed		Conclusions
	n	Age range (years)	Device	Strategy	
Safran[30] (1996)	42	5-8	Octopus 2000R	Custom two level. 12 points within central 15°	Children performed well. The detection of stimulus improved with age.
Tschopp (1998)[18] – Part 1	106	5-8	Octopus 2000R	Familiarisation phase then 15 identical tests consisting of 12 supra-threshold stimuli.	Children as young as 5 can undergo a form of ASP. Reliability and endurance increased significantly with age.
Tschopp[56] (1998) – Part 2	118	5-8	Octopus 2000R	Familiarisation phase then 3 threshold tests to build up a 76 point visual field exam.	Threshold values for 5- and 6- year olds was not as reliable. 7- and 8- year olds were able to provide reliable normative threshold values.
Donahue[28] (2001)	24	6-18	HFA	SITA 24-2 (threshold test)	SITA shortens test time significantly.
Stiebel-Kalish[58] (2004)	26	2-11	HFA	SITA 24-2 (threshold test)	Can be performed at 4 years old.
Morales[20] (2001)	50	6-12	Octopus 1-2-3	TOP-32 (threshold test)	Successfully performed on as low as 6 years. Most reliable results obtained after 7 years.
Brown[29] (2005)	142	6-13	Octopus 1-2-3	TOP-32 (threshold test)	6 year old results excluded due to high inter-subject variability.
Wabbels[59] (2005)	28	5-14	Twinfield perimeter	CLIP and FT	Test performance dependent on age, maturity and ability to communicate. CLIP was easier than FT (especially in those younger than 8 years)
Akar[60] (2008)	68	6-13	HFA	Fast-Pac and SITA Fast	The children older than 8 years produced significantly higher test reliability scores. SITA Fast seemed to be the more reliable method of visual field assessment.

Table 4.1: Summary of literature involving children and Automated Static Perimetry (ASP).

examiner bias and is dependent upon the examiner's skills and knowledge.[23] Test data does also not provide quantitative information for serial comparison.

There are few publications in the recent literature exploring the lower limits of age when using the manual kinetic approach. Instead, studies have either used the method of kinetic perimetry for investigating specific visual field defects in children because it is the most appropriate method for doing so. For example studying the type of field defects present in paediatric glaucoma[12], children who received cryotherapy as infants[61], or those treated with Vigabatrin[62–64] or for examining normative values of the visual field in children[21,22]. These studies have predominantly used Goldmann Kinetic Perimetry and while the youngest age tested was 4 years, most studies did not attempt testing in children as young as this opting to test 6 years and above only.

Studies which have involved even younger children have predominantly used the double-arc perimeter.[65–70] These studies were concerned with measuring the extent of the visual field only. However, the technique could be performed in the very young (infants).

One study has looked at the use of more recent automated kinetic perimetry in children to overcome the problems of examiner bias.[71] They found that children as young as 5 years could be reliably tested.

Both the ASP and manual kinetic perimetry methods still suffer from the same problems when looking to examine the visual field in young children, in that they both require the need for continuous fixation on a central target and high levels of concentration and endurance. As such there is a distinct lack of perimetry testing in children below the age of 5 using these methods even in research, and these are the main reasons why these methods have never been widely introduced into paediatric clinical practice.

4.1.2 Recent "computer graphics" perimetry techniques

Several newer methods of perimetry which use a personal computer and a liquid crystal display (LCD) screen along with techniques which differ from the classical differential light sense measurements, i.e. estimates of simple achromatic contrast thresholds, have emerged in recent years. These can loosely be termed "computer graphics" perimetry techniques and each has its own advantages which has led to the plausibility of using it in children or for exploring a particular paediatric disease. As a result these "computer graphics" perimetry techniques have been investigated for use with children. Each of the techniques and their use in children is reviewed here in sections corresponding to each perimetry technique.

4.1.2.1 Rarebit perimetry

In recent years, new methods of perimetry that use a personal computer with LCD screens have emerged. Once such method is rarebit perimetry. The conventional "white-on-white" perimetry, that is where white light stimuli are projected onto a white background screen, has been shown to have poor sensitivity to early neural damage in glaucoma.[72,73] One possible contributing factor to this effect is that test targets are relatively large and so will be assessing many overlapping visual receptors. Rarebit perimetry was developed in order to overcome this issue.[74] The test presents tiny light stimuli ("rare bits" or also referred to as "microdots") half the normal minimum angle of resolution. The microdots are presented in test areas (a total of 30 areas each 5 degrees in diameter) within the central 30 degrees of visual field. In each test area two dots are shown at a time and the patient must report if they see none, one or two microdots. Microdots are shown at different locations 5 times within each test area resulting in 10 microdots for each test area. Rarebit perimetry does not return threshold values, but rather, returns a hit/miss rate for each test area. A normal subject should return close to a 100% hit-rate implying that the visual neural architecture is complete, whereas in disease, loss of connections of retinal ganglion cells or disconnection further along the visual pathways results in a lower hit-rate. It is designed to enable the detection of mild visual functional damage and so is useful in early detection of glaucoma.

Martin (2005)[75] investigated the use of rarebit perimetry in children and adults. In addition to rarebit perimetry, frequency doubling perimetry was also investigated on the same group of participants but will be discussed separately in the next section "frequency doubling technology perimetry". There were 21 healthy children included in the study with an age range of 6.5 to 12 years and it was found that reliable results were obtained using rarebit perimetry in 76% of the children. There was a significant correlation between age and fixation errors and it was concluded that the test was suitable for children aged 7 years and older. A disadvantage of rarebit perimetry is the high false positive response rate which reduces the reliability of the test. Moreover, subjects need to possess fairly sophisticated motor skills to respond to the test appropriately (i.e. single or double button presses to indicate the number of microdots seen). However Martin found that rarebit perimetry was popular amongst many of the children due to its similarities to a computer game and does not require the subject to place their head in an immersive bowl screen but does use a chin rest.

Martin et al. (2007)[76] again investigated the use of rarebit perimetry in children. Fifteen children aged 6-15 years with paediatric glaucoma, and 15 age and sex matched healthy children performed rarebit perimetry and were also examined by Goldmann manual kinetic perimetry. All children in the control group showed a normal hit-rate with rarebit perimetry. 8 eyes from the paediatric glaucoma group were found to have a normal rarebit hit-rate compared with

15 eyes found to be normal using Goldmann Kinetic Perimetry. It was concluded that rarebit perimetry was able to detect glaucomatous damage in various types of paediatric glaucoma among children as young as 6 years.

4.1.2.2 Frequency doubling technology perimetry

Frequency doubling technology (FDT) perimetry is a technique also developed fairly recently.[77–79] Frequency doubling refers to a perceptual effect seen when an achromatic sinusoidal grating of low spatial frequency (less than 3 cycles per degree) undergoes counterphase flickering at a high temporal frequency (larger than 7Hz), the apparent spatial frequency of the grating appears to be doubled.[80,81] FDT perimetry does not require a judgement on behalf of the patients as to whether doubling is present, rather FDT simply measures grating contrast detection thresholds for sinusoidal stimuli that fall within the frequency-doubling range. This is a technique which has shown promise for detection of glaucomatous visual field loss in adults[82] and has now more recently been used in several studies to investigate its usage in children because it can have a shorter test time than ASP (less than 6 minutes per eye), uses a larger stimulus target, has tolerance to relatively large refractive errors and consists of a more convenient office setup. The most notable advantage of FDT that is relevant in children is that the fixation target appears to move and this attracts the child's attention more effectively. The children's head is placed on a visor in front of an LCD screen and not in a bowl which can cause some children to feel claustrophobic. Several studies have looked into how reliable FDT perimetry is in children, as follows:

Becker et al. (2003)[83] aimed to determine if children could complete a screening program of FDT perimetry reliably. 259 normal children (mean age 10.7 years, range 4-17 years) were recruited to perform a FDT screening test and results were analysed for reliability using the false positive error and fixation loss counts and also the detection of visual field defects. False positive errors were below 1 among all groups except the youngest (4 year-olds) and fixation errors decreased as age increased. It was concluded that children aged 10 years and older can reliably complete the FDT screening test.

Nesher et al. (2004)[84] also tested the feasibility of FDT perimetry in children. 40 Children aged 5 to 10 years were recruited to perform the C20 threshold test on the Carl Zeiss Meditec FDT analyser in both eyes. In contrast to Becker et al. it was found that test reliability was similar between children aged 5 to 7 years and those aged 8 to 10 years, possibly due to the more stringent reliability criteria used by Becker et al.

Blumenthal et al. (2004)[19] recruited 40 children aged 4 -14 years to also complete the C20 threshold test. Two consecutive tests were performed on one randomly chosen eye and the better of the two examinations (as indicated by mean deviation from normal threshold levels)

was used for analysis of reliability indices which again included fixation losses, and false positive and false negative errors. In addition global indices of mean deviation (MD) and pattern standard deviation (PSD) were recorded and used as an assessment of reliability. MD and PSD are values which show how much the whole field departs from what is expected to be normal. At younger than 8 years of age, 43% of the visual field tests were considered unreliable, compared with 23% from children over the age of 8 years. Again, reliability as measured by the reliability indices and MD were found to be highly correlated with an increase in age.

Martin (2005)[75] investigated the use of FDT perimetry (and also rarebit perimetry as described in the previous section) in children and adults. There were 21 healthy children aged 12 years or younger included in the study with the youngest being 6.5 years. Also included in the study were 30 teenagers and young adults (aged 14 to 20 years). Participants performed two types of FDT tests: (i) a screening program (C-20-5), and (ii) a threshold program (N-30). 57% of the children in the younger group produced reliable test results for the C-20-5 screening test according to the criteria, defined by the manufacturer, of less than 30% erroneous responses as measured by both fixation losses and false positives. However, all of the unreliable results in this group were as a result of fixation errors and if the more strict criteria defined by Becker et al was used,[83] only 3 of the 21 children (14%) were able to produce reliable test results. The reliability was vastly improved when considering the older group where 95% produced reliable results. 57% of the younger group also produced reliable results when performing the FDT N-30 threshold program, and 90% of the older group produced reliable results for the N-30 threshold test (when using the manufacturer reliability guidelines). The group had concluded that children could reliably perform RB perimetry from 7 years of age. However, the children found FDT perimetry more difficult to perform and the majority (88% of all participants) preferred RB perimetry to FDT perimetry.

Most recently Quinn et al. (2006)[85] aimed to test visual field thresholds of normal children using FDT. They assessed testing times, fixation losses and MD with respect to age and used test results to produce some normative paediatric threshold data for FDT perimetry. Ninety four children (aged 5 to 17 years) participated in the study and were asked to perform a screening test lasting approximately 1 minute (as a "practice" test), before performing threshold testing in each eye with a break as appropriate. 9% of the children were deemed too unreliable at performing the screening test to proceed with the threshold testing. These children amounted to 21% of the total number of 5- to 9-year-olds. Testing time decreased with increasing age (from approximately 7.5 minutes for the youngest children) as did fixation losses although with some amount of variability in each age group. MD increased significantly with age (up to the age of 14 years, where normal adult values were obtained).

4.1.2.3 High pass resolution perimetry

High pass resolution (HPR) perimetry (also known as ring perimetry) is another form of perimetry using a standard computer display screen. It was developed as a method for providing an estimate of retinal ganglion cell density.[86,87] HPR uses ring shaped, spatially high-pass filtered targets to determine resolution over the central 30 degrees of the visual field. The perimeter determines resolution thresholds (the smallest ring able to be seen) for 50 locations. The pace of the HPR test alters to the current reaction time of the subject. However, HPR still requires the need for a continuous fixation on a central target during the test. HPR has been found to be useful in the detection of visual field loss due to glaucoma and is a reasonably rapid test (lasting approximately five minutes), and is well tolerated by patients.[88]

Marraffa et al. (1995)[89] conducted a study involving 15 children (mean age 8.7 years, ranging from 6 to 11 years) affected by congenital glaucoma to discover which of two perimetry techniques, HPR and static computerised perimetry (using the Humphrey field analyser), were most suitable for these younger patients. They concluded that HPR perimetry was more suitable for children because of the shorter test time and following a questionnaire it was found that many of the children liked the HPR task more as they found it easier and it appeared similar to a game (in comparison to the Humphrey test). Tests were performed twice in order to measure reproducibility. Two tests (of the same type) were considered reproducible if they showed the same defect with an averaged threshold of no greater than $\pm 2dB$. The Humphrey test proved reproducible in 47% of eyes tested while the HPR test was reproducible in 68% of the eyes tested (this was without statistical significance).

4.1.2.4 Multifocal visual evoked potential

Visual evoked potentials (VEP), recorded using electroencephalography (EEG), are caused by sensory stimulation of the visual field. Advancements in electrophysiology have made it possible to evaluate the visual field by assessing a collection of VEP (multifocal VEP perimetry).[90] Multiple locations of the visual field are simultaneously stimulated using a cortically scaled (in a dart board type pattern) pseudo-randomly black and white reversing pattern stimulus and VEPs corresponding to each visual field location can be recorded and analysed for amplitude where a reduced signal amplitude has been shown to correlate with visual field defect.[91] Multifocal VEP in its current form requires little cooperation from the patient, is not dependent on subjective responses and has a short test time (approximately 4 minutes per eye). Because of these features, several groups have investigated using multifocal VEP in children.

Harding et al (2002)[92] aimed to develop a field-specific VEP technique for identifying visual field defects in epileptic children being treated with Vigabatrin who were unable to perform other types of perimetry. A VEP "test stimulus" was specifically developed for detecting the

visual field losses associate with the drug which used a central (0-5 degrees) stimulus and peripheral (30-60 degrees) stimulus consisting of black and white checks increasing in size with eccentricity. They enrolled 39 children (3 to 15 years) with epilepsy who were being treated with Vigabatrin (for at least 3 months) and performed their field-specific VEP test and also, where possible, they undertook formal static perimetry using the Humphrey field analyser 135-point suprathreshold test to determine the diagnostic performance of the field-specific VEP test using the Humphrey as a "gold standard" test. Of the 39 children, 35 were able to comply with the field-specific VEP test but only 12 were able to comply with the static perimetry. The mean age of the children able to complete both was 12.2 years (range: 8-15 years). Results from these 12 patients gave good sensitivity (75%) and specificity (87.5%) values for the field-specific VEP test using comparison with the "gold standard" Humphrey test. It was concluded that the test was well tolerated by children aged 3 years and older and is reliable at detecting Vigabatrin associated visual field loss. This study highlights the lack of a good "gold standard" perimetry technique in young children. Other studies have also found multifocal VEP to be useful for monitoring the visual field in epileptic children taking vigabatrin.[10,93]

Balachandran et al. (2004)[94] aimed to study the maturation of multifocal VEP in normal children and to apply the normative results to determine visual field loss using multifocal VEP in three clinical situations of optic pathway diseases. Normative VEP data (amplitude and latency) was recorded from 70 children (aged 5-16 years) and it was found that a scaled amplitude remained largely unchanged until 11 years where there was a sudden increase (40%) until the age of 13 years and remained stable thereafter. Latency was found to decrease gradually with age and plateau at 13 years. This data was then used to make an aged matched comparison with three children with advanced optic nerve disease where results correlated well with existing clinical findings. It was concluded that multifocal VEP is a test that can be performed by children as young as 5 years and one which holds promise in being able to diagnose and monitor visual field defects in children.

Kelly (2006)[95] more recently looked at comparing pattern VEP to perimetry as a method of detecting visual field loss in children with optic pathway gliomas. 40 patients with optic pathway gliomas were recruited to perform VEP testing. 15 of the patients (8-20 yrs) were also able to perform visual field testing using Goldmann Kinetic Perimetry and four of those 15 additionally performed ASP (SITA Fast). In those who performed both VEP and a form of comparative perimetry, VEP amplitudes were significantly reduced at the midline electrode in all eyes with visual field loss leading the authors to conclude that VEP may be a viable alternative in children that are intolerant to standard visual field testing who have visual field loss due to optic pathway gliomas.

Kim et al. (2006)[96] assessed the use of mVEP tests to measure the visual field in epileptic children 6-15 yrs. They collected normative mVEP measurement data from 21 healthy chil-

dren and used normative latency and peak amplitude measurements to compare with mVEP measurements made from 3 patients with epilepsy in whom standard perimetry testing was not possible (aged 5-8 yrs). In each of the three patients abnormal waves measured by mVEP were detected in the quadrants corresponding to lesion sites demonstrated by neuroradialogical images and it was concluded that mVEP was useful in evaluating visual field defects in these children.

4.1.2.5 Multi fixation perimetry

In order to solve the problem of fixation loss errors in static perimetry, one group has previously developed a novel form of perimetry which uses a moving fixation target. The idea was first described by Damato in 1985[97] where a simple method of perimetrytermed "oculokinetic perimetry" was described which used a paper test chart where the subject looks at 100 locations on the chart in turn and records if they are able to see a central point on the chart each time. The points are strategically placed so as to produce a map of the patient's visual field when the completed chart is rotated by 180 degrees. The test was designed to be a simple and very low-cost method of self-test perimetry, but the idea was later extended in an effort to improve perimetry testing in children.[16] The same research group developed the idea to run automatically on a computer, where this time the fixation target moved across a display screen and the subject must move a circle using a mouse or joystick in order to maintain it over the fixation target while it moves across the screen. "Test stimuli" are displayed only when the circle is correctly positioned over the fixation target, and the subject must respond to seeing the "test stimuli" by pressing a button. Children enjoyed the game-like nature of the developed test and the youngest child able to perform the test was 4 years of age.

The technique was later developed into a system named the computer assisted moving eye campimeter (CAMEC) and was used in children by Mutlukan et al (1993).[15] 32 children were examined using blind spot test programs of CAMEC and a commercial device (Dicon auto-perimeter). Among those who completed both tests the blind spot was detected in 75% of eyes tested by the Dicon auto-perimeter and 100% of eyes using CAMEC leading the authors to conclude that fixation was greatly improved using CAMEC and therefore allows better quantification of scotomas and the test is suitable for children aged more than 4 years.

4.1.3 Summary of perimetry in children literature

ASP is known to be unreliable in children and many previous research efforts have concentrated on investigating ways to improve the lower age limit of children able to perform ASP. These have been based around familiarisation strategies and use of faster testing strategies as they have become available. A summary of this literature is shown in table 4.1. The youngest aged

Study	Subject details		Tests performed		Conclusions
	n	Age range (years)	Technique	Strategy	
Martin[75] (2005)	21	6.5-12	Rarebit	Version 3.0	Significant correlation between age and fixation errors. Test is suitable for children aged 7 years and older.
Martin[76] (2007)	30	6-15	Rarebit	Version 3.0	Rarebit perimetry able to detect glaucomatous damage in various types of paediatric glaucoma among children as young as 6 years
Becker[83] (2003)	259	4-17	FDT	Screening test	Children aged 10 years and older can reliably complete the FDT screening test
Nesher[84] (2004)	40	5-10	FDT	C20 threshold test. Carl Zeiss Meditec FDT analyser	Test reliability was similar between children aged 5 to 7 years and those aged 8 to 10 years
Blumenthal[19] (2004)	40	4-14	FDT	C20 threshold test. Carl Zeiss Meditec FDT analyser	reliability highly correlated with an increase in age. At younger than 8 years of age, 43% of the visual field tests were considered unreliable.
Martin[75] (2005)	21	6.5-12	FDT	First a screening program (C-20-5) and then a threshold program (N-30)	All unreliable results were as a result of fixation errors. Using criteria defined by Becker et al.[83] Only 14% were able to produce reliable test results.
Quinn[85] (2006)	94	5-17	FDT	N-30-5 screening program 30-2. ZEST threshold program	fixation losses decreased with increasing age. 21% of the total number of 5- to 9-year-olds unable to do screening test
Marraffa[89] (1995)	15	6-11	HPR	Ring test	HPR perimetry more suitable than ASP for children
Harding[92] (2002)	39	3-15	Multifocal VEP	Vigabatrin field specific test	Test was well tolerated by children 3 years and older and is reliable at detecting Vigabatrin associated field loss.
Balachandran[94] (2004)	70	5-16	Multifocal VEP	Collected normative VEP data	Normative data was used to make age matched comparison in three children with optic nerve disease. Results correlated well with existing clinical findings.
Kelly[95] (2006)	15	8-20	VEP	Patients with optic pathway gliomas had VEP recording compared with those of control subjects	Reduced amplitude and signal-to-noise ratio in VEP recordings was a good indicator of visual field defect.
Kim[96] (2006)	3	5-8	VEP	Latency and peak amplitude of VEP in epilepsy patients were compared with normative recordings	Abnormal VEP waves were measured in visual field quadrants which corresponded with the lesion sites demonstrated by neurological imaging.

Table 4.2: Summary of literature involving children and perimetry techniques other than automated static perimetry (ASP) and kinetic perimetry.

children still able to produce reliable results are about 7-8 years of age. Given the nature of ASP it is impressive that threshold visual field testing has been reliably performed in children as young as this in some of the studies reviewed. However, the technique of ASP is still not routinely used in children of this age clinically, perhaps because of the length of time required to appropriately train them in the task.

In addition to these reported "youngest age" studies, other studies in the literature have used the ASP technique to assess the visual fields in children as part of research looking at other clinical aspects.[98–103]. However, these studies generally have not included children younger than 10 years of age, presumably for the very reason that reliability is a problem.

Goldman kinetic perimetry is a more popular method of perimetry in children as the test can be controlled by the examiner and adapted to the developmental age of the child. However, there are significant disadvantages with this technique as it is dependent on a trained skilled examiner. Both the ASP and kinetic perimetry methods still suffer from the same problems. They both require the need for continuous fixation on a central target and high levels of concentration and endurance. As such there is a distinct lack of perimetry testing in children below the age of 5 using these methods and these are the main reasons why these methods have never been widely introduced in to young paediatric clinical practice.

Researchers have also assessed the use of other "computer graphics" perimetry techniques with children, as they have emerged. A summary of the studies carried out using these techniques with children is shown in table 4.2. The youngest age at which these techniques can be reliably carried out by children varied depending on the reliability criteria used and the type of tests being carried out. However, almost all studies reported a correlation with reliability indices (predominantly fixation errors) and increasing age, and each of these tests still requires central fixation, stationary head position and most importantly an understanding of the task required to perform the tests reliably.

Multifocal visual evoked potentials have shown some promise in detecting visual field defects in children because of the quicker nature of the test and more importantly the lack of any subjective response from the patient. From the literature, the youngest ages able to carry out some form of multifocal VEP has been from 3 to 5 years and it has been found to be useful for monitoring the visual field in epileptic children taking vigabatrin. However, the technique still requires a stationary head position, constant central fixation and also requires the patient to wear electrodes. Additionally the waveforms of VEP traces can vary even for normal subjects meaning that it can be difficult to interpret them as objective evidence for visual field defects.[104,105] Improvements have been made in multifocal VEP recording and analysis. However, the technique has not been widely taken up.

Multi fixation perimetry has previously proved useful at assessing the visual field in young chil-

dren (older than 4 years) after reducing the problem of fixation errors. This form of perimetry still requires a subjective response from the subject in the form of pressing a button and suppression of the natural gaze response of looking towards peripheral stimuli when seen as well as a stationary head position which greatly inhibits using this technique with younger children.

There are virtually no commonly used perimetry techniques which are suitable for children younger than approximately 8 years of age and there exists no form of perimetry which is able to describe the visual field in a more accurate manner than confrontation in children younger than 3 years old. Most of the research efforts described in this review do not address the fundamental problems inherent in performing perimetry on children and it is a new, child friendly technique which overcomes these issues, that is required.

A novel technique and system for assessment of visual fields in children has therefore been developed and is the basis of this research thesis.[31] The system makes use of relatively new advances in eye tracking technology and is more suitable for use with children. The Technique and system, named "saccadic vector optokinetic perimetry" (SVOP), builds on original ideas by Damato et al. who first developed the idea of oculokinetic perimetry where the point of fixation varies during a perimetry test.[97,106] SVOP comprises a personal computer, display screen, an eye-tracking device (Tobii x50, Tobii Technology, Danderyd, Sweden), and software developed under this research program that controls the eye-tracking device, displays visual stimuli on the display screen, and interprets eye gaze responses in "real time".

A thorough search of the literature as to the novelty of using eye tracking to assist with perimetry produced two articles from the proceedings of "Vision 2005", both from the same research group.[107,108] The work included the collection of some basic early data on the possibility of using saccade as an index for visual field measurement and it was concluded that an objective measurement of visual fields is possible using the measurement of saccades in response to visual stimuli. However, since these articles there has been no further work published.

4.2 Research proposal and aims

Given the problems that arise in the methods of perimetry used in children, a proposal for a new method of perimetry for children is described here. Saccadic vector optokinetic perimetry (SVOP) detects a child's saccadic eye movement when a stimulus is presented in the periphery of their visual field. The only task required of the child is to follow their natural reaction to fixate on the stimulus of interest if they see it.

SVOP does not require any cooperation or understanding from the child. The child is not required to learn any task nor to give any subjective response. When subjective responses from the child are not used in the mapping of visual field, this removes the need for vigilance,

endurance or understanding of the test method on the part of the child. SVOP does not restrict the child's movement (headrest not needed) and does not form any physical contact with the child (e.g. no electrodes). A continuous fixation on a stationary central fixation target is not needed in the proposed test.

There are two main stages to this research: (i) the development of the technique and system of SVOP for assessment of visual fields in children, and (ii) an assessment of the validity of the developed system as a diagnostic tool for visual field assessment. The aims associated with each stage of the research are outlined below.

(i) Development of the technique and system of SVOP for assessment of visual fields in children. The aims are to:

- develop the theory of operation of SVOP based on current eye tracking technology;
- assess eye tracking equipment suitable for developing SVOP;
- develop the algorithm which will assess patient eye gaze reactions to visual stimuli;
- create a suitable full SVOP system (hardware and software); and
- conduct a feasibility trial using the developed SVOP system.

(ii) Assessment of the validity of the developed system as a diagnostic tool for visual field assessment. The aims are to:

- conduct a "validation trial" of the developed SVOP system using large number (n=120+) of healthy volunteer children and adults, and child and adult patients with visual field defects;
- compare the SVOP test with an equivalent test on an established perimeter, and compare SVOP test results with patient clinical diagnosis and history in the cases where an equivalent clinical visual field assessment is not possible or is inaccurate; and
- assess the variability of tests performed in the "validation trial".

Chapter 5

System development and feasibility

5.1 Theory of operation

5.1.1 Hardware and system setup

5.1.1.1 Eye tracking devicerequirements and specifications

The eye tracker must be non-contact, unobtrusive, allow freedom of head movement and be able to provide data in "real time". For these purposes "real time" can be considered a sample rate of 30 Hz or greater. In addition, the two most important specifications are those related to (i) the point of gaze data, and (ii) the 3D eye location data provided by the eye tracker. A set of minimum requirements for the range, accuracy and resolution for each of these two specifications are set out in table 5.1 and the reasoning is further discussed in the following paragraphs.

	Gaze data	3D eye location data
Range	Horizontal: ±15° Vertical: 30°(above the eye tracker)	Eye location volume: 200 x 100 x 200mm (Width x Height x Depth with respect to the eye tracker location)
Accuracy	±2.5°	$\pm 20mm$
Resolution	1.5°	$5mm$

Table 5.1: The minimum requirements for the range, accuracy and resolution of the eye tracker characteristics of "gaze" and "3D eye location" data.

Gaze data requirements

The range of the gaze data is the largest gaze angle which an eye tracker is able to assess. The proposed SVOP system must be able to assess the first ±30° of the visual field. The eye tracker

will be located centrally, directly beneath a display screen which will present the visual stimuli. Because the point of fixation will not be kept at the same central location, this reduces the minimum horizontal range required to $\pm 15^\circ$ (e.g. to assess a visual field angle of 30° to the right, fixation could be stationed at a location corresponding to 15° to the left of centre and a test point could be located 15° to the right of centre) . However, the minimum required vertical range must be $+30^\circ$ due to the fact that the eye tracker will be positioned below the display screen.

The gaze data will be used to determine: (i) if a subject is looking at a "fixation stimulus", and (ii) if and when a subject changes their fixation point in response to the presentation of a visual field "test stimulus". The accuracy of the gaze data required for the proposed system needs only to be within $\pm 2.5^\circ$. This is because at all stages the screen location of any visual stimuli will be known, and also because there will only ever be a single visual stimuli on the screen at any particular time. What is perhaps more important is the precision of the gaze data when a subject has their fixation in one location. So long as the precision is to within approximately 1.5°, then it can be inferred that the subject is maintaining fixation at a known "fixation stimulus" location. In addition, a change in fixation can be detected as a difference between successive gaze data samples of greater than 1.5°.

The resolution of the gazed data must simply be equal to or less than the required precision of the gaze data.

3D eye location data requirements

The range of the 3D eye location data is essentially the volume of head movement allowance the eye tracker will tolerate. Clearly the larger this is the better because the proposed SVOP system is to be used with children who are potentially likely to move about. However, if a child can be captivated by the testing procedure, then a relatively small volume would suffice. A subject's head is less likely to move up/down as compared to left/right and forward/back (relative to the eye tracker position). Given these reasons, a minimum head movement box size of 200mm x 100mm x 200mm (Width x Height x Depth relative to the eye tracker) is required.

Both accuracy and precision of the 3D eye location data are important because this data will be used to calculate the position of "test stimuli" on the display screen. An error in this data will result in an error in the screen position of specific visual field test points. A detailed assessment of the effects of error in the 3D eye location is performed in section 5.5. Here it is sufficient to say that the accuracy of this data should be within +/- 20mm to enable accurate positioning of visual field test stimuli.

The requirements for the resolution of the 3D eye location data again relate to the required

precision. A precision of within 5mm is required so as not to induce further errors in the "test stimuli" screen locations calculated.

The reasoning behind these minimum requirements may become clearer as the theory and details of the proposed SVOP system are explained in the remainder of this "development" chapter. However, it is important to provide a set of parameters here in advance of discussing the eye tracker devices which are considered for this research.

At the commencement of this research project, non-contact, unobtrusive eye tracking devices requiring no head or eye mounted equipment were beginning to become more commercially available. Four of these commercially available devices were considered for their suitability in this research. The four eye trackers were the Tobii x50 [Tobii Technology, Karlsrovägen 2D, S-182 53 Danderyd, Sweden], SMI iView X- RED [SensoMotoric Instruments GmbH, Teltow, Germany], ASL R6 [S. Oliver Associates, Northumberland House, Popes Lane, London W5 4NG, UK], Seeing Machines FaceLab 4 [GPO Box 782, Canberra ACT 2601, Australia]. The main specifications and characteristics of each eye tracker (provided by the manufacturers) are shown in table 5.2.

Specific to this project, there were several considerations to take into account when selecting the eye tracking device to be used for developing a visual field assessment system for children.These considerations are outlined below and are based on the specifications provided by the eye tracker manufacturers.

Eye position

The position of the eyes must be known in real time if the subjects are allowed freedom to move. In order to assess specific visual field angles during a test, the position of the eyes must be known, so that each stimulus can be presented in the correct position. Each of the eye tracking systems considered is able to provide data on the position of each eye in real time. However, for the SMI iView X- RED and ASL R6 this requires the use of a magnetic head tracking (MHT) device which requires the subject to wear a magnetic headband. There are no details given regarding the accuracy of the eye position data and this information will be determined experimentally (the methods and results relating to this are in section 5.2.2).

Freedom of head movement

Each of the eye trackers offer similar ability to allow head movement, and can all meet the minimum requirements of 200 x 100 x 200mm (Width x Height x Depth). The Seeing Machines FaceLab 4 has two modes: "classic" and "precision". The classic mode allows more head movement at the cost of eye gaze data accuracy. However, for movement to be possible with the SMI device and the ASL R6, it was advisable to use MHT.

Specification	Tobii x50	SMI iView X-RED	ASL R6	Seeing Machines FaceLab 4
				
Eye tracking technique	Pupil/Corneal reflection	Pupil/Corneal reflection	Pupil/Corneal reflection	Stereo camera pair
Moving parts?	No	Yes (pans and tilts)	Yes (pans and tilts)	No
Ability to track custom display	Yes	Yes	Yes	Yes
Head movement allowance	20 x 15 x 32cm (W x H x D at 60cm from tracker)	Preferably still (without magnetic tracking)	1 sq foot	Classic: 30 x 20 x 60 (W x H x D) Precision: 25 x 15 x 30 (W x H x D)
Sample Rates	50Hz	50 – 60Hz	50 – 60Hz	60Hz
Accuracy	0.5-0.7 degrees	0.5 - 1 degrees	0.5 degrees	Classic: +/- 5° rotational error Precision: within 1° rotational error
Resolution	0.35 degrees	0.1 degrees	0.25 degrees	1 degree
Distance of optics to eye	45 - 75cm	40 - 100 cm	Up to 100cm	Classic: 0.5 – 1.1m Precision: 0.5 – 0.8m
Max Gaze Angle	+/- 35 degrees (H) +/- 35 Degrees (V)	+/- 30 degrees (H) +/- 25 Degrees (V)	+/- 25 degrees (H) +/- 20 Degrees (V)	Gaze rotations of +/- 45 degrees
Applicable raw data available	Time. Gaze position for each eye (x & y). Position of each eye (x & y). Camera to eye distance. Pupil size. Validity code.	Time. x and y eye gaze position coordinates. Pupil diameter	x & y eye gaze position coordinates. Pupil diameter.	Eye position. Eye rotation. Eye gaze position against screen. Pupil diameter.

Table 5.2: The four eye tracking systems considered and their main specifications and characteristics.

Gaze accuracy

According to the specifications, the accuracy of each of the eye tracking devices is within 1° (with the exception of the "Classic" mode offered by the Seeing Machines FaceLab 4, which has less accuracy at ±5°),meaning that they would all meet the gaze accuracy requirements of ±2.5°.

Maximum gaze angle (range)

The maximum gaze angle that the eye tracker is able to detect will be a factor in the maximum visual field angle which could potentially be assessed. The range of maximum gaze angles which the 4 eye trackers are capable of is ±35° to ±45° (horizontally) and ±25° to ±45° (vertically). The FaceLab 4 is capable of the largest gaze angles but does not offer the greatest gaze accuracy or resolution. All four eye trackers provide horizontal gaze ranges greater than the required ±15°. The requirement of 30° vertical range in gaze angle is only met by the Tobii x50 and the FaceLab 4.

Conspicuousness

The eye tracking device needs to be discreet so as not to attract the attention of any "inquisitive" children. Neither the Tobii x50 nor Seeing Machines FaceLab 4 has any moving parts, unlike the other two eye tracking devices which pan and tilt to follow the subject's eyes. These moving systems have the potential to distract the attention of a child during an examination of their visual field.

Subject constraints

There is to be no constraints placed on the subject, i.e. there must not be any head mounted equipment. This is true for all the systems considered. However, the SMI iView X- RED and ASL R6 also require MHT if the position of the head is to be known. As head position data is essential and there are planed to be no constraints placed on the subject, these two eye tracking systems were not considered.

Raw data and software development

It is essential that the chosen eye tracking device is able to provide real time gaze and eye position data. The Tobii x50 and Seeing Machines FaceLab 4 are able to do this without the use of additional head mounted equipment. In addition the Tobii x50 comes with a software development kit (SDK) which allows control of the eye tracking device through any desired programming software. This is an important requirement of the eye tracking device if the perimetry system is to be comprised within our own software.

Summary and suitability of Tobii x50 eye tracker

Considering the specifications and characteristics important for this research of each of these eye trackers, it became clear that the Tobii x50 eye tracker was the most suitable. The Tobii

x50 eye tracker is an eye tracker which uses infrared (IR) light and does not move (i.e. pan or tilt) to maintain contact with a subject's eyes as the camera has a relatively large field of view. These features make the x50 eye tracker unobtrusive and discrete, which are important factors considering the device will be used with children. Additionally, the x50 allows some freedom of head movement (as it uses the pupil/corneal reflection technique described in section 3.2.2.2) within the camera field of view, meaning that head restrictions do not need to be imposed on the subject. Because the x50 eye tracker has allowance for an amount of head movement, it also is able to provide "real time" data which allows the calculation of three dimensional eye position which is measured using an optical technique rather than requiring any additional head tracking equipment. The x50 can be used with a custom chosen display screen by defining the size and relative position of the display to the eye tracker. It has also previously been used with children (for research purposes other than perimetry) and additionally allows control of the eye tracker through development of custom software through the use of the SDK.

5.1.1.2 Display screen requirements and specification

Display screen size is an important aspect of the visual field assessment system developed in this research because the screen size (along with the maximum visual angle which the eye tracker can tolerate) ultimately dictates the maximum size of the visual field which can be assessed using the proposed SVOP system. The vast majority of visual field assessment tests carried out clinically concentrate on the central 30°. This is because the most common reasons for assessing the visual field are due to glaucoma and neurological diseases which can both be diagnosed effectively with information about the first 30° of visual field.[109–111] Additionally, the Humphrey Field Analyser has a suprathreshold test pattern (C-40 test pattern) with a maximum visual field angle of 25°, and also a threshold test pattern which contains test points within the central 30° which is one of the most commonly used test patterns for threshold testing, namely the 24-2 test pattern which has maximum visual field angle of 27°. With these test patterns in mind, a display screen size was selected which would enable the replication of the C-40 test pattern for comparative studies in this research, and also with future development in mind the replication of the threshold 24-2 test pattern. These values also fall within the maximum visual angle which the Tobii x50 eye tracker is able detect.

The largest visual field angle which can feasibly be used with any particular size display screen depends upon the screen dimensions and how far away the subject's "test eye" is. From figure 5.1, the maximum visual field angle possible (ϕ_H and ϕ_V, horizontal and vertical angles respectively) for any particular display screen size can be calculated from:

$$\tan\left(\frac{\phi_H}{2}\right) = \frac{w}{2D}$$

Similarly:

$$\tan\left(\frac{\phi_V}{2}\right) = \frac{h}{2D}$$

where ϕ_H is the maximum visual angle in a horizontal direction, ϕ_V is the maximum visual angle in a vertical direction, w is the screen width, h is the screen height and D is the screen to eye distance, where:

$$D = L \sin \varepsilon$$

Where ε is the angle which the eye tracker's camera makes with the vertical. ε is adjusted such that with the subject's eyes at a distance L from the camera, they are also positioned centrally (vertically) in front of the display screen (so ε is also dependent upon the screen size).

From these equations, for a standard 20 inch display screen which has the dimensions w=435mm and h=274mm, $\varepsilon =\sim 70°$ and the screen would be able to display a maximum horizontal visual field angle of $\phi_H = 42.2°$ and a maximum vertical visual field angle of $\phi_V = 27.4°$. These values are calculated with the optimum eye tracker camera to "test eye" distance of (L) of 600mm, but these angles could be further increased if we were to move the test eye closer to the display screen.Therefore a 20 inch screen with the above dimensions will be adequate for the proposed SVOP system.

The screen resolution will be related to the accuracy of visual stimuli location and size. The size of stimulus which will be mostly used in this research is the Goldmann III size (table 2.2 on page 22) which corresponds to a subtended angle of 0.43°. An angular screen resolution of 0.04°would represent a maximum error in the stimulus size of less than 10% which would be an acceptable minimum requirement for the proposed suprathreshold perimetry application. A typical screen resolution for the above mentioned 20 inch display is 1680x1050 pixels. The angular screen resolution can be calculated using the horizontal and vertical screen dimensions, and an approximate location of a test subjects eye. Using the above stated dimensions and using a screen-to-eye distance (D) of 564mm (calculated using an eye tracker camera-to-eye distance (L) of 600mm), the screen resolution of 1680x1050 equates to an angular resolution of 0.026° .

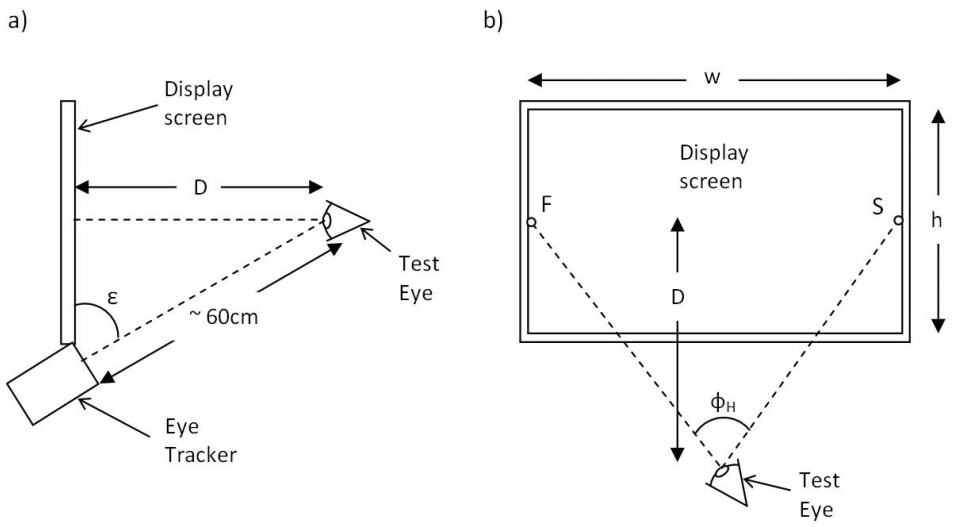

Figure 5.1: Variable and constant values to consider for calculation of the maximum possible visual field angle a display screen can display. a) Side view of an eye tracker and display screen where the eye tracker camera is set up at an angle of 70 degrees to the vertical and a test eye is located optimally from the eye tracker at a distance of 60cm. b) Front view of display screen showing the maximum horizontal visual field angle possible considering a fixation point (F) at one side and a stimulus test point (S) at the other side of the display screen.

The brightness uniformity of the chosen display screen and its capability to display brightness values accurately and consistently was also a consideration when selecting a suitable display screen. These characteristics are assessed in a later section (section 5.2.3).

5.1.1.3 Proposed SVOP system setup

Figure 5.2 shows a schematic of the proposed setup for the SVOP system. The primary display screen is a 20" LCD monitor which the patient views and on to which the visual stimuli are presented. The eye tracker (Tobii x50), set at an angle of 70° to the vertical, is located directly below the primary display screen. A personal computer (PC) controls the eye tracker, collects raw data about eye gaze position and eye location from the eye tracker and also controls what is displayed on the primary display screen based on this data. The eye tracker and primary display screen are located on a height adjustable surface to allow for different sized patients (i.e. small children through to adults) and different seating arrangements. A secondary display screen can be used to set up tests, input patient information and monitor patient position. The values in figure 5.3 represent how the x50 eye tracker is set up for SVOP testing.

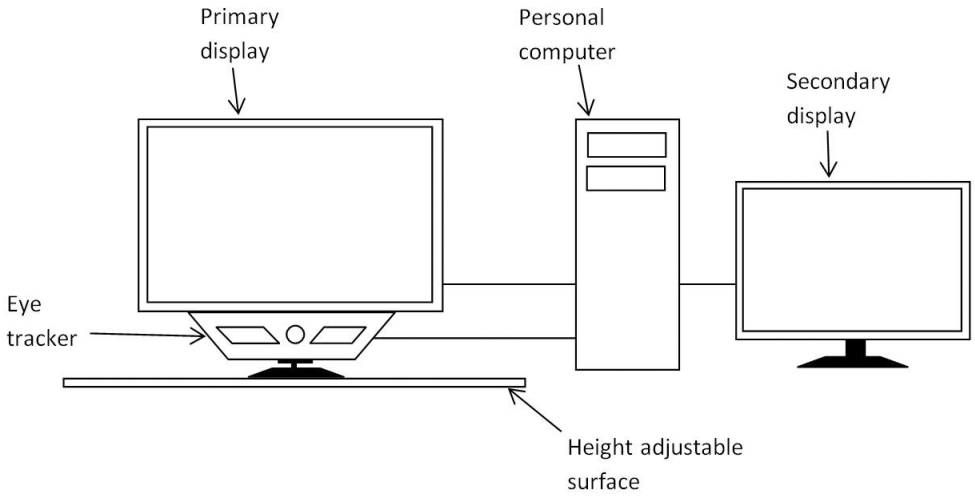

Figure 5.2: Schematic diagram of SVOP system setup.

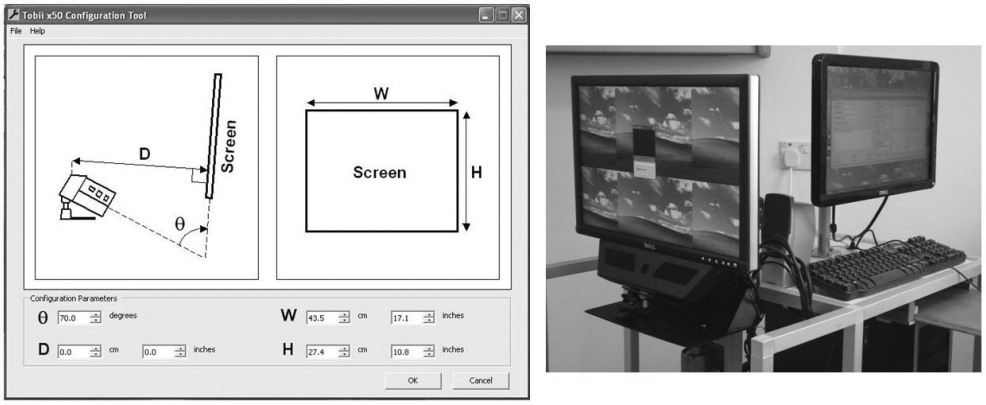

Figure 5.3: The positional setup of the X50 eye tracker for SVOP testing showing the positional values used in the Tobii configuration tool and a photograph of the setup.

5.1.2 Calculation of eye position

Figure 5.4 demonstrates how the screen position for a visual field point being assessed is dependent upon the 3D position of the subject's eyes relative to the display. The figure shows two examples, (a) and (b), which show the position of a stimulus on a display screen given a visual field angle of ϕ. In each case ϕ and the point of fixation (F) remain unchanged, but the position of the "test stimulus" (S) changes as a function of the position of the patient's eye relative to the point of fixation on the screen. Hence, to ensure that there is an accurate measure of the patient's visual field at a particular field angle, the 3D position in space of each eye has to be known so that the stimulus can be positioned correctly.

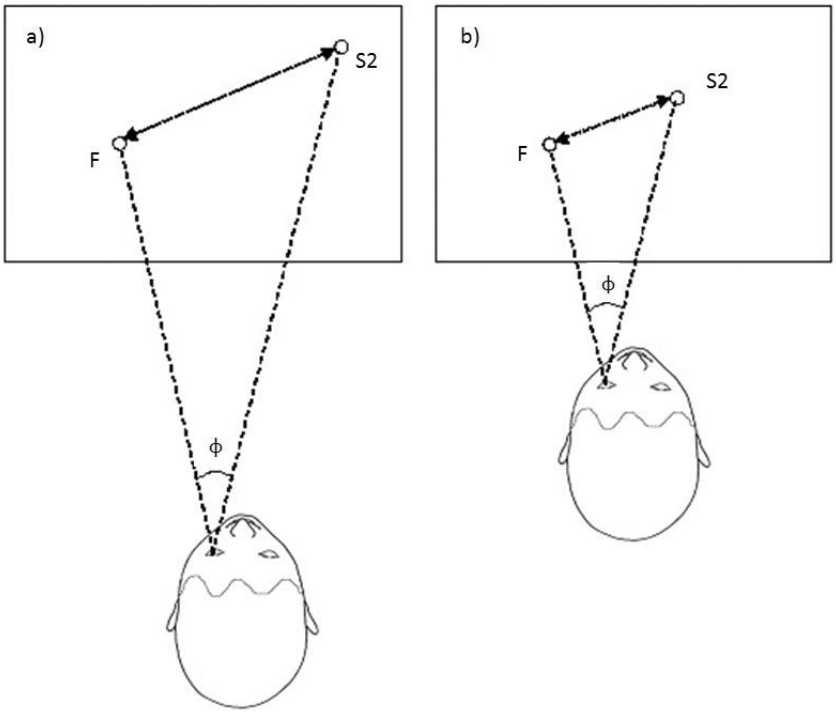

Figure 5.4: The effect of "test eye" to screen distance on the stimulus location. a) With the test eye further from the display screen, the position of the "test stimulus" (S) is further from the fixation point (F). b) With the test eye closer to the display screen, the position of S is closer to F.

In addition to the position of any particular "test stimulus" varying as a function of the location of the patient's eye, the displayed size of a "test stimulus" may also differ in size. This is also dependent on the distance between the subject's eyes and the fixation point at the time at which the stimulus is to be shown (figure 5.5).

In order for calculations to be made for the position and size of any "test stimulus" the 3D position of the "test eye" (or "test eyes" for binocular visual field assessment) must be calculated. This can be achieved using data provided by the eye tracker. All data fields provided by the eye tracker are shown in Appendix B. The key data fields required for calculating the location of the eyes are shown in table 5.3. In addition to this data, several constant values are required to enable correct calculation of eye location. These constants are the horizontal and vertical sizes of the camera's field of view at a specific known distance from the eye tracker. This information is detailed by the x50 eye tracker specifications as 200mm x 150mm (horizontal x vertical size respectively) at a distance of 600mm, and so are known values. However, for this section of theory these constants will be defined as Cam_H $(= 200mm)$, Cam_V $(= 150mm)$, and Cam_D $(= 600mm)$.

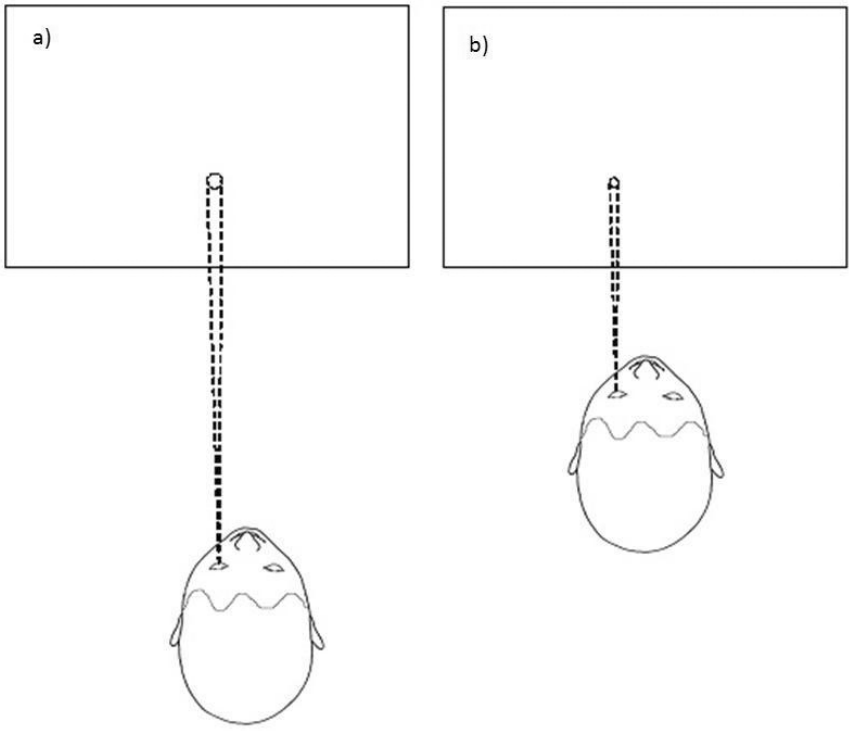

Figure 5.5: The effect of "test eye" distance from screen on the size of the stimulus that is presented (for a constant angular "test stimulus" size). a) With the test eye further away from the screen the displayed "test stimulus" size is larger. b) With the test eye closer to the screen the displayed "test stimulus" size is reduced.

Data Field	Description (units)
Left eye horizontal position as seen by eye tracker camera	X position of left eye in eye tracker camera field of view (0-1, where 0 is furthest left point)
Left eye vertical position as seen by eye tracker camera	Y position of left eye in eye tracker camera field of view (0-1, where 0 is top most point)
Left eye distance	Distance of the left eye from the eye tracker (mm)
Right eye horizontal position as seen by eye tracker camera	X position of right eye in eye tracker camera field of view (0-1, where 0 is furthest left point)
Right eye vertical position as seen by eye tracker camera	Y position of right eye in eye tracker camera field of view (0-1, where 0 is top most point)
Right eye distance	Distance of the right eye from the eye tracker (mm)

Table 5.3: Data fields supplied by the Tobii x50 eye tracker (at a frequency of 50Hz) which are used to calculate the 3D position of the eyes.

Figure 5.6 shows the eye tracker camera's field of view (FOV) and an example location of an eye within that field of view. Also shown in the figure is the horizontal and vertical size of the

camera's FOV at the specific distance of 600mm (Cam_D) from the camera and the location (E) of an eye within the camera FOV, given by three values ($e_{x'}$, $e_{y'}$ and $e_{z'}$) which are the x, y and z components of the eye position in a coordinate system with its origin at the eye tracker camera, the positive z-axis extending out through the centre of the camera FOV, the positive x-axis horizontal to the display screen and extending to the right of the display screen, and the y-axis relative to the z- and x-axis. An additional point (P) is shown which corresponds to a point which is related by a ratio to the eye position, but located within the camera FOV which is at the specific distance Cam_D (600mm) from the camera. This point is described by three values ($p_{x'}$, $p_{y'}$ and $p_{z'}$) which relate to the x, y and z components of the point P using the same coordinate system. The distance D is the direct distance between the eye tracker camera and the eye and this distance data is provided by the eye tracker. Also provided by the eye tracker is the horizontal and vertical position of the eye within the camera field of view, these values are given as a number between 0 and 1, with the zero values corresponding to the top left of the field of view (when looking towards the eye tracker camera).

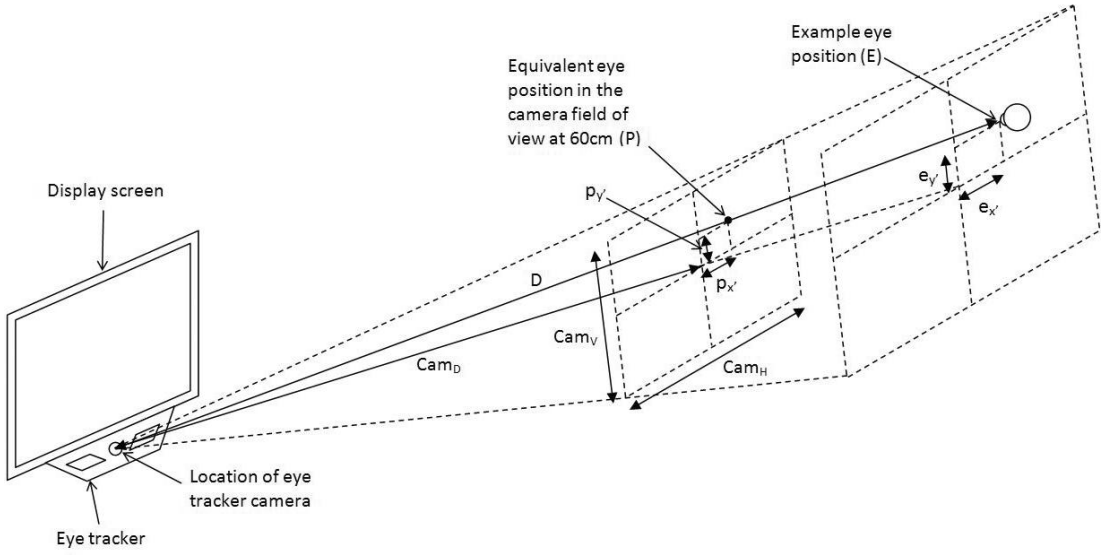

Figure 5.6: The eye tracker camera's field of view and an example location of an eye within that field of view. Also shown on the figure is the horizontal and vertical size of the field of view at a specific distance (60cm) from the camera. D is the distance of the eye from the eye tracker camera (this data is given by the eye tracker). $e_{x'}$ and $e_{y'}$ are the horizontal and vertical components of the eye position within the camera field of view (considering a coordinate system which has a z-axis with its origin at the camera and increases through the centre point of the camera's field of view).

In order to calculate the position of the eye ($e_{x'}$, $e_{y'}$ and $e_{z'}$) in the coordinate system described, the x and y position of the eye within the camera field of view must first be converted so that the zero values correspond to the centre of the field of view rather than the top left corner. This can be done using the following:

$$x'_{cam} = 2x_{cam} - 1$$

$$y'_{cam} = -2y_{cam} + 1$$

where x_{cam} and y_{cam} are the values given by the eye tracker, and x'_{cam} and y'_{cam} are these same values converted so that a value of zero corresponds to the centre of the FOV, values of -1 correspond to the bottom-left, and values of +1 correspond to the top-right of the camera field of view.

Then, the 3D position of point P can be calculated by:

$$p_{x'} = x'_{cam} \times \left(\frac{Cam_H}{2}\right)$$

$$p_{y'} = y'_{cam} \times \left(\frac{Cam_V}{2}\right)$$

$$p_{z'} = Cam_D$$

Next, using the fact that the geometry of the position of P and E has equal ratios, The position of the eye can be calculated from:

$$e_{x'} = p_{x'} \times \left(\frac{D}{D_p}\right)$$

$$e_{y'} = p_{y'} \times \left(\frac{D}{D_p}\right)$$

$$e_{z'} = p_{z'} \times \left(\frac{D}{D_p}\right)$$

where D_p is the direct distance from the camera to the point P and $D_p = \sqrt{600^2 + p_{x'}^2 + p_{y'}^2}$ and D is the direct distance from the camera to the eye (data given by the eye tracker) in mm.

Finally, because the eye tracker is tilted at an angle, the camera field of view is also tilted in this same direction and the calculated eye position $(e_{x'}, e_{y'}, e_{z'})$ are coordinates of the eye position in this same direction (figure 5.7). It is more desirable to have the 3D coordinates of the eye position in a coordinate system which makes more sense relative to the display screen. To calculate the eye position in a coordinate system with the x-axis along the horizontal of

the display screen, the y-axis along the vertical of the display screen, the z-axis extending horizontally out from the eye tracker camera, and the camera as the origin point, a rotation matrix which will rotate the coordinate system about the x'-axis (into the page in figure 5.7) by the angle γ, can be used:

$$\begin{bmatrix} e_x \\ e_y \\ e_z \end{bmatrix} = \begin{bmatrix} 1 & 0 & 0 \\ 0 & \cos\gamma & \sin\gamma \\ 0 & -\sin\gamma & \cos\gamma \end{bmatrix} \begin{bmatrix} e_{x'} \\ e_{y'} \\ e_{z'} \end{bmatrix}$$

$$e_x = e_{x'}$$

$$e_y = e_{y'}\cos\gamma + e_{z'}\sin\gamma$$

$$e_z = -e_{y'}\sin\gamma + e_{z'}\cos\gamma$$

Where $\gamma = 90° - \varepsilon = 20°$ (from figure 5.1)

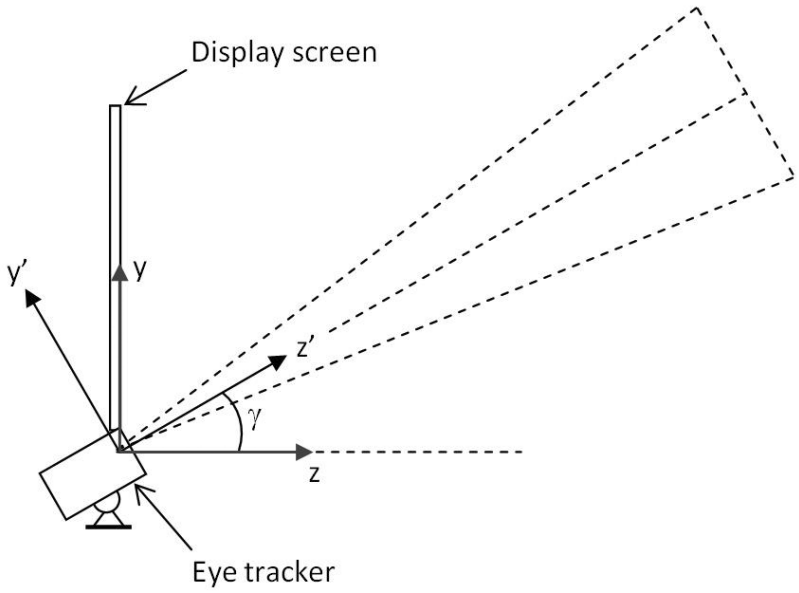

Figure 5.7: Side view of display screen and eye tracker. The eye tracker is positioned at an angle to the horizontal and so its field of view is also at this angle.

5.1.3 Calculation of a "test stimulus" screen position

Once the 3D position of the test eye(s) has been determined, the position of a "test stimulus" can then be calculated using this positional data. A point within the visual field can be described

by two angles (figure 5.8):

- ϕ, which is the angle at the eye made by lines to the point of fixation (F) and the point (S) - the eccentric visual field angle; and
- θ, which is the angle from the horizontal on the plane which has the line of gaze (from the eye to F) as its normal - the rotational visual field angle.

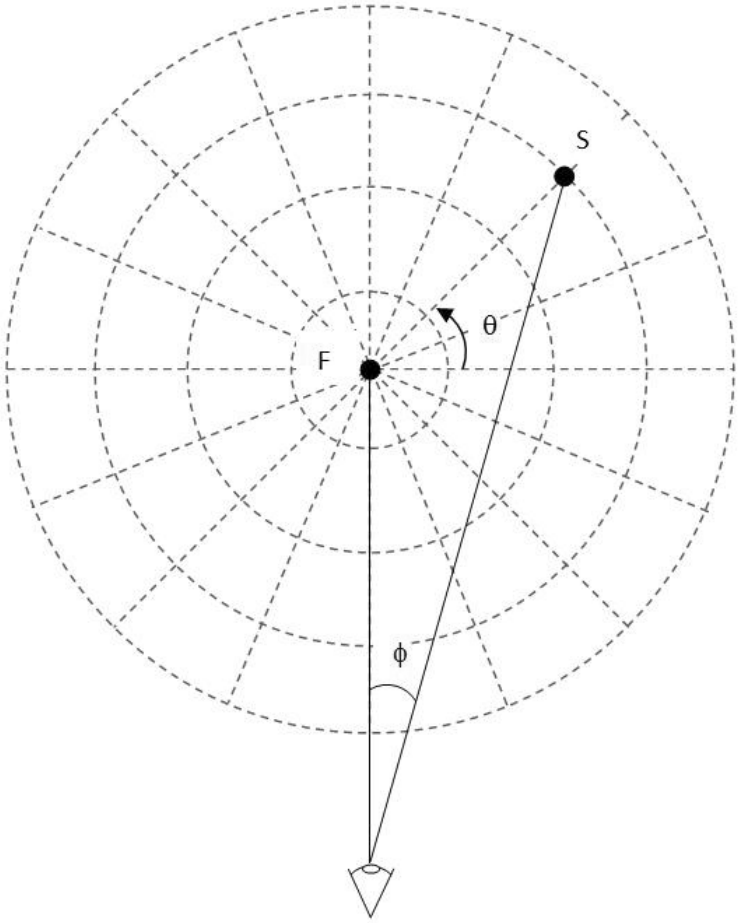

Figure 5.8: A visual field point as described by two angles, ϕ and θ. Where ϕ is the angle at the eye made by lines to the point of fixation (F) and the point (S) and θ is the angle from the horizontal on the plane which has the line of gaze (from the eye to F) as its normal.

In standard perimeters stimuli are presented on a screen in locations which correspond to specific retinal visual field locations and because the position of the patient's eye is fixed, the position on the screen at which a specific stimulus is shown is always the same. However, in the system proposed for this research, the patient's head is not maintained in a fixed position and in addition, the fixation point location can also vary throughout the test. As a result the

screen location for any particular "test stimulus" corresponding to a specific retinal location is dependent upon the position of the eye relative to the point of fixation.

This section provides the theory behind the calculation of where a stimulus should be presented on the screen based on the 3D position of the test eye (calculated in the previous section 5.1.2), the position of gaze on the screen, and the two angles which describe the visual field point that is to be tested (ϕ and θ).

The variables calculated in section 5.1.2 for the 3D position of a test eye from the eye tracker (e_x, e_y and e_z) can be transformed so that the values of these variables are described relative to a point of fixation (which is a known screen location where a "fixation stimulus" is displayed). Figure 5.9 shows this in terms of a coordinate system with the fixation point (F) at the origin, the xy plane corresponding to the plane in which the screen is positioned and the point E is the 3D location of the test eye relative to F. The vector EF ($\overrightarrow{EF}$) is the line of sight.

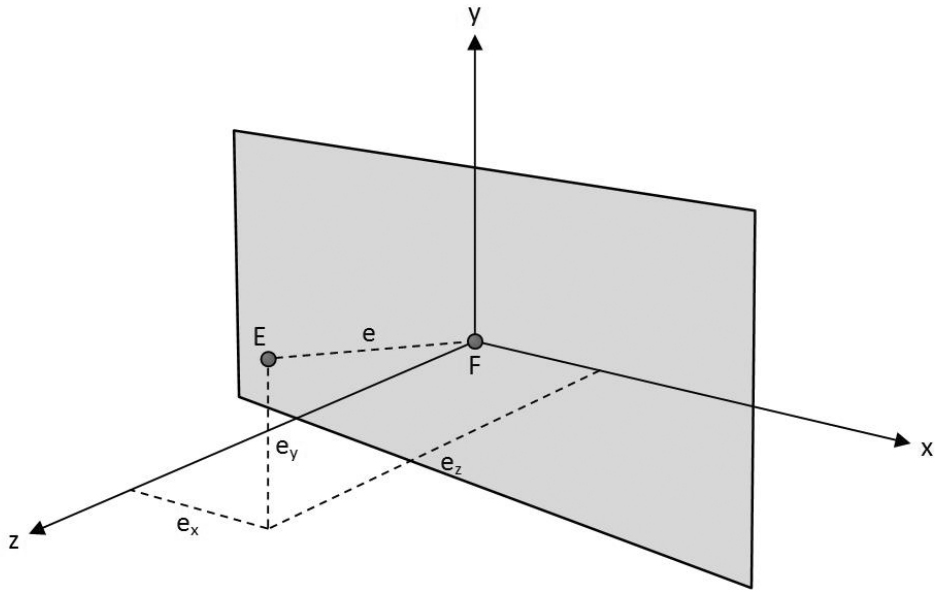

Figure 5.9: Coordinate system with the fixation point (F) at the origin. The xy plane corresponds to the plane in which the screen is positioned. The point E corresponds to the 3D location of the test eye relative to F.

Now, imagining a plane surface perpendicular to the direction of gaze (the vector $\overrightarrow{EF}$). This plane lies on the x'y' axis of a new coordinate system x'y'z' where the line of sight lies along the z' axis, and the origin is still at the point of fixation, F (figure 5.10). The position of a "test stimulus" (S') on this plane within this new coordinate system can be calculated:

$$S'_{x'} = e \tan\phi \cos\theta \tag{5.1}$$

$$S'_{y'} = e \tan\phi \sin\theta \tag{5.2}$$

$$S'_{z'} = 0 \tag{5.3}$$

where $e = \sqrt{e_x^2 + e_y^2 + e_z^2}$

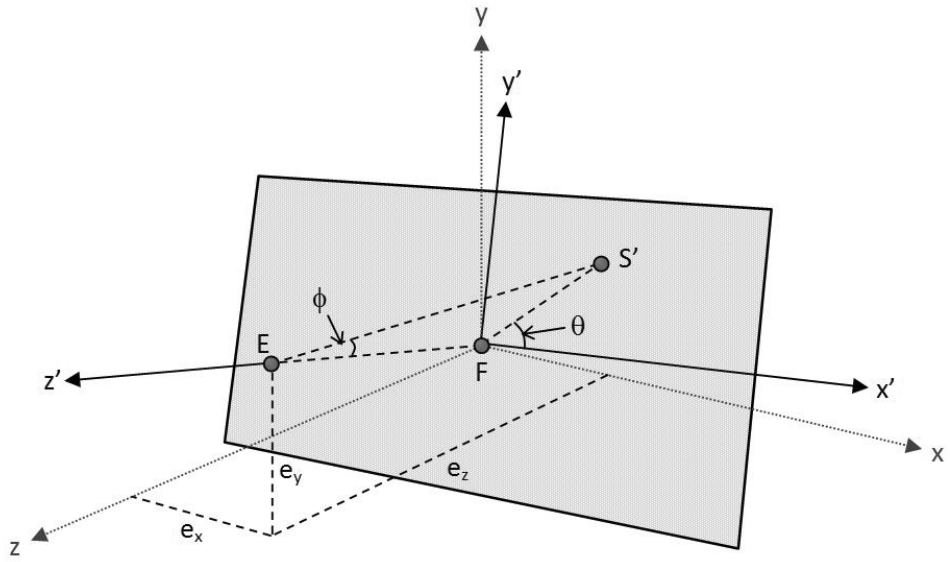

Figure 5.10: A new surface, which is the x'y' plane within a new coordinate system x'y'z', where the line of sight lies on the z' axis. The position of a stimulus S' on the x'y' plane can be described by the two angles ϕ and θ with respect to the position of the test eye (E) and the point of fixation (F).

This gives the 3D position of the "test stimulus" relative to the point of fixation, with respect to the 3D eye position (e_x, e_y and e_z) and the point in the visual field we are testing (ϕ and θ). However, this point is on the plane x'y' and is described in the coordinate system x',y',z'. It is now desirable to find the coordinates of S' in the original coordinate system x,y,z before being able to determine where the line ES' intersects the plane xy to find the position of the "test stimulus" on the display screen.

To find the coordinates of S' in the coordinate system x,y,z, 3D rotation matrices can be used. In general terms, the rotation matrices for rotating the x- and y-axes in a counterclockwise direction when looking towards the origin are given by:

$$R_x(\alpha_x) = \begin{bmatrix} 1 & 0 & 0 \\ 0 & \cos\alpha_x & \sin\alpha_x \\ 0 & -\sin\alpha_x & \cos\alpha_x \end{bmatrix}$$

Where α_x is the angle by which the x-axis is rotated.

$$R_y(\alpha_y) = \begin{bmatrix} \cos\alpha_y & 0 & -\sin\alpha_y \\ 0 & 1 & 0 \\ \sin\alpha_y & 0 & \cos\alpha_y \end{bmatrix}$$

Where α_y is the angle by which the y-axis is rotated.

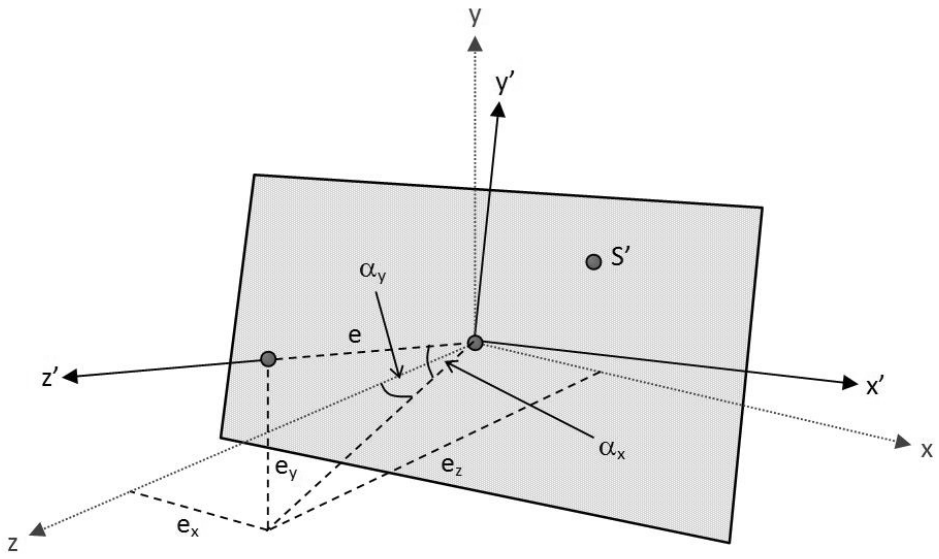

Figure 5.11: The rotation angles required to rotate the x',y',z' coordinate system to the x,y,z coordinates system. $\alpha_x$is the angle by which the x'-axis is to be rotated (counterclockwise in the situation shown) and α_y is the angle by which the y'=axis is to be rotated (clockwise in the situation shown).

Figure 5.11 shows the angles by which the x'- and y'-axes need to be rotated and demonstrates the direction of rotation of these axes to rotate the coordinate system x',y',z' to the coordinate system x,y,z. In the situation shown in figure 5.11 the x'-axis needs to be rotated in a counterclockwise direction by the angle α_x, and then the y'-axis must be rotated in a clockwise direction by the angle α_y. In this case the two rotation matrices (R1 and R2) required are:

$$R1(\alpha_x) = \begin{bmatrix} 1 & 0 & 0 \\ 0 & \cos\alpha_x & \sin\alpha_x \\ 0 & -\sin\alpha_x & \cos\alpha_x \end{bmatrix}$$

$$R2(\alpha_y) = \begin{bmatrix} \cos\alpha_y & 0 & \sin\alpha_y \\ 0 & 1 & 0 \\ -\sin\alpha_y & 0 & \cos\alpha_y \end{bmatrix}$$

These rotation matrices hold no matter what the position of the eye (E) because when either of the rotation angles α_x or α_y become negative due to the location of E, this also reverses the direction of the rotation to be performed.

So, the 3D position of S' after the first coordinate system rotation, R1, is:

$$S'_{R1} = \begin{bmatrix} 1 & 0 & 0 \\ 0 & \cos\alpha_x & \sin\alpha_x \\ 0 & -\sin\alpha_x & \cos\alpha_x \end{bmatrix} \begin{bmatrix} S'_{x'} \\ S'_{y'} \\ S'_{z'} \end{bmatrix} \tag{5.4}$$

and the 3D position of S' after the second coordinate system rotation, R2, will be:

$$S'_{R2} = \begin{bmatrix} \cos\alpha_y & 0 & \sin\alpha_y \\ 0 & 1 & 0 \\ -\sin\alpha_y & 0 & \cos\alpha_y \end{bmatrix} \begin{bmatrix} S'_{R1_x} \\ S'_{R1_y} \\ S'_{R1_z} \end{bmatrix} \tag{5.5}$$

Also, from figure 5.11:

$$\sin\alpha_x = \frac{e_y}{e} \tag{5.6}$$

$$\cos\alpha_x = \frac{\sqrt{e_x^2 + e_z^2}}{e} \tag{5.7}$$

$$\sin\alpha_y = \frac{e_x}{\sqrt{e_x^2 + e_z^2}} \tag{5.8}$$

$$\cos\alpha_y = \frac{e_z}{\sqrt{e_x^2 + e_z^2}} \tag{5.9}$$

Using equation 5.4, the 3D position of S' relative to the fixation point (F) after the first rotation of the coordinate system (R1) can be described in terms of eye position and the visual field angles (ϕ and θ):

$$S'_{R1_x} = S'_{x'}$$
$$= e \tan\phi \cos\theta \qquad \text{(substituting equation 5.1)} \tag{5.10}$$

$$S'_{R1_y} = S'_{y'} \cos\alpha_x + S'_{z'} \sin\alpha_x$$
$$= \tan\phi \sin\theta \sqrt{e_x^2 + e_z^2} \qquad \text{(substituting equations 5.2, 5.3 and 5.7)} \tag{5.11}$$

$$S'_{R1_z} = -S'_{y'} \sin\alpha_x + S'_{z'} \cos\alpha_x$$
$$= -e_y \tan\phi \sin\theta \qquad \text{(substituting equations 5.2, 5.3 and 5.6)} \tag{5.12}$$

Using equation 5.5, the 3D position of S' relative to the fixation point (F) after the second rotation of the coordinate system (R2) can also be described in terms of the eye position and the visual field angles (ϕ and θ):

$$S'_{R2_x} = S'_{R1_x} \cos\alpha_y + S'_{R2_z} \sin\alpha_y$$
$$= e \tan\phi \cos\theta \cos\alpha_y - e_y \tan\phi \sin\theta \sin\alpha_y \qquad \text{(substituting equations 5.10 and 5.12)}$$
$$= e \tan\phi \cos\theta \frac{e_z}{\sqrt{e_x^2 + e_z^2}} - e_y \tan\phi \sin\theta \frac{e_x}{\sqrt{e_x^2 + e_z^2}} \qquad \text{(substituting equations 5.8 and 5.9)}$$
$$= \frac{\tan\phi}{\sqrt{e_x^2 + e_z^2}} (e e_z \cos\theta - e_x e_y \sin\theta) \tag{5.13}$$

$$S'_{R2_y} = S'_{R1_y}$$
$$= \tan\phi \sin\theta \sqrt{e_x^2 + e_z^2} \qquad \text{(substituting equation 5.11)} \tag{5.14}$$

$$S'_{R2_z} = -S'_{R1_x} \sin\alpha_y + S'_{R1_z} \cos\alpha_y$$
$$= -e \tan\phi \cos\theta \sin\alpha_y - e_y \tan\phi \sin\theta \cos\alpha_y \qquad \text{(substituting equations 5.10 and 5.12)}$$
$$= -e \tan\phi \cos\theta \frac{e_x}{\sqrt{e_x^2 + e_z^2}} - e_y \tan\phi \sin\theta \frac{e_z}{\sqrt{e_x^2 + e_z^2}} \qquad \text{(substituting equations 5.8 and 5.9)}$$
$$= -\frac{\tan\phi}{\sqrt{e_x^2 + e_z^2}} (e e_x \cos\theta + e_y e_z \sin\theta) \tag{5.15}$$

Now the coordinates of S' in the original coordinate system (x,y,z) are known (as such the notation of these coordinates is now changed to S'_x , S'_y and S'_z). The next step is to find where the visual field point stimulus will be displayed on the display screen. This new point

(S) corresponds to the point where a line from the eye (E) to S' intersects the xy plane (i.e. the display screen). Figure 5.12 demonstrates this.

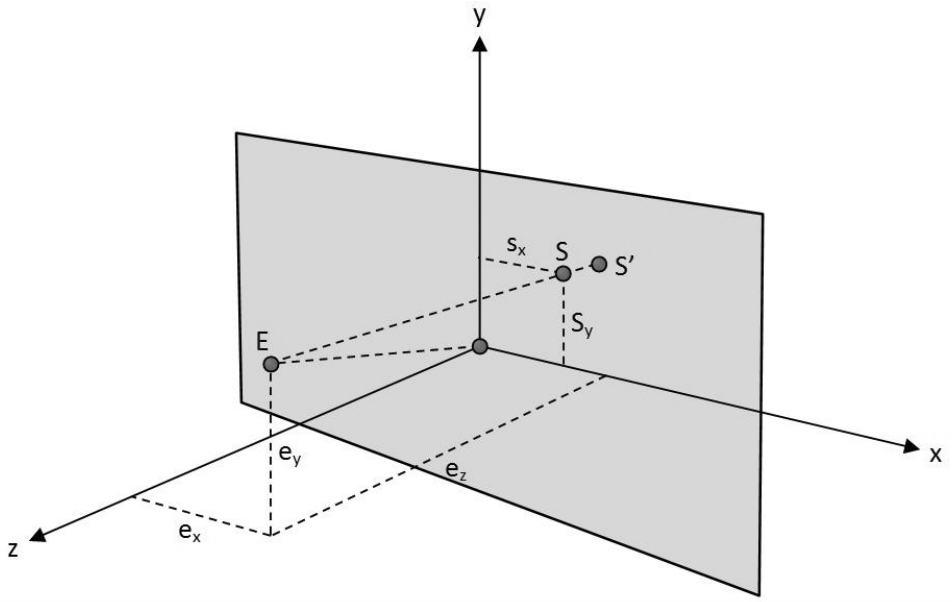

Figure 5.12: The position of the visual field point stimulus (S) on the display screen (which corresponds to the xy plane in the original coordinate system. S is the point where a line from E (the eye) to S' intersects with the plane xy. We wish to find the position of S on the display screen (i.e. the values S_x and S_y).

This intersection point (S), is the point on the screen which corresponds to the visual field point we wish to test. The general equation of a line can be written as:

$$P = P_0 + t(P_1 - P_0) \tag{5.16}$$

Where P is the position vector of a point on the line which passes through two other points with position vectors P_0 and P_1.

The general equation of a plane can be written as:

$$N \cdot (P - P_2) = 0 \tag{5.17}$$

Where P is the position vector of a point on the plane which also has a point on it with position vector P_2 and N is a vector normal to the plane.

The point of intersection of the line and plane is (putting 5.16 into 5.17):

$$N \cdot (P_0 + t(P_1 - P_0)) - N \cdot P_2 = 0$$

Which gives:

$$t = \frac{N \cdot (P_2 - P_0)}{N \cdot (P_1 - P_0)}$$

In the situation in figure 5.12, the normal to the plane, $N = (0, 0, 1)$, a point on the plane, $P_2 = (0, 0, 0)$, $P_0 = (e_x\,, e_y\,, e_z)$ and $P_1 = (S'_x\,, S'_y\,, S'_z)$. So:

$$\begin{aligned} t &= \frac{(0,0,1) \cdot ((0,0,0) - (e_x\,, e_y\,, e_z))}{(0,0,1) \cdot \big((S'_x\,, S'_y\,, S'_z) - (e_x\,, e_y\,, e_z)\big)} \\ &= -\frac{e_z}{S'_z - e_z} \end{aligned} \tag{5.18}$$

Substituting this into equation 5.16 gives:

$$(P_x\,, P_y\,, P_z) = (e_x\,, e_y\,, e_z) - \frac{e_z\left((S'_x\,, S'_y\,, S'_z) - (e_x\,, e_y\,, e_z)\right)}{S'_z - e_z}$$

Where the point P corresponds to the screen position of the visual field point (S). So, the coordinates of S are:

$$S_x = e_x - e_z\left(\frac{S'_x - e_x}{S'_z - e_z}\right)$$

$$S_y = e_y - e_z\left(\frac{S'_y - e_y}{S'_z - e_z}\right)$$

$$\begin{aligned} S_z &= e_z - e_z\left(\frac{S'_z - e_z}{S'_z - e_z}\right) \\ &= 0 \end{aligned}$$

Where S'_x , S'_y and S'_z are given by equations 5.13, 5.14 and 5.15 (where they are labelled as S'_{R2_x} , S'_{R2_y} , S'_{R2_z} respectively) so that these coordinates on the display screen are calculated using the variables of visual field angles (θ and ϕ) and the 3D position of the test eye (e_x , e_y , e_z).

5.1.4 Calculation of a "test stimulus" size and shape

The size of a "test stimulus" is described in terms of an angle subtended from the eye (section 2.2 on page 22). Traditional perimetry devices use a bowl shaped screen with stimuli projected on to it. The bowl shape allows stimuli to be displayed as circular test points which are always

presented at the same size and shape for a given subtended angle size (e.g. Goldmann III) because each point on the bowl is theoretically equidistant from the test eye. Due to the fact that the proposed SVOP perimetry system in this research uses a flat screen, and additionally allows the patient freedom to move their head, each "test stimulus" will vary in displayed size. Additionally, the shape of the each stimulus has the potential to vary, again because the proposed SVOP system uses a flat display screen. As each stimulus is defined by a subtended angle at the eye, this can be imagined as a cone, the tip of which is located at the eye. If each stimulus is presented on a bowl shaped screen (as in traditional ASP) where every point on the screen is the same distance from the eye, it can be seen that any location on the screen (corresponding to different visual field locations) will result in a circular shaped stimulus of the same size because the screen always intersects the cone at 90° (figure 5.13).

However, a flat screen acts as a plane intersecting the cone, potentially at an angle other than 90° (figure 5.14a). The flat display screen intersection with the cone creates a stimulus which is a "conic section". This results in an elliptical shape with the centre line through the cone at one focus of the ellipse (figure 5.14b).

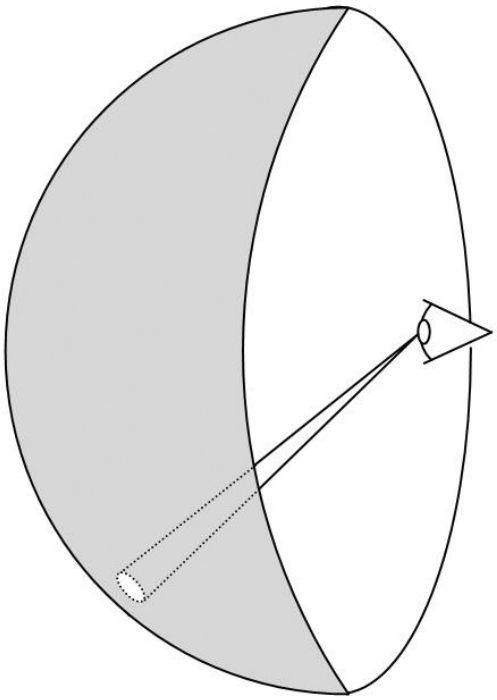

Figure 5.13: A bowl shaped screen (as in traditional ASP) where every point on the screen is the same distance from the eye, resulting in a circular shaped stimulus of the same size at every location.

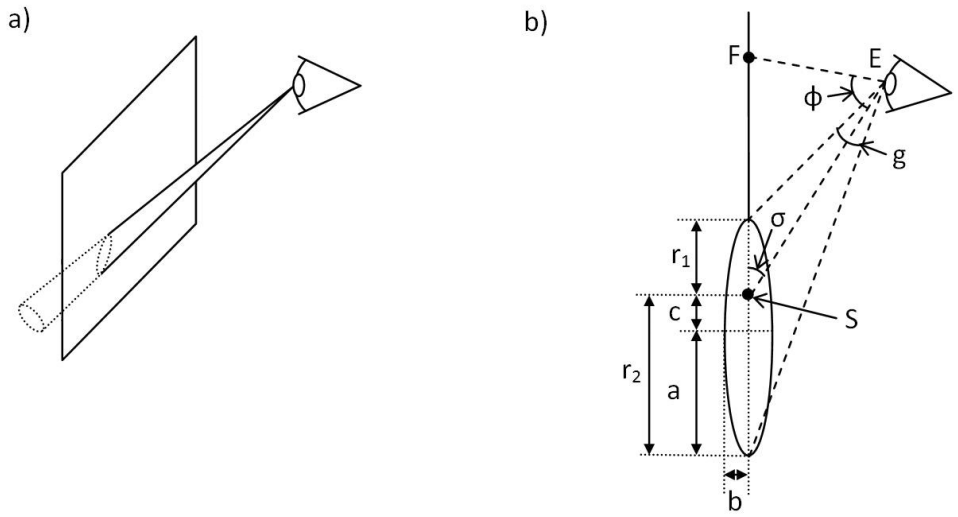

Figure 5.14: a) A flat screen acts as a plane intersecting the cone, resulting in a "conic section" stimulus potentially with an elliptical shape with the centre of the cone at one focus of the ellipse. b) the dimensions of the "conic section" and the variables used to calculate those dimensions.

To establish the dimensions of the ellipse, the major and minor semi-axis (a and b respectively in figure 5.14b) must be found. These can be calculated by first finding the values of r_1, r_2 and c which are the distances from one focus to either end of the ellipse, and to the centre of the ellipse respectively.

From the sine rule:

$$\frac{\sin\sigma}{EF} = \frac{\sin\phi}{FS}$$

Where σ is the angle made between the display screen and the line from the eye to the display screen through the centre of the cone, ϕ is the visual field angle being assessed, EF is the distance from the eye (E) to the point of fixation (F), and FS is the distance between the point of fixation to the point of the "test stimulus" (S), which is defined as the point where the centre line through the cone intersects with the screen.

$$\therefore \sin\sigma = \sin\phi\frac{EF}{FS} \tag{5.19}$$

The value of ϕ is known, and because the position of the eye (E) and the position of the stimulus (S) have previously been calculated, both EF and FS are known. Hence a value for σ can be found.

Again, using the sine rule:

$$\frac{\sin\left(\frac{g}{2}\right)}{r_1} = \frac{\sin\left(180-\sigma-\frac{g}{2}\right)}{ES}$$

Where g is size of the stimulus described by an angle subtended at the eye and ES is the distance from the eye to the stimulus point. Both of these values are known, and σ is given by equation 5.19.

$$\therefore r_1 = ES\frac{\sin\left(\frac{g}{2}\right)}{\sin\left(\sigma + \frac{g}{2}\right)} \tag{5.20}$$

Also, again from the sin rule:

$$\frac{\sin\left(\frac{g}{2}\right)}{r_2} = \frac{\sin\left(180 - \frac{g}{2} - (180 - \sigma)\right)}{ES}$$

$$\therefore r_2 = ES\frac{\sin\left(\frac{g}{2}\right)}{\sin\left(\sigma - \frac{g}{2}\right)} \tag{5.21}$$

The major semi-axis (a) can be given by:

$$a = \frac{r_1 + r_2}{2}$$

where r_1 and r_2 are given by equations 5.20 and 5.21.

Now, the distance from a focus to the centre of the ellipse (c) is given by:

$$c = a - r_1$$

And the minor semi-axis (b) can be calculated from a characteristic of ellipses which states that:

$$b = \sqrt{r_1^2 - c^2}$$

Thus, we have the dimensions of the stimulus to be displayed on the screen.

5.1.5 Proposed SVOP software

As described in section 5.1.1.3 the SVOP system comprises a personal computer, display screen, and a Tobii x50 eye tracker. This section outlines the proposed software which will control the eye tracker, display visual stimuli on the display screen and interpret eye gaze responses in real time.

A test begins with a "fixation stimulus" displayed on the screen. The purpose of a "fixation stimulus" is to provide a fixation point for the patient and to allow the system to confirm that

the patient is indeed looking at a specific screen location by comparing the "fixation stimulus" location with real time eye gaze location data. Once verification that the subject is looking at the "fixation stimulus" is obtained, a visual field point to be assessed is selected and a visual "test stimulus" corresponding to this visual field point is displayed on the screen while at the same time the original "fixation stimulus" is erased. The "test stimulus" is displayed for 200ms (which is the same stimulus presentation time used by the Humphrey Field Analyser) and is presented at screen coordinates corresponding to a specific location within the patient's visual field. For each "test stimulus", the task required of the patient is to follow their natural reaction to fixate towards the area of the screen where the "test stimulus" was seen. By monitoring the eye movements of the patient, changes in eye gaze position can be detected and the vector of the saccadic eye gaze movements in response to the "test stimulus" will provide an indication as to whether the patient has perceived it or not. The time interval between presentation of the stimulus and the patient's response (i.e. the patient's reaction time) can also be used to assist in confirming that the eye movements are, or are not, a reaction to the visual field "test stimulus" presented.

In order to allow the calculation of the appropriate screen position for any particular visual field point being assessed, the position of the eye(s) in 3D space relative to the display screen must be known. The Tobii x50 eye tracker provides "real time" data (at a sample rate of 50Hz) for the distance of each eye from the eye tracker's camera and also provides values for the position of each eye within the camera's field of view. This information allows the "real time" calculation of the 3D position of each eye relative to any point on the display screen and so provides the values for determining the correct size, shape and screen location of the "test stimuli" to be presented on the screen at any moment, for any particular visual field point that is to be assessed (as described in the previous sections).

A subject's eye gaze is to be monitored when "test stimuli" are shown in different positions on the display screen throughout a test, each position corresponding to different points within a subject's visual field. A software algorithm is to be used to decide whether the subject was able to see the new stimulus or not, based on the direction and magnitude of any eye movements (i.e. the vector of a fixation change), in addition to the timing of that eye gaze movement. If a subject perceives a "test stimulus" presented on the display screen, the natural response is to gaze towards it. If the point is not seen there is a different type of eye gaze movement response (or no response at all). It is the job of the algorithm to automatically distinguish between these two types of responses in "real time" based on the vector of any fixation change made following the presentation of a new visual field "test stimulus", and the timing of any such fixation change. To make this automated decision, the vector change in fixation point is compared directly with the vector corresponding to the change in screen position of the "fixation stimulus" to the "test stimulus". In practice, there will be a natural variation in the difference

between the vector change in fixation point and the vector change in the screen position of the stimuli (i.e. the accuracy with which the patient can fixate at the location where the "test stimulus" was presented). Hence, it is important to know how much variation is acceptable before a "test stimulus" is labelled as "unseen". To deal with this, parameters used within the algorithm designed to make this decision will be based on eye response data collected as part of this research program.

Figure 5.15 shows the software steps of a visual field test using the proposed SVOP technique. In practice, this software is to be implemented using a custom developed computer program running on a personal computer which also controls the eye tracker and display screen. At the start of the test a visual "fixation stimulus" (for example a circular point or small cartoon face for children) is displayed in the centre of the screen. When the initial "fixation stimulus" is displayed the eye tracker's gaze data are used to verify that the patient is gazing at the "fixation stimulus". In the event that the gaze data suggests that the patient is not fixating on the correct point after a certain number of gaze samples, additional visual prompts could be used to attract attention if required.

After it is determined that the patient is fixating at the first "fixation stimulus", a new visual field test location is selected (from a pre-selected list of visual field points) and the position, size and shape of the associated "test stimulus" are calculated within one sample time period (20ms). The position of the "test stimulus" is calculated using the distance from the current fixation point (in this case the central "fixation stimulus") to the subject's test eye(s), as measured using the eye tracker's data, and the visual field point that is to be assessed. For any particular visual field examination there will be a number of different visual field points to be assessed. The order in which the selected points are assessed is randomised. Once the "test stimulus" position, size and shape is determined, the "fixation stimulus" is erased and the "test stimulus" is displayed in the calculated location for a period of 200ms. A countdown timer (which runs in the background) is started as soon as the "test stimulus" is displayed. If the displayed stimulus is not detected as "seen" within this time then the stimulus is categorised as "not seen". The countdown time is set to a pre-determined limit (for example 1 second) which will provide a sufficient amount of time for a patient to react to a "test stimulus" if seen.

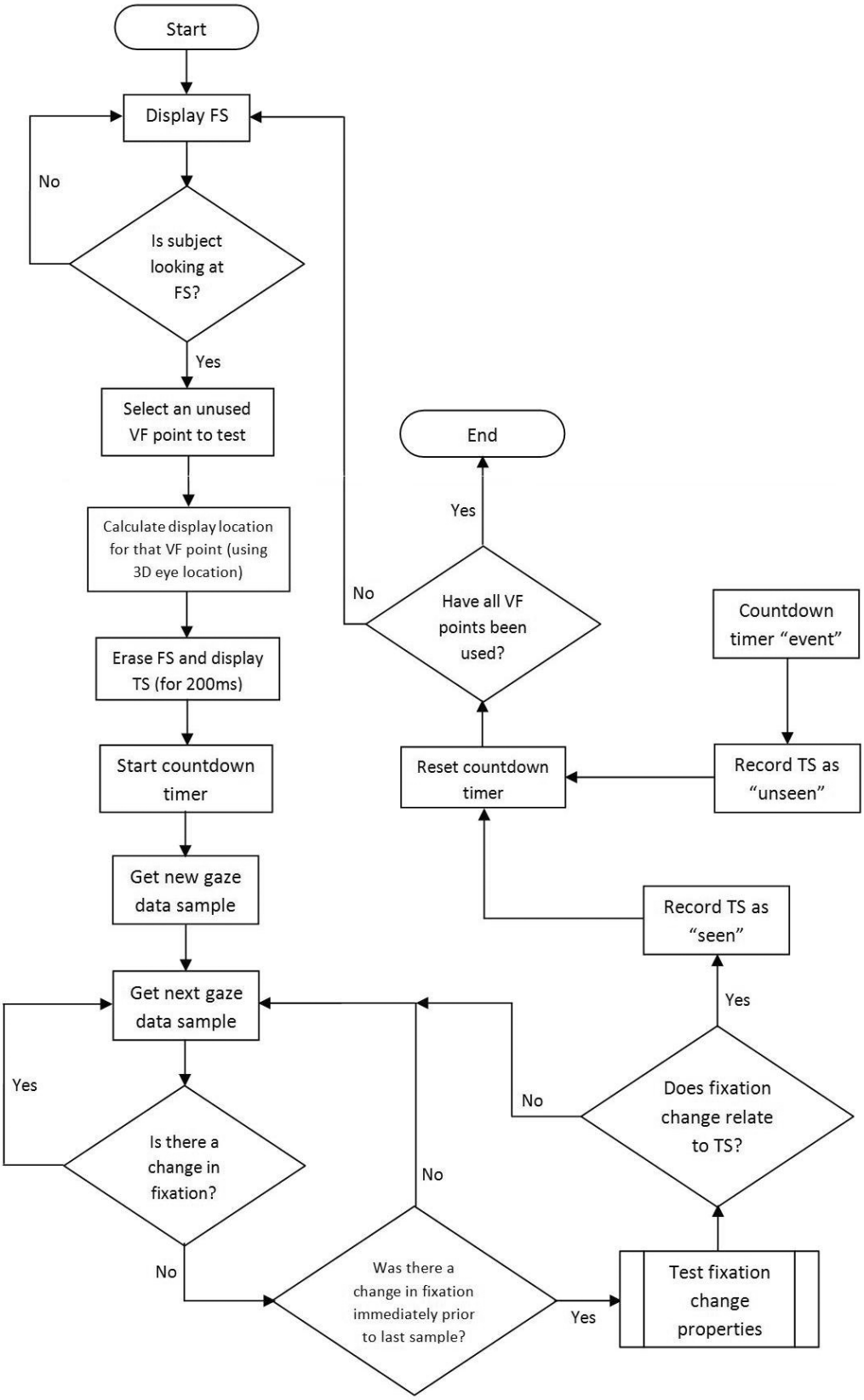

Figure 5.15: Flow diagram of the proposed software program for an SVOP test. The step "Test fixation change properties" relates to further software steps outlined in figure 5.16. FS = "fixation stimulus". TS = "test stimulus". VF = Visual Field.

As soon as a "test stimulus" has been displayed, gaze data are continually monitored every sample (every 20ms). The gaze data are used to determine whether there has been a change in the fixation point. If, for any particular gaze datum sample, there has been a considerable change in the fixation point (which could be determined for example as a screen distance between gaze data samples greater than a specified number of pixels), the very next gaze data sample is used to determine whether there has been a further change in the fixation point, this process continues until no considerable change in fixation point is found between consecutive data samples. In this manner the movement of the user's eye towards a new fixation point can be found. If there is no significant change in fixation between subsequent gaze data coordinates and the prior gaze data point did indicate a change in fixation then this indicates the end of the subject's fixation change and hence the vector of the fixation change can be found. Once a fixation change vector is detected, the properties of the fixation change are tested to identify whether the fixation change corresponds to the vector associated with the "fixation stimulus" to the "test stimulus".

Figure 5.16 illustrates the programmatic steps used to determine if the characteristics of any fixation change found can be matched with the "test stimulus" which was displayed. The direction of the fixation change is compared with the direction from the "fixation stimulus" to the "test stimulus". Additionally, the amplitude (measured as a visual angle subtended at the eye) of the fixation change is compared to that of the visual field angle being tested. If these two characteristics are in agreement (within a range of specific values) then the fixation change is considered to relate to the "test stimulus" presented on the display screen and that point is recorded as "seen". A further check could be to assess the reaction time of the eye movement to assist with the decision. If the reaction time is outwith certain limits a re-test of this visual field point could be made. If either of the vector properties of the fixation change do not relate to the corresponding properties between the "fixation stimulus" and "test stimulus" then the fixation change is considered not to relate to the new stimulus and the system returns to the capture gaze data step of figure 5.15 (note that upon this occurrence, the visual field point is not labelled as "unseen" at this step in the program).

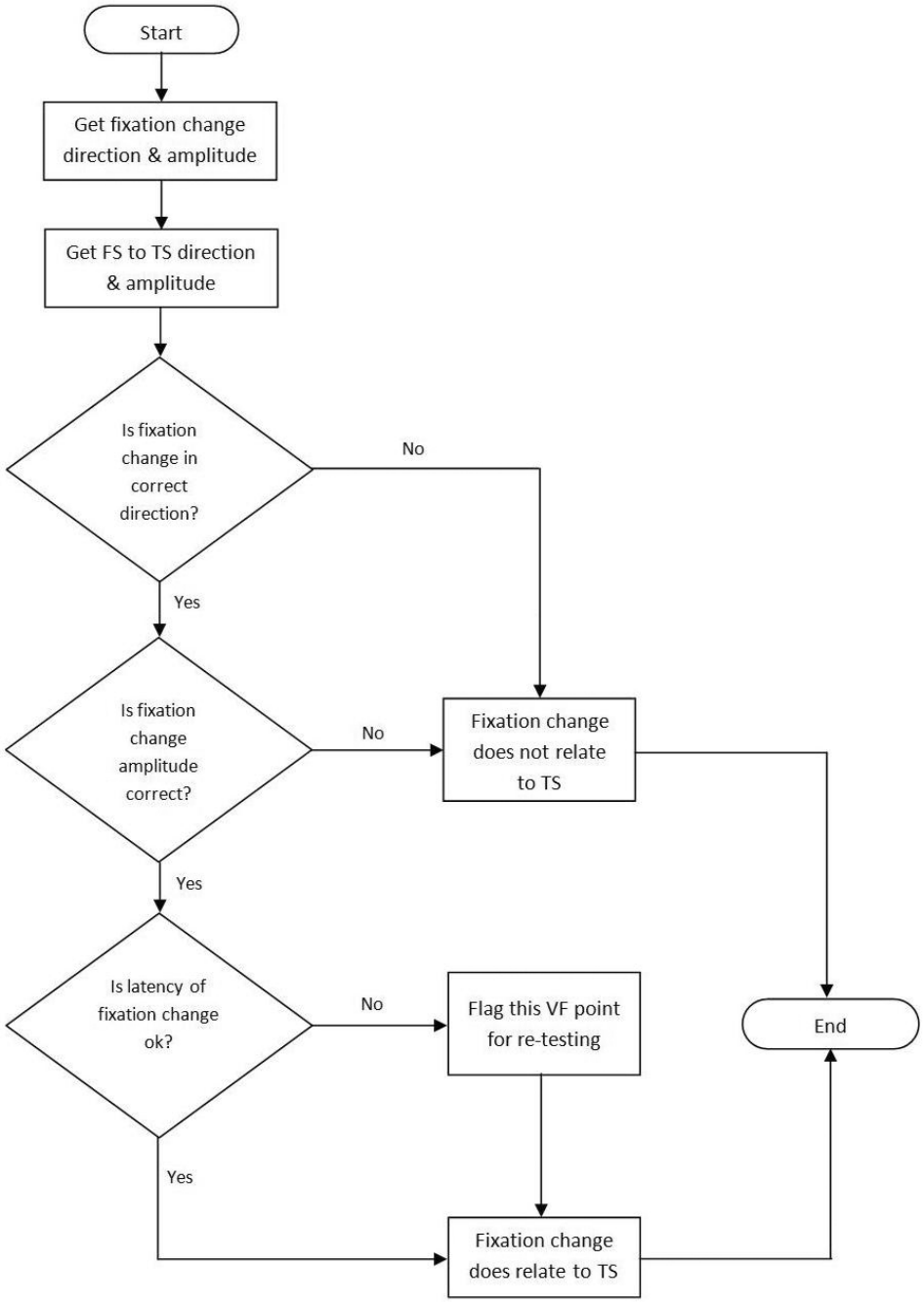

Figure 5.16: Flow diagram for the assessment of fixation change characteristics following the presentation of a "test stimulus". This diagram represents the programmatic steps contained within the "Test fixation change properties" step in figure 5.15.

Returning to Figure 5.15, in the event that the "test stimulus" is identified as having been "seen", this event is recorded and the countdown timer is reset. If any fixation changes are not recorded as "seen" (or indeed if there are no fixation changes detected) before the countdown timer reaches zero, this triggers the countdown timer "event" and the stimulus is initially recorded as "unseen"

and this point will be flagged for retesting at a later stage during the test. Upon retesting any initially "unseen" stimuli, if it is again "unseen", then that will be the final result for that stimulus point. If at any time a stimulus point is determined as "seen", then "seen" is the final result of that stimulus point. If not all points have been tested then the process is run again with a new visual field point with the last "test stimulus" point becoming the location for a new "fixation stimulus". Otherwise, the test is completed. By way of example, figure 5.17 shows an illustration of a visual field point being tested and "seen". The solid lines indicate the gaze location data changes every 20ms.

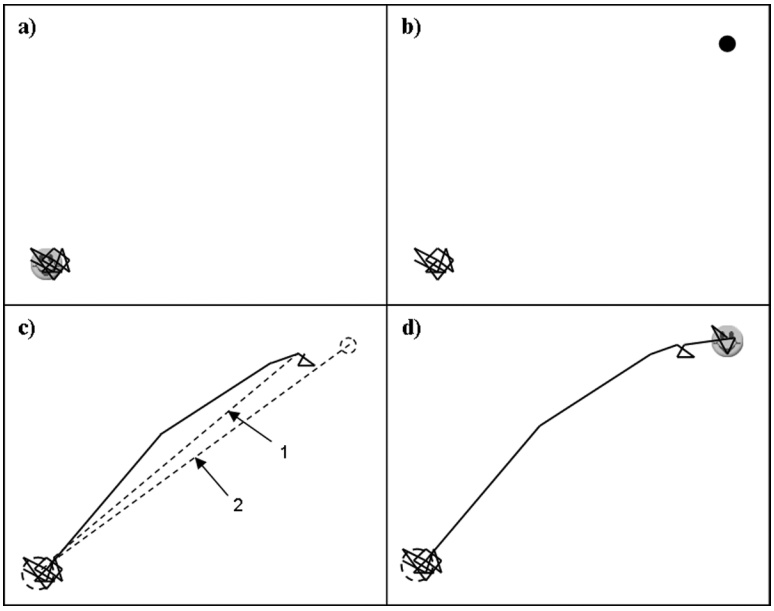

Figure 5.17: Illustration of a visual field point being tested and "seen". The solid lines indicate the gaze point changes every 20ms. a) The subject fixates on a "fixation stimulus". b) A "test stimulus" is displayed corresponding to a visual field point. c) A change in fixation is detected (dashed line 1) and compared with the positional change in stimuli (dashed line 2). d) A new "fixation stimulus" is displayed ready to repeat the process.

The "test stimuli" presented can be of the same type throughout a test (i.e. a defined angular size and a defined brightness). However, to keep the test interesting for children, once a "test stimulus" has been detected as "seen" it is changed to an interesting audio-visual animation appropriate to their developmental age. For instance, small cartoon face animations are used for younger children. This may help to motivate child patients to submit to the test. The test can also be interrupted at appropriate times by additional visual prompts (with sound if necessary) to draw the attention of a distracted child back to the screen.

In order to create this proposed SVOP system, the hardware components of the system will need to be assessed. For example, the eye tracker's gaze and distance data accuracy and the display screen brightness uniformity will need to be investigated. Additionally, to create the "decision algorithm" proposed above, the fixation change characteristics relative to displayed

"test stimuli" must first be investigated so as to determine specific numerical limits which the algorithm can use to make its automated decision. These aspects are discussed in the following sections (5.2 "Assessment of SVOP Hardware" and 5.3 "Assessment of Eye Gaze Response to Test Stimuli").

5.2 Assessment of SVOP hardware

In order to develop the system proposed in the previous section of theory, the selected eye tracking hardware must be capable of providing sufficiently accurate eye gaze data and eye positional data so as to allow an accurate assessment of patient fixation, accurate calculation of the "test stimuli" positions and accurate assessment of patient gaze response to the "test stimuli". The following sections detail the methods and results for assessing the eye gaze data and eye positional data provided by the Tobii x50 eye tracker (sections 5.2.1 and 5.2.2 respectively). In addition, another specification related to the Tobii eye tracker which is important to the accurate functioning of the proposed SVOP system has been assessed as part of the methods in section 5.2.2. This is the horizontal and vertical head movement box size at a known distance (600mm) from the eye tracker's camera. It is important to assess these specific constant values as they are used in the calculations which determine 3D eye position relative to the eye tracker.

Another important hardware aspect of the SVOP system concerns how capable the LCD screen is at faithfully reproducing different levels of luminance (brightness). The SVOP system should produce "test stimuli" at a specific luminance level which will allow an SVOP test to be compared directly with a clinically accepted automated static perimetry device (e.g. the Humphrey Field Analyser). A method for displaying visual stimuli at specific luminance levels using LCD grey-scale colour levels, is described and assessed in section 5.2.3.

5.2.1 Gaze data accuracy

Two methods were used to assess the gaze data accuracy of the Tobii x50 eye tracker. An initial gaze accuracy assessment consisted of collecting gaze data while subjects fixated at 15 specific screen locations and subsequently analysing the data for accuracy at each screen location. A second, more detailed assessment was used to assess gaze data accuracy under conditions similar to those expected during an SVOP test. The following sections present these two methods and associated results.

5.2.1.1 Methods and subjects

Method 1: Gaze accuracy at 15 specific screen locations

A computer program was written (using Visual Basic .Net within the Microsoft Visual Studio 2005 development environment) to assess the accuracy of the gaze data provided by the Tobii x50 eye tracker. The hardware setup for these methods was the same as that described in section 5.1.1.3 on page 61. The program was designed to display a visual stimulus (in the form of a cross) on the display screen at 15 specific locations in a random sequence (figure 5.18 shows the screen positions used). Test subjects were instructed to fixate their gaze on the centre of the cross when it stopped at each location. Whilst the subject's gaze was fixating at each location, the program collected 20 data samples (at a sample rate of 50Hz). Each sample contains multiple fields of data and all available data fields were recorded (Appendix B shows all the data fields available from the Tobii x50 eye tracker which were collected for each sample). For each sample the program calculated the total gaze error, in pixels, using the X and Y gaze location data and the X and Y screen location of the centre of the visual stimulus (the cross). This was done for both the left and right eye data individually. From the 20 calculated gaze error values at each screen location, the average and standard deviation was calculated. The error could also be calculated in degrees of visual angle. This was done by using the "eye distance" and "X and Y eye position" data to calculate 3D eye location (as described previously in section 5.1.2) and subsequently calculating the error as a distance described by the angle subtended at the eye. Only data with validity codes of 0 (corresponding to definitely valid data) were used for these calculations. Data with validity codes other than 0 which could correspond to the eye tracker's inability to track one or both of the subject's eyes or possibly the subject blinking was analysed separately. These samples did not have any gaze data associated with them and are defined as "dropouts". Information on validity codes and their meaning is also listed in Appendix B.

The Tobii x50 eye tracker requires that a calibration procedure be performed for any particular subject's eyes in order to subsequently produce accurate gaze point estimation data. The calibration procedure presents a visual stimulus at a series of locations on the display screen. The calibration point visual stimulus is, by default, a circle which moves to, stops and repeatedly shrinks and grows at each defined screen location, but it can also be customised to be made more child friendly. During this time, the subject must fixate on the calibration stimulus, most importantly when it stops at any particular location. The number of points at which the calibration stimulus stops can also be customised. The default is 5 screen locations and the calibration procedure lasts for approximately 10 seconds.

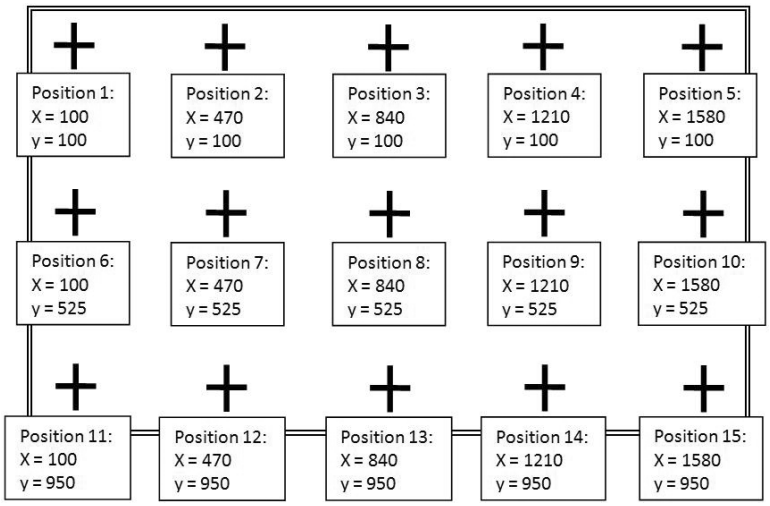

Figure 5.18: The 15 screen locations used by the gaze data accuracy program. Each screen position is numbered (1-15) and associated with a specific X and Y screen position in pixels. The screen has a resolution of 1680 by 1050 pixels in the X and Y direction respectively.

10 test subjects performed the 15 point accuracy test. All subjects performed a new default 5 point calibration prior to each of the 15 point tests. Each test was performed with a natural head movement with the eyes starting location at approximately 600mm from the eye tracker's camera and in a central location within the camera's field of view.

Method 2: Gaze accuracy under SVOP test conditions

The methods described above for the 15 point accuracy test were designed to give an early indication of the gaze data accuracy capability of the Tobii x50 eye tracker. A more in depth test was required which would assess gaze data accuracy at many more screen locations and with a larger number of test subjects with a greater age range (including healthy volunteers and also patients with visual field defects).

To do this, a first version of the SVOP software was created with the aim of data collection (rather than attempting to make any automated assessment of visual field defects). The software was written in Visual Basic .Net (within the Visual Studio 2005 development environment) and was designed to simply display a "fixation stimulus", then when a subject was gazing at the "fixation stimulus" calculate the position of a visual field point "test stimulus", display it (for 200ms) and repeat this procedure from the screen position of the last "test stimulus" while all the data given by the eye tracker was continually exported to a text file and the screen location of all the "fixation stimuli" were exported to another text file. The text files also contained time stamp data so that the screen location values could be matched to the gaze data during post test analysis. The software was designed so that it would import a series of visual field points from another text file prior to starting the process. This text file contained a list of visual field

points described by two values, ϕ and θ, which are the two angles used to define a visual field point (as described in section 5.1.3 and figure 5.8 on page 68). In this manner, any visual field test pattern consisting of any number of visual field points could be used with the software (providing of course that the visual field locations are able to fit on the display screen from any particular fixation location). The "test stimuli" corresponding to the various visual field points were designed to be displayed in a random sequence so long as they could be presented on the display screen based on the current "fixation stimulus" position. If a situation was reached where no remaining "test stimuli" could be displayed (i.e. if they would be off the screen) from a fixation point being used, a new "fixation stimulus" point would be displayed which would allow at least one of the remaining "test stimuli" to be displayed, and the test would continue in this manner until all the visual field test points had been displayed. The diagram in figure 5.19 gives a diagrammatic representation of the software program to accompany this written description.

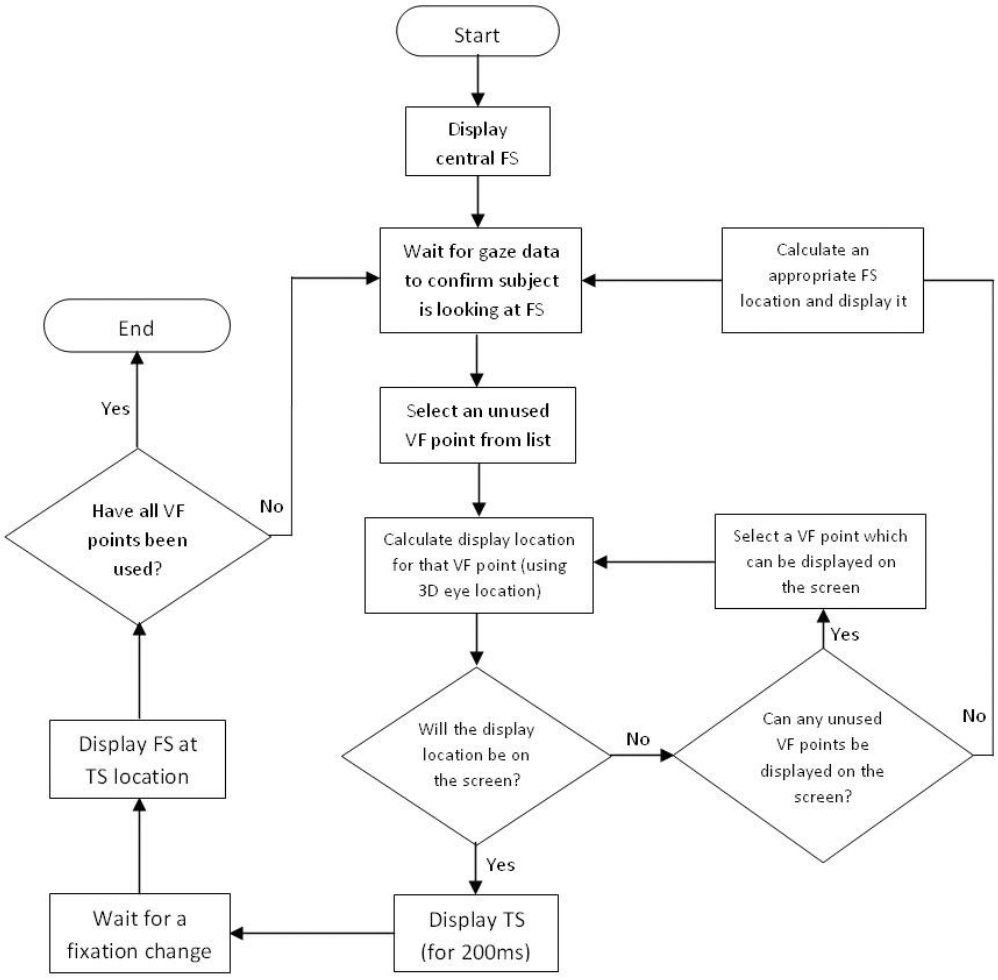

Figure 5.19: Flow diagram of an early version of SVOP software designed for data collection only. FS = "fixation stimulus". TS = "test stimulus". VF = visual field.

For these methods three different "test stimuli" test patterns were used. Two of the test patterns were used for the left and right eye respectively and were matched to the HFA C-40 screening test pattern. The third pattern used was a custom designed 40-point pattern, to be used as a binocular test pattern, which consisted of 40 points located within the first 25 degrees of the visual field and was based on a combination of the left and right eye test patterns. Figure 5.20 shows the three test patterns used. All "test stimuli" were presented at a specific luminance brightness equivalent to the 14dB level on the HFA. The method for displaying "test stimuli" at this specific brightness is detailed in a later section (section 5.2.3 on page 106), but essentially the procedure used a specific background grey-scale colour and "test stimulus" grey-scale colour to produce a "test stimulus" brightness corresponding to the HFA 14dB luminance level. All "test stimuli" were presented at the Goldmann III size for a period of 200ms.

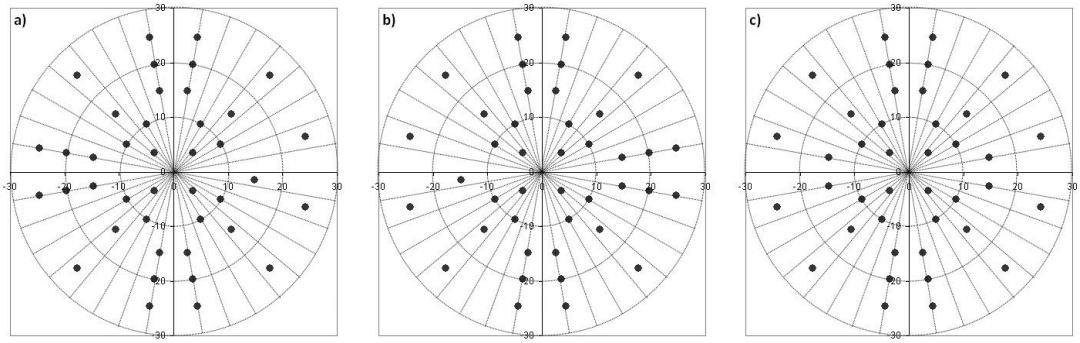

Figure 5.20: The three visual field test patterns used in the program for assessing gaze data accuracy. a) A test pattern equivalent to the right eye HFA C-40 screening test. b) A test pattern equivalent to the left eye HFA C-40 screening test. c) A custom test pattern designed for binocular testing.

38 subjects were recruited with the aim of performing the procedure 3 times (using each of the 3 test patterns once). When using the left and right eye test patterns the subject was also instructed to occlude the opposing eye with a hand held eye occluder. The eye occluder was custom built and was made out of a plastic material which was designed to transmit infrared wavelengths but block visible light. Using this material allowed the occlusion of an eye while still allowing the eye tracker camera to perceive the occluded eye. The reason this strategy was used was because of an inability of the eye tracker to provide constant data when it could only perceive a single eye. In reality not all subjects were able to perform all three tests, for example younger subjects were unable to hold the eye occluder and so only performed the procedure using the binocular test pattern. The subjects recruited and tests performed are outlined in table 5.4.

Subject groups	Number	Age (years)		Tests performed		
		Mean	Range	Binocular	Left	Right
Healthy adult	14	35.1	21-68	14	14	14
Adult patient	6	57.0	17-74	6	5	5
Healthy child	9	8.8	5-16	9	9	9
Child patient	9	7.8	2-15	9	5	5
Total	38	29.7	2-74	38	33	33

Table 5.4: The test subjects recruited and tests performed for the gaze accuracy tests.

5.2.1.2 Results

Results of method 1: Gaze accuracy at 15 specific screen locations

Figure 5.21 shows the average (± 1 standard deviation) error between the location of the visual stimuli on the screen (in the form of a cross) and the gaze data samples collected from the eye tracker while each subject was instructed to look at the centre of the visual stimuli. The 15 screen locations (labelled 1 to 15) are shown in the previous methods section (figure 5.18 on page 87). The left and right eyes were assessed separately and the error was calculated in degrees of visual angle. Figure 5.22 on the following page shows the average number of dropouts (± 1 standard deviation). One dropout is defined as when the eye tracker is unable to produce a sample which has gaze information, this occurs when the eye tracker is unable to detect the eye for any reason. Again data were collected with each subject gazing at the 15 different screen locations. At each location 20 data samples were collected, so the number of dropouts at each location per subject could range from 0 (all samples provided gaze data) to 20 (no samples provided gaze data).

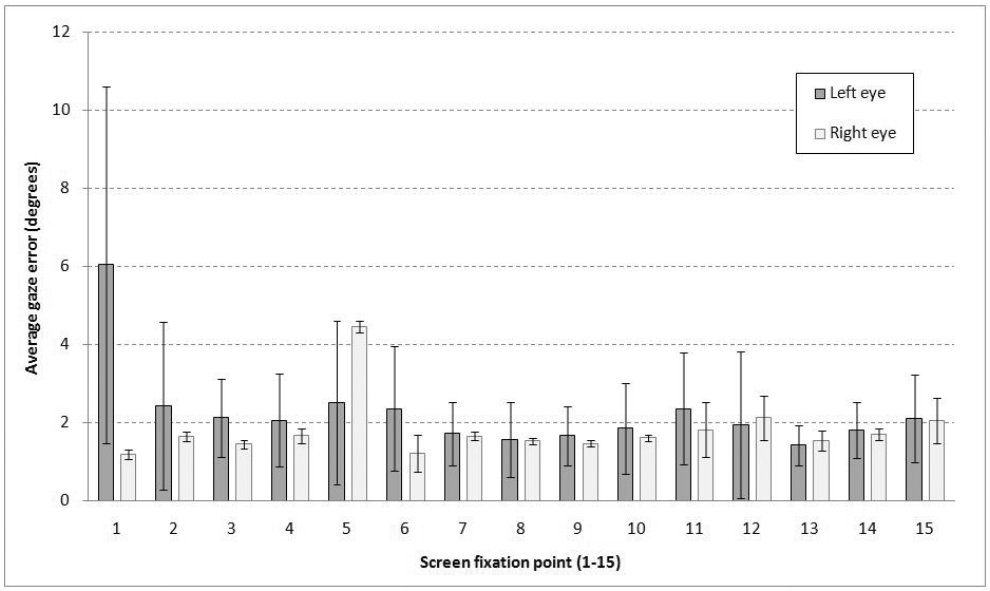

Figure 5.21: The average gaze data error (in degrees) for each of the 15 screen fixation locations for both the left eye and right eye data. Error bars are ± 1 standard deviation.

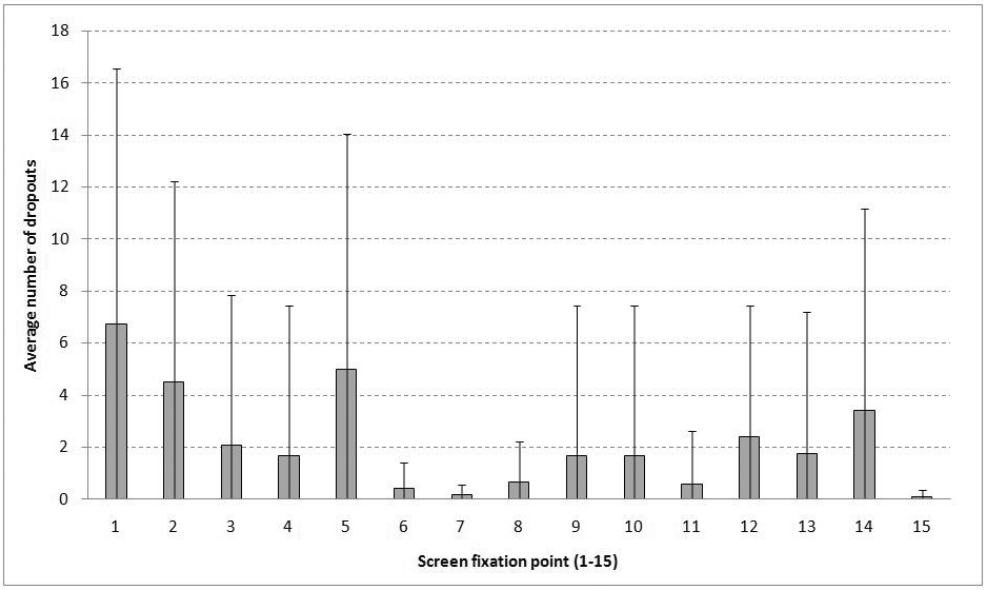

Figure 5.22: Average number of dropouts for either eye for each of the 15 screen fixation locations. Error bars are ± 1 standard deviation.

Results of method 2: Gaze accuracy under SVOP test conditions

As an example of the gaze data available from a test, figure 5.23 shows the screen coordinates of every gaze data sample collected from a single test. Also shown are the screen coordinates of each "fixation stimulus" used during the test. From this figure, the nature of the gaze data

which typically constitutes "fixation" can be visualised. There is typically a "cluster" of gaze data coordinates in an area close to the "fixation stimulus", with a varying degree of accuracy of the gaze data. Gaze data coordinates which do not belong to any "clusters" (in figure 5.23) are samples which happen to have occurred while the test subject was in the process of moving their fixation from one screen location to another.

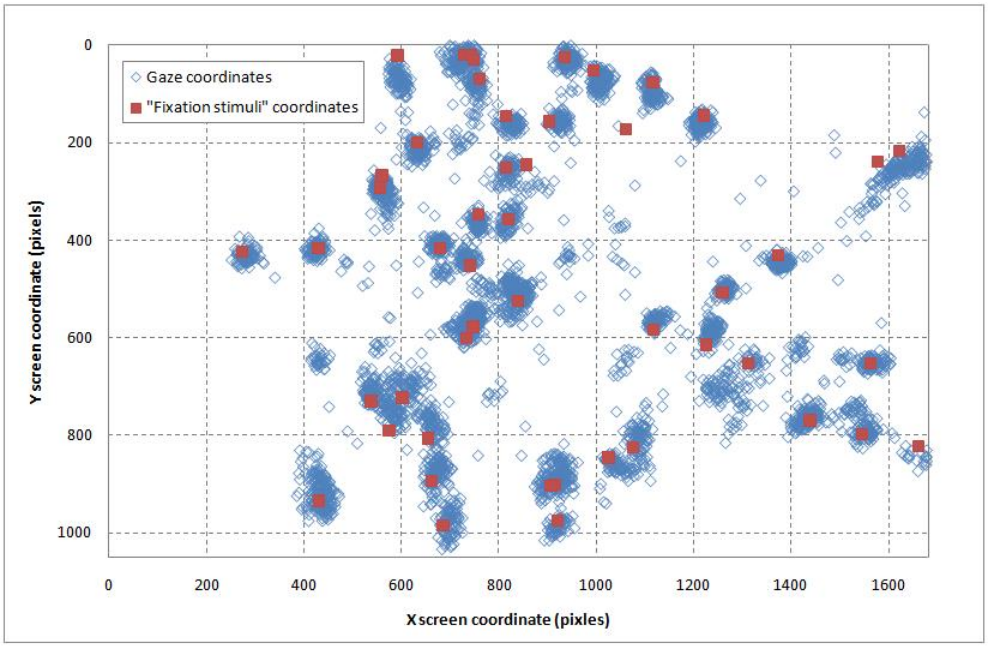

Figure 5.23: Example of all the gaze data coordinates and "fixation stimuli" coordinates from a gaze data test.

From the data collected from each test, the average gaze data error (difference between the fixation stimulus coordinates and the gaze data coordinates) was computed using 20 gaze data samples following the presentation of each "fixation stimulus", this data was then categorised according to the screen location of the "fixation stimulus" such that the screen was divided up into a grid of rectangular sections measuring 168x175 pixels each. All the error data values (previously computed) which were located within each individual grid "square" was then averaged. Figure 5.24 shows this data in contour plots (for both the average error values and one standard deviation) separated into data from binocular, left eye and right eye tests.

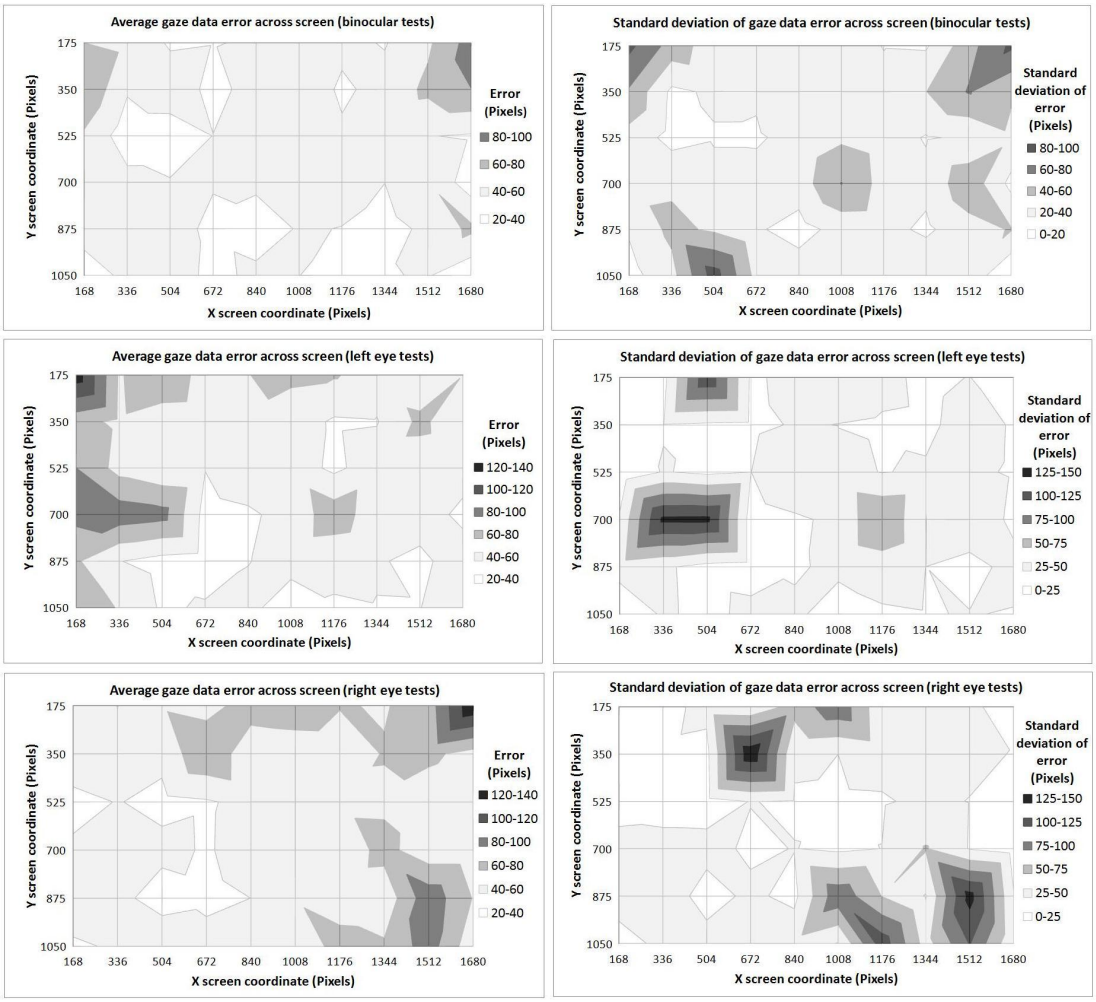

Figure 5.24: Average (left hand plots) and value of 1 standard deviation (right hand plots) of gaze data error in pixels for locations across the display screen for binocular (top row), left eye (middle row) and right eye (bottom row) tests.

The same procedure was used to calculate the average and standard deviation of the number of dropouts during each of the 20 data samples collected such that the average number of dropouts for different screen location grid "squares" are calculated for each type of test (left, right and binocular). This data is shown in figure 5.25 as separate contour plots for the average values and one standard deviation, for each type of test (binocular, left and right eye).

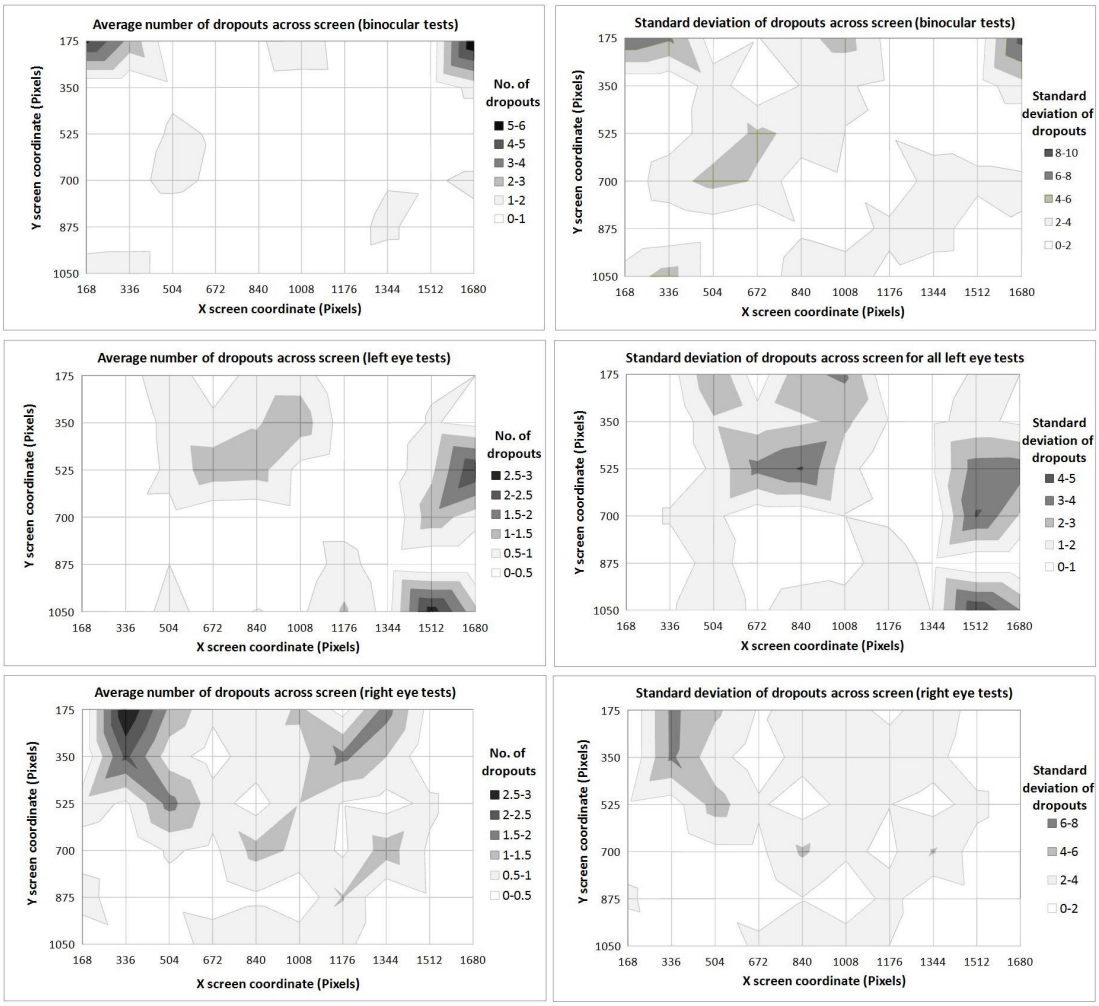

Figure 5.25: Average (left hand plots) and value of 1 standard deviation (right hand plots) of the number of dropouts for locations across the display screen for binocular (top row), left eye (middle row) and right eye (bottom row) tests.

5.2.1.3 Discussion

The 15 point gaze accuracy test was designed as an initial test following the purchase of the Tobii x50 eye tracker, and was performed with normal, healthy subjects. The main purpose of these tests was to investigate the general performance of the eye tracker's gaze data accuracy and provide an early assessment of its suitability for the proposed SVOP system. The second gaze accuracy test methods (gaze accuracy under SVOP test conditions) were designed to act as a more detailed look at gaze accuracy under conditions similar to that of a SVOP test with the inclusion of adult and child patients in addition to healthy adult and child volunteers.

The average gaze errors were measured to be less than the previously described minimum gaze error requirement of $\pm 2.5°$ (5.1 on page 54). Only when gaze location was fixating towards the top left and top right corners of the display screen did the gaze error increase to a level above

the minimum required gaze accuracy.

The results from both gaze data accuracy test methods showed similar results in terms of screen locations where the eye tracker provided less accurate gaze data. Less accurate areas (or "problem areas") were mostly confined to the corners and vertical sides of the display screen, in particular the top two corners, the left side of the screen when testing a subject's left eye and the right side of the screen when testing the right eye. However, not all subjects showed reduced gaze data accuracy in these screen corner regions. This can be seen by the increased variability in these areas (from the contour plots of the standard deviation of gaze errors in figure 5.24). Decreased gaze data accuracy on the same side as the eye being tested in uniocular tests was at first surprising but may be explained by the relative position of the eyes and the eye tracker's centrally located camera. Even with uniocular tests the eye being tested was not located centrally in the camera's field of view. Instead, it would normally be located slightly to one side of the camera depending on the eye in question. As a result it is possible that it becomes harder for the eye tracker's camera to accurately identify the required reflections from the eye when it is rotated more away from the direction of the camera's field of view, and hence harder to produce as accurate gaze data.

Dropouts (or areas where the eye tracker lost track of one or both eyes) also occurred in some similar "problem areas" as those where the gaze data accuracy was reduced. It is not surprising that dropouts had a greater tendency to occur when fixation was towards the vertical edge screen locations. However, the side of the screen where dropouts occurred was predominantly the opposite side the the eye being tested in uniocular tests. This was unusual but may simply be due to a lack of data available for analysis on the sides which did not demonstrate a larger amount of dropouts (as the low standard deviation in these areas indicates).

These tests have identified some approximate areas of the screen where eye-tracking may not always be possible or where gaze data accuracy could potentially be reduced. These "problem areas" were not consistent across all subjects tested. However, it is useful information to be considered in the development of the SVOP testing system.

Using the eye tracker in these tests with some patients with visual field defects also highlighted some potential problems with eye tracking in this patient population. With one patient, there was no eye tracking data obtained for one of their eyes which had a persistent right enlarged pupil. This highlights that eye tracking may not be possible in certain patients where the eye shape has been changed in some way (for example due to surgical procedures). Further descriptions and details of eye tracking problems within patients is described in a section dedicated to the limitations of the SVOP system (section 5.5 on page 139) which appears at the end of this chapter.

The gaze data results obtained here can be used to create a fixation algorithm for the proposed

SVOP software which is designed to define when a subject is fixating at a particular stimulus. Fixation data from the eye tracker consisted of a series of gaze data coordinates which correspond with what was presented on the screen (i.e. the stimulus which the subject was fixating on). From the data collected it can be seen that a series of gaze coordinates, which correspond to a fixation point, vary in coordinates from sample to sample (samples occur every 20ms). This is due mainly to small errors in the eye tracking in this situation (rather than naturally occurring fixational "micro-saccades"). Two possible scenarios occur: (i) either a series of gaze coordinates is well "clustered" at the screen coordinates of the "fixation stimulus"; or (ii) there is an error in the location of the gaze coordinates, but they are still well "clustered". In either case it can be inferred that a subject is gazing at any particular known "fixation stimulus" location if this "clustering" is within a certain range of the "fixation stimulus" coordinates and remains well clustered for a set period of time. From these data, a fixation detection algorithm was developed which used some simple rules to determine fixation. If, over a time period equal to 20 consecutive gaze data samples (400ms), every one of those 20 gaze coordinates is within ± 100 pixels (approximately equal to $\pm 2.5^{\circ}$ visual angle) of the "fixation stimulus" then this constitutes fixation on that "fixation stimulus".

5.2.2 Distance data accuracy

The proposed SVOP visual field assessment system allows the patient some freedom of head movement during the test so long as they stay within the Tobii x50 eye tracker's camera field of view. This is made possible because the eye tracker provides data which allows the calculation of the 3D location of the patient's eye(s) in real time. This means that at any point during the test the position of the subject's eye(s) should be known. This 3D eye positional data then allows the calculation of the "test stimulus" screen location for any particular point within the patient's visual field which is to be assessed (as described in the theory section 5.1.3). As such, the accuracy of any particular "test stimulus" location (i.e. how well the calculated "test stimulus" screen location corresponds to the intended visual field point which is to be assessed) is related to the accuracy of the calculations which describe of the 3D position of the patient's eye(s). As described in section 5.1.2, the calculation of the 3D position of the eye(s) depends primarily on the "eye distance" data provided by the eye tracker.

Because the accuracy of the screen position of the "test stimuli" are clearly a very important aspect of the proposed SVOP system, the methods and results sections which follow describe an assessment of the accuracy of the eye tracker distance data which can be used to assess how this accuracy (or rather any error) impacts upon the accuracy of the calculated "test stimuli" screen location.

There are two methods described in this section. The first is used to assess the accuracy of the

distance data provided by the eye tracker, and the second is used to assess the accuracy of the 3D eye position calculated data (e_x , e_y , and e_z).

5.2.2.1 Methods

Method 1: Stationary head

The computer program used in section 5.2.1.1 to assess the Tobii x50 eye tracker's gaze data accuracy at 15 specific screen locations was used, again with the same system setup as described in section 5.1.1.3 on page 61. The program displayed a visual stimulus (in the form of a cross) on the display screen at 15 different locations in a random sequence and a test subject was instructed to fixate their gaze at the cross when at each of the 15 screen locations. However, during this test subjects had their head maintained in a fixed position. Because the head location (and hence 3D eye location with respect to the eye tracker) was kept stationary, theoretically the distance data provided by the eye tracker should remain constant throughout the test. As described in the gaze data accuracy methods, the computer program collected 20 data samples (at a rate of 50Hz) when a subject was fixating at each screen location. However, this time the program was altered to calculate the average and standard deviation of the distance data provided by the eye tracker (for both the left and right eyes) with fixation at each screen location, rather than make gaze error calculations.

10 test subjects performed the 15 point test. All subjects performed a new default 5 point calibration prior to each of the 15 point tests. Each test was performed with the eyes at a location of 600mm from the eye tracker's camera and in a central location within the camera's field of view.

Method 2: Head movement

In order to make an assessment of the 3D eye position data (calculated using data fields provided by the eye tracker) while a subject is moving within the eye tracker camera's field of view, a secondary method of accurately monitoring 3D eye location and motion relative to a fixed point is required. One method of gaining this secondary positional data is by using magnetic tracking. Magnetic tracking uses a transmitter and a receiver (or sensor) to provide real-time 3D positional data (x, y and z coordinates) of the receiver relative to the transmitter which can be kept at a fixed point.

Magnetic trackers operate by measuring the electromagnetic field strength, at a sensor location, of magnetic fields generated by a transmitter.[112,113] Usually the sensor is attached to some moving object which is to be tracked, with the other placed at a fixed location, serving as a reference point. Magnetic tracking devices function by measuring the strength of the magnetic

fields generated by sending current through three orthogonal electromagnets in the transmitter. The receiver also has three orthogonal wire coils embedded in it. By sequentially activating each of the transmitter electromagnets and measuring the magnetic fields generated on each of the three perpendicular sensor wire coils, the resultant set of data contains sufficient information to determine both the position and orientation of the sensor relative to the transmitter.

A magnetic tracking device (WinTracker II from VR-Space Inc. Taiwan) hereafter referred to as the Magnetic Head Tracker (MHT) was selected to be used as the secondary motion tracking device which would enable an assessment of the accuracy of the Tobii eye tracker's eye positional data. Before the MHT could be used for this purpose an assessment of its own accuracy needed to be made. If the accuracy of the MHT can be defined, this will allow accurate statements to be made about the precision of the eye tracker positional data. The manufacturers specification on the accuracy of the MHT state that it has a 1.52mm RMS (root mean square) static accuracy at a distance of 750mm. This information is not particularly useful as it only provides accuracy data when the receiver is stationary in one location. What would be more useful is knowledge about the errors dependence on the distance between the transmitter and receiver.

The MHT accuracy was assessed by positioning the receiver at known 3D locations (x, y and z coordinates) from the transmitter and collecting the MHT positional data, so providing a 3D map of the MHT's accuracy. The MHT was found to have the most accurate positional data when the receiver was located within a specific volume of space with respect to the transmitter. This error was found to be within approximately $\pm 20mm$ when the transmitter to receiver distance was greater than 100mm and less than 400mm. This fact was used to construct an "add-on" for the SVOP system equipment such that the transmitter was positioned as shown in fig 5.26 allowing the receiver (which would be attached to the subject's head using a head band) to be situated within this "accurate volume" when a subject's eye(s) were positioned at approximately 600mm from the tracker camera and located centrally within the camera's field of view.

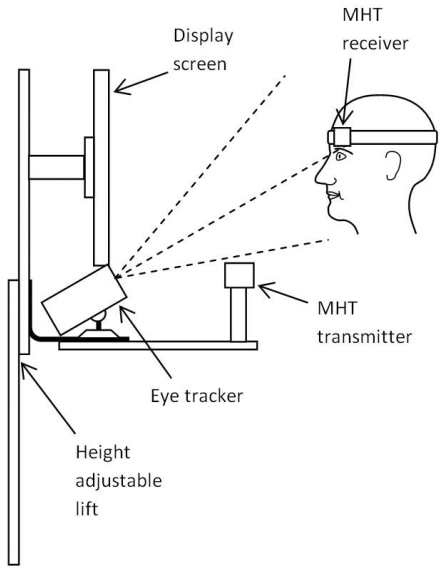

Figure 5.26: Experimental setup for distance data tests using a magnetic head tracker (MHT).

A computer program was written to continually collect positional data (x, y and z) from both the eye tracker and MHT, each at the same rate of 50Hz. This was accomplished by using the fact that new data from the eye tracker was known to be sent to the PC at the rate of 50Hz, and so each time the program received data from the eye tracker, it would also collect a positional data set from the MHT. The 3D eye positional data (x, y & z coordinates) for the eye tracker were calculated using the calculations outlined in the theory section 5.1.2 on page 62. The program was designed to continually export both sets of 3D positional data to a text file until the computer operator manually stopped the process.

A subject was positioned as shown in figure 5.26. They had one eye covered and were positioned so that the uncovered eye was positioned at 600mm from the eye tracker's camera and was located centrally within the camera's field of view. The MHT sensor was placed just above the uncovered eye by the use of a head band. While the program was running and collecting the positional data, with the subject kept stationary and fixating at a stimulus located centrally on the display screen, the whole SVOP setup was moved in a horizontal direction perpendicular to the direction in which the subject was facing. The direction of the horizontal movement was reversed each time the eye moved outside of the eye tracker's camera field of view. The SVOP system was mounted on a movable trolley, allowing it to be moved in this manner. Secondly, this process was repeated with vertical movements by raising and lowering the height of the SVOP system (i.e. the eye tracker, display screen and MHT transmitter) again reversing the vertical movement direction each time the eye moved outside the eye tracker Camera's field of view. These processes were repeated until several direction changes had been completed.

The data collected using these methods:

1. allows a direct comparison of positional data between the eye tracker and the MHT; and
2. gives values for the box size at a specific distance of 600mm from the eye tracker. The effect of keeping the subject's eye stationary, but moving the eye tracker and MHT has the effect of a moving subject but allowed the movement to be precisely controlled, thus allowing an accurate measure of the box size lengths (while at the same time allowing an assessment of the eye positional data accuracy).

5.2.2.2 Results

Results of method 1: Stationary head

Figure 5.27 shows an example of the distance data recorded with a fixed head position whilst the eye gaze point is varied to fixate on the previously described 15 display screen locations. The actual camera-to-eye distance was kept constant at 600mm, so this chart reveals the error in this distance data when eye fixation is positioned at varying locations on the screen.

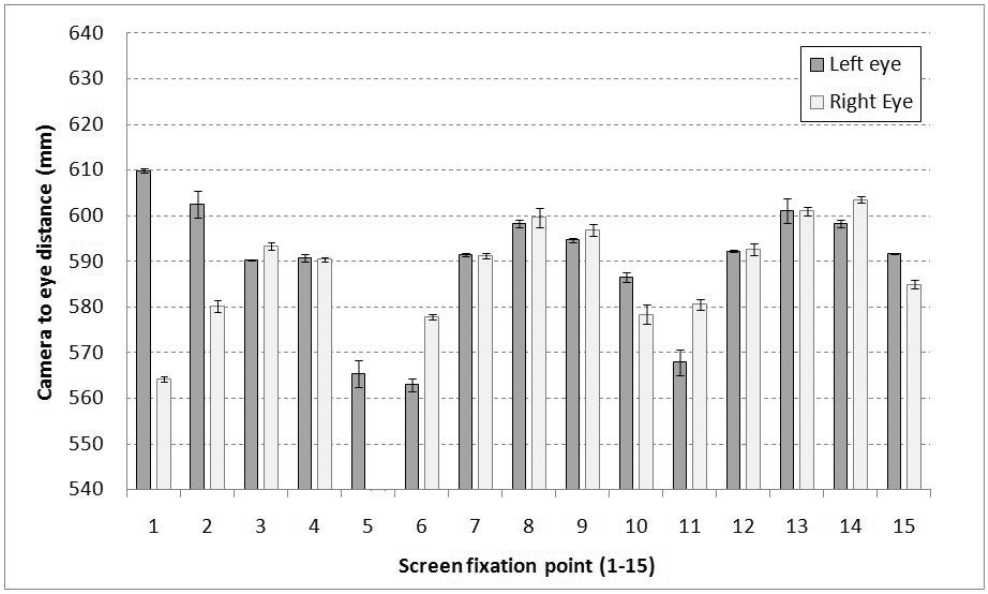

Figure 5.27: Distance data variation with stationary head position while varying the point of fixation.

Results of method 2: Head movement - including MHT accuracy

Figure 5.28 shows four charts which represent the 3D location of the single eye, as it repeatedly moves in a horizontal direction across the eye tracker camera's field of view, as represented by

the data (and subsequent calculation) collected from the eye tracker and data collected from the magnet head tracker (the WinTracker). There are four charts, one each to represent the x, y, and z coordinates from the eye tracker camera (charts a, b and c), and the absolute distance (chart d). Theoretically, the x coordinate should increase and decrease about zero such that the difference between the minimum and maximum values equals the horizontal size of the eye tracker camera's field of view (at a specific distance of 600mm from the camera). Also, theoretically, the y and z coordinates should remain constant as the eye should be moving in a horizontal direction only. The absolute value should increase as the eye moves away from the centre horizontal point (where x = 0) and decrease as the eye moves towards the centre horizontal point.

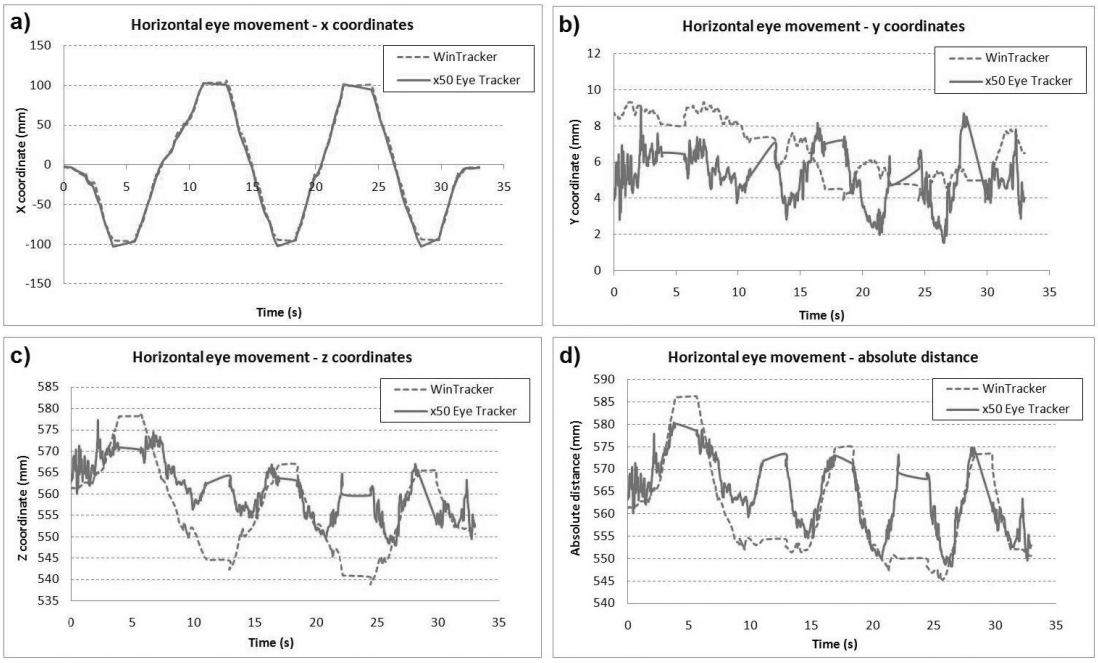

Figure 5.28: Horizontal eye movement x, y, z and absolute values as recorded by the eye tracker and MHT.

Figure 5.29 also shows four charts which represent the 3D location of the single eye, this time as it repeatedly moves in a vertical direction through the eye tracker camera's field of view, as represented by the data (and subsequent calculation) collected from the eye tracker and data collected from the magnet head tracker (the WinTracker). There are four charts, one each to represent the x, y, and z coordinates from the eye tracker camera (charts a, b and c), and the absolute distance (chart d). Theoretically, the y coordinate should increase and decrease about the zero value. The difference between the minimum and maximum values of y should be slightly more than the vertical size of the eye tracker camera's field of view (again at a the distance of 600mm from the camera) because we are taking a vertical "slice" through the field of view which is set at an angle of 70 degrees to the vertical. Also, theoretically, the x and

z coordinates should remain constant as the eye is moving in a vertical direction only. The absolute value should increase as the eye moves away from the centre vertical point (where y = 0) and decrease as the eye moves towards the centre horizontal point.

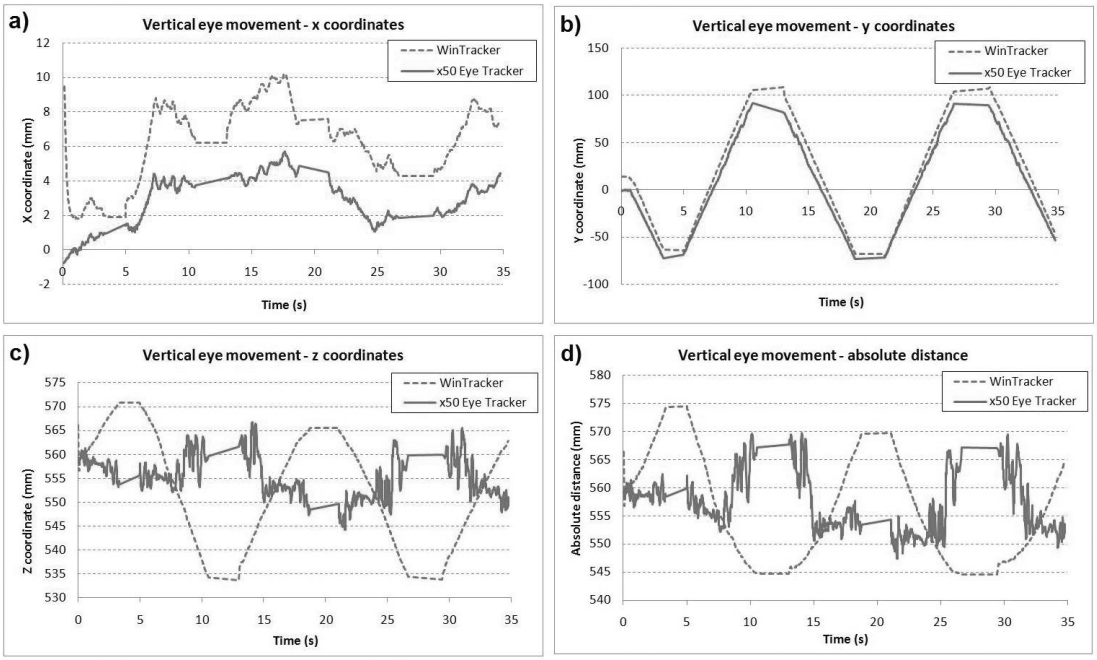

Figure 5.29: Vertical eye movement x, y, z and absolute values as recorded by the eye tracker and MHT.

Table 5.5 details the values of the horizontal and vertical box size as measured using the maximum and minimum values obtained from the eye tracker data and the MHT data.

Tracking device	Horizontal (X) direction (mm)		Vertical (Y) direction (mm)	
	Average	Standard deviation	Average	Standard deviation
Eye Tracker	199.6	3.1	159.6	3.8
MHT	197.5	2.2	172.7	3.1

Table 5.5: X50 eye tracker head movement box size at a camera-to-eye distance of 600mm.

5.2.2.3 Discussion

1. Stationary head

The Tobii x50 eye tracker uses a triangulation method to calculate the distance of the eyes from the eye tracker camera.[114] The distance is calculated using the known separation of the two infrared light sources located either side of the centrally located camera, the distance between

the reflections from the eye of each of the two separate infrared light sources (as seen by the eye tracker's infrared camera), and an assumed value for the radius of curvature of the eye.

The accuracy of this method for calculating distance was assessed in a simple manner using the "stationary head" assessment methods with a subject's eyes positioned at a known distance from the eye tracker's camera (through the use of a specifically positioned chin-rest). Distance data from the eye tracker was recorded while the subject held their gaze at 15 different screen locations in turn. The purpose was to investigate the accuracy of the distance data and also to assess the effect of eye fixation location on the distance data accuracy. Figure 5.27 shows clearly how the point of fixation has an effect on the accuracy of the eye tracker's distance data, with the most accurate data provided when the subject was fixating more towards the centre of the screen (where the centre of the screen is located directly above the eye tracker's camera). As gaze position moved further towards the display screen left and right (and also to an extent the top) edges, the distance data showed an increase in error.The effect is seen most notably with fixation at the top corners of the screen where the distance data error increased by up to 40mm. However, the distance data errors when fixation was in these areas were significantly larger than at any of the other fixation points. If these areas were to be excluded, the error reduces to a maximum of 20mm and therefore will meet the minimum requirement for the eye location accuracy outlined in table 5.1 on page 54.

These results suggest that if a subject was looking at far left or right areas of the screen (in particular the top corners) and the distance data was used to make the calculation for a visual field "test stimulus" screen location at that moment, there would be a larger error in the calculated "test stimulus" screen location. As a result, these far left and right areas are not used as "fixation stimulus" locations.

The implications of the errors in the distance data on visual field "test stimulus" screen location are assessed in a separate section dedicated the assessment of "test stimulus" screen location (at the end of this chapter) where the error values found here (excluding the extreme errors with fixation in the left and right sides) are used to model and assess the implications on "test stimulus" screen location error.

2. Head movement

The purpose of the "head movement" experiments was to make an assessment of the accuracy of the 3D location data of an eye with respect to the eye tracker's camera (as calculated using the eye tracker distance data and horizontal and vertical eye location data within the camera's field of view. The details of this calculation are outlined in section 5.1.3). In addition, these measurements were also designed to provide an assessment of the two constant values used in the aforementioned calculations, namely the horizontal and vertical camera field of view

size at the specific camera-to-eye distance of 600mm. These values are given in the Tobii x50 eye tracker specifications as 200mm and 150mm respectively, and these experimental methods would also allow these values to be verified.

Figure 5.28 shows the horizontal eye movement x, y, z coordinates and absolute distance value as recorded (and calculated) by the eye tracker and MHT. Chart a) of this figure demonstrates that the x-coordinate of both the MHT and eye tracker calculated values are in close agreement and the size of the horizontal camera field of view (measured as the average range between the minimum and maximum x-coordinate values) are also in good agreement (table 5.5). Importantly, these values are also in agreement with the horizontal field of view size defined in the eye tracker's specifications (200mm). Charts b) and c) of figure 5.28 demonstrate possible error values in the y-coordinate and z-coordinate directions respectively. Theoretically these values should have remained constant during the experiment as only movement in the x-direction was created. The error measured in the y-coordinate direction equates to just a few mm for both the MHT values, and eye tracker calculated values, and up to 20mm in the z-coordinate direction for the eye tracker calculated values but almost double that for the MHT values in the z-coordinate direction. This larger error with the MHT could indicate that there is increased error in the MHT data when the receiver is located at these larger absolute distances from the transmitter. This is also consistent with what was previously calculated when considering the ideal transmitter location setup.

In figure 5.29, chart b) shows the y-coordinate values measured when the movement was in the y-coordinate (vertical) direction, and again good agreement between the MHT values and the eye tracker calculated values was obtained. However, the agreement was not as accurate as that obtained with the x-coordinate values during horizontal movement. The average range of the vertical movement calculated using the two measurement techniques (MHT and eye tracker calculated values) were in disagreement by $\sim 13mm$ ($\sim 160mm$ for the eye tracker values and $\sim 173mm$ for the MHT values, table 5.5) and neither of these values matched the stated Tobii x50 specification of 150mm for the vertical field of view at 600mm from the camera. However, the values measured under these experimental conditions were in fact a vertical slice through the eye tracker camera's field of view which was tilted at an angle of 20° to the horizontal (figure 5.30). When this is taken into consideration, the theoretical vertical "slice" length through the camera's field of view is 160mm which is in very good agreement with the eye tracker calculated average value. Chart c) in figure 5.29 which shows the z-coordinate values again casts doubt over the accuracy of the MHT values because in theory the z-direction values should remain constant under the described experimental conditions. The eye tracker calculated z-coordinate values show an error of $\sim \pm 13mm$, whereas the MHT shows an error of $\sim \pm 15 - 20mm$ which appears to vary in a very well defined way, increasing as movement of the MHT receiver's absolute distance from the transmitter increases.

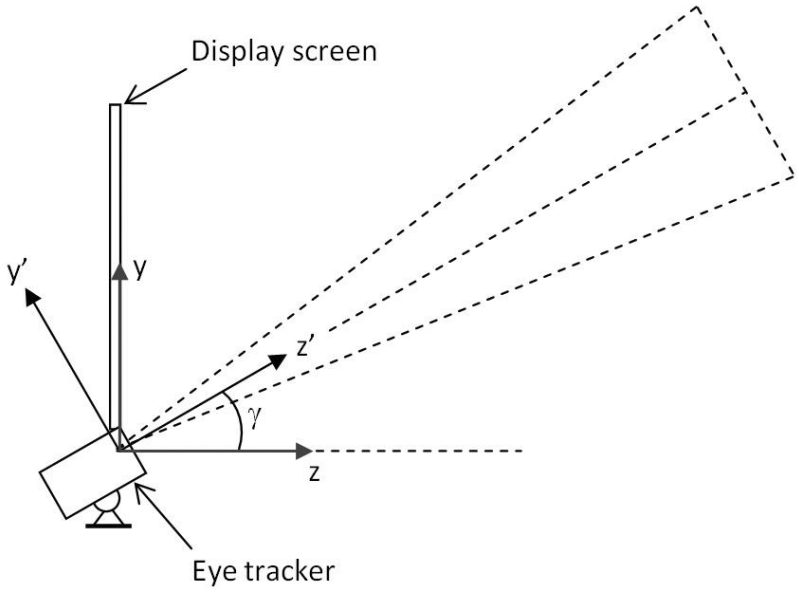

Figure 5.30: Side view of display screen and eye tracker. The eye tracker is positioned at an angle to the horizontal and so its field of view is also at this angle.

Some positive outcomes are seen from these results. There is good agreement between the eye tracker calculated values for camera horizontal and vertical field of view sizes and relatively small errors observed. The agreement observed between the eye tracker calculated values for the camera's horizontal and vertical field of view (at a distance of 600mm) and the values stated in the x50 eye tracker's specifications is perhaps not too surprising as the calculations used these specified constant values. However, these results have given some confidence to the 3D eye location coordinates as calculated by the eye tracker distance data. The errors measured here are later used in a detailed assessment of errors and their implications in section 5.5 at the end of this chapter.

There is a question over whether the MHT technique can be used to accurately evaluate the accuracy of the x, y and z eye location measurements of the eye tracker because the MHT also has error associated with its data. Although the MHT error was measured to be less than 20mm when the transmitter was within approximately 400mm from the transmitter, the error had a dependence on the transmitter to receiver distance. Additionally, there are other errors associated with using the MHT. It is difficult to determine the exact location of the receiver (worn on the subject's head) relative to the subject's eye. However, the MHT was practical for the experimental methods used here to confirm the eye tracker's horizontal and vertical camera field of view dimensions. As with the "stationary head" methods these experiments were only done with a single subject and a more detailed analysis would include additional subjects to further verify the results obtained.

5.2.3 Screen luminance

Another important hardware item to consider in the SVOP system is the display screen. To enable a comparative test (with the HFA) and also to obtain meaningful specific brightness values for the "test stimuli" to be displayed, a method of presenting stimuli of specific known screen luminance levels must be created, and the display screen's ability to display them accurately must be assessed. As discussed in section 2.3.2.4 on page 19, many of the well-known perimetry devices use different luminance levels to display stimuli of varying brightness intensity. This allows particular numerical values to be assigned to the "test stimuli" used and hence allows a numerical description to be assigned to a patient's visual field. The HFA for example, uses a projection system and light attenuating filters to display stimuli at specific luminance levels on a bowl shaped screen which is illuminated with a specific background luminance.

Because the proposed SVOP system uses a flat panel LCD screen rather than a projection system (as seen in the HFA for example), the way in which different luminance levels are displayed will be inherently different. LCD screens work by producing coloured images by filtering a white back-light. The back-light is typically provided by fluorescent tubes positioned at the back of the LCD screen.

An LCD is made of several layers. Light from the fluorescent back-light passes through a layer of light polarising material, a layer containing the liquid crystal material, and another layer of polarising material rotated by 90 degrees with respect to the first polarising material layer. Light can pass through the arrangement of layers when the liquid crystal component has a small electric current passed through it, forcing it to align with the orientation of the polarising filters. LCD monitors allow each pixel to be activated individually. Individual liquid crystal pixels, arranged in a grid, each allow a metered amount of the white light through. Each pixel contains three sub-pixels which are each paired with a coloured filter to remove all but the red, green or blue portion of the light from the original white source. The sub-pixels are small enough that when the display is viewed from even a short distance, the individual colours blend together to produce a single pixel of colour. The shade of colour for each pixel can be controlled by changing the relative intensity of the light passing through each of the sub-pixels.

So, with an LCD screen, the light provided by the back-light (fluorescent lamps) is essentially being attenuated and filtered to produce different colours. Because of this fact, different colours will produce varying levels of luminance as more or less back-light is allowed to pass. This property can be used to develop a method which comprises different colours to produce different levels of luminance. Colour produced by pixels in a LCD screen can be expressed as an RGB triplet (R,G,B), corresponding to a red, green and blue component. Each component can vary from zero to a defined maximum value. If all the components are at zero the resultant colour is black, if all values are at a maximum, the result is the brightest white that the screen is capable

of displaying (which is related to the brightness of the florescent tube back-light). Typically in computing the component values are stored as integer numbers in the range 0 to 255, which is the range that a single 8-bit byte can offer (by encoding 256 distinct values). Bearing this in mind, the most obvious method for generating various distinct levels of luminance would be to use the luminance levels generated by different colours to produce a scale of increasing luminance. Grey-scale level colours are produced by setting the R, G and B (red, green and blue) levels equal to each other, and would be a simple method to employ. The maximum luminance will have RGB level of (255, 255, 255) and the minimum will have RGB = (0, 0, 0). Grey-scale levels in-between will produce levels of luminance between the minimum and maximum values.

In order to implement this method of using grey scale levels to present stimuli of specific luminance in the proposed SVOP system, the luminance values of the grey-scale levels which the display screen produces first needs to be assessed. Additionally, the uniformity of the display screen must also be assessed in order to identify any uniformity variation in brightness across the screen. This is important because the proposed SVOP system could feasibly present a "test stimulus" almost anywhere on the display screen. Any display screen brightness uniformity variation would result in a "test stimulus" being of a slightly different brightness in one screen location as compared to another, even if both stimuli were presented at the same grey-scale level (i.e. the same intended luminance).

The following sections detail the methods and results used to:

1. assess the LCD screen brightness values produced by varying grey-scale levels in order to quantify the possible levels of brightness which the SVOP system can produce using an LCD screen,

2. assess the LCD screen brightness uniformity in order to assess how a stimulus of a single grey-scale level could potentially vary in brightness when displayed at different screen locations.

These two assessments can be made using the same methodology and experimental setup which is described in the next section.

5.2.3.1 Methods

A luminance meter (L203 photometer from Macam Photometrics Ltd. Livingston, UK) was used to make luminance measurements from 77 different screen positions. A computer program was written (using Visual Basic .Net within Microsoft Visual Studio 2005 development environment) which would run on a PC which controlled the LCD display and which was also

connected to the luminance meter via an RS232 serial port connection. The program was run each time the light meter's sensor was positioned facing toward each screen location. The program displayed grey-scale level colours on the LCD screen from an R=G=B value of 0 up to 255 in steps of 15. While each colour was displayed on the screen the program would instruct the light meter to start collecting luminance values. At each grey-scale colour level 20 luminance values were collected and were exported to a separate text file. The program was run with the luminance meter sensor directed at each of the 77 different screen locations, resulting in both luminance values for varying grey-scale level values and also an indication of the luminance variation across the display screen. This method was performed by positioning the photometer sensor in two different ways. First, each of the 77 screen locations was assessed by placing the sensor in direct contact with the screen at each location. Secondly, with the photometer sensor placed at a central location in front of the display screen and at a distance of 600mm from the eye tracker (resulting in a distance of 564mm from the centre of the LCD screen). The photometer had a measuring angle of 6 degrees, so the screen positions were arranged such that the screen area subtended by 6 degrees from the central photometer location would always fully contain display screen pixels (i.e. all of the measured area would be from the display screen) and adjacent screen positions overlapped by approximately 20mm. Figure 5.31 shows this setup.

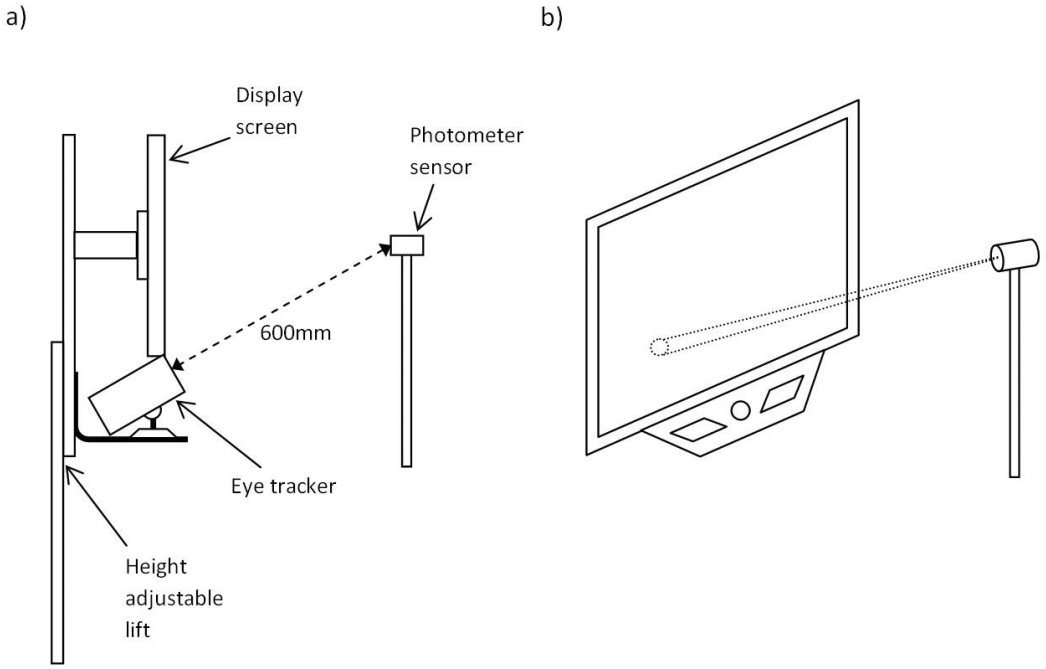

Figure 5.31: Experimental setup for luminance measurements.

5.2.3.2 Results

Figure 5.32 shows the luminance measurements made when the photometer's sensor was placed directly on to the display screen at each of the 77 screen locations. Each chart within the figure shows the luminance values (in Cd/m^2) represented as a colour contour map based on the 77 locations. The 4 charts represent the luminance measured from the screen while it was displaying 4 different grey-scale colours across the whole screen. These grey-scale colours correspond to RGB levels equal to 45, 105, 165 and 225. These luminance measurements were performed with 18 different grey-scale RGB levels. However, only 4 are shown here as examples of how the luminance from the display screen increases as the grey-scale RGB value increases, and to demonstrate the variation in luminance across the display screen.

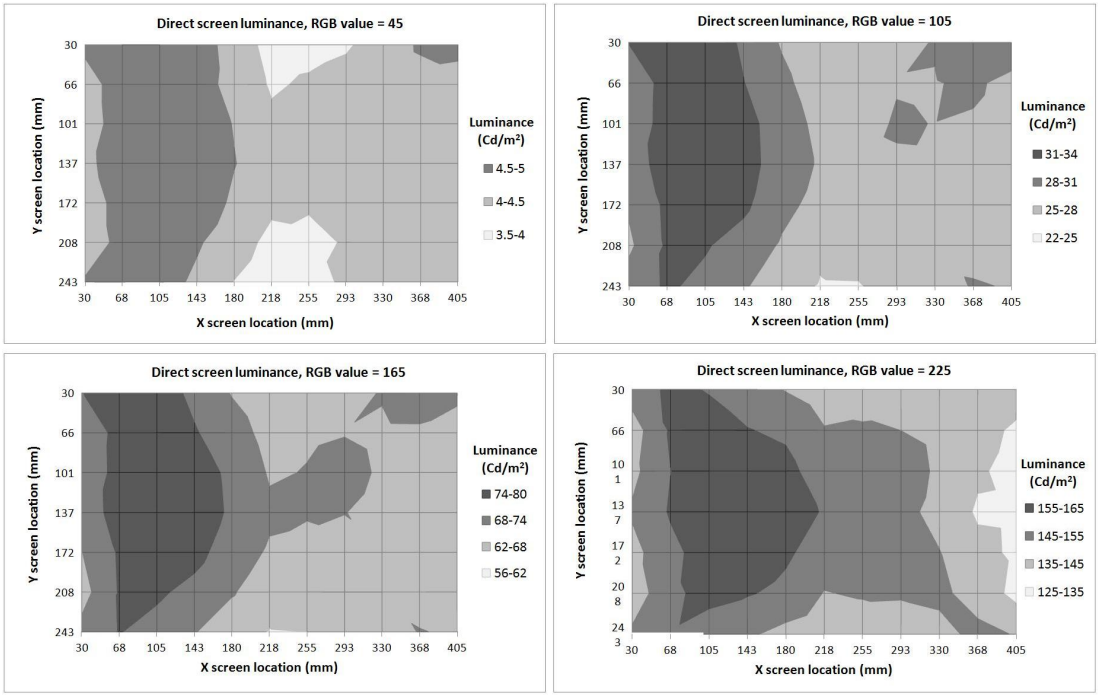

Figure 5.32: Four examples of across screen luminance variation from display screen using direct measurements. The four examples are from different RGB screen grey levels of 45, 105, 165 and 225.

A more realistic situation, when considering the proposed SVOP system and technique, is the display screen luminance viewed from a location in front of the screen which more closely matches the approximate location of a patient's eye(s) during an SVOP test. Figure 5.33 shows the luminance measurements made with the photometer's sensor placed at a location corresponding to a central location in front of the display screen and at a distance of 600mm from the eye tracker, corresponding to the proposed starting location of a patient's eye(s) at the beginning of an SVOP test. Again, each chart within the figure shows the luminance values (in Cd/m^2) represented as a colour contour map based on the 77 measurements made. The

4 charts represent the luminance measured from the screen while it was displaying 4 different grey-scale colours across the whole screen. These grey-scale colours corresponded to RGB levels of 45, 105, 165 and 225 to give four examples of how the luminance from the display screen once again increases as the grey-scale RGB value increases, and also to demonstrate the variation in luminance across the display screen when viewed from this specific location in front of the display screen.

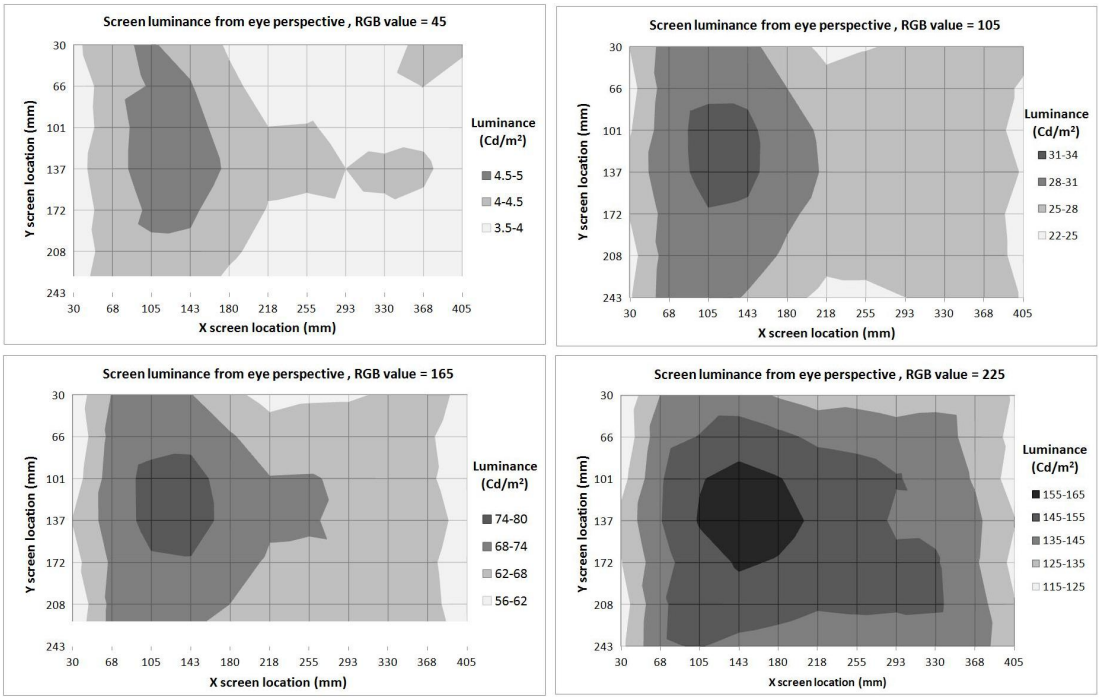

Figure 5.33: Four examples of across screen luminance variation from display screen using eye perspective measurements. The four examples are from different RGB screen grey levels of 45, 105, 165 and 225.

Because both direct screen luminance measurements and luminance measurements from the described central location in front of the display screen have been made, this allows for the analysis of the bias between them. The resulting bias between the measured luminance's at each screen location (for each grey-scale level tested) would give an indication of how much of the luminance variation seen in the measurements taken from the central location in front of the screen, were due to factors other than the display screen luminance variation. The resultant variation in the bias values must be related to other factors (most likely the angle at which an area of the display screen is being viewed, as this is known to degrade the luminance as this angle increases). Figure 5.34 shows the bias luminance measurements (in Cd/m^2) represented as colour contour maps based on the measurements made at the 77 screen locations. Again, the 4 charts represent the bias luminance while the screen was displaying 4 grey-scale colours across the whole screen, corresponding to the RGB levels of 45, 105, 165 and 225.

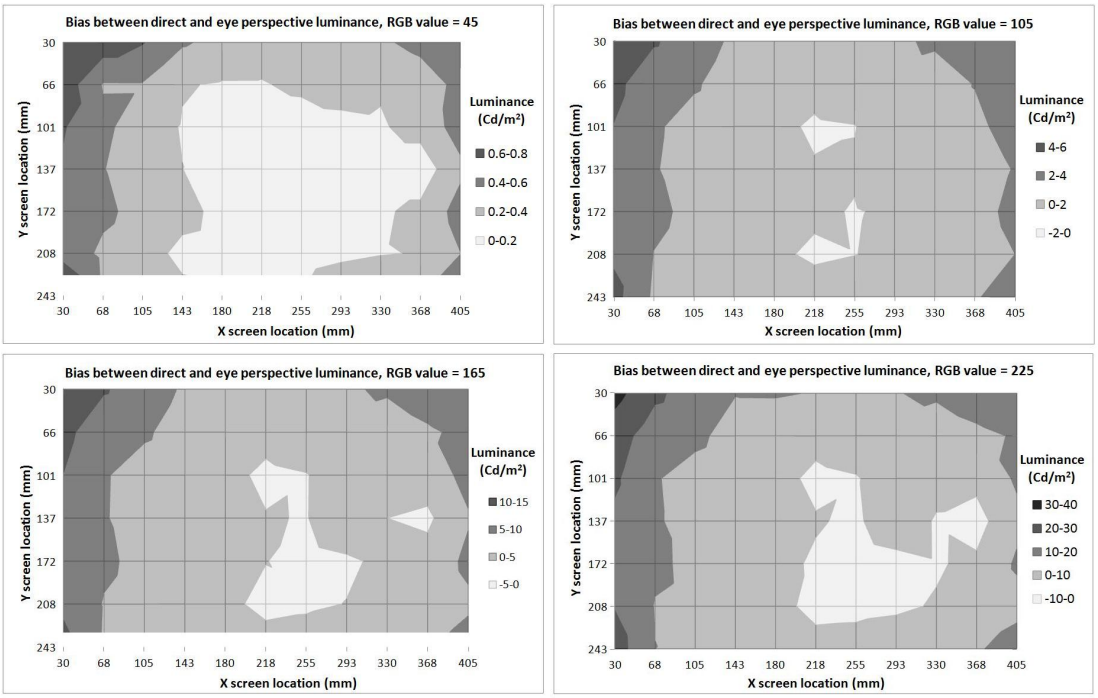

Figure 5.34: Four examples of bias between direct and eye perspective screen luminance measurements. The four examples are from different RGB screen grey levels of 45, 105, 165 and 225.

Using the luminance values measured with the photometer's sensor at the centred location in front of the display screen, the across-screen average values of luminance were calculated at each grey-scale level. Figure 5.35 shows this data. Also shown on the chart (depicted using dashed lines) are the grey-scale RGB values 66 and 223 which correspond to two specific luminance values. The RGB value of 66 corresponds to a luminance value of $10Cd/m^2$. This value is significant because it is equivalent to the background luminance used by the HFA. The second RGB value, of 223, corresponds to a luminance value of $136.7Cd/m^2$. This luminance value corresponds to a specific luminance level which the HFA is able to produce as a "test stimulus" brightness and on the HFA is described as a decibel (dB) level of 14dB. The reason this value is shown on the chart is because this "test stimulus" brightness level was selected to be used quite widely in this research program (for example as the "test stimulus" brightness in the developed SVOP test which will be compared directly with a HFA screening test which uses the 14dB "test stimulus").

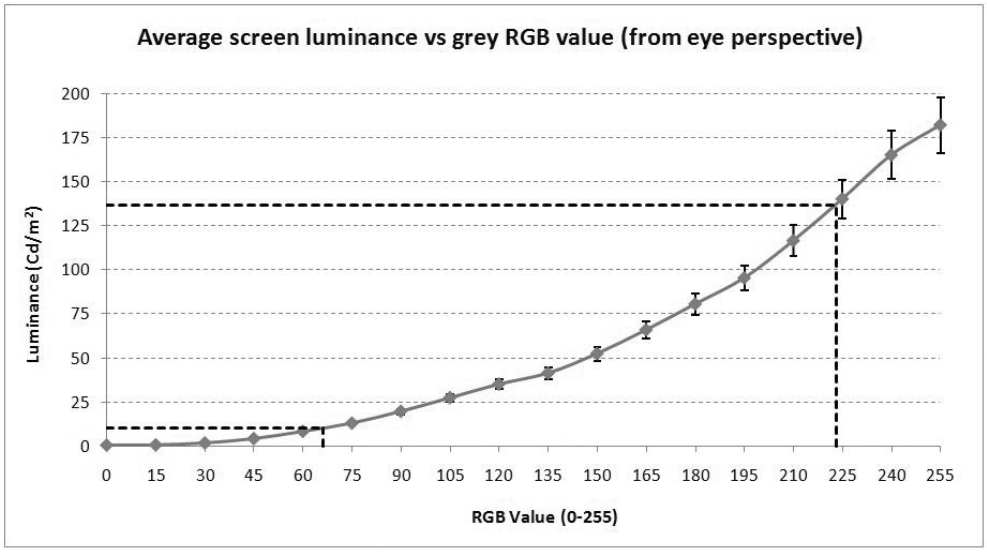

Figure 5.35: Average (±1 standard deviation) of screen luminance values from all screen positions, from eye perspective, across all grey scale RGB values.

Table 5.6 shows all the luminance dB levels which the HFA uses along with the associated luminance values of each dB level. In addition, the table also shows the equivalent RGB grey-scale level which corresponds (where possible) to each HFA dB level. The way in which these are calculated is by taking the HFA level brightness (which corresponds to the difference between the background and the "test stimulus" on the HFA) and adding the background luminance to give the appropriate stimulus luminance value at which a "test stimulus" should be displayed on the LCD screen in the proposed SVOP system in order for it to correspond to any of the particular HFA dB levels.

Figure 5.36 on page 114 shows the luminance values vs grey-scale RGB values taken from two specific screen locations. The two locations correspond to that which had the highest luminance and that which had the lowest luminance (i.e. the brightest and dimmest screen locations respectively) from the measurements taken when the photometer's sensor was located centrally with respect to, and in front of, the display screen. The brightest screen location corresponded to the measurements taken at a screen location of (143,137) and the dimmest screen location corresponded to the measurements taken at a screen location of (30,30) in (x,y) coordinates from the top left of the screen. This chart allows a measurement of the range of luminance values which a "test stimulus" displayed at a single RGB value could possibly have if it was displayed at any location on the screen and was viewed from the location of the photometer sensor. Table 5.7 on page 114 shows the calculated ranges of how "test stimuli" displayed on the LCD screen could potentially vary in luminance difference, when considering the difference between the "test stimuli" brightness and background brightness RGB levels, as a result of using the brightest and dimmest locations of the display screen as viewed from the described location

used for the photometer sensor (at a distance of 600mm from the eye tracker's camera and located centrally in front of the display screen).

HFA dB level	luminance contrast between stimuli and background Cd/m^2	stimulus luminance Cd/m^2	Equivalent LCD RGB value
0	3183.1	3193.1	-
1	2528.3	2538.4	-
2	2008.5	2018.6	-
3	1595.4	1605.4	-
4	1267.2	1277.2	-
5	1006.5	1016.5	-
6	799.6	809.6	-
7	635.0	645.1	-
8	504.5	514.5	-
9	400.8	410.8	-
10	318.3	328.3	-
11	252.7	262.8	-
12	200.9	210.9	-
13	159.5	169.5	243
14	126.7	136.7	223
15	100.6	110.6	206
16	79.9	89.9	190
17	63.7	73.7	173
18	50.6	60.6	159
19	40.1	50.1	147
20	31.8	41.9	136
21	25.1	35.2	120
22	20.1	30.1	110
23	15.9	25.9	102
24	12.7	22.8	96
25	10.2	20.2	91
26	8.0	18.0	87
27	6.4	16.4	83
28	5.1	15.1	81
29	4.1	14.2	78
30	3.2	13.2	76
31	2.5	12.6	-
32	1.9	11.9	-
33	1.6	11.6	-
34	1.3	11.3	-
35	1.0	11.0	-

Table 5.6: HFA stimuli luminance values and the corresponding grey-scale RGB values on the LCD screen.

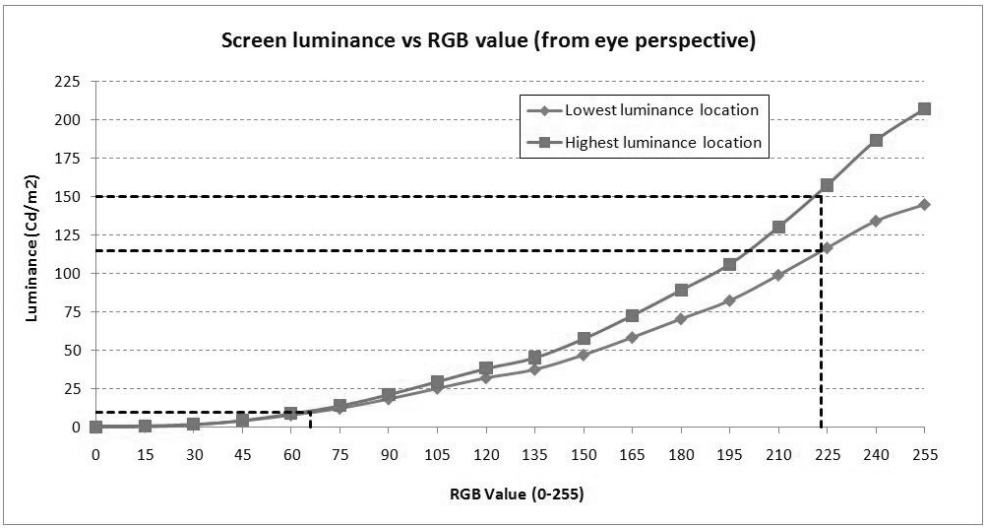

Figure 5.36: Luminance values, from eye perspective, for all grey scale RGB values from two screen locations which correspond to the locations with the lowest luminance values and the highest luminance values.

HFA "test stimuli" luminance levels		Equivalent LCD RGB value	Equivalent luminance based on RGB value (Cd/m^2)		Difference between equivalent stimulus and background (Cd/m^2)		Total range (Cd/m^2)
dB	Cd/m^2		Dimmest	Brightest	Dimmest	Brightest	
13	169.5	243	136.3	187.2	127.0	177.5	50.4
14	136.7	223	114.6	150.4	105.3	140.6	35.3
15	110.6	206	95.0	120.3	85.7	110.5	24.8
16	89.9	190	78.3	96.0	69.0	86.2	17.2
17	73.7	173	63.3	75.3	54.0	65.5	11.5
18	60.6	159	53.1	61.8	43.8	52.1	8.3
19	50.1	147	45.5	52.3	36.2	42.5	6.3
20	41.9	136	39.4	44.8	30.1	35.0	4.9
21	35.2	120	31.4	35.2	22.0	25.4	3.4
22	30.1	110	26.7	29.8	17.4	20.0	2.6
23	25.9	102	23.2	25.7	13.9	15.9	2.0
24	22.8	96	20.6	22.7	11.3	12.9	1.6
25	20.2	91	18.5	20.3	9.2	10.5	1.3
26	18.0	87	18.1	19.8	8.8	10.1	1.2
27	16.4	83	15.3	16.6	6.0	6.9	0.8
28	15.1	81	14.6	15.8	5.3	6.0	0.7
29	14.2	78	13.5	14.5	4.2	4.7	0.5
30	13.2	76	12.7	13.6	3.4	3.9	0.4

Table 5.7: The maximum range of luminance values, for each equivalent HFA stimuli level, on the LCD screen when considering the brightest and dimmest screen locations (as measured from a location 600mm from the eye tracker's camera and centrally in front of the display screen).

5.2.3.3 Discussion

The described method of using grey-scale colour levels for producing specific luminance level "test stimuli" on a computer display screen relies to a certain extent on having screen luminance uniformity of an acceptable level. There are two main aspects of display screen uniformity which are of importance in this research program: (i) direct uniformity characteristics specific to the display screen, due mainly to poor uniformity of the back-lighting of the screen; and (ii) the uniformity "appearance" of the screen as a result of different viewing angles. It was expected that both these factors would be a feature of the display screen being tested. Figure 5.32 demonstrates that the direct screen shows a non-uniformity in luminance measured directly from the display screen with an increase in luminance on the left side of the screen. This increased luminance was a consistent feature at all the grey-scale levels measured and so can be considered to be a characteristic of the display screen used.

The more realistic situation (in terms of the proposed SVOP system) of screen uniformity measured from a location which corresponds more appropriately with where a test subject's eye(s) would be located is shown in figure 5.33. The increased luminance area to the left side of the screen which was revealed by the direct screen measurements is still observed. However, in addition there is reduced luminance in areas towards the edges of the screen (in particular the left and right sides). This additional reduction in luminance can be attributed to the effect of reduced luminance with increased viewing angle. The effect of viewing angle alone is seen in figure 5.34 by having the previously measured direct screen luminance uniformity subtracted out, and demonstrates quite clearly that the reduction in luminance effect as a result of wider viewing angles occurs more significantly towards the left and right edges of the display screen.

In addition to assessing screen luminance uniformity, the purpose of these experimental methods was to obtain luminance values for different grey-scale levels which could then be used in the proposed SVOP system. Because the LCD luminance was not uniform, the "across-screen" luminance values at each measured grey-scale level were averaged. Each average value would then represent a luminance value for each of the grey-scale levels measured (as shown in figure 5.35).

Using these averaged values it is possible to compare the display screen's capability in displaying "test stimuli" luminance's which correspond to those which are used by the HFA. Table 5.6 shows that from the wide range of luminance levels which the HFA is able to produce there is a range of luminance levels which the display screen is capable of displaying. There are 12 luminance levels on the HFA scale which are brighter than the display screen is capable of displaying. This is because the display screen has a maximum brightness which is related to the back-light used and there is no need for a normal computer screen to be any brighter than this maximum luminance. There are also HFA stimulus luminance levels at the lower (or dimmer) end of the

scale which the display screen has problems displaying correctly. The reason for this is that at these lower brightness levels, the equivalent HFA stimulus luminance starts to lie between two adjacent grey-scale levels. For the purposes of the proposed SVOP system these lower brightness levels are not required as the system is designed to be a suprathreshold screening test using a relatively bright level of "test stimuli".

However, the problem of the screen non-uniformity still persists, and with each display screen stimulus level which corresponds to a HFA stimulus level there is an associated potential error in the luminance displayed in comparison with the specific HFA luminance. This is because an "across-screen" average is used to describe each stimulus luminance level when in fact there are a range of "possible" luminance levels which could be displayed for any particular "intended" stimulus brightness level depending on the screen location of the "test stimuli". The largest potential errors using the measurements made are described in figure 5.36 and table 5.7. The largest potential error is calculated by the luminance difference between the background and "test stimulus" level from the brightest and dimmest screen locations. This reveals a luminance "range" for each specific HFA stimulus level which could be reproduced using the display screen. Taking the largest potential error to be $\pm\frac{1}{2}$range, then the error is at an acceptable level for this application (when assessing the measurements made) as the largest potential error for any particular equivalent HFA level does not cross over into another adjacent (above or below) brightness level on the HFA scale. These errors can be reduced further by making sure that the far left and far right sides of the screen, where luminance is reduced further due to the increased viewing angle, are not used as locations to present "test stimuli". However, there is also a risk of an increase to these errors because in the proposed SVOP system the test subject is allowed to move their head. Head movement will change the viewing angle to each part of the screen (increasing viewing angle to some areas while reducing it to others). The effect of this could add further to the potential brightness level error. However, this variation is tolerable for proposed suprathreshold system because a test subject only has a certain amount of allowable head movement before they will move outside the eye tracker's field of view (under which condition the test would not be able to proceed). This prevents extremely large viewing angles to occur.

5.3 Assessment of eye gaze response to "test stimuli"

In order to develop a software algorithm which is capable of automatically deciding, in real time, whether or not visual field "test stimuli" have been seen or not, it is important to assess the characteristics of eye gaze responses to the presentation of the "test stimuli". An eye gaze response can simply be described as a change in fixation position (i.e. from the "fixation stimulus" point to a new point). So, an eye gaze response here is termed "fixation change" and

it is these "fixation changes" which will be assessed in this section. The developed algorithm will need to determine when fixation change eye movements correspond to a patient having seen a visual field "test stimulus". Three properties of any fixation change movement will be assessed to make this decision:

- Direction - the direction in which fixation change movement takes place.
- Amplitude - the magnitude of the fixation change movement.
- Latency - the reaction time of the fixation change movement.

5.3.1 Methods

The first version SVOP software previously described in section 5.2.1.1 on page 87 was altered to collect data on gaze fixation change movements in response to visual "test stimuli". As a reminder, the software program was designed to display a "fixation stimulus", then when a subject is gazing at the "fixation stimulus" calculate the position of a visual field point "test stimulus" and display it for 200ms and repeat this process with a predetermined set of visual field locations while constantly collecting gaze data. Figure 5.19 on page 88 shows the program flow of this software. The program was altered slightly in terms of the data collection such that in addition to collecting the raw gaze and distance data, it would also calculate and export data about the characteristics of fixation changes which occur in response to the "test stimuli" which were displayed. These characteristics and their associated data are described in the following paragraphs (headed "Direction", "Amplitude" and "Latency Characteristic") which describe the three properties associated with the fixation changes that are detected.

A total fixation change was defined by a start and end gaze location. The change in screen position (measured in pixels) of all consecutive gaze data points was continually monitored. The start of a fixation change was detected by looking for a change in gaze location between consecutive gaze data samples (at the 50Hz sample rate) which was greater than 50 pixels (this relates to an angular change of approximately 1.3°). The start point of a fixation change was defined as the start point of the >50 pixels gaze change. The end location of a total fixation change was defined by the point at which 5 consecutive gaze data samples are separated by a distance less than 50 pixels and must occur after the detection of a fixation change start point. The software flow of this fixation change detection algorithm is shown in figure 5.37. In this algorithm, it is possible that many data samples can make up a single detected fixation change.

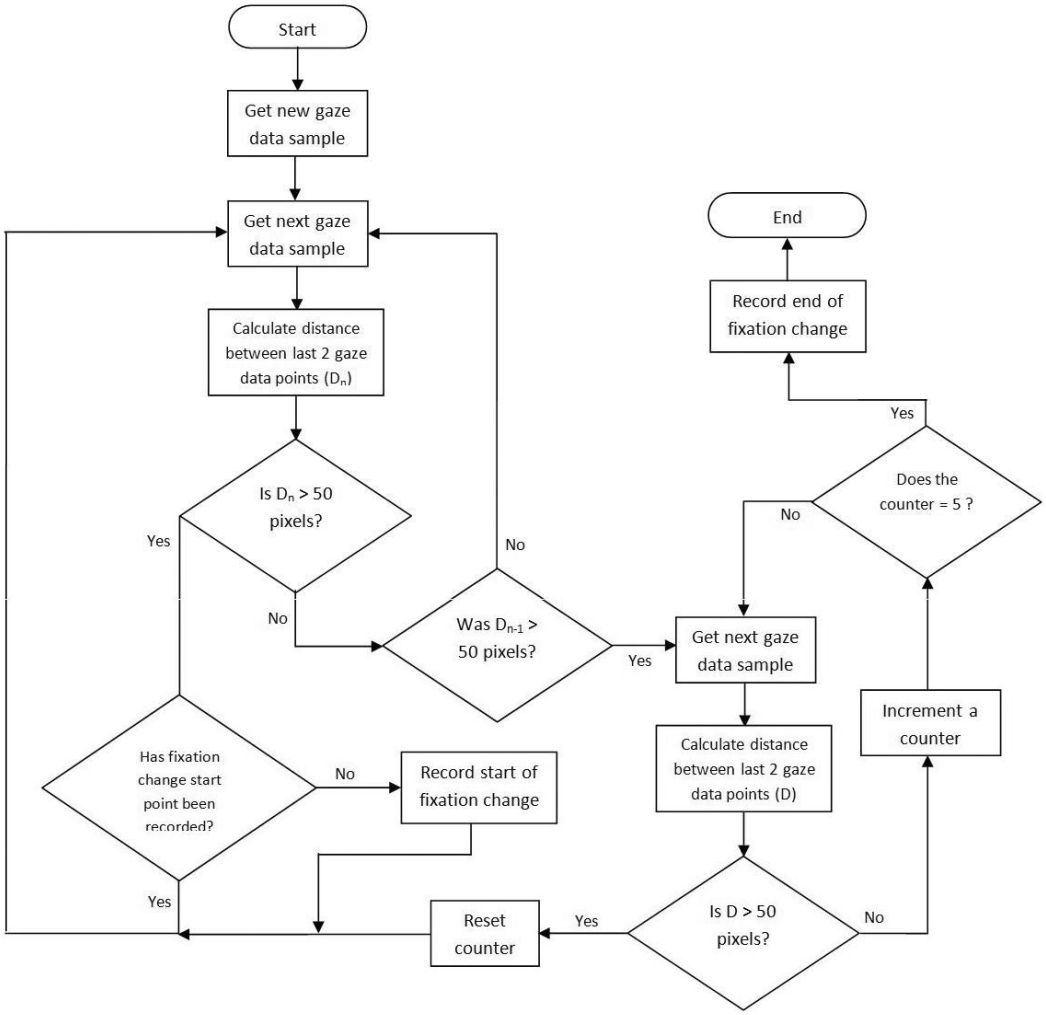

Figure 5.37: Flow diagram of the fixation change detection software algorithm.

Direction characteristic

The direction of any detected fixation change was calculated as an angle between an imaginary horizontal line extending out to the right of the fixation change start point, and the line of the fixation change. In addition, the direction between the centre of the "fixation stimulus" point and the centre of the "test stimulus" point was calculated as an angular direction using the same procedure (this angle is termed "stimulus change direction"). The bias between these two direction angles was then calculated, with a positive bias value representing a fixation change direction which is greater than the stimulus change direction. These values were calculated in degrees. An example of this is shown in figure 5.38, with the bias value calculated as follows:

$$Direction\ Bias = \theta_F - \theta_S$$

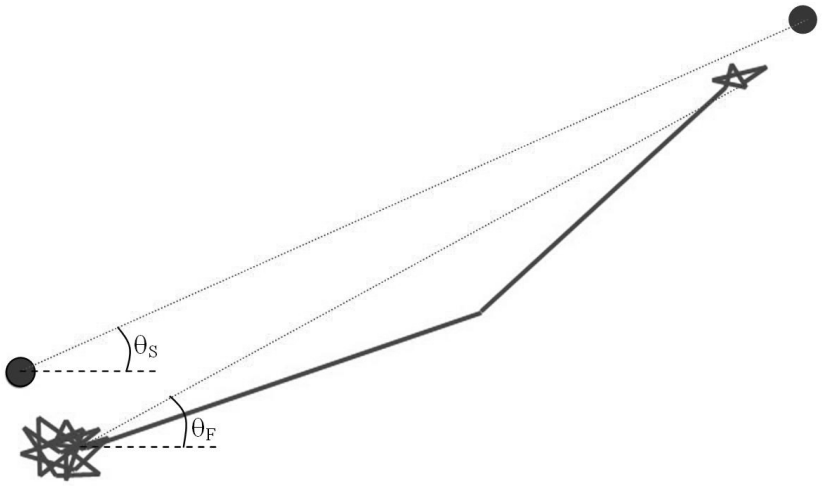

Figure 5.38: An example of values used to calculate the direction bias of a fixation change.

Amplitude characteristic

The amplitude (or magnitude) of any detected fixation change was calculated as a visual angle subtended at the eye rather than by a distance in pixels on the display screen, in this way it could be compared directly to the visual field angle which was used to display the "test stimulus". The visual angle corresponding to the fixation change was calculated by using the eye positional data (x, y and z coordinates) at the start of the detected fixation change, which could be calculated from the distance data provided by the eye tracker corresponding to the start point data sample. As the eye position is known along with the position of the start and end points of the fixation change, the angle of the fixation change (at the eye) could be calculated. The bias between the fixation change angle and the "test stimulus" angle (which is already known) was calculated and represented as a % difference. Positive values represented a fixation change angle which was larger than the "test stimulus" visual field angle, and negative values represented a fixation change angle which is less than the displayed "test stimulus" visual field angle. An example of an amplitude fixation changes is shown in fig 5.39, with the % bias value calculated as follows:

$$\%\ Amplitude\ Bias = \left(\frac{\phi_F}{\phi_S} - 1\right) \times 100$$

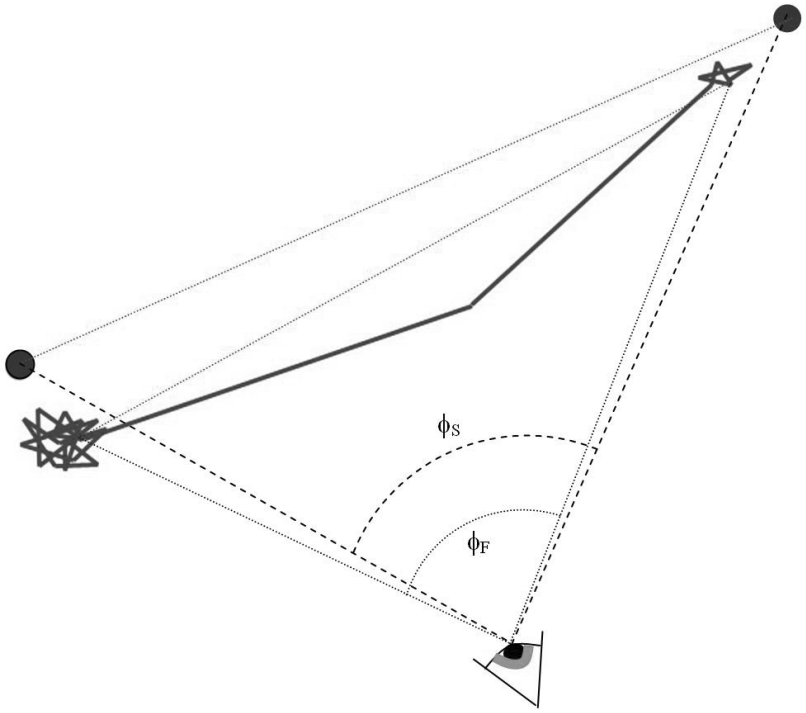

Figure 5.39: An example of values used to calculate the amplitude bias of a fixation change.

Latency characteristic

The latency characteristic can also be described as the eye reaction time in response to the "test stimulus". Latency was calculated (measured in ms) simply by taking the time difference between the time the "test stimulus" was initially presented on the display screen and the time at the beginning of the first detected fixation change subsequent to a "test stimulus" being displayed.

Test patterns, "test stimuli" and subjects

For these methods, as in section 5.2.1.1 on page 87, three visual field test patterns were used. These were the test pattern for the left and right eyes as based on the HFA C40 screening test pattern and a custom designed 40-point visual field pattern which consisted of 40 points located within the first 25 degrees of the visual field which was based on the left and right eye test patterns (figure 5.20 on page 89 shows the three test patterns used). The "test stimuli" were presented at a specific luminance brightness of $136.7Cd/m^2$ HFA equivalent to 14dB. One reason for doing this is that in future comparative studies, data on direction, amplitude and latency of reactions to a specific luminance level will be used to create a test which can

be compared to a screening test which can be created on the HFA for clinical feasibility and validation studies.

The main aim of this data collection process was to produce a set of "normative" data to describe gaze reaction characteristics in response to "seen" "test stimuli" so that an algorithm can be created to detect when any particular "test stimulus" has been seen.

Healthy volunteers and also patients with visual field defects of a range of ages were recruited to perform three tests each (corresponding to the three field test patterns described above). The subjects and tests which were performed are outlined in table 5.8.

Subject groups	Number	Age (years)		Tests performed		
		Mean	Range	Binocular	Left	Right
Healthy adult	14	35.1	21-68	14	14	14
Adult patient	6	57.0	17-74	6	5	5
Healthy child	9	8.8	5-16	9	9	9
Child patient	9	7.8	2-15	9	5	5
Total	38	29.7	2-74	38	33	33

Table 5.8: Subjects for fixation change characteristics tests

5.3.2 Results

Direction characteristic

Figure 5.40 shows five frequency distributions for gaze direction bias following the presentation of "test stimuli". The five different frequency distributions relate to five different eccentric visual field angles ($5^\circ - 25^\circ$ in steps of 5°). These frequency distributions detail the direction bias characteristics for gaze responses to "seen" "test stimuli". These data can then be used to define a set of limits of "permissible" direction bias values for use in an algorithm which automatically decides, in "real time", if a displayed "test stimulus" has been seen.

These limits were chosen to be the average direction bias values ± 3 standard deviations using the data for each eccentric visual field angle assessed ($5^\circ - 25^\circ$ in steps of 5°). Figure 5.41 shows a chart representing the chosen direction bias limits with increasing eccentric visual field angle for use in the SVOP decision algorithm.

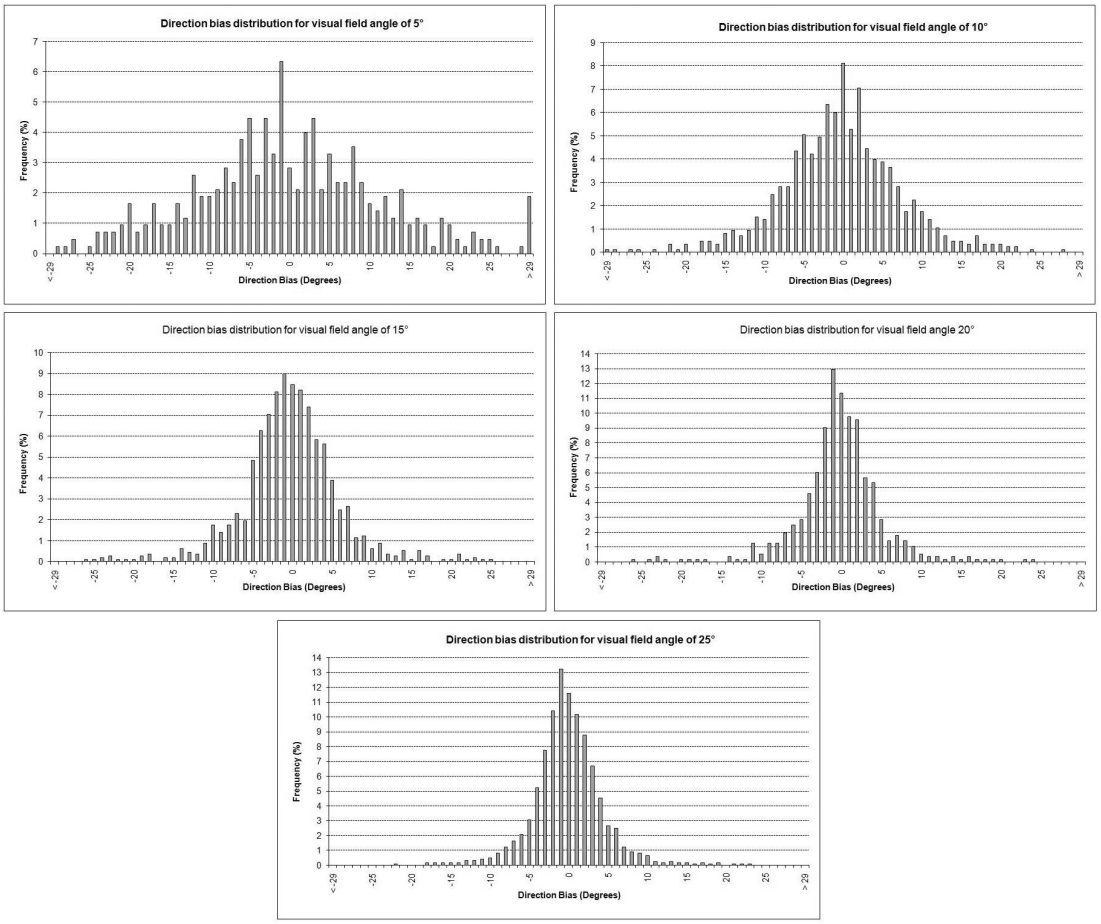

Figure 5.40: Distribution of direction bias values at each of the tested visual field angles

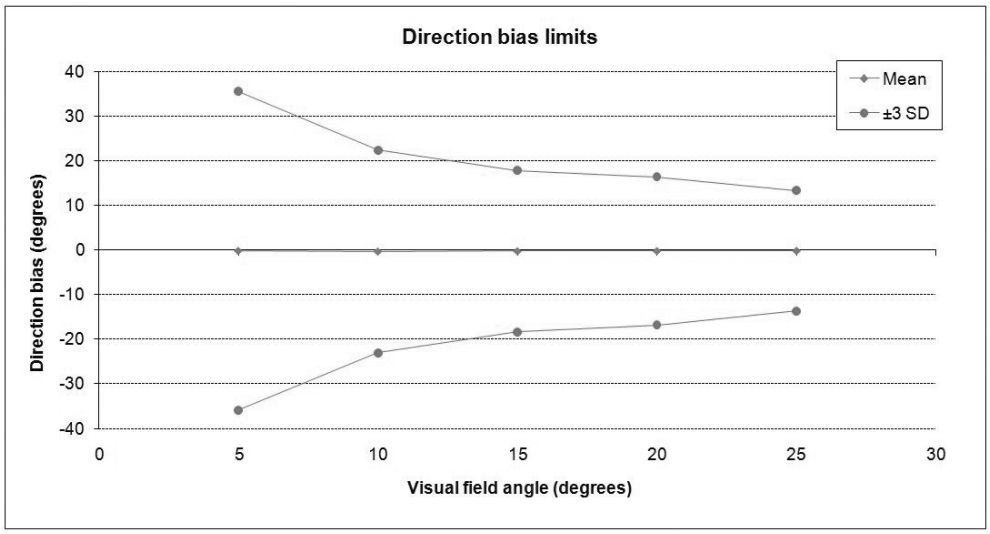

Figure 5.41: Average, ±3 standard deviations (equivalent to the limits used), of direction bias values for each of the tested visual field angles

Amplitude characteristic

Figure 5.42 shows five frequency distributions for gaze amplitude bias following the presentation of "test stimuli". The five different frequency distributions relate to five different eccentric visual field angles ($5° - 25°$ in steps of $5°$). These frequency distributions detail the amplitude bias characteristics for gaze responses to "seen" "test stimuli". This data can then be used to define a set of limits of "permissible" amplitude bias values for use in an algorithm which automatically decides, in "real time", if a displayed "test stimulus" has been seen.

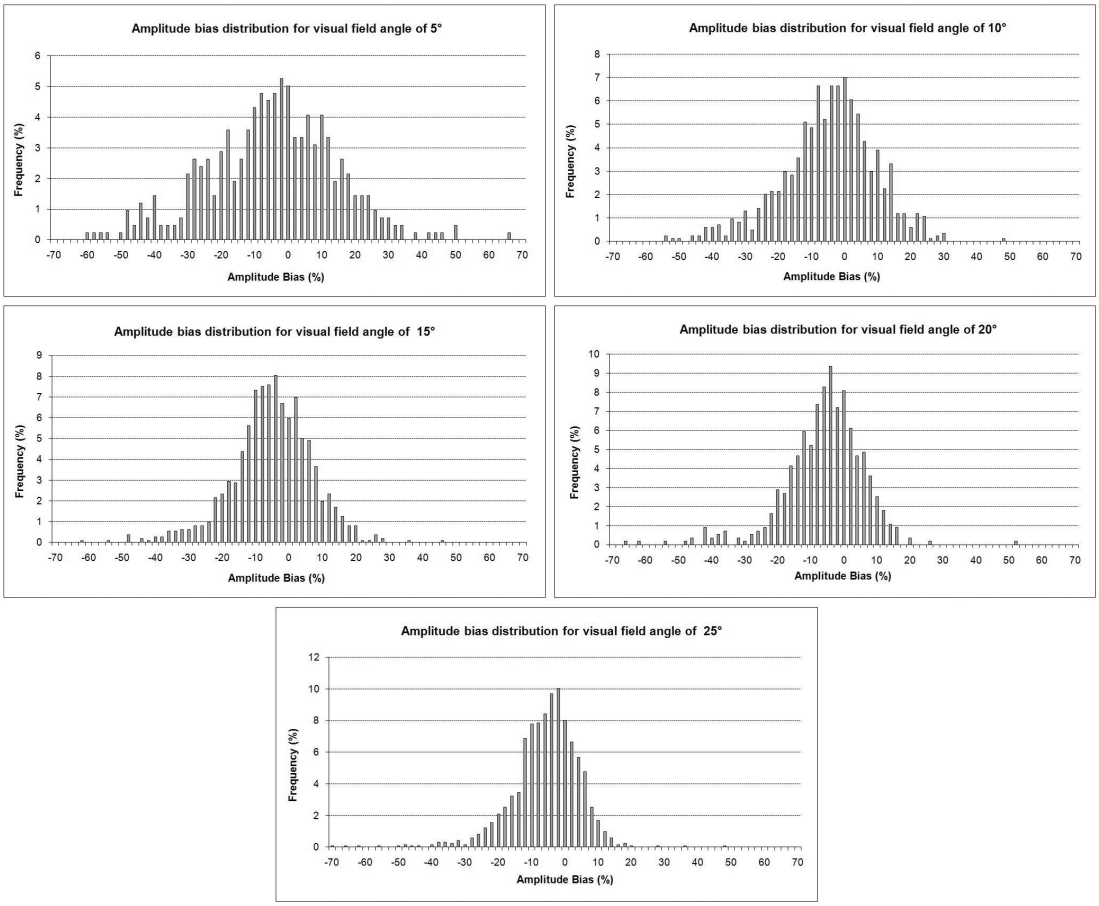

Figure 5.42: Distribution of amplitude bias values at each of the tested visual field angles

These limits were chosen to be the average amplitude bias values ± 3 standard deviations using the data for each eccentric visual field angle assessed ($5° - 25°$in steps of $5°$). Figure 5.43 shows a chart representing the chosen direction bias limits with increasing eccentric visual field angle for use in the SVOP decision algorithm.

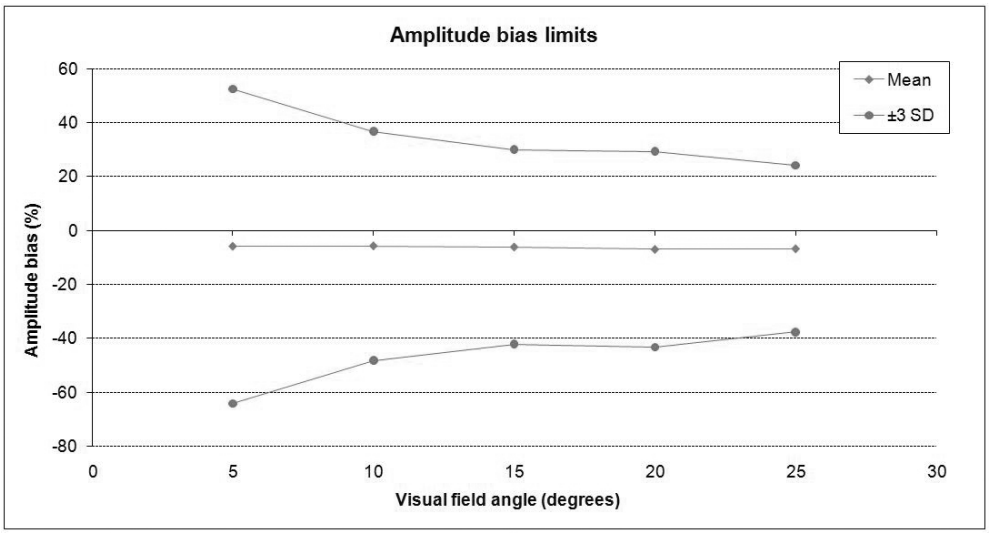

Figure 5.43: Average, ±3 standard deviations (equivalent to the limits used), of amplitude bias values for each of the tested visual field angles

Latency characteristic

Figure 5.44 shows all the reaction times in response to "test stimuli" which were considered as "seen", and the average ±1 standard deviation. This chart demonstrates the range of reaction times observed for each eccentric visual field angle. Clearly there is some erroneous data where there are very short reaction times $<$ 50ms. These fast reaction times can be attributed to the method of reaction time measurement. A simple algorithm was deigned to detect a reaction by calculating the difference between the presentation of the "test stimuli" and the first gaze movement. The gaze movement was simply defined as a change in gaze coordinates of $>$50 pixels and it was likely that this could occur from the gaze data without the subject having actually responded.

The reaction times were also assessed for gaze reactions to "test stimuli" which were considered to be "unseen". Figure 5.45 charts the average reaction times (±1 standard deviation) for each subject who had "test stimuli" that were considered both "seen" and "unseen" as part of their set of "tests" such that the "seen" and "unseen" reaction times could be plotted together.

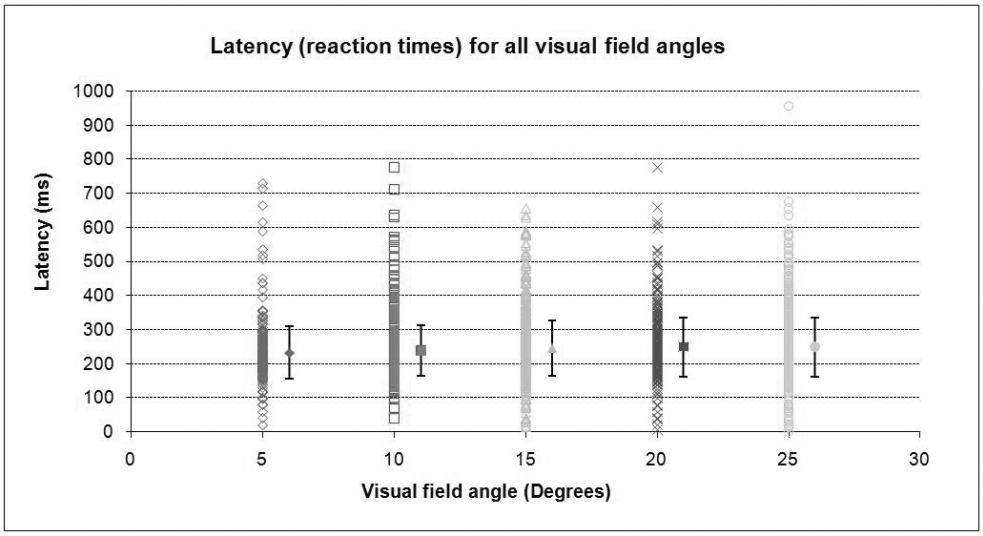

Figure 5.44: Spread and average (±1 standard deviation) of latency values for each of the tested visual field angles

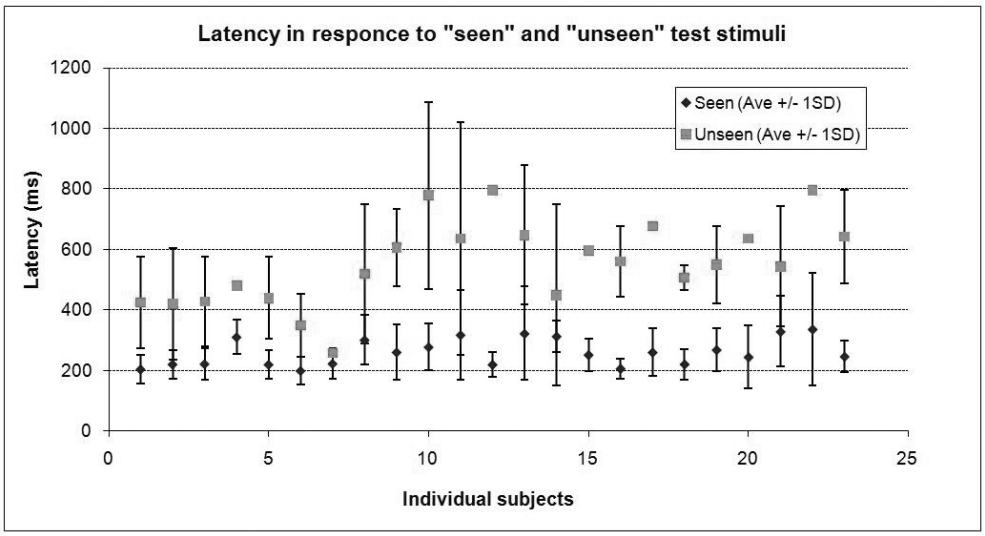

Figure 5.45: Latency values for "seen" and "unseen" points. (Average ±1 standard deviation).

5.3.3 Discussion

The methods described in this section were designed to collect and analyse data regarding subject gaze responses to visual field "test stimuli" which will eventually be used in the proposed SVOP system. A subject's gaze response was defined as the first "fixation change" immediately following the presentation of a "test stimulus". A "fixation change" was defined as having a start and end pair of fixation coordinates which were determined using the algorithm outlined in figure 5.37. Data regarding three characteristics of each "fixation change" in response to "test stimuli" were collected. These characteristics comprised: (i) the direction, (ii) the amplitude,

and (iii) the latency of the gaze response. The direction and amplitude were compared directly with the direction and amplitude of the direct vector between the "fixation stimulus" and "test stimulus" screen coordinates to produce bias values. The purpose of collecting these data was to enable the development of an algorithm which could use the data to make automated decisions on whether any particular "test stimulus", in the proposed SVOP system, has been "seen".

The bias data collected about direction and amplitude characteristics of fixation changes were expected to be in the form of normal distributions. This was shown to be the case. However there was an influencing factor which had an effect on the shape of the normal distributions. The eccentric visual field angle of the "test stimuli" used had an effect on the width of the distributions for both the direction bias and amplitude bias characteristics (figures 5.40 and 5.42 respectively). As the eccentricity of the visual field angle used increased, the distributions showed a reduced overall width. The reason for wider distributions of these bias characteristics at smaller eccentric visual field angles is due to the natural error in the gaze data which is sometimes seen (as discussed in section 5.2.1). There can sometimes be an error in the data provided by the eye tracker which is generally not a problem for determining when a subject is fixating on a "fixation stimulus" because, so long as the error is not too large, it can still be inferred that the subject is looking at the "fixation stimulus". An error in the gaze data at either, or both ends of a "fixation change" could result in a wider range of direction and amplitude bias values the closer the "fixation stimulus" is to the "test stimulus" (i.e. the smaller the eccentric visual field angle is).

The average value for the direction bias was effectively zero for any eccentric visual field angle, while for the amplitude bias the average values were slightly shifted below zero indicating that subjects tended to slightly underestimate the position of the "test stimulus" when considering the finishing point of their first fixation change in response to the "test stimulus".

As a result of the varying distribution widths with eccentric visual field angle, data was analysed separately according to the eccentric visual field angle of the "test stimuli". The average and standard deviation values for the direction and amplitude bias distributions could be used as the basis for the "decision algorithm" to be used in the proposed SVOP system which would make the automated decision about whether any particular "test stimulus" has been "seen". The "decision algorithm" will use a set of limits determined by the results gathered in these methods such that a "test stimulus" will only be considered as "seen" if the "fixation change" response has direction and amplitude bias characteristics which both fall within limits set at the average $\pm$ 3 standard deviations of the distribution data collected (as shown in figures 5.41 and 5.43). The reason for using the $\pm$ 3 standard deviation level was to ensure that all appropriate fixation changes are labelled correctly as "seen". Because the algorithm must consider two separate variables to make a "seen" decision it is necessary to increase the range of acceptable values.

As an added insurance, it is also proposed that any visual field points not considered as "seen"

by the decision algorithm the first time the "test stimulus" is shown will be retested and only finally be described as "unseen" if the test point is still not determined as being "seen" a second time.

The third characteristic of any particular "fixation change" response following the presentation of a "test stimulus" is the latency. Latency was recorded whether the responses were considered to have been "seen" or "unseen". The decision regarding whether a "test stimulus" was "seen" or "unseen" in these methods was slightly subjective and was based on post test reviewing of the gaze reactions. Generally, it was very obvious when a gaze response was in fact due to the "test stimulus" presented having being "seen". "Unseen" reaction times (latency) were really a reaction to the disappearance of the "fixation stimulus" (rather than the appearance of the "test stimulus") and were generally significantly larger than those which were "seen" (figure 5.45). This data provides another possible insurance method for automatically verifying that "test stimuli" have been "seen". Latency can not be relied on completely due to the large variability in this value for any particular subject. However, a further rule to be implemented in the "decision algorithm" could be that any particular visual field test point should be retested if there was a significantly slower reaction time as compared to previously "seen" "test stimuli" which have already been tested.

The described method of detecting "seen" stimuli using a vector of eye movement is potentially more reliable than the detection method used in current automated static perimeters. The method described here uses multiple data variables to accomplish a decision (direction, amplitude and latency of eye movements) whereas standard automated perimeters have only a single button press to signal that "something" has been seen and there is no way of verifying that a patient has definitely "seen" the stimulus which was presented other than the timing of the button press. The described eye movement vector detection method may be a considerable improvement on the single button press used ubiquitously in many automated static perimeters.

5.4 Clinical feasibility study

5.4.1 Introduction

The developed SVOP system is so far described in a theoretical basis and by using data gathered on eye gaze reactions to "test stimuli". However it has not been assessed in any way against another clinically accepted visual field assessment test. Before embarking on a large clinical validation trial, it was important to test the feasibility of the developed system against a comparative, clinically accepted visual field test device in healthy volunteers and patients with visual field defects able to perform the comparative test reliably. In addition, it would also be important to "try out" the developed system with its target age group of children, including

healthy children and children with visual field defects whether or not they can perform a comparative visual field test reliably or not.

5.4.2 Subjects and Methods

Four groups of children and adult subjects were recruited (table 5.9). Subjects performed 3 SVOP tests. In the first two tests, a subject's left and right eye's visual field was tested by performing uniocular SVOP tests which replicated the Humphrey Field Analyser's (HFA) Central-40 point left and right eye suprathreshold screening test patterns (hereafter referred to as HFA C-40 test) with the addition of a 41st point in the SVOP tests positioned at the blind spot. Subjects also performed a custom made binocular SVOP field test which was based on the HFA C-40 uniocular test patterns (figure 5.46). Exceptions to this procedure were very young children unable to effectively hold the occluding eye cover which was used (two subjects). These children performed the SVOP binocular visual field test only. There were 4 (1 child, 3 adults) subjects unable to perform one of the SVOP tests for various additional reasons (e.g. very poor or absent vision in one eye), in which case tests were not performed on that eye.

		Age (Years)	
Subject Group	Number of subjects	Mean	Range
Normal Adults	12 (5 m, 7 f)	29.8	16-61
Normal Children	4 (3 m, 1 f)	7.5	5-9
Adults with visual field defect	8 (5 m, 3 f)	63.3	17-77
Children with suspected visual field defect	5 (4 m, 1 f)	5.8	4-9

Table 5.9: Subjects and subject groups recruited for the feasibility trial.

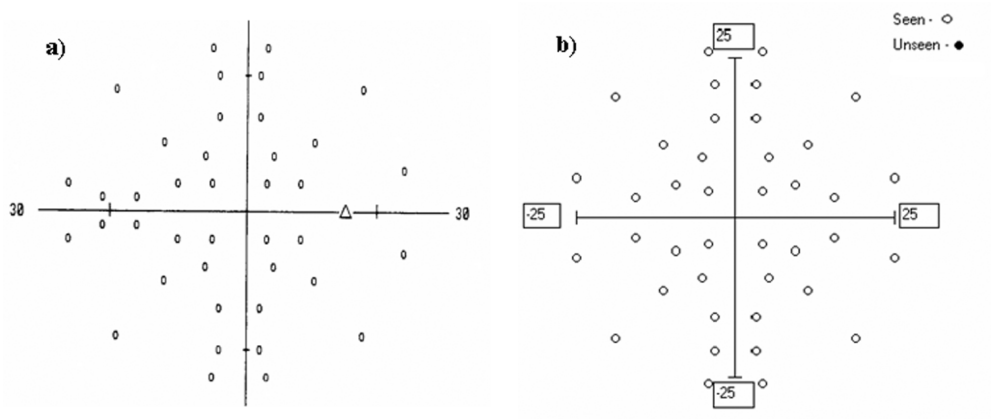

Figure 5.46: a) The Humphrey Field Analyser (HFA) C-40 Point screening test pattern for the right eye including blind spot (Δ). The test pattern for the left eye is a mirror image of this. b) The 40 point test pattern developed for binocular Saccadic Vector Optokinetic Perimetry (SVOP) tests. Numbers displayed indicate visual field in degrees from point of fixation.

Prior to each set of 3 SVOP visual field tests, each subject performed the calibration procedure. Subjects were required to look at the display screen and follow a stimulus with their eyes to 5 different locations on the screen. The stimulus used for adults and older children was a simple filled circle which moved to each location in turn (this is the Tobii eye tracker's standard calibration procedure). For younger children a custom calibration procedure was used. In these cases, the circle was replaced with a cartoon character which moved to each of the 5 screen locations where a simple animation with sound was played, lasting just a few seconds, in order to keep the attention of the child.

The SVOP tests performed by adults and older children used a simple small cartoon face to create a "fixation stimulus". The visual field stimuli used during the test were of size Goldmann III (0.43 degrees angular diameter) and duration 200ms. Adults and older children were given the simple instruction "If you see anything on the screen just look towards it". For younger children the "fixation stimulus" of a cartoon face was replaced with a variety of small short cartoon character animations with sound effects so as to encourage attention and generate interest. Younger children were not given any instruction, but were merely encouraged to look at the display screen.

The adults with visual field defects also performed the HFA C-40 test with the left and right eyes. The HFA's standard screening tests use an age matched hill of vision where stimuli are presented at 6dB brighter than the expected hill of vision value. The HFA's C-40 tests were purposely altered so that all stimuli were presented at a constant intensity level of 14dB to match the SVOP visual field tests which were also tailored to display stimuli at an intensity level of 14dB (stimulus intensity of 429Asb and background 31.5Asb) as stipulated in the HFA manufacturer manual. The stimulus size and duration used in the HFA C-40 tests was Goldmann III and 200ms respectively. The SVOP tests performed by the normal adults and children were compared with a normal healthy visual field, and the SVOP right and left eye tests performed by the adults with visual field defect were compared with the equivalent HFA C-40 left and right eye visual field tests.

5.4.3 Results

Normal adults

11 of the 12 normal adults performed all three SVOP tests (binocular, left eye, and right eye). The remaining 1 adult performed the SVOP binocular visual field test and left eye visual field test. All adults had normal visual fields confirmed by HFA testing. Figure 5.47 shows examples of SVOP test results from a normal subject, where all points from each of the three tests were correctly identified, i.e. all points were correctly identified as 'seen' except the blind spots

present in the left and right eye tests respectively which were determined to be 'unseen'. Table 5.10 gives a summary of the results obtained for the 'normal adult' group.

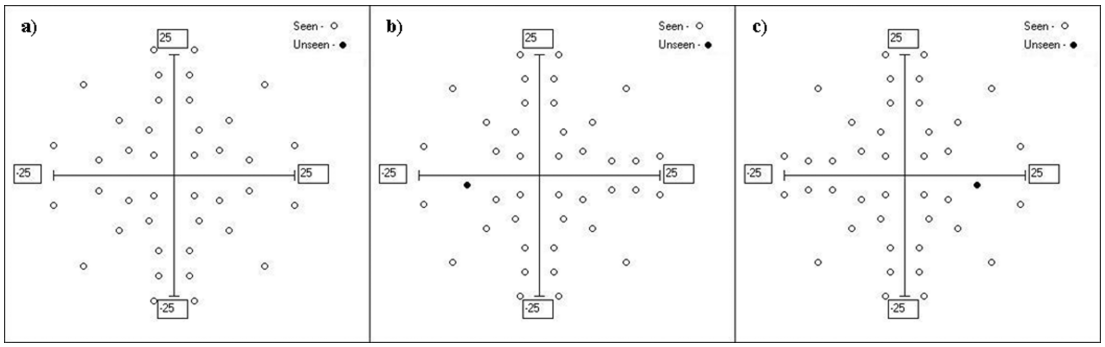

Figure 5.47: Example of SVOP test results from a normal subject depicting the 'seen' and 'unseen' points. a) Binocular visual field test, b) left eye test, c) right eye test.

	Visual Field Test Type		
Test Result Characteristics	Binocular	Left Eye	Right Eye
Number of subjects performing test	12	12	11
Number of Visual field points in test	40	41	41
Mean (±SD) number of correctly diagnosed points	39.9 ± 0.3	40.7 ± 0.8	40.7 ± 0.5
% of correctly diagnosed points	99.8	99.2	99.3

Table 5.10: Results from the 'normal adult' group. Correctly diagnosed points are those which correspond with a normal healthy visual field.

The blind spots were correctly identified as 'unseen' in all of the left and right eye SVOP tests apart from one in which the subject was able to see the stimulus presented in the blind spot area. This test was repeated in order to assess this anomaly and again the blind spot was recorded as being "seen". Currently, in the SVOP system, each subject's blind spot is not "found" by the system as is the case with the HFA, instead the point tested is specifically located at 15 degrees temporally and 1.5 degrees below the horizontal midline.

Normal children

The youngest subject (aged 5 years) in this group performed only the SVOP binocular test. All other subjects performed all three SVOP tests. HFA tests were not attempted in the child subjects because clinical experience has consistently reported its unreliability. Designation of a normal child group was prospectively inferred from subject sampling. Table 5.11 summarises the results for this subject group. All blind spot locations tested were correctly identified as 'unseen' for all of the right and left visual field tests performed in this group except for one subject where the blind spot location was labelled as 'seen' in their right eye visual field test.

Test Result Characteristics	Visual Field Test Type		
	Binocular	Left Eye	Right Eye
Number of subjects performing test	4	3	3
Number of Visual field points in test	40	41	41
Mean (±SD) number of correctly diagnosed points	40.0 ± 0.0	40.7 ± 0.6	40.7 ± 0.6
% of correctly diagnosed points	100	99.2	99.2

Table 5.11: Results from the 'normal child' group. Correctly diagnosed points are those which correspond with a normal healthy visual field.

Adults with visual field defect

Within this group the left and right eye SVOP tests were compared with the HFA C-40 left and right eye visual field tests. The individual eyes with visual field defects and those with no defects were compared independently. One subject did not perform the left eye test due to very poor vision in that eye. Table 5.12 summarises the results for this subject group.

Test Result Characteristics	Visual Field Test Type			
	Abnormal Eyes		Normal Eyes	
	Left Eye	Right Eye	Left Eye	Right Eye
Number of subjects performing test	3	7	4	1
Number of Visual field points in test	41	41	41	41
Mean (±SD) number of correctly diagnosed points	35.0 ± 1.7	37.6 ± 2.6	40.5 ± 0.6	40.0
% of correctly diagnosed points	85.4	91.6	98.8	97.6

Table 5.12: Results from the 'adults with visual field defect' group. Correctly diagnosed points are those which correspond with the HFA C-40 screening test visual field results.

HFA threshold examinations (test type 24-2) which had been performed on each subject were obtained to act as a further visually-comparative test result in addition to the direct quantitative comparisons performed. Figures 5.48, 5.49 and 5.50 show the SVOP 41 point test, the equivalent HFA C-40 test and the most recent threshold test for three different patients within this subject group. The patient in figure 5.48 was previously diagnosed with primary open angle glaucoma. The patient in figure 5.49 was previously diagnosed with right normal tension glaucoma. The patient in figure 5.50 was previously diagnosed with a tilted optic disc.

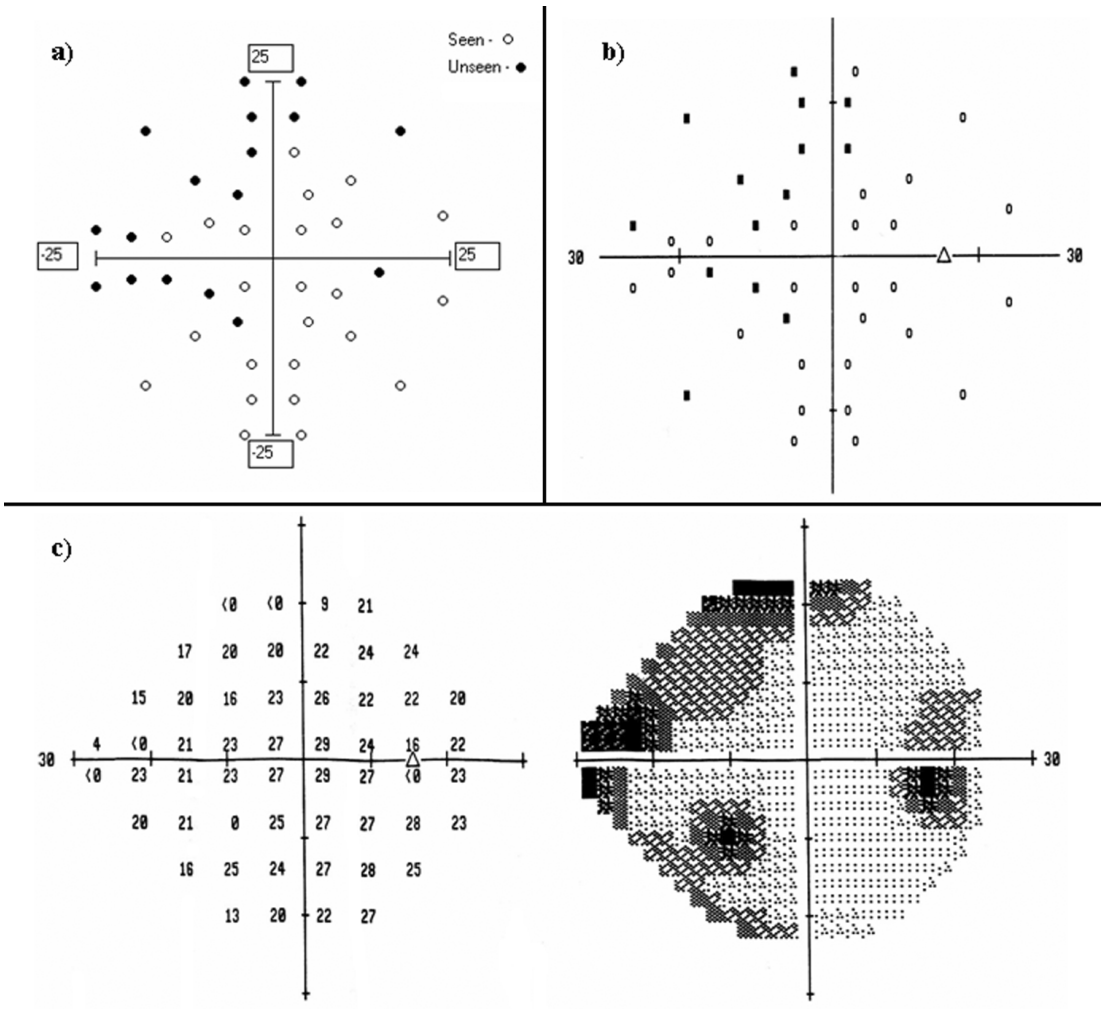

Figure 5.48: Test results from a subject within the 'adults with visual field defect group'. a) The SVOP test result, b) the equivalent HFA C-40 test result, and c) the patient's most recent full threshold HFA 24-2 test result. This patient was previously diagnosed with primary open angle glaucoma.

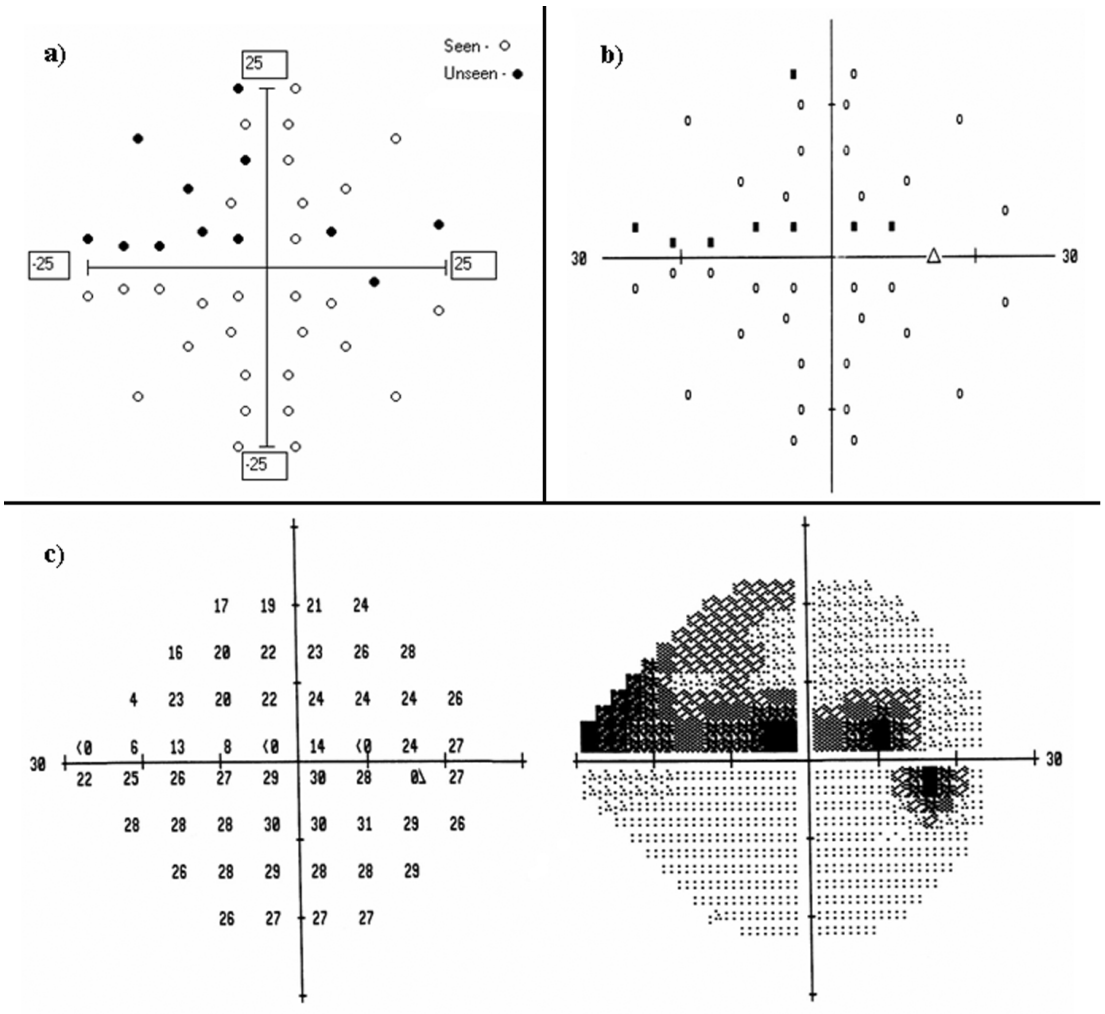

Figure 5.49: Test results from a subject within the 'adults with visual field defect group'. a) The SVOP test result, b) the equivalent HFA C-40 test result, and c) the patient's most recent full threshold HFA 24-2 test result. This patient was previously diagnosed with right normal tension glaucoma.

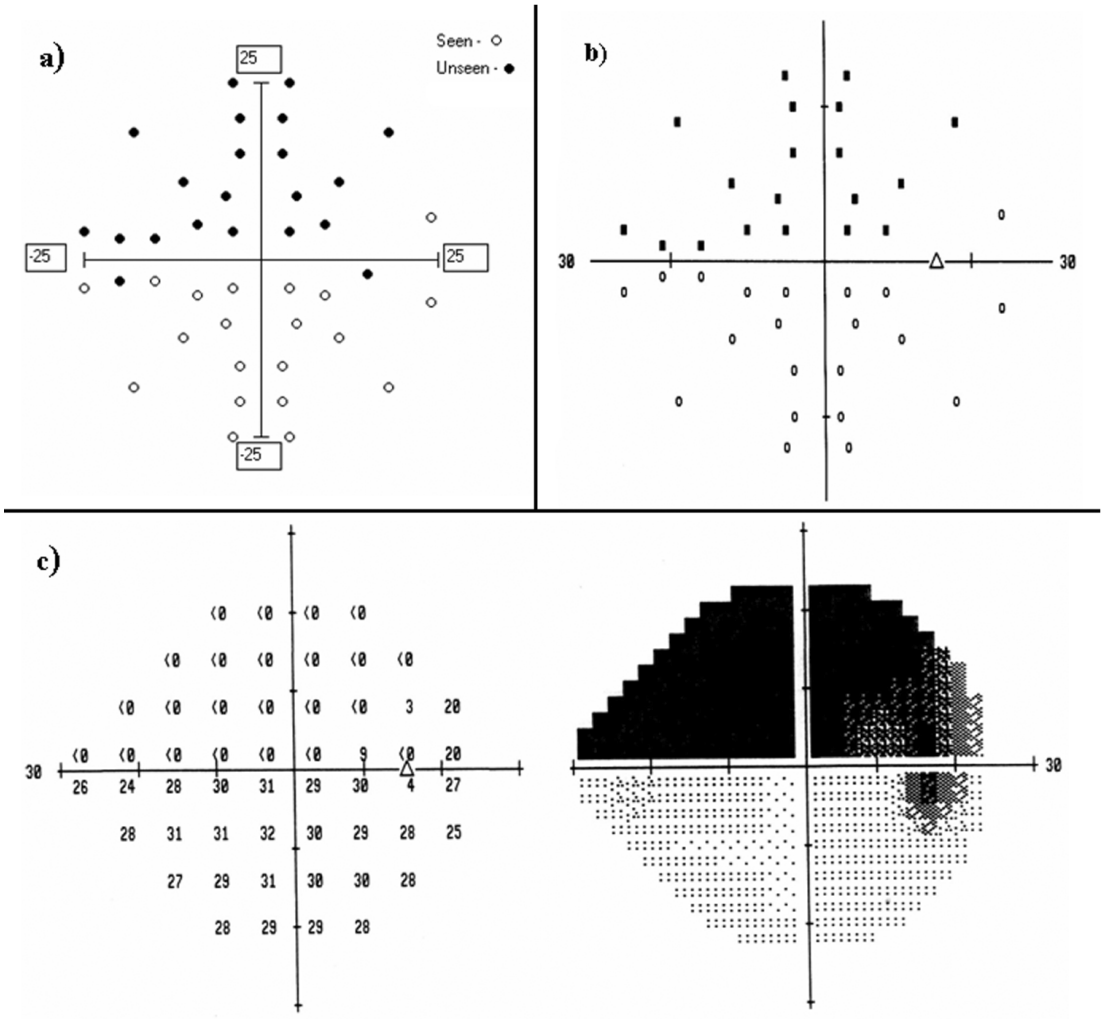

Figure 5.50: Test results from a subject within the 'adults with visual field defect group'. a) The SVOP test result, b) the equivalent HFA C-40 test result, and c) the patient's most recent full threshold HFA 24-2 test result. This patient was previously diagnosed with a tilted optic disc.

Children with suspected visual field defects

As with the "normal children" group, no comparative HFA visual field testing was carried out with these children because of known problems with HFA test reliability. Additionally, several of these children only performed a binocular SVOP test for which there was no equivalent HFA test. Figure 5.51 shows the binocular SVOP tests of the three youngest subjects (two 4 years, and one 5 years of age).

The first patient (figure 5.51a) was a 4 year old boy with left hemiplegic cerebral palsy consequent on a haemophilus meningitis at 3 years of age. He additionally had a left homonymous hemianopic visual field defect which was detected on confrontational visual field testing prior to performing the SVOP test.

The second patient (figure 5.51b) was a four year old boy who suffered a severe non-accidental

injury at 7 months of age with bilateral extensive retinal haemorrhage, rib fractures, encephalopathy and raised intracranial pressure. This resulted in a cortical visual loss with a suspected right visual field impairment, nystagmus and optic atrophy. Prior to performing the SVOP test clinical visual field testing had proved difficult because of the marked nystagmus and short attention span.

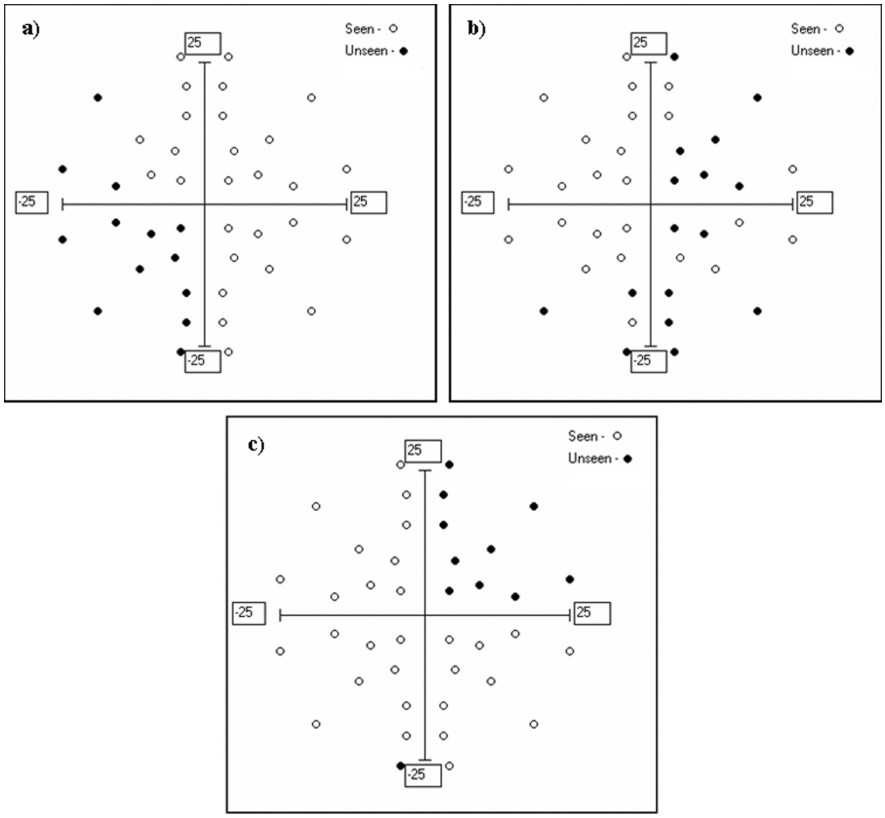

Figure 5.51: The SVOP binocular tests completed by the three youngest participants in the 'children with suspected visual field defects' group. Subject a) a 4 year old diagnosed with suspected left homonymous hemianopia following confrontational visual field testing, b) a 4 year old with suspected right sided visual field impairment following previous raised intracranial pressure from a non-accidental injury. c) a 5 year old with hypothalamic and optic nerve glioma with chiasmal involvement and no vision in his left eye.

The third patient (figure 5.51c) was a five year old boy diagnosed with hypothalamic and optic nerve low grade glioma previously treated with chemotherapy. At presentation he had total loss of vision in his left eye and confrontational visual field testing suggested a loss of peripheral vision on the temporal side of the right eye. Despite no changing evidence of enlargement of the tumour an increased visual field defect was clinically suspected. The SVOP binocular test (no vision in left eye) showed visual field loss in the superior right temporal quadrant.

A summary of the results obtained for normal adults and children, and adults with visual field defects groups is shown in figure 5.52. The number of correctly diagnosed points in the normal right and left eye tests is the number which agree with a normal visual field. The number of

correctly diagnosed points in the eyes with visual field defects is the number of points which agree with the equivalent HFA C-40 test. The left and right eye SVOP tests had a total of 41 points. The average percentage of points agreeing with a normal visual field in the normal adult and normal child eyes was 99.2% and 99.1% respectively. The percentage of points agreeing with the HFA C-40 screening test in the adult eyes with visual field defect was 89.8%

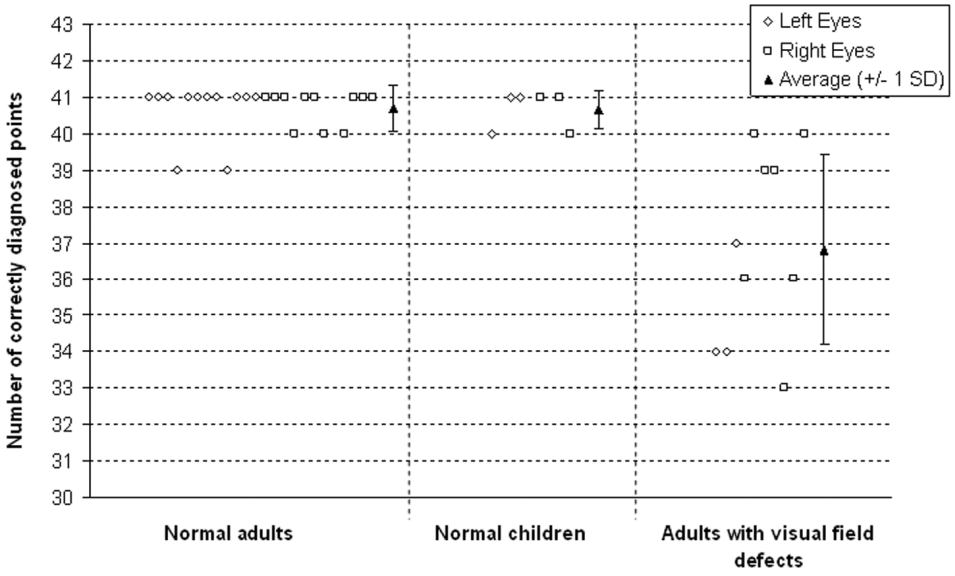

Figure 5.52: Number of tested visual field points corresponding to a normal visual field for the normal adults and children, or corresponding to the equivalent HFA C-40 screening test. SD = 1 standard deviation.

There were varying test times for the different groups. The average time for normal subjects to complete a 41 point SVOP test was 120 ± 42s. The average test time for patients with visual field defects was 269 ± 125s. There was an average increase of 65s in tests incorporating the animations designed for young children as compared to those without.

5.4.4 Discussion

This study's aim was to determine the feasibility of the SVOP technique. In order to do this, a variety of normal subjects and subjects with visual field defects were used. Adults were included as they could provide comparable results by undertaking the HFA C-40 test in addition to the SVOP test. Children were included to demonstrate that the technique is both feasible and acceptable to them.

In both the normal adult and child eyes, good comparison with a normal visual field was found with the SVOP tests. A good comparison was also found between the HFA C-40 screening test and the equivalent SVOP test in the adult eyes with visual field defects. However, the number

of correctly matched points between the two equivalent tests in this group was less than the number for the normal groups. There are two possible reasons for this lower agreement: (i) The brightness contrast level was matched between the two tests (SVOP and HFA C-40) as closely as possible. However, when using a standard LCD display for the SVOP tests there is inevitably some brightness variation across the screen depending upon the viewing angle of the subject, resulting in a variation in the brightness contrast of the presented stimuli. This effect is minimised by using an average level of brightness contrast corresponding to an averaged measurement of brightness across the screen and by preventing stimuli being presented in the far left and far right areas of the screen where there is a significant change in the brightness. Despite this brightness variation, it was measured that the largest difference in brightness contrast possible on the screen was less than 1dB on the HFA's decibel scale. (ii) Potentially it would be more difficult to achieve a pair of well matched visual field test results (SVOP and HFA C-40) in patients with more complex visual field defects where reduced visual sensitivity is relative rather than absolute.

At this point it is not known to what extent each of the two test types (SVOP and HFA C-40) are repeatable. It is probable that there is some variation in repeatability of both the HFA C-40 test and SVOP test, particularly in those patients with complex visual field defects. An indication of this can be seen by comparing the suprathreshold tests performed with the HFA 24-2 full threshold tests (figures 5.48, 5.49 and 5.50). There are areas of the suprathreshold (stimuli presented as a constant 14dB) visual field test results which do not agree with the raw numerical sensitivity dB values suggesting that repeatability may be an issue. The reproducibility of both the HFA C-40 and SVOP tests will need to be assessed in future studies.

Despite the lesser agreement in the abnormal adult group, there was still a high percentage of agreeing points and the fact that the defective areas were picked up is highly encouraging. Similarly, identification of blind spots was obtained in virtually all the subjects. In addition, a blind spot area was detected in one child subject while performing the binocular SVOP visual field test, a correct finding attributed to the patient's poor left eye vision (figure 5.53).

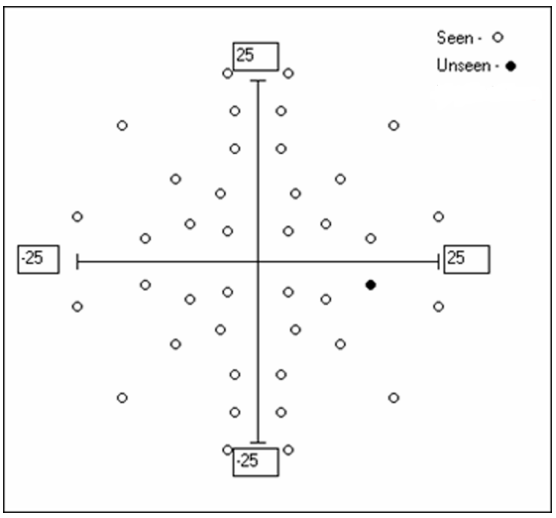

Figure 5.53: The eye tracking binocular visual field test performed by a child subject. The vision of the left eye in this subject was particularly poor resulting in the blind spot area being identified during the binocular SVOP test.

The children in both the normal and visual field defect groups were easily able to perform the eye tracking visual field test, and completed the test in between 1 to 6.5 minutes. it was particularly encouraging to see that the younger children (age 4 years) were happy undertaking the test. With the addition of the short animations during the test, it clearly became a fun procedure for some of the children. The animations which are optionally used during a test do not interfere with the testing of visual field points, but are used to maintain interest and fixation during the test. Currently the animations used are of small cartoon faces but there is no reason why different types of animation cannot be used to accommodate for different age groups or child interests, the only important criteria being that the animations are kept small so as to keep fixation to a small area.

ASP would be a very useful adjunct in the assessment of the visual fields of young children and the presented technique allows this measurement where there is currently no satisfactory alternative. Visual field defects were picked up in young children aged 4 and 5 years (figure 5.51). As there is no comparative "gold standard" visual field test for these age groups it is difficult to comment on the accuracy of the results in this group. However, given the results from the more compliant and older adult subjects and the suspected diagnoses of the children it can be inferred that the defected areas were detected with a good degree of accuracy. The test can be especially useful in refuting false positive results obtained from confrontation visual field testing in young children. By way of example, two children in our series were clinically diagnosed with complete hemianopias which were refuted by the SVOP test (figures 5.51a and 5.51c). Given the conflicting results between the clinical diagnosis' and SVOP test's in these cases, in order to confirm that the SVOP test results were not bogus they were investigated further by reviewing a video replay of the on screen test combined with the "real time" eye

gaze displayed simultaneously (in the form of lines representing eye gaze changes every 20ms overlaid on top of the screen replay). If these children had complete hemianopias, as was clinically suspected, they would not have been able to immediately fixate on many of the points that were displayed during the test. Review of the replays further confirmed the ability or inability of these children to see each individual stimulus in the areas of interest.

From this early experience, the technique of perimetry using eye tracking is a sound method of measuring visual fields in children and its advantage is that they are not required to look at one particular point throughout the test, instead the only task required of them is to perform a natural intuitive reaction in response to a visual stimulus. Neither are they required to place their heads in a fixed position as data provided by the eye tracking system gives a real time assessment of 3D eye position in space. Additionally, children take to the system well because many children are already familiar with computer displays.

Currently, the SVOP system is developed in such a way so that a test will not proceed if there is a conflict between the eye gaze data coordinates given by the eye tracker and the "fixation stimuli" coordinates used during a test. This is so that the points tested are not inaccurate. However, this is a potential limitation of the existing system because it will not allow the testing of patients with eye movement disorders who could present with eccentric fixation.

From these results, the system and technique of SVOP shows promise as a more objective visual field assessment method in young children when compared to the current confrontation perimetry technique used in clinical practice.

5.5 Errors and limitations

5.5.1 Error in "test stimuli" screen location

5.5.1.1 Methods

Due to the complex nature of the equations which govern the calculation of the "test stimuli" screen locations, and the number of variables involved, error analysis was performed using a modelling method of analysis. A mathematical simulation was created to determine the main factors which contribute to the "test stimuli" screen location errors and determine how the errors behave under various situations.

The screen position of each "test stimulus" depends on the visual field angle to be tested (described by the two angles ϕ and θ which are the eccentric and rotational visual field angle respectively) and the 3D location of the eye with respect to the point of fixation (the "fixation stimulus" location). The variables which largely contribute to the "test stimulus" screen location

error is the 3D coordinates of the eye. These 3D coordinates are calculated primarily from the distance data provided by the eye tracker. Through previous experimentation, the error in the eye tracker camera-to-eye distance (D) provided by the eye tracker is known to be approximately ±20mm (from section 5.2.2 on page 96).

Using this approximate value for the error in D, the error in screen location can be modelled and determined under various simulated situations. For example, different situations occur by using various values for visual field angles (ϕ and θ), 3D eye location (x y and z coordinates) and point of fixation on the screen. These errors were determined by using Microsoft Excel to model the maximum and minimum errors in "test stimuli" screen location using an error in D of ±20mm under the various combinations of the other variables to calculate the error using the equations previously described for calculating visual field screen location. Through an assessment of the situations which create the largest errors, a "worst case scenario" can be established. Some examples of the various scenarios are described in the following results section.

5.5.1.2 Results

Figure 5.54 describes the horizontal and vertical screen location error (in mm) for various visual field points, with fixation at the centre of the test screen and with the location of the test eye directly in front of the fixation point (as depicted in the small chart) and at a distance of 600mm from the eye tracker camera. The upper left chart in the figure shows the location from fixation (which in this situation is the centre of the screen) of 120 hypothetical visual field test locations (corresponding to eccentric visual field angles of $\phi = 5^\circ - 25^\circ$ in steps of 5°, and rotational visual field angles of $\theta = 0^\circ - 345^\circ$ in steps of 15°). This chart also shows the horizontal and vertical error (shown as horizontal and vertical error bars) for each visual field point using an associated camera-to-eye distance error of ±20mm. The lower charts show these error values in greater detail by plotting the horizontal (left chart) and vertical (right chart) error values against the rotational visual field angle (θ) for the five eccentric visual field angles (ϕ).

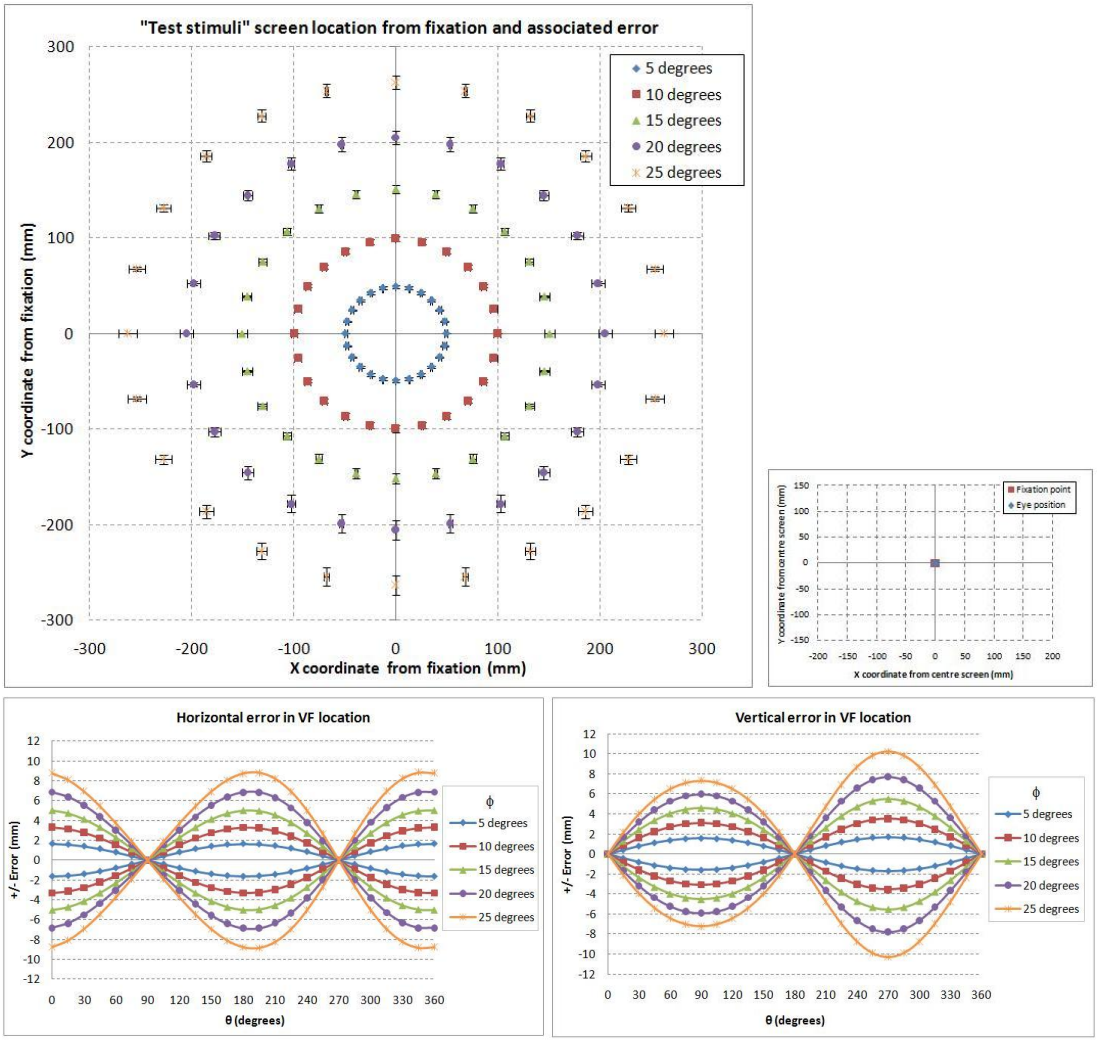

Figure 5.54: Screen location error for various visual field locations associated with a camera-to-eye distance error of ±20mm at 600mm. Fixation point is at the centre of the screen and the eye is located centrally in-front of the screen.

Each of the subsequent figures describe the screen location error of visual field points in the same way as figure 5.54, where the only things being varied are the fixation point and eye location point in relation to the fixation point changed in each situation. Many different situations were analysed as part of these modelling methods and the figures presented show just a selection of these situations where the errors become slightly more amplified and so justify presentation in this results section. The text accompanying each figure also describes each situation. However, in all the situations presented the test eye is at a distance of 600mm and the distance error used in each case is ±20mm.

Figure 5.55 shows the horizontal and vertical screen location error of 120 visual field points under a situation where fixation is at the far left hand side of the screen and with the location of the test eye as far right as the camera field of view will allow (shown by the small chart).

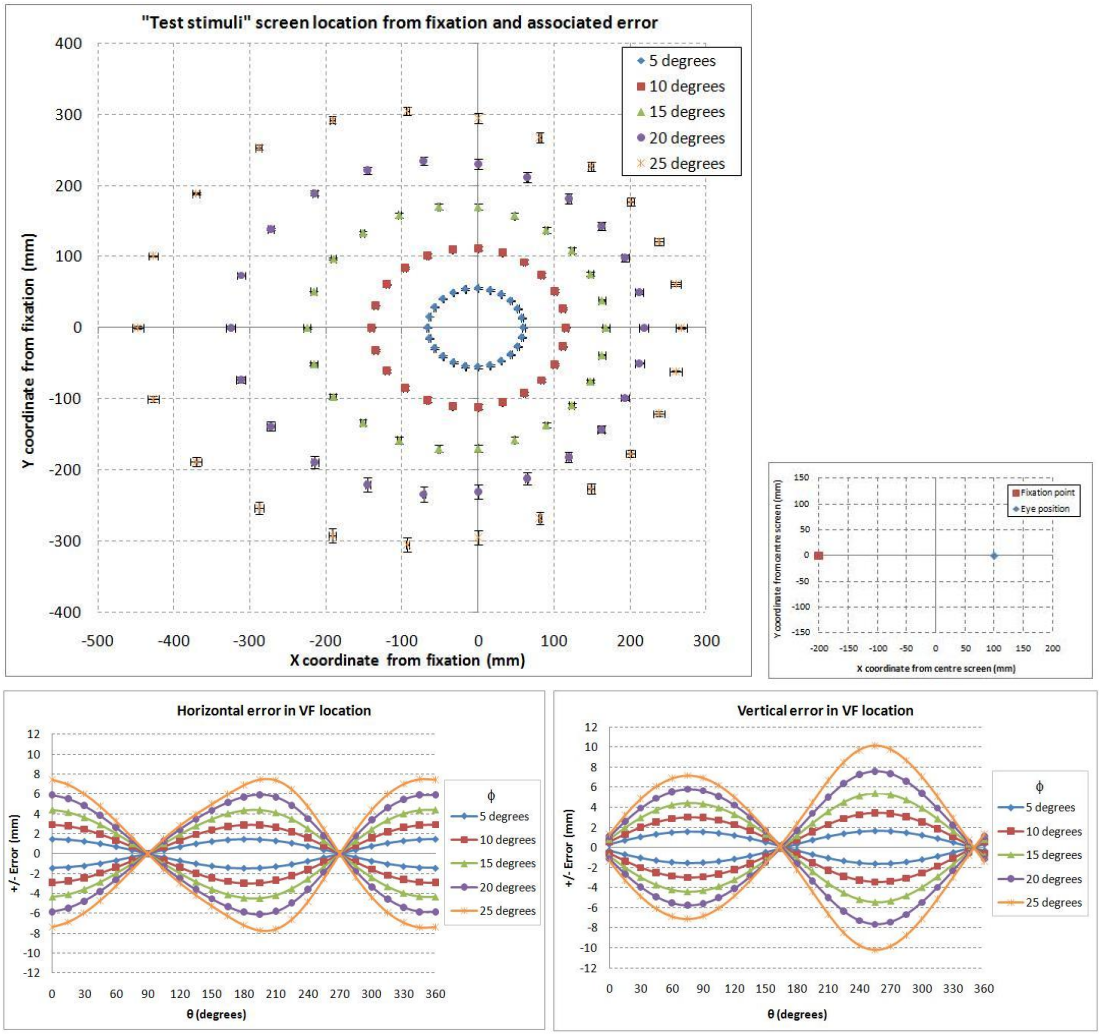

Figure 5.55: Screen location error for various visual field locations associated with a camera-to-eye distance error of ±20mm at 600mm. Fixation point is at the far left of the screen, and the eye is located approximately as far right as the camera's field of view will allow.

Figure 5.56 shows the horizontal and vertical screen location error for 120 visual field points under a situation where fixation is at the top of the screen and the location of the test eye as low down vertically as the camera field of view will allow (shown by the small chart).

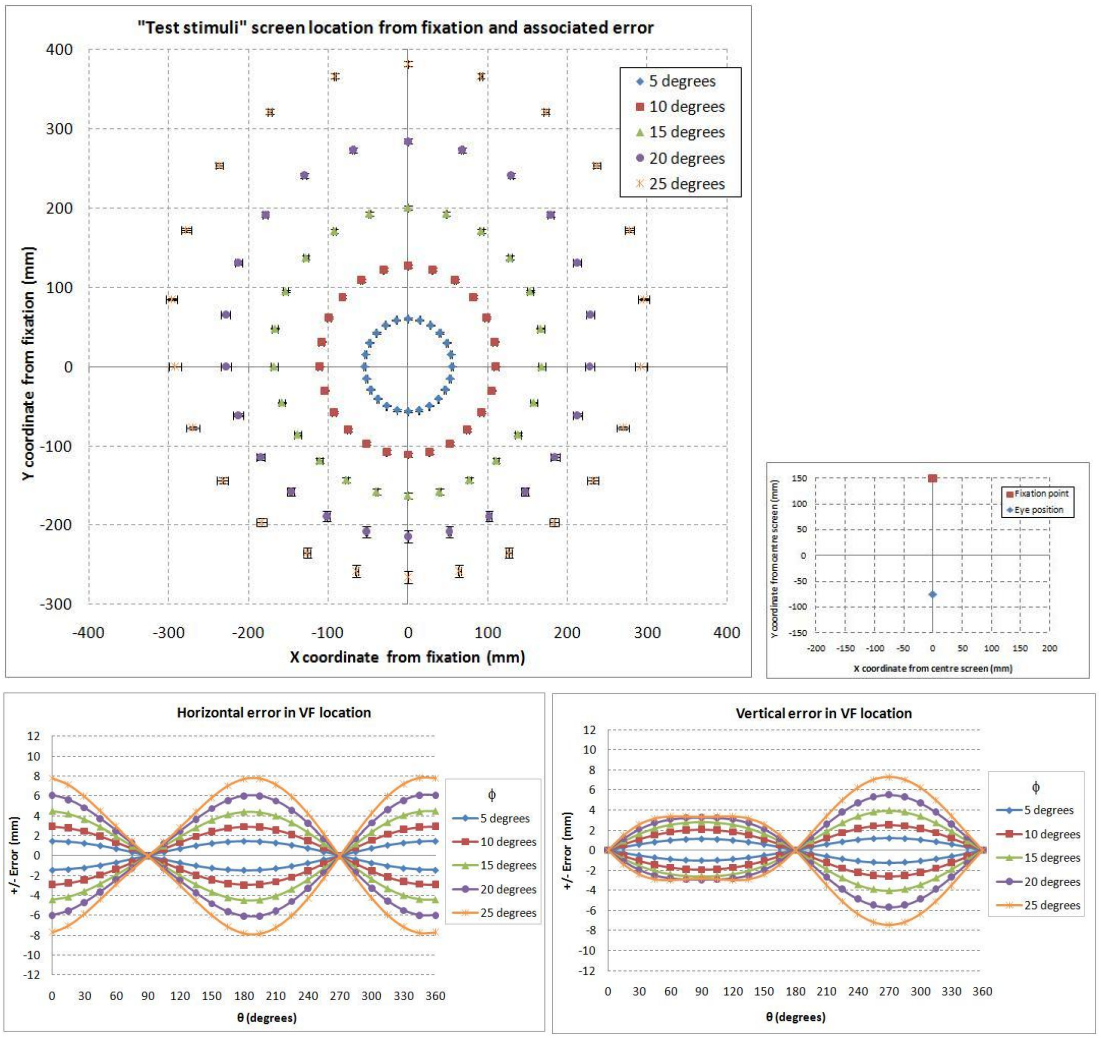

Figure 5.56: Screen location error for various visual field locations associated with a camera-to-eye distance error of ±20mm at 600mm. Fixation point is at the top of the screen, and the eye is located approximately as low down as the camera's field of view will allow.

Figure 5.57 shows the horizontal and vertical screen location error for various visual field points for a situation where fixation is at the bottom of the screen and where the location of the test eye as elevated as far as the camera field of view will allow (again shown by the small chart).

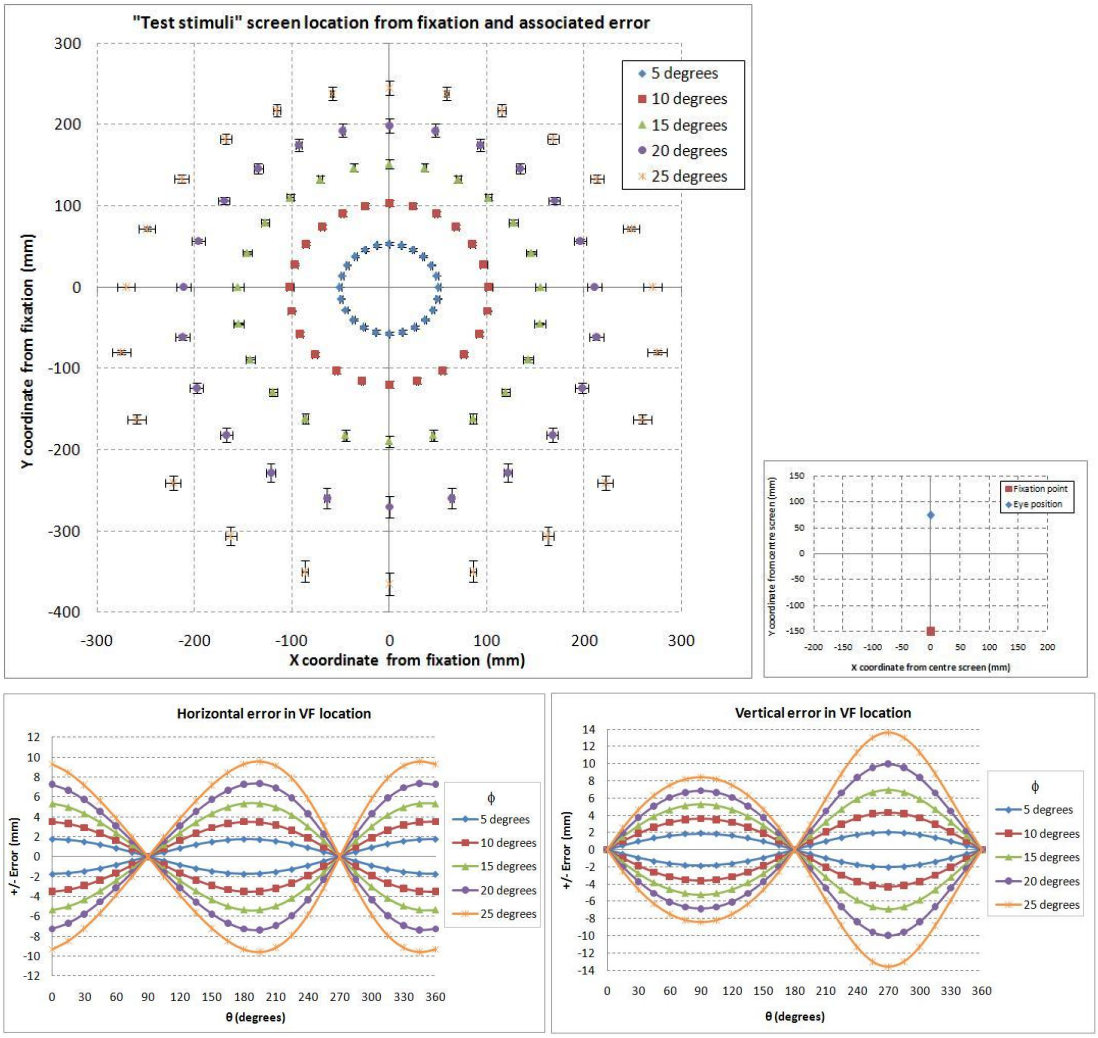

Figure 5.57: Screen location error for various visual field locations associated with a camera-to-eye distance error of ±20mm at 600mm. Fixation point is at the bottom of the screen, and the eye is located approximately as high up as the camera's field of view will allow.

Figure 5.58 shows the horizontal and vertical screen location error for the 120 visual field points under a situation where fixation is at the left hand side, and bottom of the screen and with the location of the test eye as elevated vertically and as far right horizontally as the camera field of view will allow (shown in the small chart).

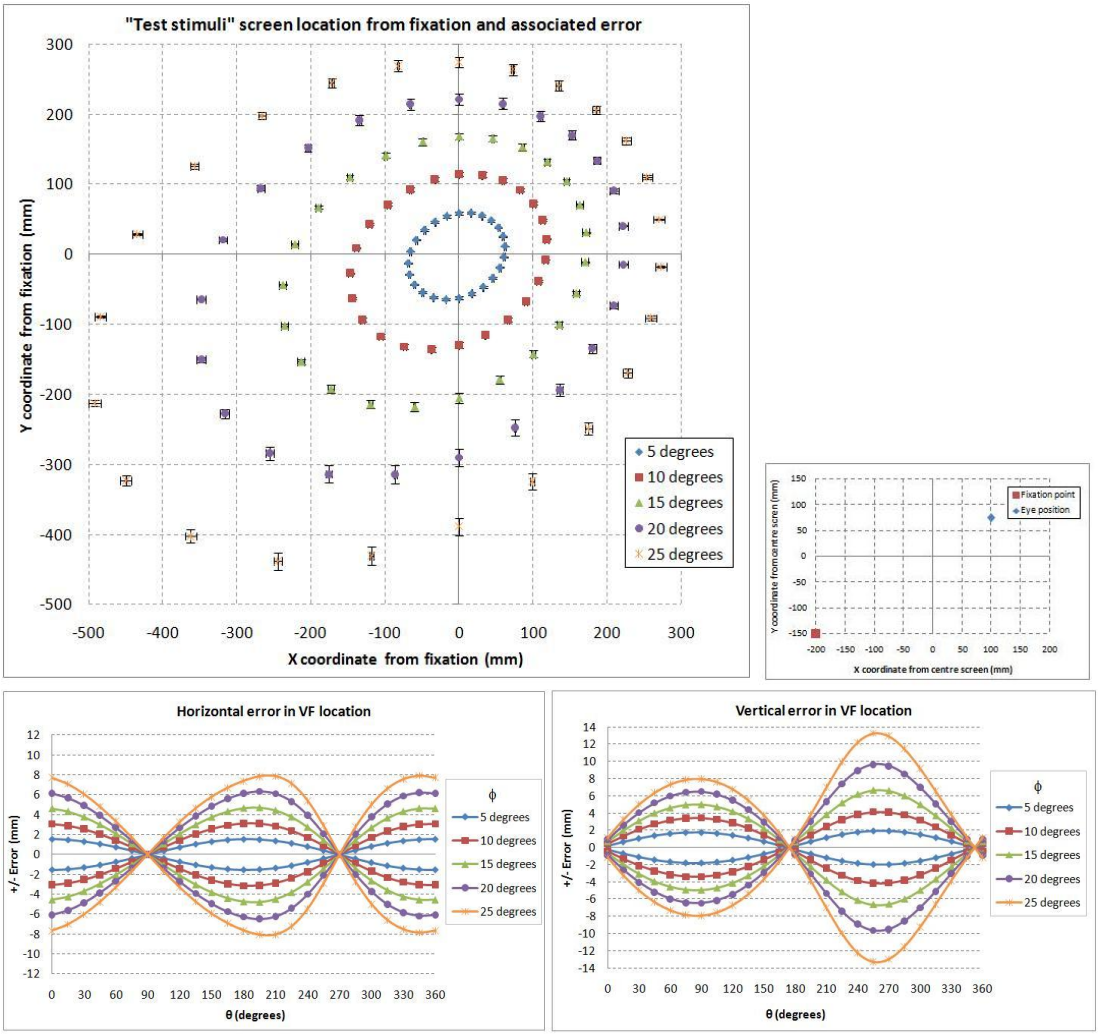

Figure 5.58: Screen location error for various visual field locations associated with a camera-to-eye distance error of ±20mm at 600mm. Fixation point is at the bottom-left of the screen, and the eye is located approximately as far top-right as the camera's field of view will allow.

Figure 5.59 shows the horizontal and vertical screen location error for the 120 visual field points under a situation where fixation is at the right hand side, and top of the screen and with the location of the test eye as low down vertically and as far left horizontally as the camera field of view will allow (shown by the small chart).

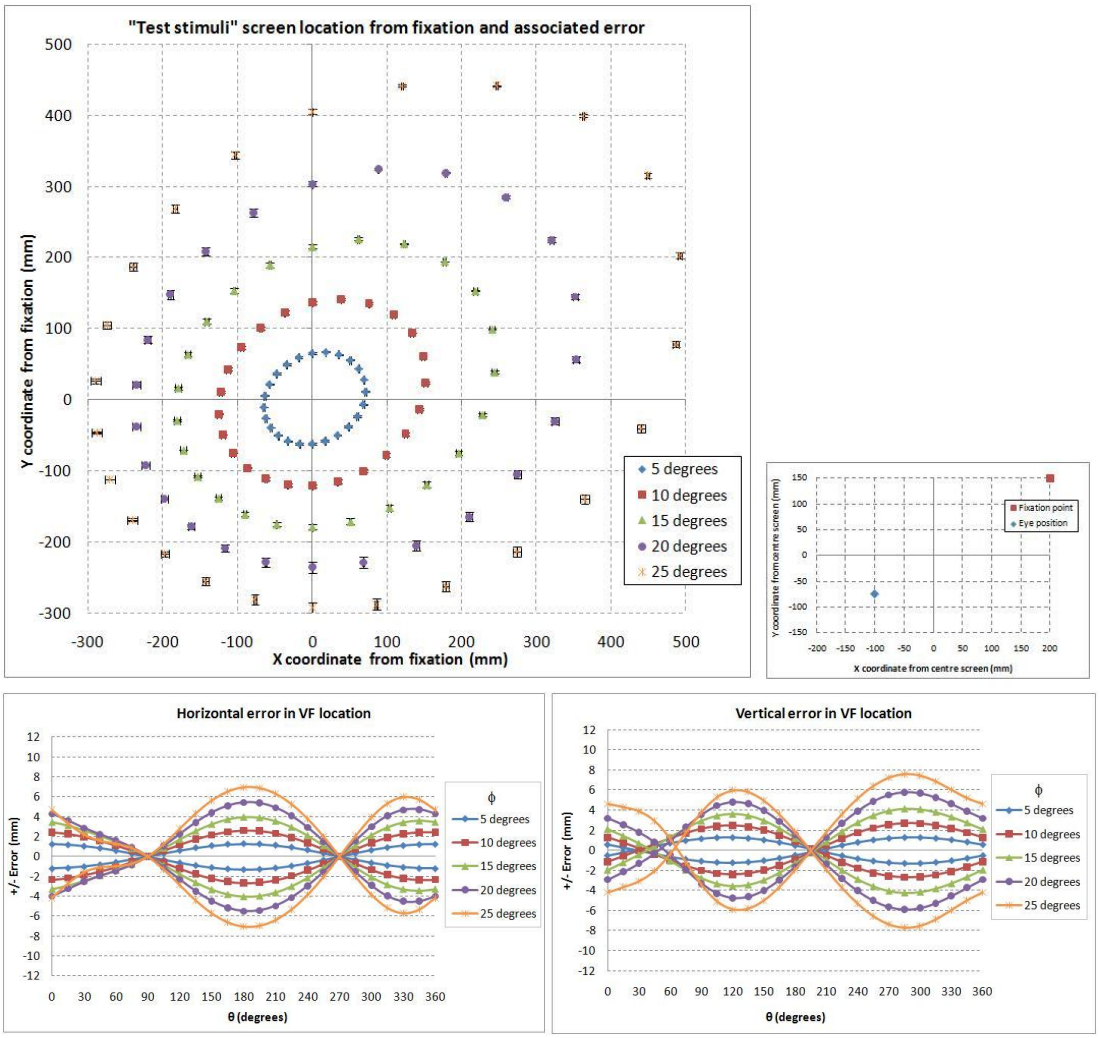

Figure 5.59: Screen location error for various visual field locations associated with a camera-to-eye distance error of ±20mm at 600mm. Fixation point is at the top-right of the screen, and the eye is located approximately as far bottom-left as the camera's field of view will allow.

Thus far, all the example situations shown have been with the test eye at a distance of 600mm from the eye tracker's camera. Because the test eye can also potentially be at different camera-to-eye distances (D), the modelling analysis was also performed at different values of D. Table 5.13 shows the largest error as seen by the modelling methods for three different values of D and for each of the eccentric visual field angles ($\phi = 5° - 25°$ in steps of 5°).

Eccentric VF angle, ϕ (Degrees)	Largest theoretical error at different eye distances, D (±mm)		
	Error when D = 500 mm	Error when D = 600 mm	Error when D = 700 mm
5	2.1	2.0	2.0
10	4.4	4.3	4.3
15	7.0	6.9	6.8
20	10.1	10.0	9.8
25	13.8	13.6	13.3

Table 5.13: Table of maximum screen location errors for different camera-to-eye distance values (D) and different values of eccentric visual field angle.

The largest observed error for each eccentric visual field angle (as given in table 5.13) always occurs as an error in y screen location, and also always occurs when fixation is at bottom of the screen with the eye location at the top of the eye tracker camera's field of view. This largest error is for visual field points with a rotational visual field angle (θ) between 180 and 360 degrees (i.e. below the fixation point), and as such cannot actually be displayed on the screen from this described fixation point. Table 5.14 gives the largest possible errors in stimulus screen position for those stimuli which can actually be displayed on the screen. Table 5.15 then gives the corresponding eccentric visual field angle value for each of the maximum screen distance errors given in table 5.14

Eccentric VF angle, ϕ (Degrees)	Largest theoretical error at different eye distances, D (±mm)		
	Error when D = 500 mm	Error when D = 600 mm	Error when D = 700 mm
5	1.9	1.9	1.9
10	3.6	3.6	3.6
15	5.3	5.3	5.2
20	6.9	6.9	6.8
25	8.5	8.4	8.3

Table 5.14: Table of maximum screen location errors for different camera-to-eye distance values (D) and different values of eccentric visual field angle, taking into account the location of fixation on the screen.

Eccentric VF angle, ϕ (Degrees)	Largest theoretical eccentric visual field angle error at different eye distances, D (±degrees)		
	Error when D = 500 mm	Error when D = 600 mm	Error when D = 700 mm
5	0.2	0.2	0.2
10	0.42	0.4	0.3
15	0.6	0.5	0.5
20	0.8	0.7	0.6
25	1.0	0.8	0.7

Table 5.15: Table of maximum eccentric visual field errors for different camera-to-eye distance values (D) and different values of eccentric visual field angle, taking into account the location of fixation on the screen.

5.5.1.3 Discussion

Using an error in D of ±20mm, the largest error in stimuli screen location was modelled as 8.5mm. The largest error values relate to the larger visual field angles (variable ϕ) with 25 degrees from fixation being the largest analysed here. Interestingly the error varies in such a way that the x and y error values fluctuate as the visual field point being tested rotates through 360 degrees around the fixation point (variable θ). Fortunately this variation is in such a way that the x error reduces to zero as it approaches 90 and 270 degrees, and for most situations the y error reduces to zero as it approaches 0 and 180 degrees. This fact is very useful as it means that the display position is not likely to cross the horizontal and vertical midlines even when taking into consideration the induced error. This is of important clinical relevance because of the way in which visual field defects resulting from cerebral visual impairment often respect the horizontal and/or vertical midlines.

The modelling methods used in these methods take into account the main error inducing variable which is the camera-to-eye distance (D) data. The error in D in turn induces errors in the calculated x, y, and z eye location. This is all taken into account in this analysis. However this analysis does not take into account the potential error in two other variables which are also used in the calculation of eye position, namely x and y eye location in the camera field of view data as it is provided by the eye tracker. It is likely that there would also be additional errors from these camera values. However, the methods of error analysis performed here have taken into account the most influencing factor (the error in D). Also, the way in which x and y locations in the camera field of view is determined is purely by the relative position of the x and y locations of the eyes as it is observed by the eye tracker, whereas the distance data are calculated by the eye tracker using some assumptions (for example with regards to the shape of the cornea) and as such it is more susceptible to error (as seen by experimentation in section 5.2.2 on page 96).

What are the implications of these calculated "test stimulus" screen location errors? The errors

are small. However, it is feasible that the error may affect the comparative data of SVOP and equivalent HFA tests if the border of a patient's visual field defect happens to lie in the area of a point or points that are being tested. However, there are also several other factors which are expected to contribute to differences in comparative data. For example, the documented problem of ASP test-retest variability.[115–118]. Additionally the known small variation in luminance of the presented "test stimuli" in the SVOP test may also contribute to any discrepancies between SVOP and HFA tests. Given the factors which contribute to variability in visual field assessment the errors in "test stimulus" screen location identified in these methods are not considered great enough to contribute significantly more than these other factors. Additionally, because of the manner in which "test stimuli" location error reduces as the visual field midlines are approached, the errors are considered acceptable for this application.

It was also interesting to note that through general observation during SVOP tests in progress (when other methods of this research were being carried out), large positional errors in the "test stimuli" locations do not seem to occur. It has often been very easy to identify which visual field point is being tested based on its position relative to the last "fixation stimulus". This has also given confidence to these suggested small "test stimuli" location errors.

5.5.2 Limitations

There are no specific methods or results for this section. However, it is important to document the known limitations of the developed system. The limitations for some aspects have been found through experimentation in previous sections (such as screen luminance variation, and distance data error for example). The limitations for other aspects have been found through observation during testing (or attempted testing). Where appropriate the relevant experimental section is referenced in the text. The main limitations of the developed SVOP system can be divided into two categories associated with the two main hardware components of the system: the eye tracker and the display screen.

The display screen has the obvious limitation due to its size. As outlined in section 5.1.1.2 on page 59 the size of the display screen imposes a limit of the maximum visual field angle that can be assessed. The size used in the developed system (20" diagonal screen size) allows standard visual field test patterns to be used (which encompass test locations within the first 30 degrees of visual field), including the 40 point screening test pattern used in this research. However, it would not be capable of presenting "test stimuli" greater than approximately 30°. The other main limitation of the display screen used in the developed system is to do with the screen's ability to display appropriate luminance levels for the "test stimuli". In addition to the variability of luminance at any single "test stimuli" luminance level (as discussed in section 5.2.3), there is also a limit to the maximum and minimum luminance that the display screen can

display. The maximum "test stimuli" luminance level is governed by the maximum brightness of the display screen (which is determined by the back-light of the LCD screen). The minimum "test stimulus" luminance level which can be displayed is governed by the screens ability to display different levels of luminance at the lower end (darker end), which in this research is the lowest luminance difference between two grey-scale colour levels (one being the background grey level and the other being the "test stimulus" grey level. These maximum and minimum values (equated to the HFA levels) were found for the screen used in the developed SVOP system and each luminance level has its own error for displaying on the test screen.

Limitations due to the eye tracking device can be further categorised according to whether or not the limitation allows any eye tracker data to be collected or not. Some problems will simply not allow eye tracking data to be provided, or will only provide very limited data. Other limitations will produce inaccurate data. Several of these eye tracking problems were not observed until during the larger "clinical validation trial" which is detailed in the next chapter. However, it is appropriate to group the known limitations of the eye tracker in a single section within this thesis. These limitations are described under the two headings below relating to: (i) situations where there is no or poor quality eye tracking, and (ii) where tracking is possible but the data is potentially inaccurate.

Reasons for no or poor quality eye tracking

Poor quality or no eye tracking data occurs when there is something which interferes with the pupil-corneal reflection technique. The eye tracker is expecting to see specific reflections from the eye which relate to reflections from the cornea and a pupil. Anything which deviates from these expected reflections means that the eye is not properly detected and data for that eye is either non-existent or sporadic in nature. Below are some examples which have been observed during this research program which have meant the eye tracker has been unable to detect subject's eyes.

Figure 5.60 shows a photograph of the eyes of a patient with a right persistent dilated pupil which could not be tracked by the eye tracker, and the left eye for comparison. The eye tracker is expecting to see a "nice" circular shaped pupil (or rather an elliptical shape pupil from the point of view of the eye tracker camera) and as a result would not detect this patient's right eye.

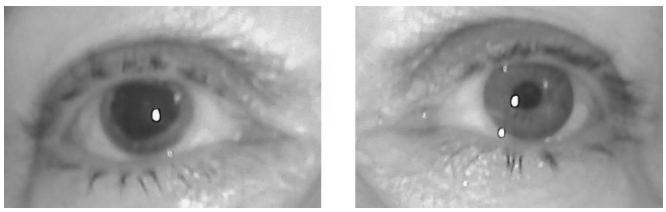

Figure 5.60: A patient's right eye with persistent dilated pupil (left hand photo) and left eye for comparison (right hand photo).

Similarly, other "visible" eye abnormalities can cause the eye tracker to not perceive an eye correctly. An example of this was patients who had undergone surgical procedures for glaucoma such as an iridectomy which involves creating a small hole in the peripheral iris. From the point of view of the eye tracker, this can create an additional reflection from the eye which in turn seemed to "confuse" the eye tracker. Figure 5.61 shows the eyes of a patient who had undergone an iridectomy procedure in their left eye (circled in the right hand photo). However, with this patient neither eye could be tracked with sufficient reliability and this could perhaps be related to this patient's previous anterior uveitis which had left slightly irregular shaped pupils in both eyes. Although this patient had two visible abnormal features in their left eye which contributed to poor quality eye tracking, there were other patients with poor quality eye tracking where the only obvious issue was an iridectomy, so it is suspected that an iridectomy alone can disrupt the eye tracking ability. However, it should also be mentioned here that yet another patient with an iridectomy was able to complete the testing without any problems in eye tracking quality. These iridectomy "holes" can vary in size and location, so it seems as though it could be that with smaller sized, or more peripherally located "holes" eye tracking is possible. These results are rather subjective at present. However, it is important to document them here as possible limitations to performing SVOP tests. Future work should attempt to document these types of eye tracking problems further.

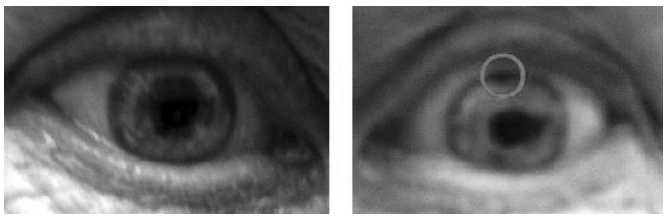

Figure 5.61: A patient's right (left hand photo) and left eye (right hand photo) showing area of iridectomy (circled). This patient also demonstrated a slightly irregular shaped pupils as a result of bilateral uveitis.

Further problems with eye tracking quality can be caused by objects coming between the eye tracker camera and the eye, thus obscuring the camera's view of the eye. Examples of this include the frames of glasses, large "bushy" eye lashes, or drooping eye lids.

Two other examples of poor quality eye tracking have been observed. One where a patient was wearing heavy, dark mascara which is known to cause problems with eye tracking as it makes it difficult for the eye tracker to detect accurately the boundary of the elliptical features of the eye.[119] Additionally, another patient was wearing large highly reflective ear rings which created additional reflections, thus confusing the eye tracker. Once the ear rings were removed, there were no eye tracking problems.

Reasons for inaccurate gaze or distance data

It may be that the eye tracker has no problems detecting the eye(s) and providing gaze and distance data, but under certain situations the eye gaze data or the eye distance data may still be unreliable. The main example of this is that with corrective lenses there is a false increase or decrease in the distance data. This can be compensated for as the increase or decrease relates directly to the power of the corrective lens, but would also require specialist spectacle frames constructed in such a way as to not obstruct the eye tracker's view of the eye.

Strabismus is a condition where the two eyes are not aligned correctly and therefore do not fixate at the same location.[120] The condition can affect one or both eyes, be intermittent and vary in severity of miss-alignment. These factors all play a part in the accuracy of the gaze data provided by the eye tracker. In some cases the eye tracker may actually be providing accurate data, and instead it is the subject that is inaccurate with their fixation. In other cases (for example if the strabismus is intermittent) it will depend on how the eye was behaving during the calibration procedure. These effects can, in some cases, be compensated for by choosing to use data from only one eye (an unaffected eye), or by patching of the opposite eye which will then in many cases force the affected eye to adjust correctly.

Fortunately many of these described problems are less relevant for young children (certain surgery procedures for glaucoma treatment, mascara, earrings). Unfortunately, strabismus can be a prominent feature of children who attend ophthalmology clinics and of those who have who may need their visual field tested. Further work may be required to quantify more fully the full extent of eye tracking problems in children with strabismus.

Chapter 6

Clinical validation trial

6.1 Introduction

Following the promising early results of the "feasibility study" (section 5.4 on page 127), a clinical trial with a larger cohort of participants was devised in order to more thoroughly evaluate the developed SVOP testing system. This chapter details the subjects, methods and results for the larger clinical "validation trial". The aim of the validation trial is to assess the validity of the developed SVOP test system as a diagnostic tool for suprathreshold visual field assessment by comparing SVOP test results directly with equivalent suprathreshold screening test results obtained using the Humphrey Field Analyser (HFA). The HFA was used as a "gold standard" for comparison where its tests could be reliably performed by the participants. Where subjects were unable to reliably perform the "gold standard" HFA tests, SVOP test results were compared with other relevant clinical findings. The HFA was chosen to act as a "gold standard" comparison test for this validation trial because there are currently no equivalent child perimetry devices which assess the visual field in the same manner as SVOP (i.e. by the method of automated static perimetry), and the HFA screening test could easily be customised and replicated (in terms of test stimuli brightness, size and location) using the SVOP system developed, in order to produce an equivalent test.

6.2 Subjects, methods and data analysis

6.2.1 Subjects

As with the previously completed feasibility study, subjects were recruited and assigned to one of four subject groups:

1. Children with suspected visual field defects (also referred to as "child patient" group).
2. Healthy children.
3. Adults with visual field defects (also referred to as "adult patient" group).
4. Healthy adults.

Adults were defined as subjects aged 16 years or older and children were defined as younger than 16 years. "Normal" (healthy) adults and children were recruited for the study had an unremarkable ophthalmological history. Adults and children with visual field defects were defined as having a known or clinically suspected possibility of visual field defects of sufficient depth so as to allow them to be identified by the suprathreshold screening tests. Subjects that were excluded from the trial were people with very severe visual impairment or with severe limitation of eye movements for any reason which would preclude visual field testing. The exclusion criteria were deliberately designed without well defined limits so as to gain an understanding of the limitations of SVOP testing.

Table 6.1 outlines the subjects recruited for the trial within each of the subject groups.

Subject Group	Number of subjects (males)	Age (Years)		Age (Months)	
		Mean (1 SD)	Range	Mean (1 SD)	Range
Child patients*	35 (19)	6.7 (3.6)	1-15	84.3 (43.9)	13-181
Healthy children	18 (9)	8.7 (3.8)	0-14	109.4 (46.1)	8-178
Adult patients	41 (19)	57.3 (15.0)	16-78	-	-
Healthy adults	28 (14)	30.4 (12.1)	16-61	-	-
Total	122 (61)				

**Several of the child patients had multiple visits to participate in the study. The mean ages given for this group are based on age at first visit.*

Table 6.1: Subjects recruited for the validation study. SD = Standard deviation.

6.2.2 Methods

The methods are described here in terms of the visual field test types. First, an explanation of the perimetry tests which were used (both SVOP and HFA) is given, then an explanation of which tests were typically performed by participants from the different subject groups.

SVOP Tests

As with the feasibility trial, three different types of SVOP test patterns used. The test patterns and number of tests performed by each subject depended upon the ability of the participant (this is explained further in forthcoming paragraphs). However, the procedure for performing

SVOP tests was the same whichever test pattern was used. The three test patterns available are shown in figure 6.1 and are described as follows:

1. A right eye and left eye test pattern consisting of 41 test points each (figure 6.1 a) and b) respectively). These test patterns are equivalent to the HFA's C-40 right and left eye screening test patterns (which each contain 40 test points each) with the exception that the SVOP test has an extra test point located at the approximate average natural blind spot location for the eye being tested.

2. A binocular test pattern consisting of 40 test points (figure 6.1 c). This test pattern has no equivalent HFA test pattern and was custom made specifically for participants who could not perform uniocular testing but it is similar in layout to the uniocular test patterns.

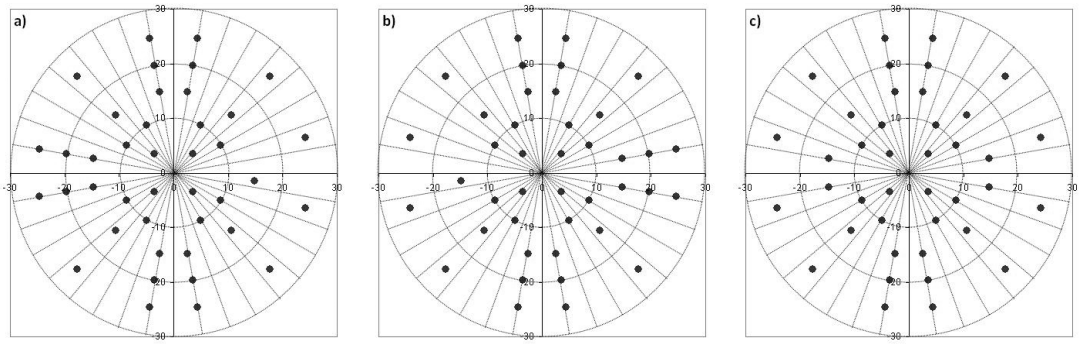

Figure 6.1: The three SVOP visual field test patterns used in the validation trial. a) A test pattern equivalent to the right eye HFA C-40 screening test. b) A test pattern equivalent to the left eye HFA C-40 screening test. c) A custom test pattern designed for binocular SVOP testing.

Prior to performing any SVOP visual field test, the subject was positioned in front of the patient display screen using appropriate seating for their age. If a uniocular test was to be performed, the subject was asked to wear an occluding eye cover over the eye not being tested. Next, with the subject looking towards the screen (with a fixation image, appropriate to the subject's age, displayed if required), the screen was moved to a location where the subject's eyes were located centrally (both horizontally and vertically) in front of the display screen and positioned at approximately 550-600mm away from the eye tracker's camera. This procedure was performed using a "Tracking Status" dialogue box which gave a representation of the location of the subject's eyes to the examiner (figure 6.2).

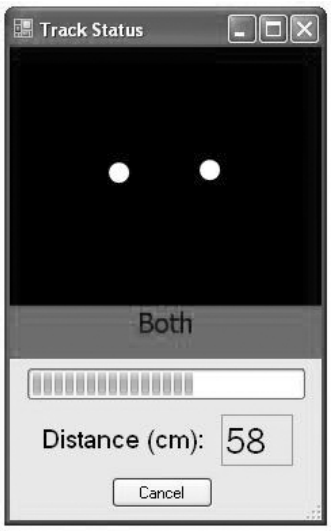

Figure 6.2: Image (screen shot) of the "tracking status" dialogue box. It shows the location of the eyes in real time (the white circles) horizontally and vertically in front of the display screen and also gives an indication of the distance to the eyes from the eye tracker's camera.

Once the subject was located in an appropriate location, a calibration procedure was performed. The calibration procedure is required in order to produce the most accurate gaze data. During a calibration procedure subjects were required to look at the display screen and follow a visual stimulus with their gaze to 5 different screen locations. The stimulus used for adults and older children was a circle which moved to each location in turn (the Tobii eye tracker's standard calibration stimulus). For younger children a custom calibration procedure was used where the circle was replaced with a cartoon character which moved to each of the 5 screen locations where upon a simple animation with sound was played, lasting just a few seconds, in order to keep the attention of the child.

Once the calibration procedure was complete, a SVOP test could be performed. Tests performed by adults and older children used a simple small cartoon face as the "fixation stimulus". For younger children the "fixation stimulus" of a cartoon face was replaced with a variety of small (similar in size to the adult "fixation stimulus") cartoon character animations with sound effects which lasted between 1 and 4 seconds, so as to encourage attention and maintain interest. The visual field "test stimuli" were all of size Goldmann III (0.43° angular diameter), duration 200ms, and luminance level equivalent to the HFA's 14dB brightness level (stimulus and background luminance of 429Asb and 31.5Asb respectively). Adults and older children were given the simple instruction "If you see anything flash up on the screen just look towards or at it". Younger children were not given any specific instructions, but were actively encouraged to look at the display screen.

HFA tests

Two different types of HFA test patterns were used. These were the HFA's left and right eye C-40 screening test patterns. The right eye test pattern is shown in figure 6.3.[121] The left eye test pattern is a mirror image of the right eye test pattern. These test patterns use 40 visual field test locations, and additionally the HFA goes through a procedure at the beginning of a test to "find" the subject's natural blind spot, this location is then identified using a triangle symbol on the test results.

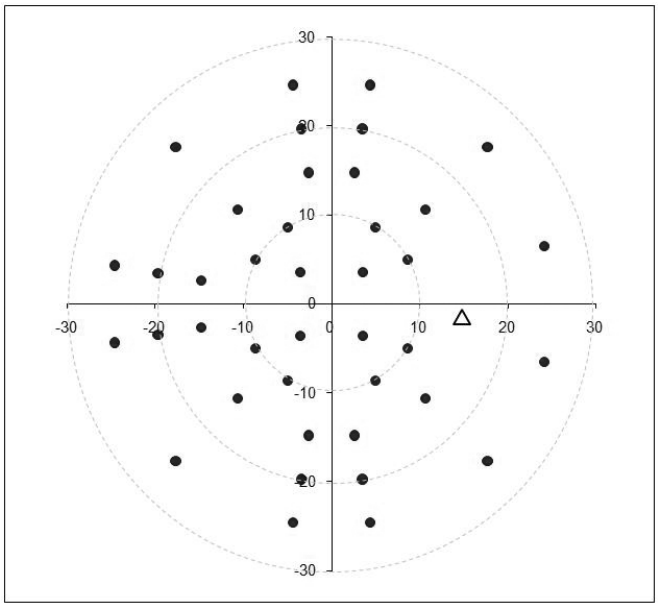

Figure 6.3: The HFA's C-40 screening test pattern for the right eye. The left eye test pattern is a mirror image of this.

To perform a HFA test, the subject had one of their eyes covered with an occluding eye patch (depending upon the uniocular test being performed), was given the patient response button, and was positioned on the appropriate side of the chin-rest (the opposite side to the eye being tested). The height of the HFA bowl (with chin-rest) was adjusted so that the subject was at a comfortable height. The subject was then asked to stare at the "fixation light" located centrally in the bowl while the chin-rest was moved using the motorised "fine adjustment" movement controls until the eye was located directly in front of the "fixation light" (this is made possible using the live video image of the eye with centrally located cross-hairs shown on the examiner's screen).

The HFA's standard screening tests use an age-matched "hill of vision" where stimuli are presented at 6dB brighter than the expected threshold value at each test location for the patient's age. These age-matched values are taken from a database of normative subject data. However, the exact values are not disclosed by the manufacturer, so in order to create a pair of exact

equivalent HFA and SVOP tests, the HFA's C-40 tests were purposely altered so that all stimuli were presented at a constant intensity level of 14dB, thus matching the SVOP visual field tests which were also tailored to display stimuli at the HFA intensity level of 14dB (stimulus intensity of 429Asb and background 31.5Asb as stipulated in the HFA manufacturer manual[121]). The stimulus size and duration used in the HFA C-40 tests was Goldmann III and 200ms respectively.

Subjects were given the instruction "You must always stare at the central light and only press the button when you see other lights flash up around about the central light. The lights which flash up may be bright or dim."

Tests performed

Ideally every participant would complete a full testing protocol consisting of a left and a right eye SVOP test followed by a left and a right eye HFA test before taking a break. The type of test to be performed first (be it SVOP or HFA) was randomised. Following the break, the 4 tests already completed were repeated but in a reverse order in terms of the device used. This "ideal" protocol results in a total of 8 visual field tests comprising of 4 SVOP tests (2 left eye and 2 right eye) and 4 HFA tests (again 2 left eye and two right eye). Not all subjects were able to perform the full set of 8 visual field tests. In children where uniocular testing was deemed not possible or not tolerable, two binocular SVOP tests were performed without any HFA equivalent.

6.2.3 Data analysis

The main forms of data analysis to be performed can be described in three categories:

- direct comparison of SVOP and HFA tests,
- repeatability of SVOP and HFA tests, and
- other indirect comparisons.

Direct comparison of SVOP and HFA tests

A measure of sensitivity and specificity can be obtained for the SVOP test by using the HFA test points as a reference or "gold standard". Each visual field point in a subject's HFA test is classified as either "unseen" (a positive result) or "seen" (a negative result), and the equivalent SVOP test can be used as a direct comparison to categorise each outcome as one of the following:

- True positive (TP) - "Unseen" points on a HFA test which the equivalent SVOP test also "correctly" diagnosed as "unseen".

- False positive (FP) - "Seen" points on a HFA test which the equivalent SVOP test "incorrectly" diagnosed as "unseen".
- True negative (TN) - "Seen" points on a HFA test which the equivalent SVOP test also "correctly" diagnosed as "seen".
- False negative (FN) - "Unseen" points on a HFA test which the equivalent SVOP test "incorrectly" diagnosed as "seen".

Using these definitions, the sensitivity and specificity (and positive and negative predictive values) can be calculated as demonstrated in table 6.2.

		HFA test points ("gold standard")		
		Positive ("unseen")	Negative ("Seen")	
SVOP test points	Positive ("unseen")	True positive (TP)	False positive (FP)	→ Positive predictive value $= \frac{TP}{TP+FP}$
	Negative ("Seen")	False negative (FN)	True negative (TN)	→ Negative predictive value $= \frac{TN}{TN+FN}$
		↓ Sensitivity= $\frac{TP}{TP+FN}$	↓ Specificity= $\frac{TN}{TN+FP}$	

Table 6.2: Calculation of sensitivity, specificity, and positive and negative predictive values.

The sensitivity is a measure of how good a test is at correctly identifying the presence of disease (in this case visual field locations which are identified as "unseen"). The specificity is a measure of how good a test is at correctly identifying those that are healthy (in this case visual field points which are labelled as "seen"). The positive predictive value is a measure of the chance that a positive test result is correct and the negative predictive value is a measure of the chance that a negative result is correct. Sensitivity and specificity are unaffected by the prevalence of disease in a tested population whereas the predictive values have a certain dependence on the prevalence of disease, where a reduction in prevalence results in a fall of the positive predictive value and a rise in the negative predictive value (in a test where sensitivity and specificity remains the same).[122]

For each uniocular SVOP test with a HFA "gold standard" comparison test there were 41 points which could be assessed (including the blind spot location). The sensitivity and specificity outcomes can be applied to various situations by counting up the total true positive, false positive, true negative and false negative points within different situations for example all tests or specific subject groups. The types of analysis performed are described fully in the results section.

Repeatability of SVOP and HFA tests

Where tests have been repeated during the same visit (i.e. either SVOP or HFA tests of the same eye(s) performed twice), Cohen's kappa statistic was used to obtain a measure of agreement between the repeated tests. Cohen's kappa statistic is traditionally used as a measure of agreement between two raters measuring something which has a binary output (i.e. two possible outcomes).[123] It was introduced as a measure of agreement which avoids the problem associated with a simple percentage agreement analysis which has the potential to be inflated due to chance agreement.

The kappa statistic, κ is given by:

$$\kappa = \frac{P(a) - P(e)}{1 - P(e)} \tag{6.1}$$

where P(a) is the relative observed agreement between two raters, and P(e) is the hypothetical probability of chance agreement calculated using the observed data to determine the probabilities of each observer randomly producing each result category.

In this visual field test repeatability situation, if we have data for two visual field tests of the same type (i.e. two left, two right or two binocular tests on either the SVOP system or HFA perimeter), we have a similar situation to the sensitivity and specificity analysis where we have visual field points which either agree or disagree as shown in table 6.3. The labelling of the outcomes in table 6.3 is perhaps slightly misleading because true and false positives and negatives suggest that one of the tests is a "gold standard" result which is not the case here. This labelling is used simply to illustrate the similarities to the outcomes used to calculate sensitivity and specificity already described in this section.

		Test 1	
		Positive ("unseen")	Negative ("seen")
Test 2	Positive ("unseen")	True positive (TP)	False positive (FP)
	Negative ("seen")	False negative (FN)	True negative (TN)

Table 6.3: Variables used in kappa statistic calculations

The observed probability of agreement, P(a), is given by:

$$P(a) = \frac{TP + TN}{N}$$

where $N = TP + TN + FP + FN$

The probability of random agreement, P(e), is given by:

$$P(e) = \left(\frac{TP+FN}{N}\right)\left(\frac{TP+FP}{N}\right) + \left(\frac{FP+TN}{N}\right)\left(\frac{FN+TN}{N}\right)$$

where $N = TP + TN + FP + FN$

And as stated, kappa, κ is given by equation 6.1.

κ is always less than or equal to 1. A value of 1 implies perfect agreement and values less than 1 imply less than perfect agreement. In cases where κ is negative, this is a sign that the two observers (or visual field location results in this case) agreed less than would be expected just by chance. There are different interpretations as to what a good level of agreement is. The following is one widely used interpretation:[124]

- $\kappa < 0.20$, poor agreement;
- $\kappa = 0.2$ to 0.4, fair agreement;
- $\kappa = 0.4$ to 0.6, moderate agreement;
- $\kappa = 0.6$ to 0.8, good agreement;
- $\kappa = 0.8$ to 1.0, very good agreement.

Other indirect comparisons

SVOP test comparisons without a HFA equivalent will typically occur with child patients where no equivalent HFA test was performed or the HFA test result proved unreliable. The data from SVOP tests could still be assessed for repeatability if the test was performed twice. However, in terms of comparative data available, this was in the form of what was already clinically suspected on the basis of clinically performed confrontational visual field testing and other evidence which would suggest the possible presence of visual field defects such as their clinical diagnosis and results of brain scans.

6.3 Results

This results section is divided into further sections corresponding to the data collected. The first section details the testing performed, the second section presents the comparison data between SVOP and HFA tests and also the repeatability of the SVOP and HFA visual field testing. The final section takes the form of a series of case studies consisting of the more interesting visual field results (such as those children who had repeated testing over time) which had no equivalent HFA test (or where the HFA equivalent tests were unreliable).

6.3.1 Visual field tests performed

Before continuing to the main results, a summary of the testing performed is important. Ideally all subjects would complete a full set of 8 visual field tests comprising 4 SVOP tests (2 left and 2 right eye tests) and 4 HFA tests (2 left and 2 right eye tests). Not all subjects were able to complete a full set of 8 tests. In some cases participants would only partially complete a full set of 8 uniocular tests, in these situations there would still usually be comparison tests available (i.e at least 1 SVOP test with an equivalent HFA test). If a subject was deemed only able to perform binocular testing, only SVOP tests were performed as there was no comparison HFA test for this strategy. Finally, if subjects were unable to perform even the SVOP binocular testing, no further visual field tests were performed. Table 6.4 shows a summary of the number of patients which fell into each of the above categories, and figure 6.4 charts the data as a percentage of subjects within each subject group to provide a visualisation of the type of testing performed in each group. Table 6.5 shows a summary of the total number of tests performed within each group, the number of direct comparisons available for analysis and the number of repeated tests available for SVOP and HFA repeatability analysis.

Subject group	Number of subjects performing visual field tests				Total subjects
	Full set of 8 tests	Partial set of tests with at least 1 HFA comparison	SVOP tests only (no HFA comparison)	No SVOP	
Child patients*	2	8	16	9	35
Healthy children	12	0	6	0	18
Adult patients	30	5	1	5	41
Healthy adults	27	1	0	0	28
Total subjects	71	14	23	14	122

*Several of the child patients had multiple visits to participate in the study. This table shows data from their first visit only.

Table 6.4: Summary of the visual field tests performed by each subject group

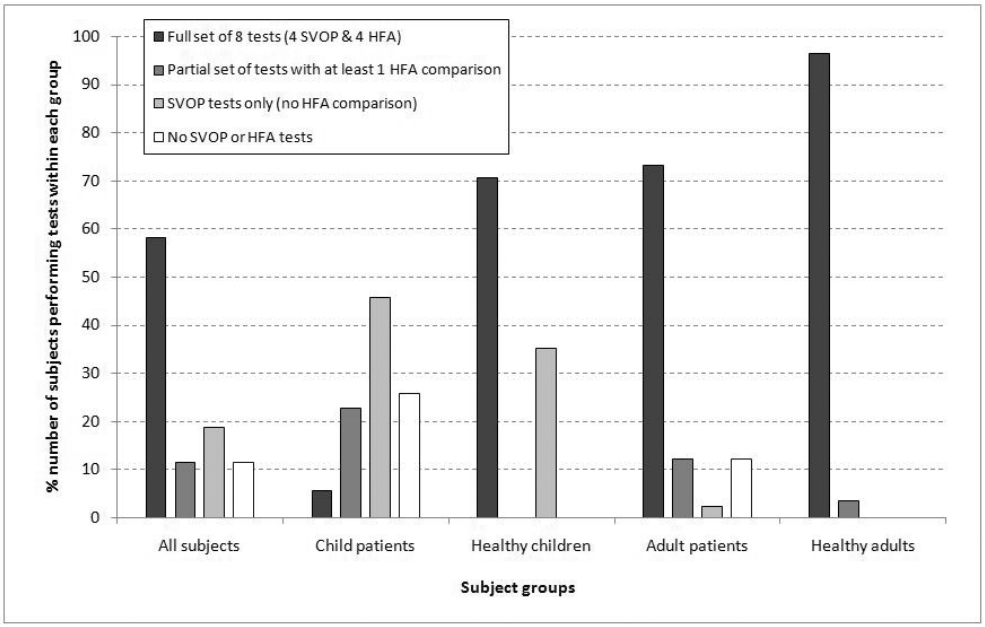

Figure 6.4: The percentage of subjects within each subject group who were able to complete a full complement of 8 tests, a partial complement (but still including at least 1 HFA comparison test), SVOP binocular tests only, and no visual field tests performed.

Subject group	Number of SVOP tests		Number of HFA tests	Number of comparison "pairs"	Number of SVOP repeatability "pairs"	Number of HFA repeatability "pairs"
	Uniocular	Binocular	(Uniocular only)			
Child patients*	41	46	32	30	34	12
Healthy children	54	8	48	48	29	24
Adult patients	130	1	130	130	63	63
Healthy adults	110	0	110	110	54	54
Totals	335	55	320	318	180	153

*Several child patients had multiple visits to participate in the study. The data shown here includes all their visits.

Table 6.5: Total number of tests performed within each subject group and the number of "pairs" of tests for comparison and repeatability analysis.

Within the adult patient group 73% of participants completed a full set of 8 uniocular tests. The most common reason for an incomplete set of uniocular tests within this group was poor quality or non-existent eye tracking data meaning that SVOP testing was not possible. Reasons for poor quality eye tracking have been outlined in Section 5.5 but to summarise, the most common

reason was due to an eye abnormality often resulting from a form of eye surgery (such as an iridectomy). Other reasons for an incomplete set of tests included tiredness resulting in an unwillingness to continue and computer problems during testing. Within the healthy adult group 96% of participants completed the full set of 8 tests with only 1 subject not completing all tests due to time constraints.

Within the child patient and normal children groups, due to the wide developmental age range there was a larger percentage of participants only performing SVOP tests (typically those under 6 years).

6.3.2 Comparison data

This section details the results of comparative testing. This includes direct comparison of SVOP test results with their equivalent HFA test results, and an assessment of the repeatability of both SVOP and HFA test results (as outlined in Section 6.2.3 on page 158). In addition to these measures, some further test parameters are also analysed. These include a comparison of test times and also, in the following sub-section, analysis of "catch trial" responses recorded from HFA tests.

6.3.2.1 HFA "catch trials" analysis

An important aspect of the HFA tests is the reliability indices (or "catch trial" data), which are used to provide an indication of the reliability of each HFA test performed. There are three reliability "trials" performed during a HFA test, these are: (i) "false positive" patient responses, (ii) "false negative" patient responses, and (iii) patient "fixation losses". These are outlined in section 2.3.2.4. However, it is worth repeating their definitions here as follows:

- The "false positive" response rate measures the tendency of a patient to press the response button even when no stimulus has been seen. During a HFA screening test false positive responses are periodically tested by the HFA making the normal mechanical motions and sounds of presenting a stimulus without actually doing so.
- The "false negative" patient response rate measures the tendency of a patient to fail to press the response button even when a distinctly visible stimulus has been presented. False negative responses are tested by presenting a stimulus at a considerably brighter light level than one which has already had a positive response from the patient.
- The patient "fixation loss" rate is a measure how steadily the patient is gazing at the central fixation stimulus. Fixation losses are estimated using the Heijl-Krakau method in which stimuli are periodically presented at the patient's pre-determined blind spot

location. Positive responses to these stimuli are recorded as fixation losses and indicate that the patient is not looking at the central fixation target.[36]

The HFA will periodically measure each of these throughout a test. HFA guidelines suggest that a test should be deemed unreliable if the false positive or false negative response rates are greater than or equal to 25%, or if the fixation loss rate is 20% or more.[125]

If a HFA test was deemed "unreliable" as a result of high reliability indices then it was not used to make a comparison with its equivalent SVOP test. Equally, they would also not be used in the assessment of HFA repeatability. In addition to providing a means of "catching" potentially unreliable HFA results, the patient responses to these "catch trials" were recorded for analysis.

Figure 6.5 shows the averaged percentages of "catch trial" response rates per HFA test for subjects who performed them. The data is arranged for each subject group and shows false positive, false negative and fixation loss "catch trial" response data. Statistical significance ($p<0.01$) was found between either of the child groups and either of the adult groups for both "false positive" and "fixation loss" responses. Statistical significance was also found between the child patients and healthy children for "false negative" responses ($p<0.01$) and "fixation losses" ($p<0.05$).

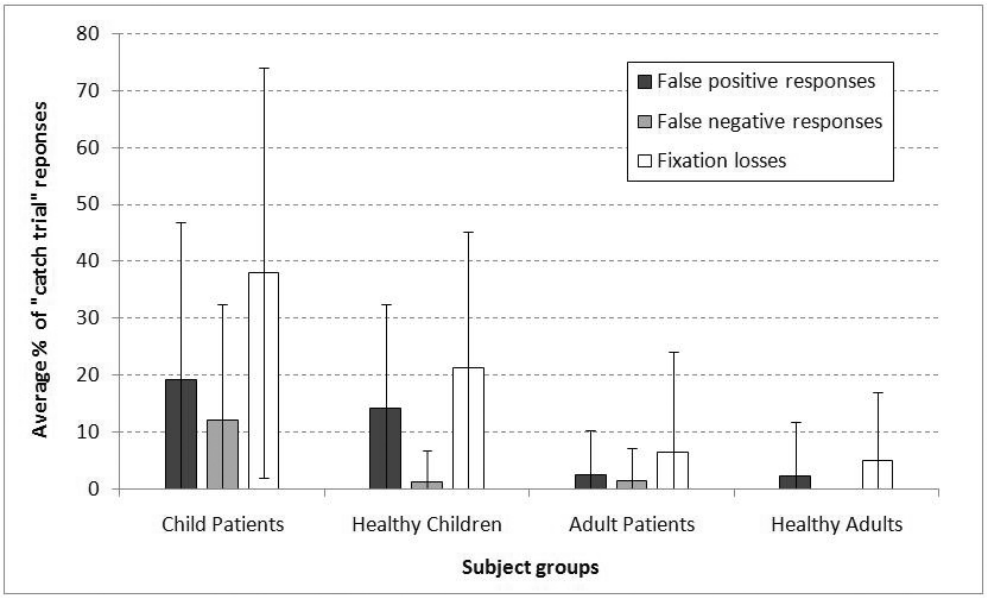

Figure 6.5: The percentage (±1 standard deviation) of responses to "catch trials" (averaged for all tests within each subject group). Catch trials include false positive responses, false negative responses, and responses to fixation loss tests.

Further analysis of these "catch trial" responses within the child subject groups is shown in figure 6.6. The chart shows the averaged percentage of false positive, false negative and fixation losses for each test performed by all the children (including both patients and normal children),

with the data split by age (those younger than 10 years and those 10 years and older). The age of 10 years was chosen as this divides the children into two approximately equal groups of tests performed (34 and 36 tests for the under- and over-10's respectively) and into two approximately equal age ranges of the children who performed HFA tests (5-9 and 10-15 years). Additionally, the age of 10 years has frequently been quoted in the literature as the age at which children can more reliably perform automated static perimetry. Statistical significance was found between the two age groups for only the "fixation losses", where the younger age group had a significantly higher rate ($p<0.01$).

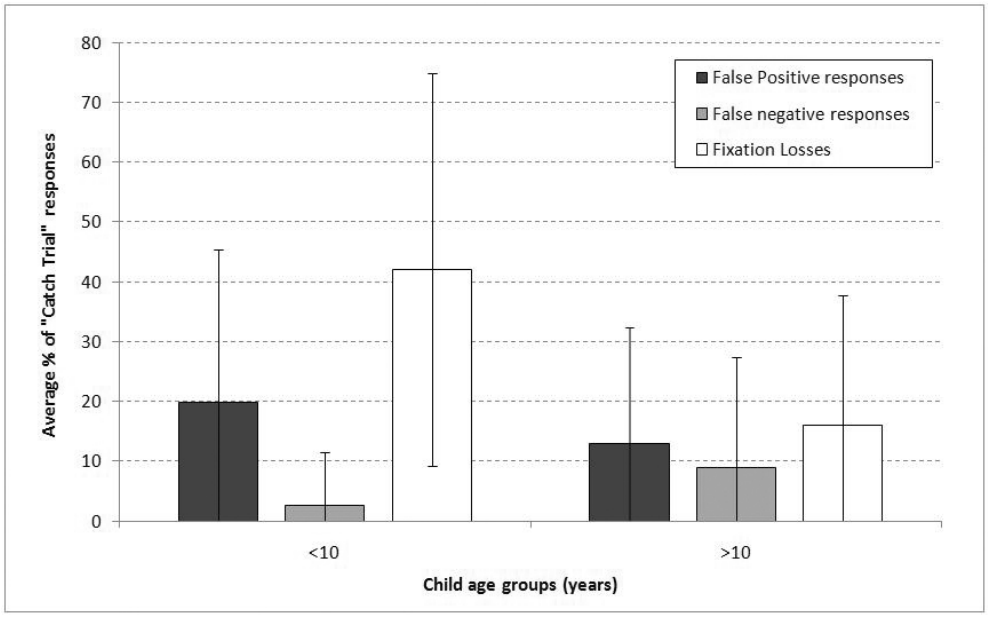

Figure 6.6: The percentage (±1 standard deviation) of responses to "catch trials" (averaged for all tests within each age group). All children were included in this analysis (patients and healthy volunteers). Catch trials include false positive responses, false negative responses, and responses to fixation loss tests.

6.3.2.2 SVOP and HFA comparison tests analysis

All tests from all subject groups

Table 6.6 details the statistical measures of sensitivity, specificity, and positive and negative predictive values for all visual field points from SVOP tests with an equivalent reliable HFA test. This analysis includes data from all patient groups and as such has a prevalence of "unseen" points (calculated from HFA test results) of just 8.4%. Figure 6.7 shows these same statistical measures calculated for each individual test comparison pair (where the HFA test was considered reliable) and averaged (±1 standard deviation) to provide an assessment of the variability of each statistical measures per individual test.

		HFA test points ("gold standard")		
		Positive ("unseen")	Negative ("Seen")	
SVOP test points	Positive ("unseen")	498	241	→ Positive predictive value = 67.4%
	Negative ("Seen")	187	7247	→ Negative predictive value = 97.5%
		↓ Sensitivity = 72.7%	↓ Specificity = 96.8%	

Table 6.6: Sensitivity, specificity and predictive values for all SVOP tests with a reliable HFA equivalent test. These data includes all assessed points from all tests within all subject groups. The prevalence of "unseen" points is 8.4%

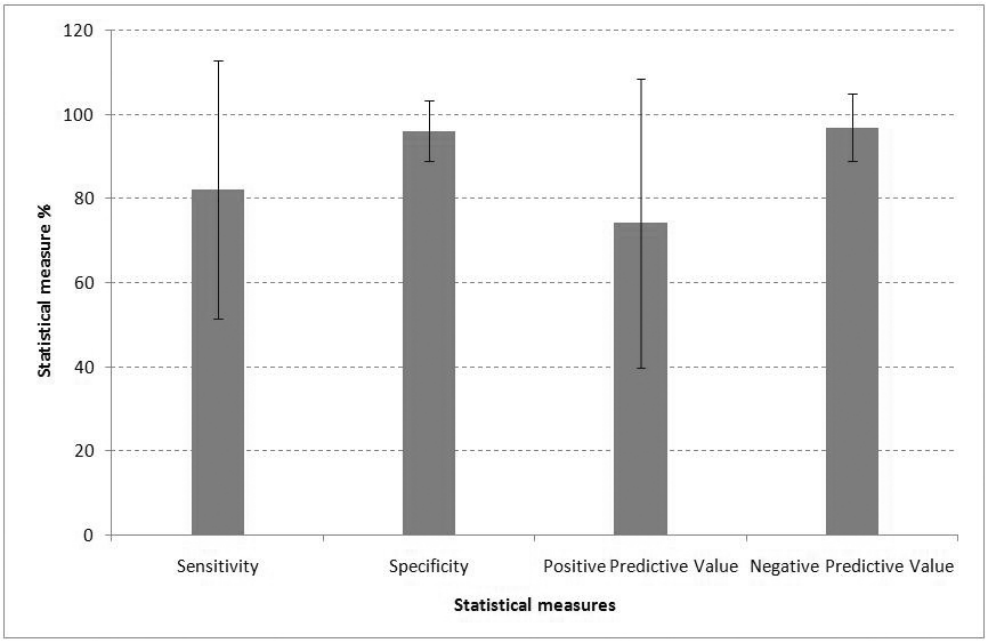

Figure 6.7: Statistical measures of sensitivity, specificity, and predictive values for all individual SVOP tests with a reliable HFA equivalent test (from all subject groups). Data shown are average ±1 standard deviation.

Adult tests

Tables 6.7 and 6.8 show two examples of a full series of 8 visual field test results (4 SVOP and 4 HFA) performed by two adult patients with known visual field defects. Table 6.7 shows the test results from a 61 year old male with pigmentary glaucoma and tilted optic discs and demonstrates a large visual field defect in the left eye. This patient had also previously

undergone a left trabeculectomy and left peripheral iridectomy. Table 6.8 shows the test results from a 65 year old female with normal tension glaucoma and visual field defect in the right eye.

Device used	Set of tests	Visual field test result	
		Left eye	Right eye
SVOP	1	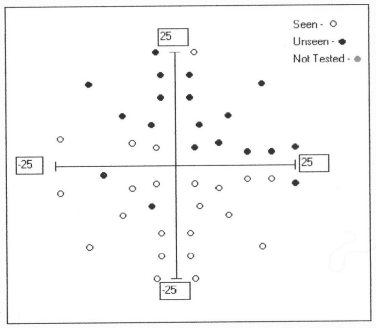	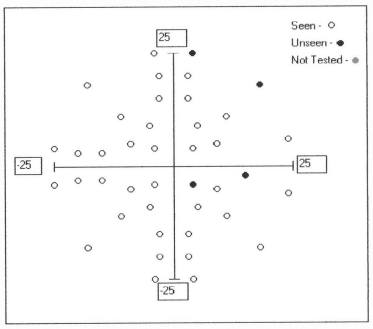
HFA	1	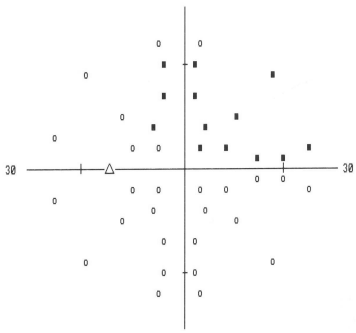	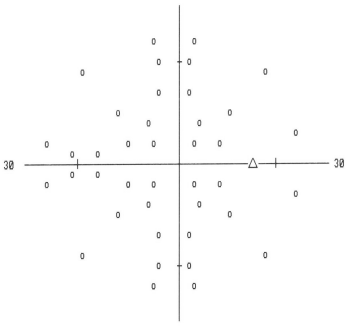
SVOP	2	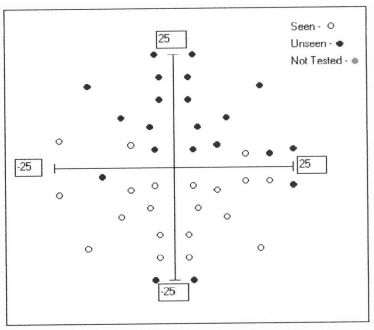	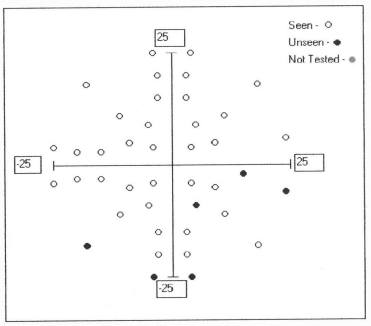
HFA	2	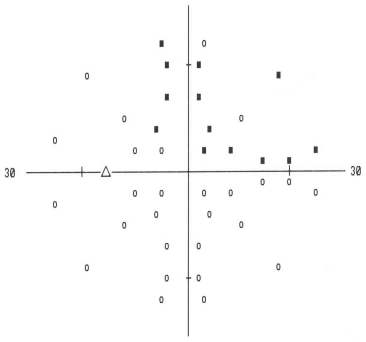	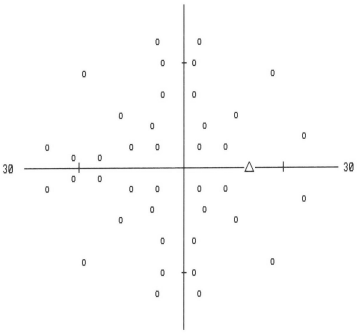

Table 6.7: A full set of 8 visual field tests (4 SVOP and 4 HFA) for an adult male with pigmentary glaucoma and tilted optic discs. This patient had also previously undergone a left trabeculectomy and left peripheral iridectomy.

Device used	Set of tests	Visual field test result	
		Left eye	Right eye
SVOP	1	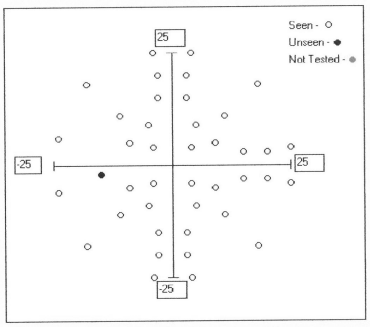	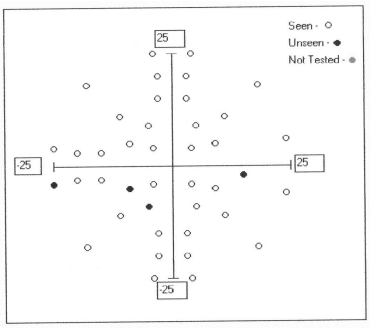
HFA	1	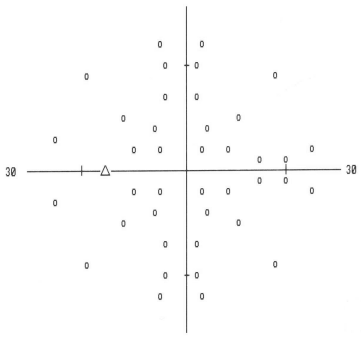	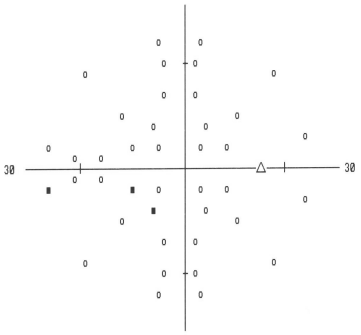
SVOP	2	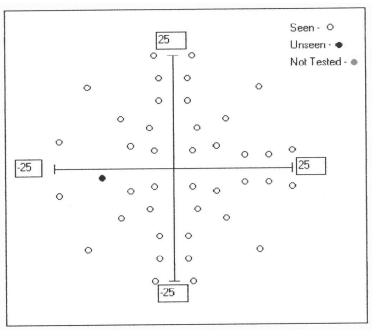	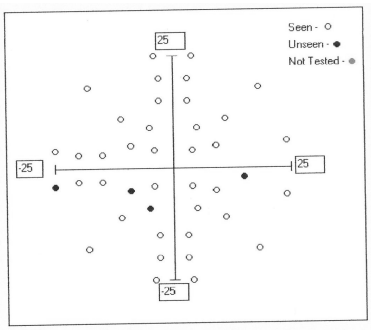
HFA	2	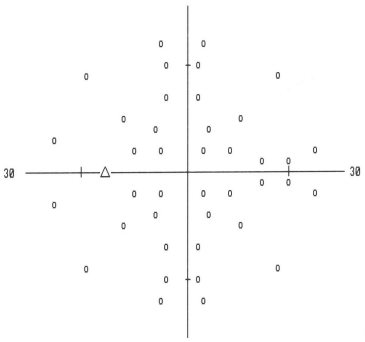	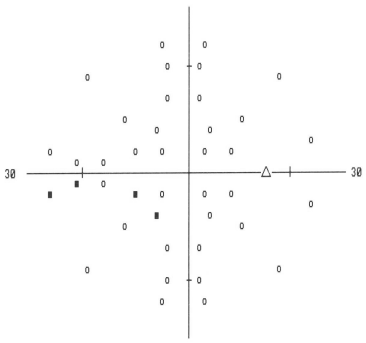

Table 6.8: A full set of 8 visual field tests (4 SVOP and 4 HFA) for an adult female with normal tension glaucoma.

Tables 6.9 and 6.10 detail the statistical measures of sensitivity, specificity, and positive and negative predictive values for all visual field points from SVOP tests with an equivalent reliable

HFA test from the "healthy adult" and "adult patient" subject groups respectively. The prevalence of "unseen" points was 2.5% for the "healthy adult" subject group which are attributed to the blind spot test locations only. For all the reliable tests performed by the "adult patient" group the prevalence of "unseen" points was 12.4%.

Not all adult patients had visual field defects, or defects which could be picked up by the suprathreshold testing performed, in both eyes. The tests which did not demonstrate any "unseen" data points (excluding the blind spot location) were subsequently defined as results from "normal" eyes. As a further form of analysis, the tests from the adult patient group were also assessed with these "normal" eye comparative tests removed from the analysis. Table 6.11 shows the statistical measures under this situation. Under these conditions the "unseen" prevalence increased to 17.8%

Figure 6.8 shows these same statistical measures. However, in this chart they have been calculated for each individual test comparison pair (where the HFA test was considered reliable) and averaged (±1 standard deviation) to provide an assessment of the variability of the statistical measures per individual test.

		HFA test points ("gold standard")		
		Positive ("unseen")	Negative ("Seen")	
SVOP test points	Positive ("unseen")	80	6	→ Positive predictive value = 93.0%
	Negative ("Seen")	3	3251	→ Negative predictive value = 99.9%
		↓ Sensitivity = 96.4%	↓ Specificity = 99.8%	

Table 6.9: Sensitivity, specificity and predictive values for all SVOP tests with a reliable HFA equivalent test from the "healthy adult" subject group. The prevalence of "unseen" points is 2.5%

		HFA test points ("gold standard")		
		Positive ("unseen")	Negative ("Seen")	
SVOP test points	Positive ("unseen")	360	220	→ Positive predictive value = 62.1%
	Negative ("Seen")	162	3461	→ Negative predictive value = 95.5%
		↓ Sensitivity = 69.0%	↓ Specificity = 94.0%	

Table 6.10: Sensitivity, specificity and predictive values for all SVOP tests with a reliable HFA equivalent test from the "adult patient" subject group. The prevalence of "unseen" points is 12.4%

		HFA test points ("gold standard")		
		Positive ("unseen")	Negative ("Seen")	
SVOP test points	Positive ("unseen")	328	202	→ Positive predictive value = 61.9%
	Negative ("Seen")	158	2039	→ Negative predictive value = 92.8%
		↓ Sensitivity = 67.5%	↓ Specificity = 91.0%	

Table 6.11: Sensitivity, specificity and predictive values for all SVOP tests with a reliable HFA equivalent test from the "adult patient" subject group with "normal" eye tests removed. The prevalence of "unseen" points is 17.8%

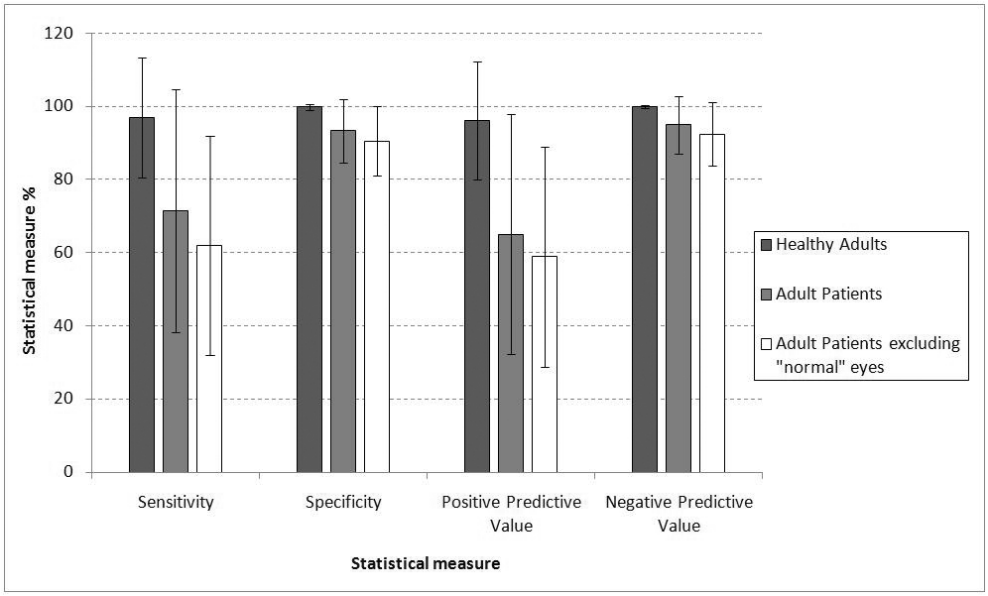

Figure 6.8: Statistical measures of sensitivity, specificity, and predictive values for individual SVOP tests with a reliable HFA equivalent test from the "healthy adult" and "adult patient" subject groups, and additionally the "adult patient" group with "normal" eye data removed. Data shown is average ±1 standard deviation.

Child tests

Tables 6.12 and 6.13 detail the statistical measures of sensitivity, specificity, and the positive and negative predictive values for all visual field points from SVOP tests with an equivalent reliable HFA test from the "healthy child" and "child patient" subject groups respectively. The prevalence of "unseen" points was 2.4% for the "healthy child" subject group (again attributed only to the blind spot locations). For all the reliable tests performed by the "child patient" group the prevalence of "unseen" points was 27.2%.

Again, not all child patients had visual field defects, or rather had defects which could be picked up by the suprathreshold testing performed, in both their eyes. Eyes with reliable HFA test results which did not have any "unseen" data points (excluding the blind spot location) were subsequently defined as "normal" eye test results. As a further form of analysis, the tests from the child patient group were assessed with the "normal" eye comparative tests removed from the analysis. Table 6.14 shows the statistical measures under this situation, and under these conditions the "unseen" prevalence was 38.5%

Figure 6.9 shows these same statistical measures. However, in this chart they have been calculated for each individual test comparison pair (where the HFA test was considered reliable) and averaged (±1 standard deviation) to provide an assessment of variability of the statistical measures per individual test.

		HFA test points ("gold standard")		
		Positive ("unseen")	Negative ("Seen")	
SVOP test points	Positive ("unseen")	6	1	→ Positive predictive value = 91.7%
	Negative ("Seen")	3	359	→ Negative predictive value = 99.2%
		↓ Sensitivity = 66.7%	↓ Specificity = 99.7%	

Table 6.12: Sensitivity, specificity and predictive values for all SVOP tests with a reliable HFA equivalent test from the "healthy child" subject group. The prevalence of "unseen" points is 2.4%

		HFA test points ("gold standard")		
		Positive ("unseen")	Negative ("Seen")	
SVOP test points	Positive ("unseen")	52	14	→ Positive predictive value = 78.8%
	Negative ("Seen")	19	176	→ Negative predictive value = 90.3%
		↓ Sensitivity = 73.2%	↓ Specificity = 92.6%	

Table 6.13: Sensitivity, specificity and predictive values for all SVOP tests with a reliable HFA equivalent test from the "child patient" subject group. The prevalence of "unseen" points is 27.2%

		HFA test points ("gold standard")		
		Positive ("unseen")	Negative ("Seen")	
SVOP test points	Positive ("unseen")	50	14	→ Positive predictive value = 78.1%
	Negative ("Seen")	19	96	→ Negative predictive value = 83.5%
		↓ Sensitivity = 72.5%	↓ Specificity = 87.3%	

Table 6.14: Sensitivity, specificity and predictive values for all SVOP tests with a reliable HFA equivalent test from the "child patient" subject group with "normal" eye tests removed. The prevalence of "unseen" points is 38.5%

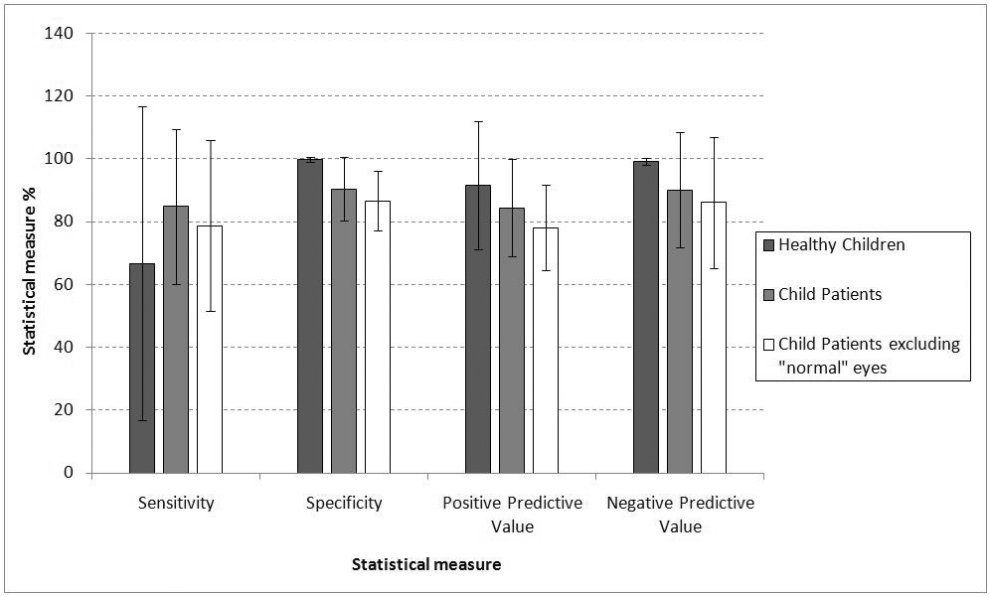

Figure 6.9: Statistical measures of sensitivity, specificity, and predictive values for individual SVOP tests with a reliable HFA equivalent test from the "healthy child" and "child patient" subject groups, and additionally the "child patient" group with "normal" eye data removed. Data shown is average ±1 standard deviation.

Summary of comparison data

Table 6.15 shows a summary of the statistical measures obtained for each of the patient groups, and additionally with the "normal" eyes taken out of the adult and child patient groups.

Subject group	Sensitivity (%)	Specificity (%)	Positive predictive value (%)	Negative predictive value (%)	"Unseen" points prevalence (%)
Healthy adults	96.4	99.8	93.0	99.9	2.5
Adult patients	69.0	94.0	62.1	95.5	12.4
Adult patients (excluding "normal" eyes)	67.5	91.0	61.9	92.8	17.8
Healthy children	66.7	99.7	91.7	99.2	2.4
Child patients	73.2	92.6	78.8	90.3	27.2
Child patients (excluding "normal" eyes)	72.5	87.3	78.1	83.5	38.5

Table 6.15: Summary of the sensitivity, specificity, positive and negative predictive values (and "unseen" point prevalence) for each subject group and also for the adult and child patient groups with "normal" eye data excluded.

6.3.2.3 HFA and SVOP test repeatability analysis

Table 6.16 details the kappa statistic values following assessment of repeated SVOP and HFA tests using all visual field points from tests from each subject group and in total. Additionally, the kappa statistic values were re-calculated with the visual field points of certain tests removed. In the case of the SVOP tests the tests excluded from this analysis were those that had not been 100% completed, and in the case of the HFA analysis, the "unreliable" (as stipulated by the HFA reliability indices) tests were excluded from the analysis. The reason for including both types of analysis in the case of the SVOP tests (inclusion and exclusion of "incomplete" tests) was to identify if "incomplete" tests could be a source of unreliability. In the case of the HFA test repeatability assessment, analysis was performed both including and excluding the "unreliable" test data because after removing this data there were no tests available for analysis in the child patient group and only one test available for analysis in the healthy children subject group.

Subject group	Kappa statistic, κ			
	SVOP tests		HFA tests	
	Analysis of all points	Excluding points from incomplete tests	Analysis of all points	Excluding points from "unreliable" tests
All groups	0.65	0.64	0.74	0.75
Healthy adults	0.86	0.88	0.99	0.99
Adult patients	0.60	0.59	0.71	0.71
Healthy children	0.46	0.62	1.00	1.00
Child patients	0.61	0.58	0.53	-

Table 6.16: Kappa statistic, κ, of repeatability for SVOP and HFA tests, for each of the patient groups.

6.3.2.4 Test time analysis

The test times of all SVOP and HFA test were recorded. Figure 6.10 shows the comparison of test times between SVOP and HFA tests for all subjects who completed both types of test, and how they compare in each subject group. Overall, in all subjects, HFA tests were on average quicker but the difference was not significant ($t(321) = 1.6$, $p=0.11$). Similarly in the child patients HFA tests were on average quicker but not significantly so ($t(30)=0.7$, $p=0.49$). In both the healthy groups (children and adults) the SVOP tests were significantly faster than the HFA tests ($t(47)=3.1$, $p<0.01$) for the healthy children, and ($t(143)=7.0$, $p=<0.0001$) for the healthy adults). The HFA test was on average significantly quicker than SVOP within the adult patient group ($t(129)=4.5$, $p<0.001$).

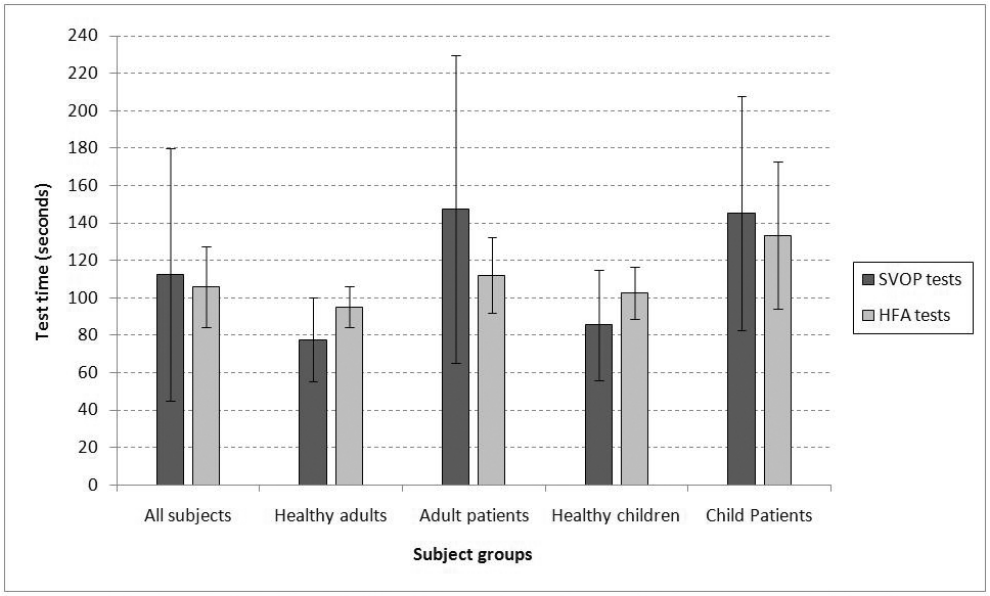

Figure 6.10: Comparison of test times between SVOP and HFA tests for all tests and for each of the subject groups. Data shown is the average (±1 standard deviation) of all tests with a comparative pair, where both tests of the pair were completed.

A one obvious reason for an increase in test time in both the SVOP and HFA tests is due to the retesting of "unseen" test stimuli. Figures 6.11 and 6.12 show the duration of SVOP and HFA tests (only including tests which were completed and which had a comparative pair) plotted as a function of the number of "unseen" points in the final test result.

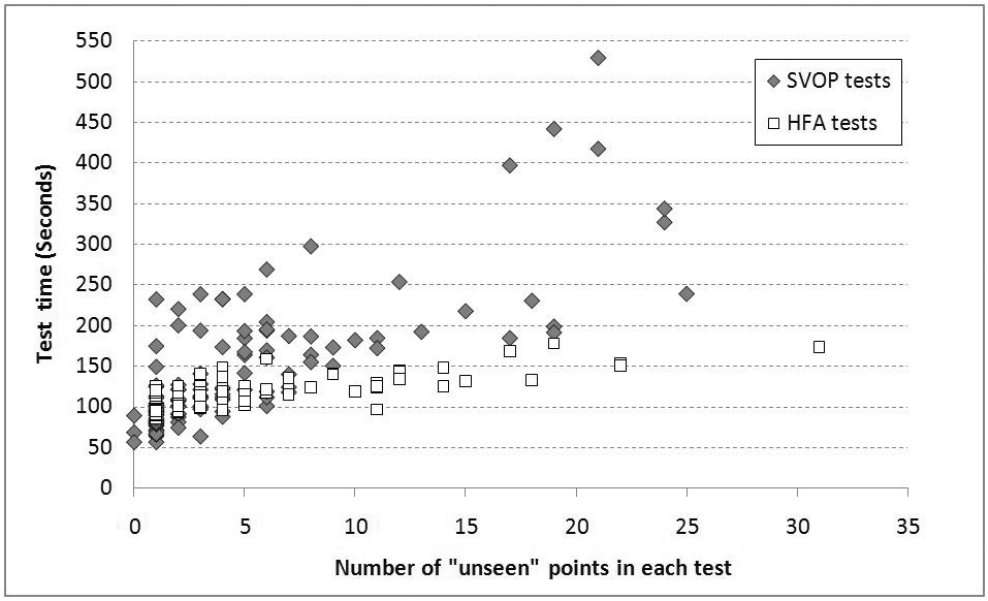

Figure 6.11: Number of "unseen" points in each test plotted against the test time for both SVOP and HFA tests from the "adult patient" subject group.

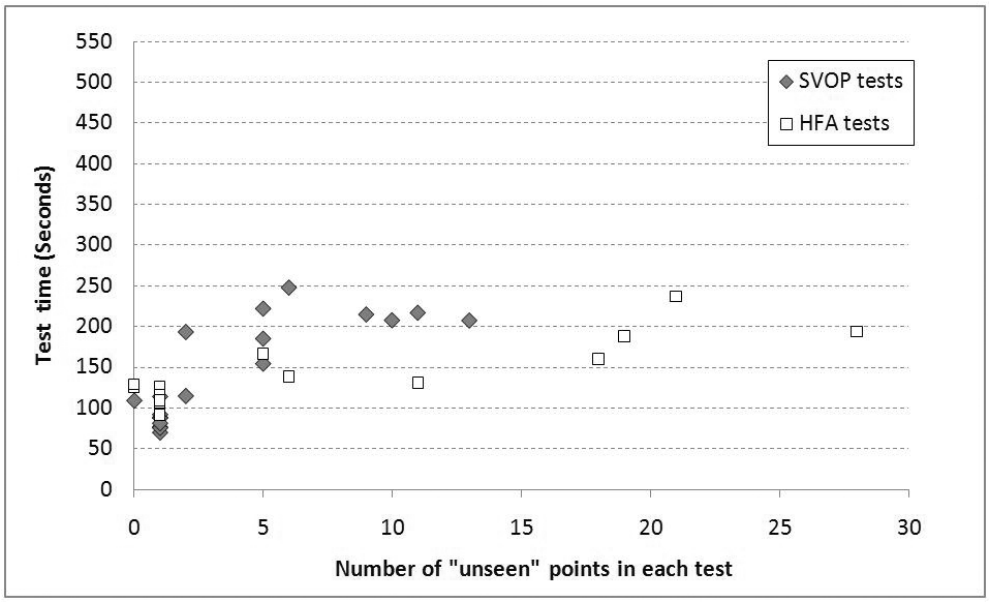

Figure 6.12: Number of "unseen" points in each test plotted against the test time for both SVOP and HFA tests from the "child patient" subject group.

6.3.3 Child patients with no reliable HFA comparison

The results in this section are presented as a series of cases. The child patients selected for presentation are those of most clinical interest, those with repeated visits to participate in the study and those with interesting results for any other particular reason. The majority of cases where there has been multiple visits to take part in the study was young child patients with visual pathway tumours. As a result this section is divided into three further sub-sections, one discussing these visual pathway tumour cases, another discussing some children with other types of cerebral visual impairment. A final case is presented in the last sub-section which details the results of the youngest participant in the study - an 8 month old healthy infant. Each patient case is presented with a table detailing the age, diagnosis, any previous treatment and previous clinical visual function assessment prior to performing SVOP tests.

6.3.3.1 Visual field defects as a result of visual pathway tumours

Case 1

Table 6.17 outlines the diagnosis, previous treatments and visual function of a 5 year old boy. All of this patient's SVOP test results are shown in figure 6.13. He performed three binocular SVOP tests prior to the start of this validation trial (during the coarse of the previously presented feasibility trial) which are also useful to present in this section, and then subsequently participated in the validation trial on four separate occasions. The months since his first SVOP

test are shown in the top left corner of each test (or set of two tests). During each of the "validation trial" visits he performed two right eye SVOP tests and two right eye HFA tests (he was blind in his left eye). On each occasion the HFA tests were not considered reliable using the HFA criteria with a high percentage of false positives and fixation losses (average of 46% and 75% respectively).

Case 1: A 5 year old (65 months) male	
Diagnosis	• Pilocytic astrocytoma in the hypothalamic optic nerve region, World Health Organization (WHO) grade I.
Previous treatments	• Complete surgical resection. • The International Society for Paediatric Oncology (SIOP, Societé Internationale pour Oncolgie Paediatrique) low grade glioma 2003 protocol (randomised to receive intensified induction chemotherapy) completed 19 months prior to first SVOP test.
Visual function prior to first SVOP test	• Blind in left eye • On confrontational visual field testing, right eye complete temporal hemianopia, which was thought to improve slightly before SVOP visual field testing. • Visual acuity: Right 6/9

Table 6.17: Case 1 patient clinical details including age on first SVOP testing, diagnosis, previous treatments and clinical visual function assessment details.

Figure 6.14 on page 180 shows the change in visual field defect according to SVOP test results by plotting the average number of "unseen" points from each visit as a function of time (in months). Only fully completed test results have been used in this analysis. Also shown on the chart is the repeatability statistic (Cohen's kappa), for any of the visits during the validation trial where there was two completed test results.

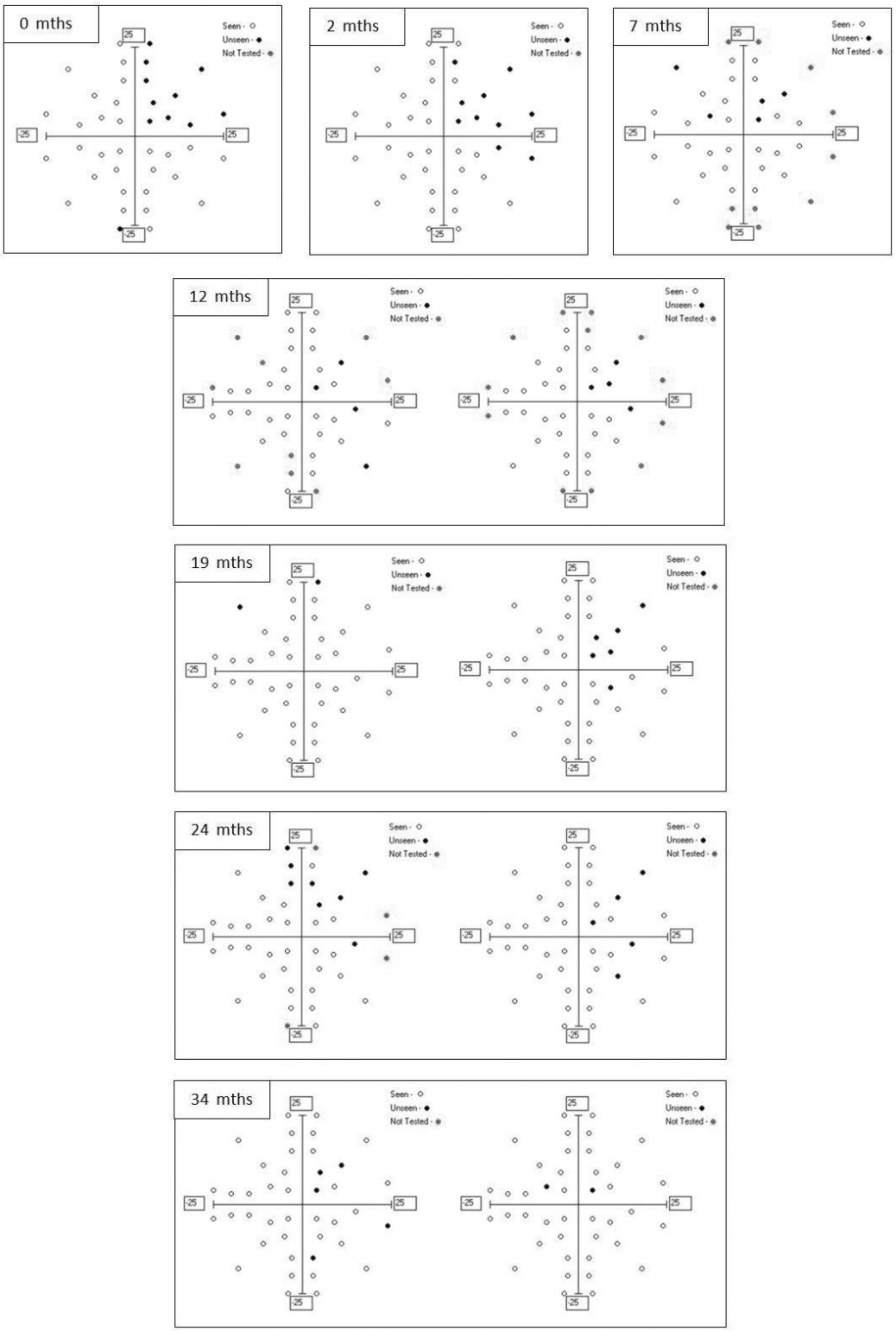

Figure 6.13: SVOP visual field test results from case 1 (see table 6.17 for details). Included are three single binocular tests performed prior to the validation trial (during the course of the feasibility trial), and 8 further right eye tests performed on 4 separate visits during the validation trial.

There was a decrease in the number of unseen points over time with the biggest change coming after the second SVOP test (performed during the feasibility study). The area consistently showing "unseen" visual field points was in his right upper quadrant. Prior to performing SVOP tests confrontational visual field testing suspected that this boy had a complete temporal hemianopia. This is clearly in conflict with the original SVOP result of an upper right quadrantanopia. The fact that this child was able to deliberately and consistently able to orient his gaze to SVOP visual field "test stimuli" presented in the lower right quadrant of his visual field is proof enough that the previous confrontational visual field result of a total right hemianopia was not entirely correct. The repeatability of SVOP testing was poor on the occasions where both tests during a single visit were fully completed (visit 2 and 4 of the validation trial results). This poor repeatability was due to one of the test results showing an upper right defect and the other during the same visit showing almost no defect in that same area. This finding are somewhat strange, but interestingly although the HFA test results were not considered reliable enough for their data to be analysed, they also showed a similar finding. Figure 6.15 shows the HFA test results from visit 1 and 2 during the validation trial. Despite the poor repeatability on these two occasions, the SVOP tests almost always showed a visual field defect in the upper right quadrant which adds credibility to the defects identified in this area from SVOP testing.

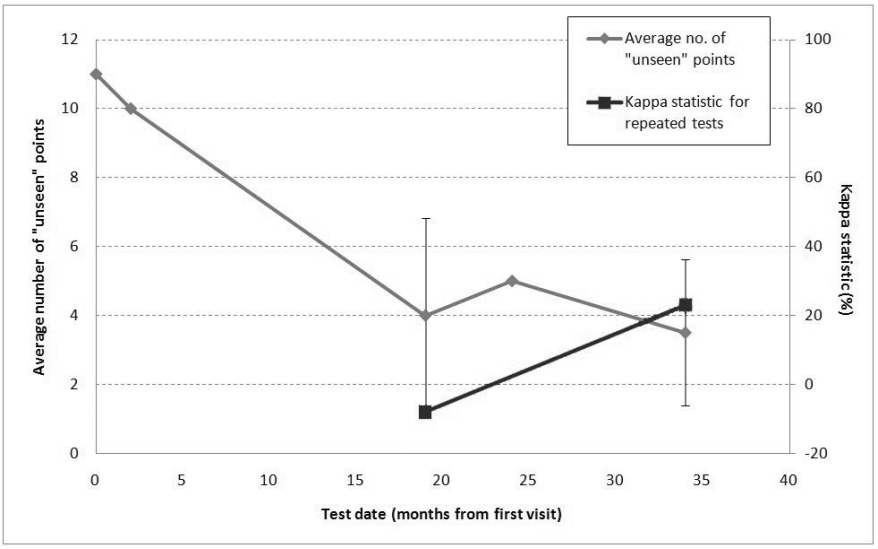

Figure 6.14: Chart of the average number of "unseen" points (±1 standard deviation where more than one test was completed in a single visit) from each visit for case 1. Only data for completed tests is shown. Where two completed tests were performed on one visit, the kappa statistic for assessment of repeatability was performed and is also shown on the chart.

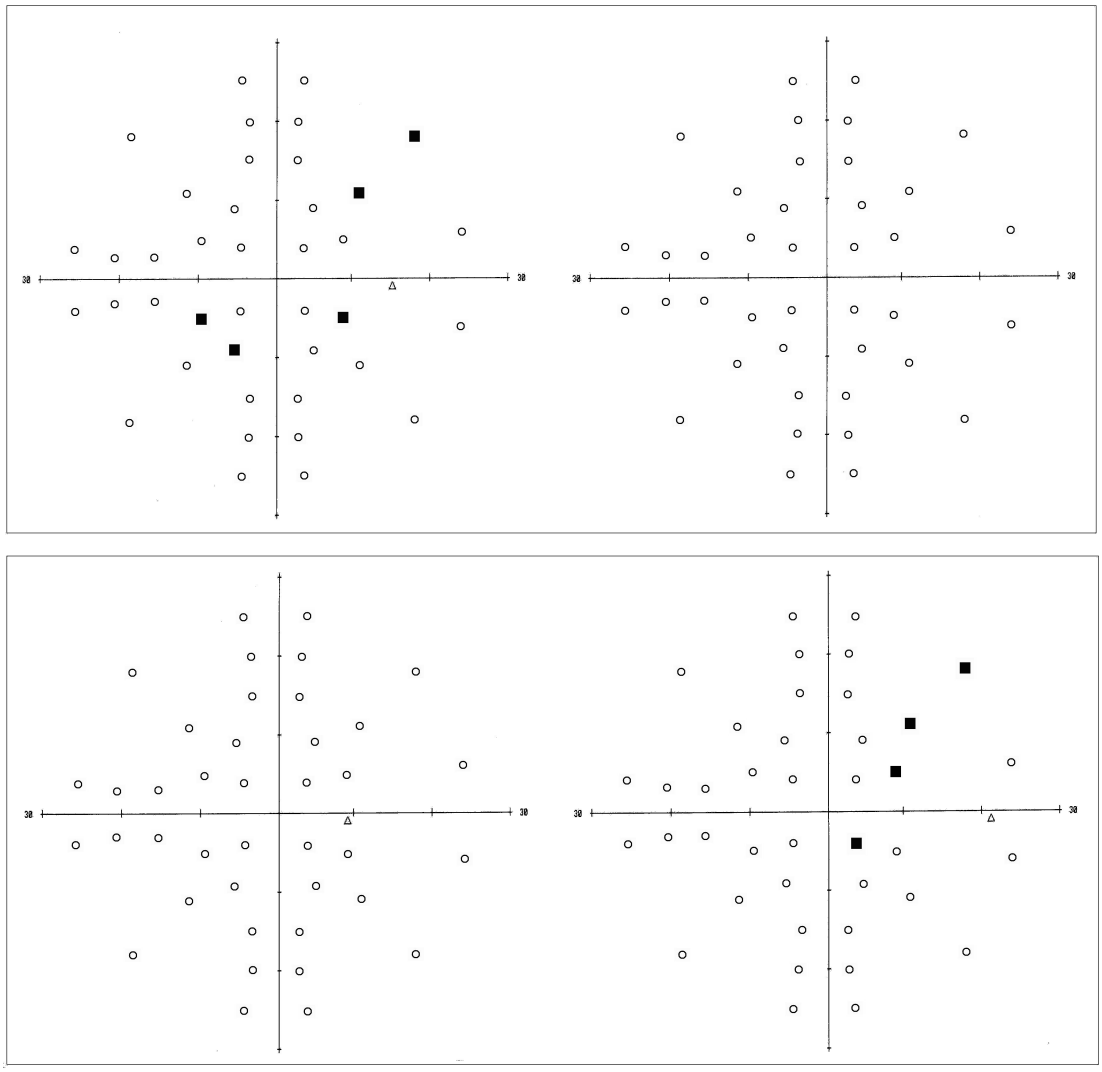

Figure 6.15: HFA test results for case 1 from two of the four visits (upper panel shows results from visit one and lower panel shows results from visit two). On each of the visits this patient performed two HFA right eye tests.

Case 2

Table 6.18 outlines the diagnosis, previous treatments and visual function of a 2 year old girl. All of this patient's SVOP test results are shown in figure 6.16. She performed two binocular SVOP tests prior to the start of this validation trial (during the course of the feasibility study), and then subsequently participated in the validation trial on five separate occasions. The months since her first SVOP test are shown in the top left corner of each test (or set of two tests). During each of the "validation trial" visits she performed two SVOP visual field tests which on some visits was with a binocular test pattern and on other visits was with a left eye test pattern (this test pattern variation was not intended for any particular reason). This young girl did not perform any HFA visual field testing.

Case 2: A 2 year old (34 months) female	
Diagnosis	• Hypothalamic pilocytic astrocytoma, WHO grade I.
Previous treatments	• Right frontal craniotomy with subtotal removal of tumour. • SIOP low grade glioma 2003 protocol (randomised to receive intensified induction chemotherapy). Completed 69 weeks 9 months after performing first SVOP test.
Visual function prior to first SVOP test	• Blind in right eye. • On confrontational visual field testing, left eye complete temporal visual field defect but not possible to get reliable nasal visual field information. • Visual acuity: Left 6/7.5

Table 6.18: Case 2 patient clinical details including age on first SVOP testing, diagnosis, previous treatments and clinical visual function assessment details.

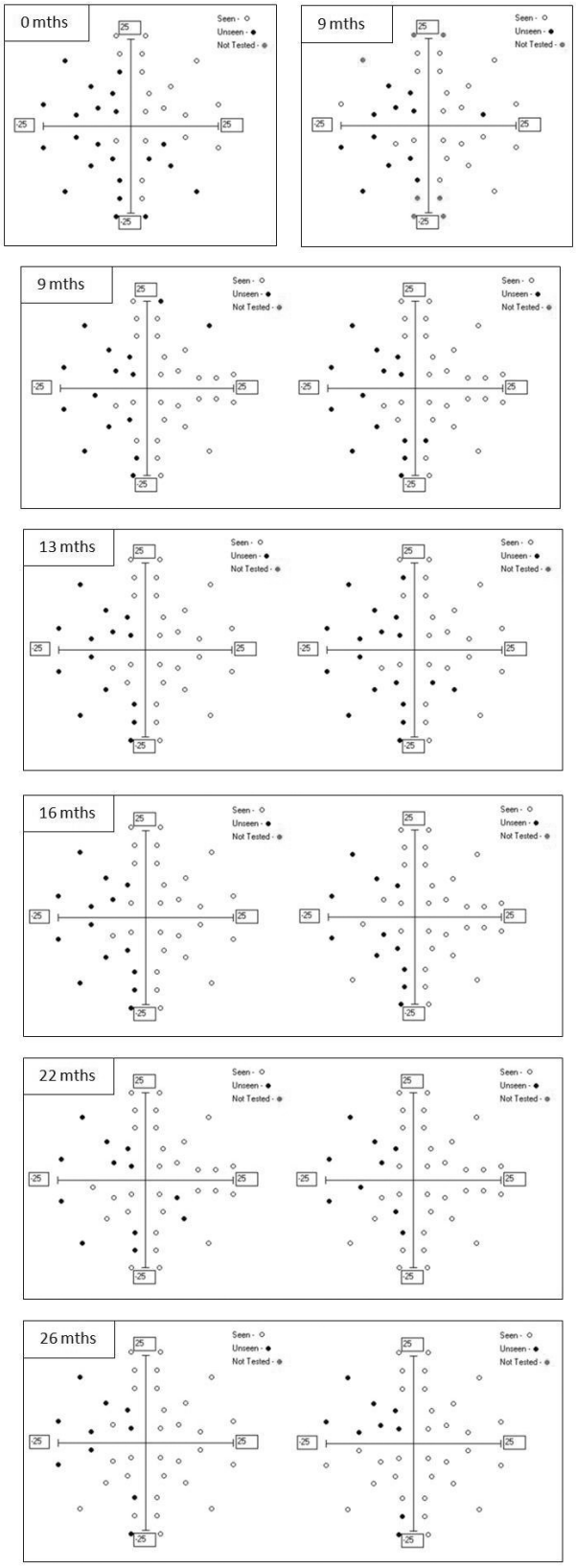

Figure 6.16: SVOP visual field test results from case 2. Included are two single binocular tests performed prior to the validation trial (as part of the feasibility trial), and 10 further tests completed on 5 separate visits during the validation trial.

Figure 6.17 shows brain scans of this patient. The left panel shows a scan taken prior to the frontal craniotomy operation, while the right panel shows the post-operative scan.

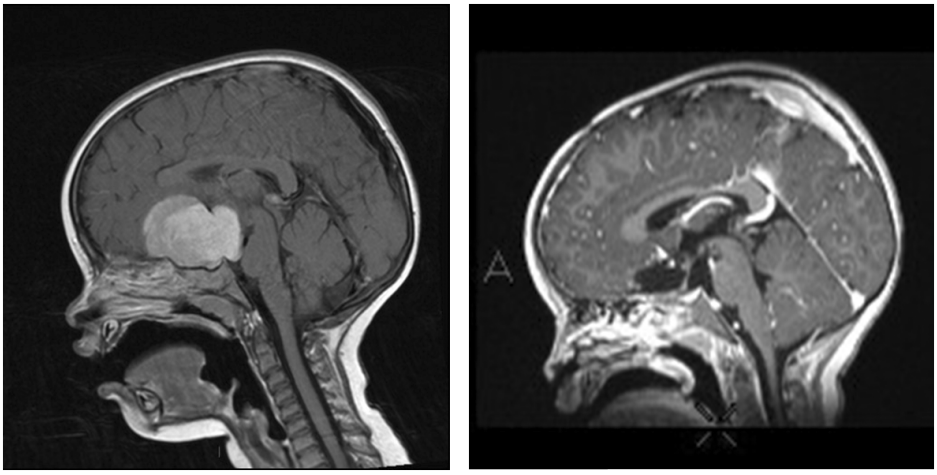

Figure 6.17: Case 2 brain scans. This patient underwent a right frontal craniotomy with subtotal removal of the tumour. Left and right panels show the pre- and post-operative scans respectively.

Figure 6.18 shows the change in visual field defect according to SVOP test results by plotting the average number of "unseen" points from each visit as a function of time (in months). Again only fully completed test results have been used in this analysis. Also shown on the chart is the repeatability statistic (Cohen's kappa), for any of the visits during the validation trial where there were two fully completed test results.

On confrontational visual field testing performed prior to the first SVOP test this young girl was believed to have a left eye complete temporal hemianopia and was known to be blind in her right eye. SVOP test results consistently showed a left sided defect in accordance with confrontational visual field testing. However, there was an additional consistent finding with the left side of this patient's visual field. On every single SVOP test there were two areas of the previously suspected complete left hemianopia that were consistently showing as "seen". These areas included points next to the vertical midline and towards the top of the upper left quadrant, and also some points in the lower left quadrant closer to the point of fixation. The points which were showing as "seen" in the lower left quadrant seemed to grow in number with each visit (figure 6.18). The Cohen's kappa statistic for the repeated tests with this patient were good with an average of 70.2 $\pm$9.8% (1 standard deviation).

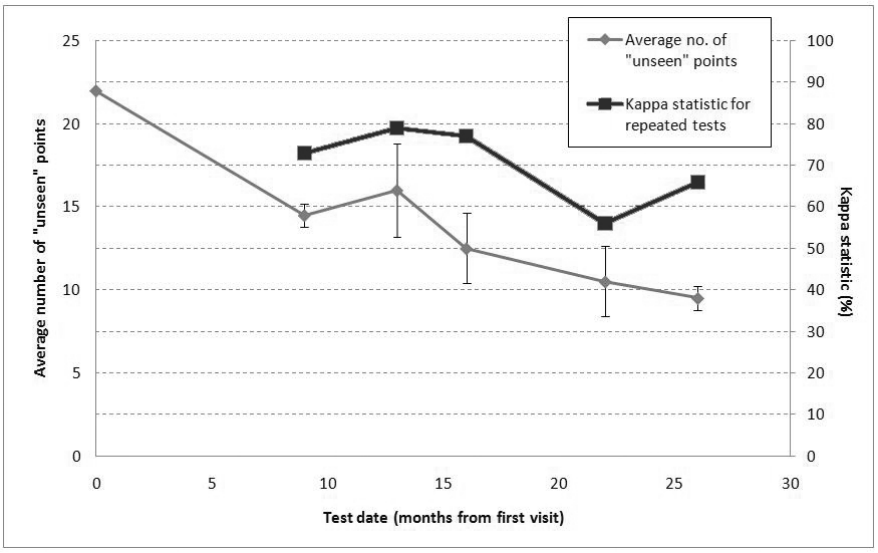

Figure 6.18: Chart of the average number of "unseen" points (±1 standard deviation where more than one test was completed in a single visit) from each visit for case 2. Only data for completed tests is shown. Where two completed tests were performed on one visit, the Kappa statistic for assessment of repeatability was performed and is also shown on the chart.

Case 3

Table 6.19 outlines the diagnosis, previous treatments and visual function of a 4 year old girl. This patient's SVOP test results are shown in figure 6.19. She performed 10 binocular SVOP tests in total (2 tests at each of 5 visits during the coarse of the validation study). The months since her first SVOP test are shown in the top left corner of each set of two tests. This girl did not perform any HFA visual field testing.

Case 3: A 4 year old (52 months) female	
Diagnosis	• Left temporal pilocytic astrocytoma, WHO grade I.
Previous treatments	• Left temporal burrhole and evacuation of cyst. • Left fronto-temporal craniotomy and debulking of tumour.
Visual function prior to first SVOP test	• On confrontational visual field testing, right homonymous hemianopia. • Visual acuity: Right 6/7.5, Left 6/9.5

Table 6.19: Case 3 patient clinical details including age on first SVOP testing, diagnosis, previous treatments and clinical visual function assessment details.

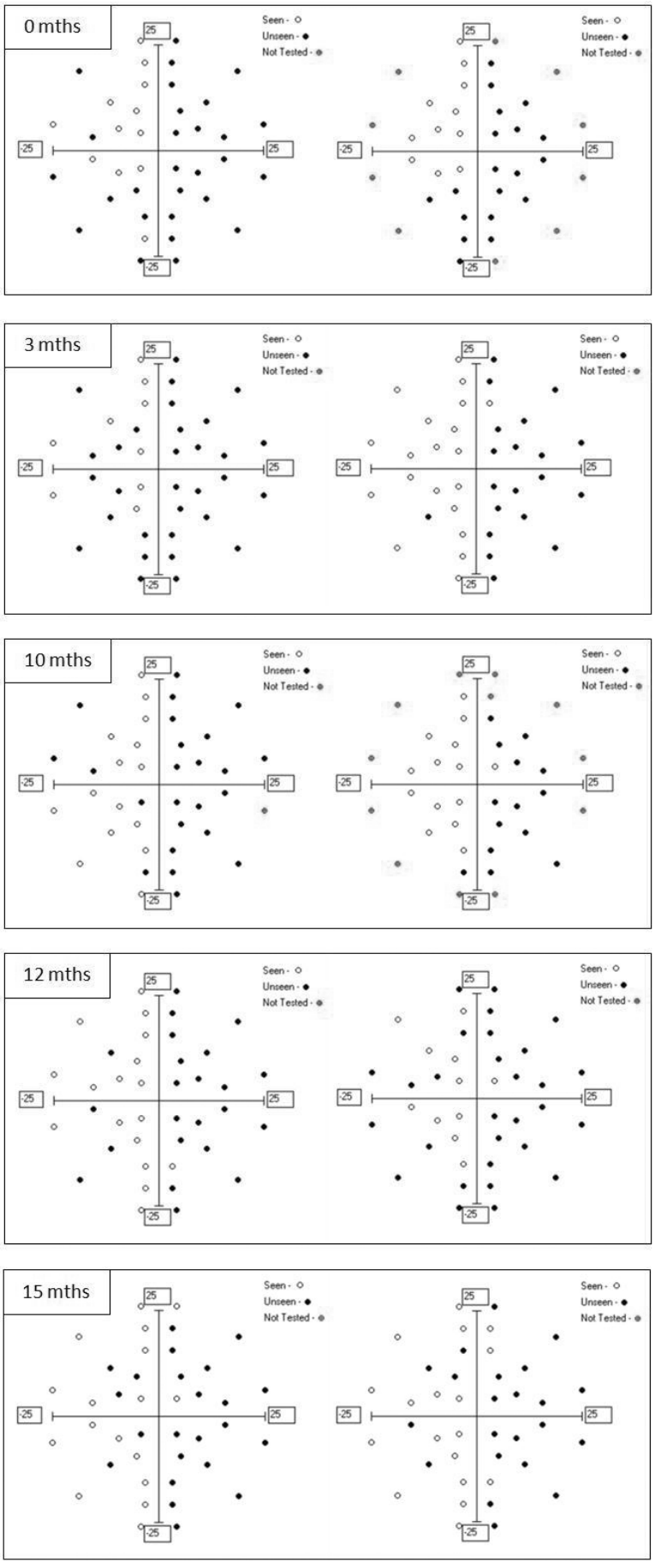

Figure 6.19: SVOP test results for case 3 including 10 binocular SVOP tests completed on 5 separate visits during the validation trial.

Figure 6.20 charts the changes in the average number of "unseen" points in SVOP tests over time (in months). As with previous charts of this type, only fully completed test results have been used in the analysis. Also shown on the chart is the repeatability statistic (Cohen's kappa), for any of the visits during the validation trial where there were two fully completed test results.

The SVOP test results demonstrate a consistently occurring right homonymous hemianopia which is in agreement with her clinical confrontational visual field testing. Harder to explain are the "unseen" points which were a regular occurrence on the left side of her visual field. However, these "unseen" points did not seem to follow a consistent pattern and were the main source of the variability in the repeatability statistics. On reviewing the post-test gaze replay of these tested points, it was became clear that the two main reasons for them not being labelled as "seen" by the SVOP software algorithm was down to either: (i) the patient did not react to the stimuli, or (ii) the patient reacted in what seemed like an appropriate manner but the decision algorithm did not correctly identify the fixation change. Reason (ii) is understandable and is a feature of many of the SVOP tests performed (throughout all subject groups) and will be discussed further in the discussion section of this chapter. Reason (i) was perhaps more puzzling due to the inconsistency of the "unseen" points which did not invoke a reaction. It is suspected that although this child would submit to performing the test, she would often become bored or disinterested as time went on. This was due in most part to the number of points which she genuinely wouldn't have seen (to the right side of her visual field), which would create long periods of inactivity during the test (from her perspective). In this scenario, there would become less incentive for her to actually react to the stimuli.

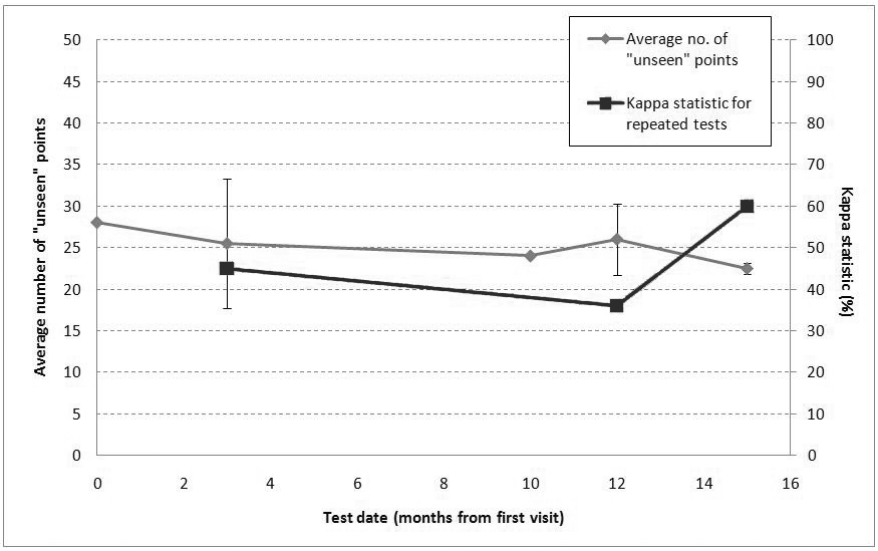

Figure 6.20: Chart of the average number of "unseen" points (±1 standard deviation where more than one test was completed in a single visit) from each visit for case 3. Only data for completed tests is shown. Where two completed tests were performed on one visit, the kappa statistic for assessment of repeatability was performed and is also shown on the chart.

Case 4

Table 6.20 the diagnosis, previous treatments and visual function of a 3 year old girl. This patient's SVOP test results are shown in figure 6.21. She performed 7 binocular SVOP tests in total (2 tests at each of 3 visits during the course of the validation study, and one test prior to those). The months since her first SVOP test are shown in the top left corner of each of the tests (or set of two tests). This girl did not perform any HFA visual field testing.

Case 4: A 3 year old (38 months) female	
Diagnosis	• Diencephalic syndrome • Hypothalamic ependymoma tumour, WHO grade II.
Previous treatments	• Left frontal temporal craniotomy and biopsy of suprasellar mass (at 10 months of age) • Baby brain chemotherapy protocol commenced at 10 months of age (received 44 cycles) • Left temporal craniotomy and excision of hypothalamic ependymoma 4 months prior to first SVOP testing
Visual function prior to first SVOP test	• Blind in left eye • Right eye difficult to assess reliably, confrontational visual field testing suggested right sided defect. • Visual acuity: Not known.

Table 6.20: Case 4 patient clinical details including age on first SVOP testing, diagnosis, previous treatments and clinical visual function assessment details.

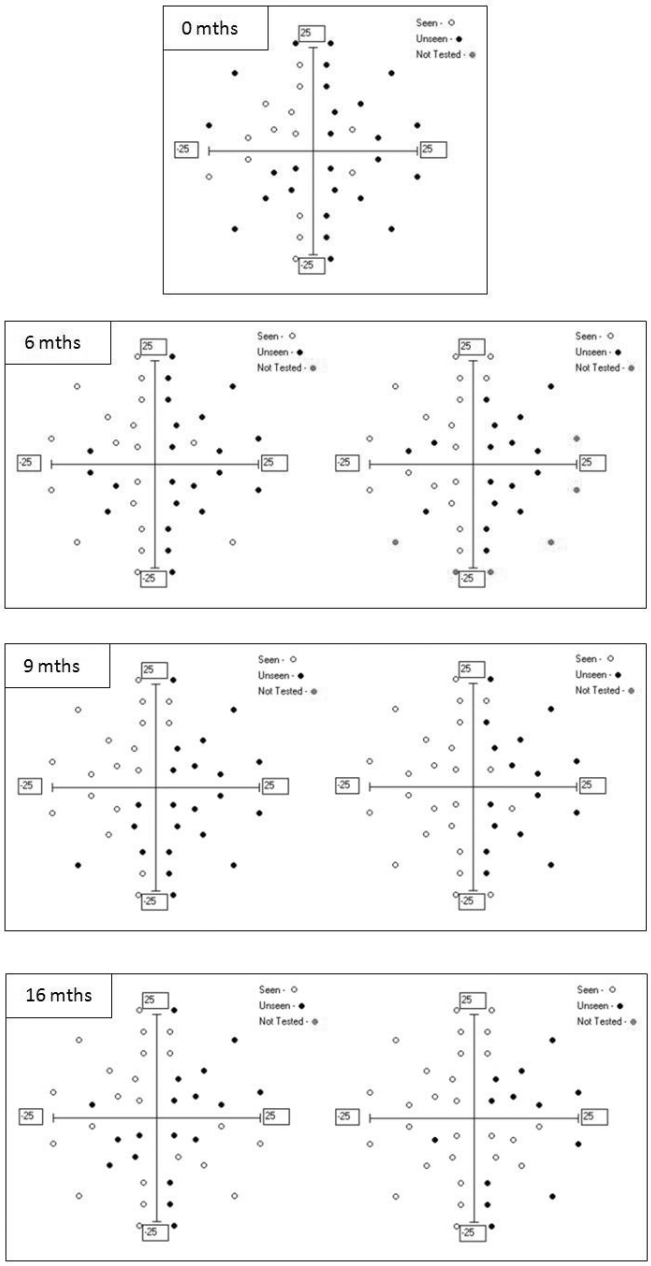

Figure 6.21: SVOP visual field test results from case 4. Included is one single binocular test performed prior to the validation trial, and 6 further tests completed on 3 separate visits during the validation trial.

Figure 6.22 shows the changes in the average number of "unseen" points in SVOP tests over time (in months). Again, only fully completed test results have been used in this analysis. Also shown on the chart is the repeatability statistic (Cohen's kappa), for any of the visits during the validation trial where there was two fully completed test results.

As with several of the other large visual field defect cases discussed in this section, there was an improvement over time in the number of "seen" points. However, with this patient's SVOP test

results there was also a sudden, more obvious change to the lower right quadrant of her visual field in her last visit results as compared to any others. Upon reviewing the post-test gaze responses to "test stimuli", it was thought possible that they could have been falsely labelled as "seen" due to a "standard" eye movement which this child performed when "test stimuli" were thought to be "unseen". This "standard eye movement appeared to be in a direction to the right and below the previous fixation point. As a result it is possible that some "test stimuli" presented in this area could have had a reaction in an appropriate direction which the software algorithm decided made them "seen" when actually the gaze movement was a "standard" reaction of this patient when nothing was seen on the screen (from her point of view). It is understandable that she may have a reaction of this type due to the right sided defect she has. It is perhaps a compensatory movement which allows her to view more of the screen. Figure 6.23 shows some examples this patients gaze movements following the presentation of some "unseen" points.

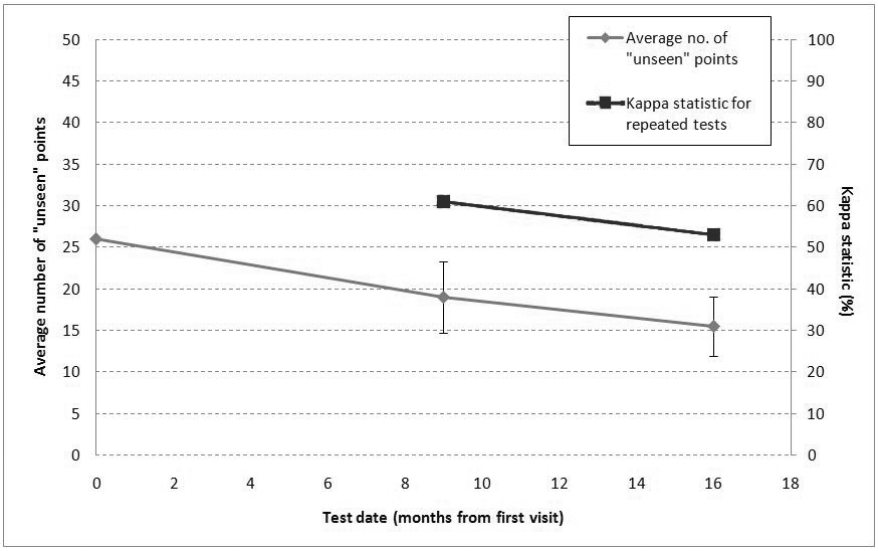

Figure 6.22: Chart of the average number of "unseen" points (±1 standard deviation where more than one test was completed in a single visit) from each visit for patient case 4. Only data for completed tests is shown. Where two completed tests were performed on one visit, the Kappa statistic for assessment of repeatability was performed and is also shown on the chart.

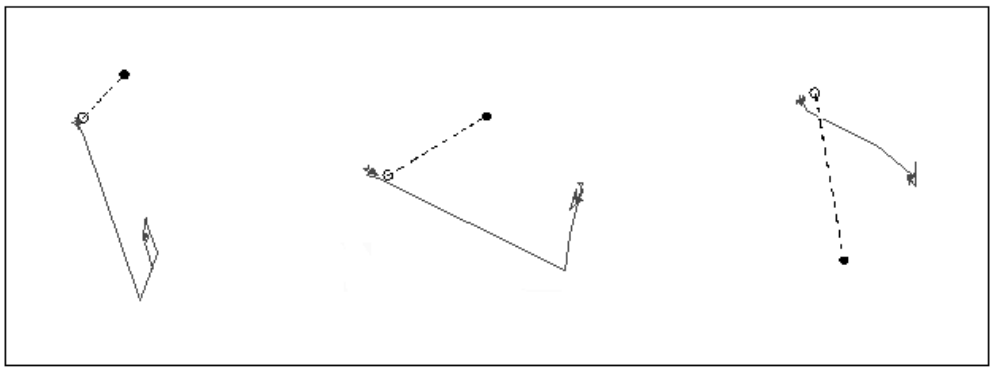

Figure 6.23: Examples of gaze reaction to "unseen" points in SVOP tests from final visit for patient case 4. The solid lines represent gaze changes every 20ms. The circles and dashed lines between them represent the relative positions of the "fixation stimulus" (white circle) and "test stimulus" (filled circle).

6.3.3.2 Visual field defects as a result of other CVI

Case 5

Table 6.21 shows the details of a 3 year old boy diagnosed with haemophilus meningitis. Confrontational visual field testing revealed a left homonymous hemianopia. Figure 6.24 shows 4 binocular SVOP visual field tests. Two of the SVOP tests were performed on separate occasions prior to the validation study, and the other two were performed during a single visit as part of the validation study. The first two test results demonstrate a large left sided homonymous defect, but not a complete hemianopia as was previously thought on confrontation. The final two SVOP tests (completed on the same visit) show an improvement to this boys visual field since the first SVOP testing, but still demonstrated defect in a similar area, although with a small amount of variation between the two tests. Figure 6.25 shows this patient's brain scan taken prior to first SVOP visual field testing and demonstrates right occipital and superior parietal cortical and subcortical enhancement which would be consistent with the a left sided homonymous visual field defect.

Case 5: A 3 year old (47 months) male	
Diagnosis	• Previous haemophilus influenza meningitis. • Mild left hemiparesis.
Visual function prior to first SVOP test	• Left homonymous hemianopia on confrontational visual field testing. • Visual acuity: 6/7.5 in each eye

Table 6.21: Case 5 patient clinical details including age on first SVOP testing, diagnosis, previous treatments and clinical visual function assessment details.

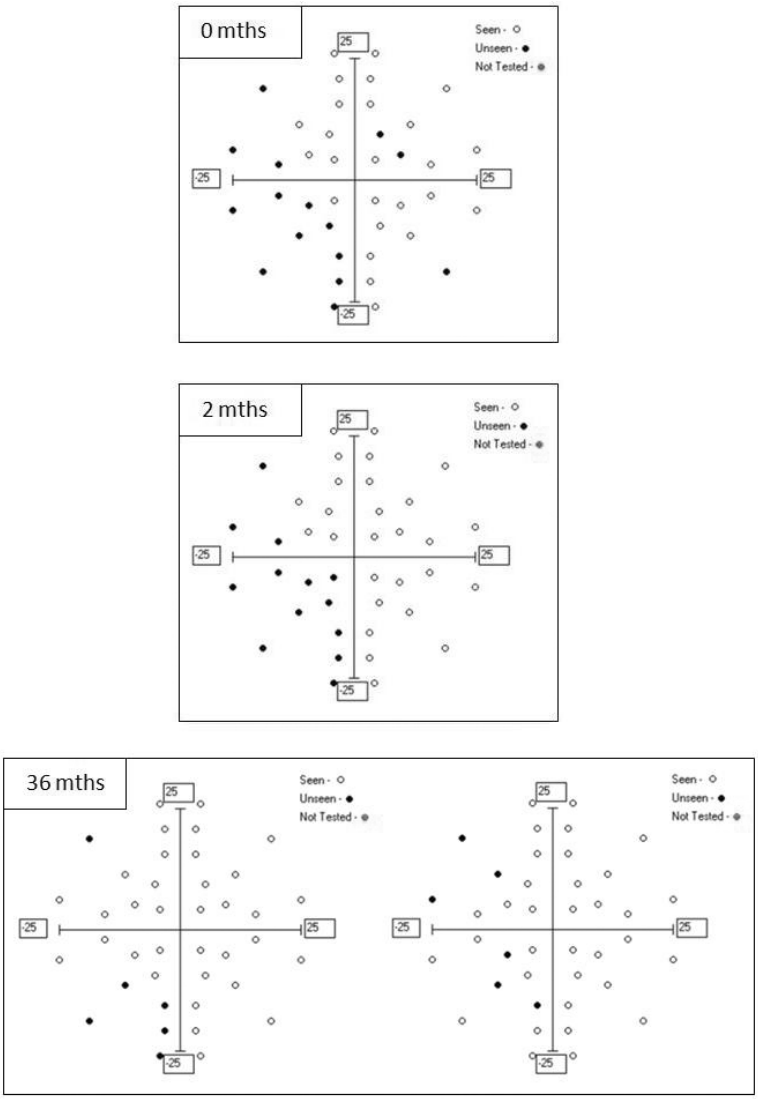

Figure 6.24: SVOP visual field test results from case 5. Included are two binocular tests performed prior to the validation trial, and 2 further tests completed on 1 visit during the validation trial.

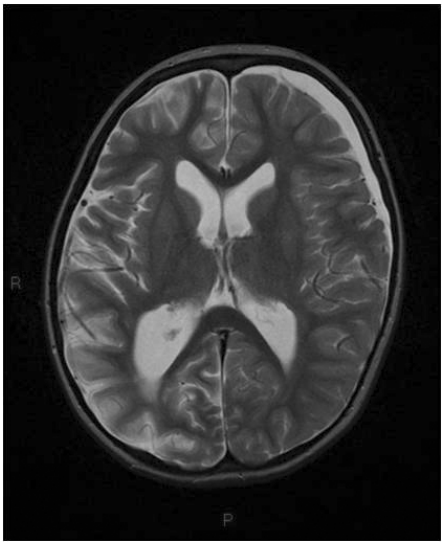

Figure 6.25: Case 5 brain scan demonstrating left frontal subdural collection of fluid with right occipital and superior parietal cortical and subcortical enhancement. This scan was taken prior to first SVOP visual field testing.

Case 6

Table 6.22 shows the details of a 3 year old boy diagnosed with possible periventricular leucomalasia (PVL). Confrontational visual field testing was suggestive of less good vision on the right side. Figure 6.24 shows 2 binocular SVOP visual field tests performed during a single visit as part of the validation study. The two SVOP tests, although not identical, do show similar areas of "unseen" visual field locations towards the lower portion of the visual field measured by SVOP.

Case 6: A 3 year old (43 months) male	
Diagnosis	• Possible periventricular leucomalasia.
Visual function prior to first SVOP test	• Confrontational visual field testing difficult. The impression was that vision was less good on the right side. • Mild visual impairment. • Visual acuity: 6/8 in each eye.

Table 6.22: Case 6 patient clinical details including age on first SVOP testing, diagnosis, previous treatments and clinical visual function assessment details.

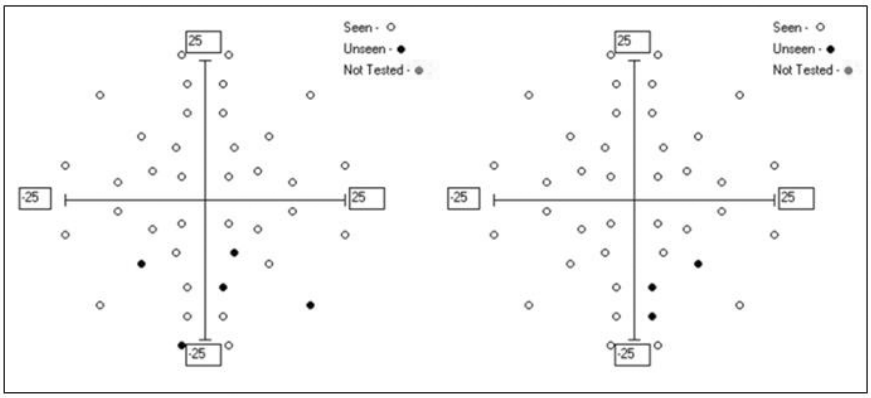

Figure 6.26: SVOP visual field test results from case 6. Two binocular tests performed on a single visit during the validation trial are shown.

Case 7

Table 6.23 shows the details of a 4 year old boy who suffered a severe non-accidental injury at 7 months of age with bilateral extensive retinal haemorrhage, encephalopathy and raised intracranial pressure. This resulted in CVI, nystagmus and optic atrophy. Prior to performing the SVOP test confrontational visual field testing had proved difficult because of the marked nystagmus and short attention span but it was thought that he had some probable right-sided visual field impairment. He performed 3 binocular SVOP tests from two separate visits. One visit prior to the validation study (as part of the feasibility study) and on the other visit performing two SVOP tests as part of this validation study. A right sided defect was a common feature of the SVOP tests performed. However, the repeatability of the two tests performed during the single visit was low at 20%

Case 7: A 4 year old (53 months) male	
Diagnosis	• Previous non-accidental head injury with bilateral sub-dural haemorrhage. • Cerebral visual impairment.
Visual function prior to first SVOP test	• Right sided visual field loss on confrontational visual field testing. • Miopia with astigmatism. • Nystagmus • Visual acuity: 6/20 (binocular)

Table 6.23: Case 7 patient clinical details including age on first SVOP testing, diagnosis and clinical visual function assessment details.

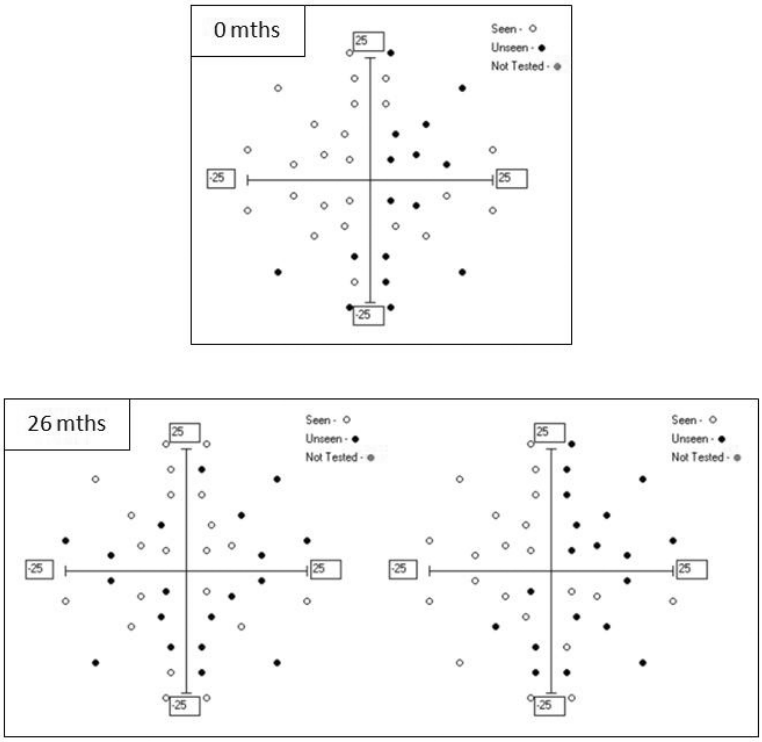

Figure 6.27: SVOP visual field test results from case 7. Included is one binocular test performed prior to the validation trial and 2 further binocular tests completed on a single visit during the validation trial.

6.3.3.3 Case 8 - A healthy infant

This subject is included here because he was the youngest participant in the study. A healthy 8 month old boy completed a single binocular SVOP test (test result shown in figure 6.28). The SVOP test result showed 37 visual field stimuli identified as "seen" and 3 as "unseen". On post test analysis of this infant's gaze movements following the three stimuli labelled as "unseen", two of them did in fact show an eye movement reaction in the direction of the "test stimuli", but the reaction was not correctly identified by the software algorithm. The final "unseen" point (located as 25° eccentricity) was the only point which did not initiate an eye gaze reaction.

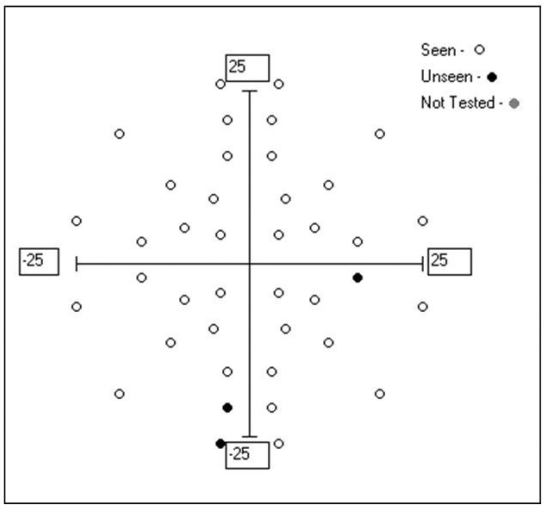

Figure 6.28: SVOP test result from a healthy 8 month old male infant.

6.4 Discussion

6.4.1 Comparison data

The results section "comparison data" (Section 6.3.2 on page 164) was divided into four further subsections. In addition to the data comparing SVOP directly with the "gold standard" HFA device and the analysis of SVOP and HFA repeatability, there were also sections which presented "catch trial" and "test time" data.

The catch trial data analysis was not designed to be a main outcome of this validation study but it was useful in demonstrating some of the issues with performing ASP in children. Many of the HFA tests performed by children were rejected due to high rates of fixation losses and false positive responses to the catch trial stimuli. The average in both child groups (patients and healthy volunteers) for fixation losses and false positive responses was greater than the previously described HFA reliable limit of 20% (figure 6.5 on page 165). Children had low rates of false negative responses. The high false positive, and lower false negative responses is representative of children tending to be more "trigger happy" with the HFA button and far more likely to press it even when there has been no stimuli presented. The high rates of fixation losses are suggestive of problems continually looking at the central fixation target. These problems are frequently noted when using ASP with children.[15,16,18–20] The data recorded during this study may be higher than some of the referenced papers where training or familiarisation strategies were used to reduce these problems. In this validation study there was no training provided for either the HFA or the SVOP test, merely encouragement during the tests. For example, during a HFA test, a child was reminded to keep staring at the "middle light" if it became clear that their fixation was wavering, or they were told to make sure to only press the button if they

see other lights flash on. And obviously many (if not all) the child subjects had not performed any HFA testing before. Perhaps in future studies it may be useful to give a child more time to practice the HFA test to enable the collection of better (or a greater amount of usable) equivalent data. These catch trial data results demonstrate very well the inherent problems with children performing ASP and some of the reasons why SVOP has been developed.

In total there was over 8000 SVOP test points directly compared to the same amount of HFA test points from almost 200 visual field equivalent test "pairs" across all subject groups leading to a good overall sensitivity and excellent specificity values (72.7% and 96.8% respectively). This means that overall, from this data, SVOP tests are better at correctly diagnosing "seen" points (i.e. no disease) than "unseen" points. However, the sensitivity value changed depending upon the subject groups, ranging from 66.7% in the healthy children to 96.4% in the healthy adults. Generally the sensitivity reduced in the patients with visual field defects and increased in the healthy subject groups, with the lowest value of 66.7% possibly due to a lack of usable comparative data in the healthy child group. Indeed, when taking out "normal" eyes within the patient groups, the sensitivity and specificity values decreased further, enforcing the result that the sensitivity values are different in different subject groups. Specificity also showed variation between subject groups, again reducing in the patient groups as compared to the healthy subject groups. However, this variation was small (5-7%) and the values remained above 90% across all groups.

Why should there be a reduction in sensitivity and specificity in patients with visual field defects as compared to healthy subjects? There are several variables which could contribute to this effect. Increased variability in both HFA and SVOP testing within the patients with visual field defects as compared to the healthy subjects is one such contributor. There is an inherent variability in the tested visual field (This is demonstrated by the HFA repeatability results). It is difficult to call the HFA a "gold standard" as it is itself not 100% repeatable. However, it was the most appropriate comparison test available and did show a better repeatability statistic than did the SVOP testing. The very nature of certain visual field defects means that the test-retest variability increases. For instance a visual field with a complex glaucomatous defect which varies in retinal sensitivity across several areas of the visual field is much more susceptible to test-retest variability than say an absolute hemianopic defect. This could be one reason why the sensitivity results of the child patient groups was slightly improved in comparison to the adult patient group, because of the likely types of visual field defects present within the two groups. This is due to the very nature of CVI being the largest contributor to childhood visual impairment, and glaucoma in adults.

Due to the natural test-retest variability in visual field testing, the point-by-point sensitivity and specificity analysis performed in this research may not have been the most appropriate method of comparative analysis. Although the results give a good indication of sensitivity

and specificity of the SVOP equipment, from a clinical standpoint it may be more appropriate to analyse each test outcome rather than an assessment of individual points. An appropriate question could have been "is there a visual field defect in each SVOP and HFA test comparison "pair" which would lead a clinician to suspect the same visual field diagnosis?", rather than "how well do all the individual points match up?"

For this reason, a more clinically relevant measure of sensitivity and specificity might be to present the test results to a number of expert clinicians who would be blinded to the device which produced each test result, and to ask them to judge on the presence or absence of visual field defect. Further, if they determine the presence of a defect they could then be asked to categorise the type of defect according to a set of previously defined types. Sensitivity and specificity would then be calculated based on how often SVOP and HFA test results from the same subject were placed in the same categories. Methodology of this type introduces an element of subjectivity to the analysis and an assessment of the clinicians interobserver agreement may also need to be performed.[126]

A further alternative, which would rely less on interobserver agreement discrepancies, would be to compare SVOP and HFA test result "pairs" with reference to more general areas within the visual field rather than the individual points. For example using the four quadrants of the visual field (separated by the horizontal and vertical midlines). Any defect identified in one quadrant of an SVOP test could be judged a "true positive" if there is also a defect within the same quadrant on the equivalent HFA test result.[127] As alternatives, and to make the assessment more rigorous, the visual field areas used could be further reduced (for example each quadrant could be divided into two or more sectors).

The lower repeatability in the SVOP tests will have also contributed to the lower sensitivity values. There are some failings in the SVOP software decision algorithm which have become apparent during this validation trial. Throughout all subject groups there are often points labelled as "unseen" in SVOP testing when, on post test review of gaze data there has been a clear gaze movement in the direction of the presented stimuli. The main reason that these points have been incorrectly determined to be "unseen" is because the "end point" of the fixation change has not been correctly detected. At present the algorithm looks for the very first change in fixation following the presentation of a "test stimulus". If, for any reason the patient moves their fixation in a different initial direction before readjusting to look towards the correct area, or if they happen to momentarily fixate while on the way to the correct area, this is the end point of the gaze change vector which is measured which could easily be incorrect or outside the previously set algorithm limits. However, this problem is fairly simple to fix by making the algorithm analyse all fixation change vectors individually and also as a whole to see if there is an appropriate gaze response. Repeatability of SVOP tests may have been increased as compared to HFA tests because of this factor.

6.4.2 Child patients

Despite the lower repeatability in SVOP testing as compared to HFA, SVOP still has the potential to measure the visual field in young children, which the HFA does not. SVOP testing in children appears to have been most useful in this study for identifying and monitoring the visual field in patients with visual pathway tumours. In several of these patients SVOP tests have repeatedly returned results which are consistent with what was previously thought by using confrontation visual field testing, but with greater detail to allow the detection of "seeing" areas of the visual field where it was previously thought there was none. SVOP clearly has the potential to detect more subtle characteristics of visual field defects in these patients than does confrontation and therefore allows better monitoring of any potential changes to visual field defects. The child patient results highlight the failings of the confrontation technique which uses a stimulus which comes in from the edge of the visual field. The confrontation method is not able to determine specific areas or "pockets" of "seen" locations, or smaller areas of scotomata closer to the central visual field.

There are some interesting issues which have arisen when testing child patients with SVOP. In almost all of the patients who had repeated visits to participate, they showed an improvement in their visual field defect over time. It is unrealistic to think that SVOP has a therapeutic effect, instead the likely cause for an improvement to these children's visual fields is a genuine one with development or more likely a learning effect with SVOP. As a child begins to understand what is happening in an SVOP test, they likely become more aware of what they are looking for (in terms of the visual "test stimuli"). It is plausible that in certain areas of reduced retinal sensitivity (but not absolute defect) that the bright "test stimuli" used in the SVOP tests appears dimmer, and it is not until the child has had a few goes of SVOP that they understand that they are actually looking for any brightness of stimuli. However, there was one patient where there seemed to be an improvement in the number of SVOP "seen" points in a false manner (case 4) who had an instinctive compensatory gaze response which was regularly in a specific direction, potentially causing several points in that direction to be labelled as "seen" when this may not have been the case. It will be important to identify such compensatory eye movements in subjects with large visual field defects so as to understand this potential limitation of SVOP.

Another point to discuss is the issue of boredom with SVOP tests. In older young children (say 5 years and above) it would sometimes be the case that that the testing procedure was not engaging enough. Many children who were tested on the HFA, although not reliable at it, enjoyed the button pressing aspect of it. With SVOP there is no obvious interaction with the test (from the point of view of the child) and this could easily lead to boredom and increased false positive results as the child "switches off" from the test. Many children are used to playing computer games with games controllers. It would be prudent to make a future version of SVOP

which also has an element of game style interaction.

So, there are several improvements which can be made to SVOP. However, in its present state is has still proved extremely useful. From a clinical point of view repeating tests as part of this validation trial protocol has been useful to eliminate false "seen" and "unseen" points but the test has proved very useful in monitoring the visual field in several patients.

Finally, the SVOP testing on the 8 month old infant should be discussed. It was thought that it may have been necessary to "try out" a few different strategies with an infant of this age. For example, larger sized "test stimuli" and "fixation stimuli" were prepared in advance. However, on attempting our standard binocular SVOP test it became clear that these other strategies would not be necessary. Out of the three points labelled as "unseen" only one appeared not to have any gaze movement reaction to it and it is interesting that this was one of the peripheral test stimuli. A child of this age certainly needs to be awake and in a reasonably attentive mood to perform an SVOP test, but the results from this infant demonstrate that it is clearly possible to obtain a measure of the visual field in infants. More infants will need to be tested using SVOP in future studies to identify how widely usable SVOP is in this age group and to identify the youngest age which it may be possible to test.

Chapter 7

Discussion and Conclusions

The aims of this research program were to develop a technique and system for ASP in children and to assess the developed system through direct comparison with an established ASP device and an assessment of test repeatability where possible. The technique and system was designed to overcome problems associated with performing ASP (the usual choice of perimetry in adults) in children by using the advantages of some fairly recent advances in eye tracking technology. The two main chapters of this thesis comprised: (i) the theory and development of the system (Chapter 5), and (ii) a clinical evaluation of the developed system (Chapter 6).

The system, named "saccadic vector optokinetic perimetry" (SVOP) was built around the idea that by monitoring a child's eye movements following the presentation of visual stimuli, it would be possible to determine whether or not the visual stimuli have been "seen" based on the direction of any gaze movement response. The system was designed to be automated to enable these decisions to be made in "real time" and the visual stimuli (or "test stimuli" as they have been referred to throughout this thesis) can be appropriately displayed at specific locations within their visual field so that testing of a number of locations during a test would reveal a plot of the child's visual field. The technique has advantages over current adult ASP techniques as it does not require the patient to stare straight ahead at one single location throughout a test and it does not require them to press a button when they perceive the "test stimuli". Hence they do not necessarily need to understand the test as there are no requirements other than to follow their natural gaze reaction to look towards visual stimuli if they see them. There is also no need for the child to have their head in a fixed position. The eye tracker provides data on the location of the child's eyes and so allows "test stimuli" to be appropriately positioned at specific visual field locations based on this positional data. All these elements were designed to be introduced as ways of overcoming the problems associated with current ASP techniques.

The SVOP system comprises a personal computer, 20" display screen, and an X50 eye tracker (Tobii Technology). The eye tracker was assessed to ascertain its suitability for use in the

proposed SVOP system. In relation to this research, the two most important data fields provided by the eye tracker were the point of gaze data, and the camera-to-eye distance data. The accuracy of both these types of data were assessed and both were found to have a dependence on subject display screen gaze location. An increase in error was found most often when a subject was gazing at certain screen location areas. These "problem areas" (as they have been referred to in previous sections) were generally confined to areas of gaze fixation towards the top corners or towards the left or right hand sides of the display screen.

The display screen itself was also assessed. The most important characteristic of the screen was its luminance uniformity, and based on that how faithfully it could reproduce specific luminance levels in all screen areas. Due to the natural characteristics of standard LCD screen technology, it was expected that the screen would not be perfectly uniform and in addition that the viewing angle would likely contribute to luminance variability. Indeed, this was found to be the case with areas to the far left and right hand sides of the display screen being most affected due to a reduction in luminance at increased viewing angles.

Because varying screen gaze location had these effects on gaze data accuracy, distance data accuracy and luminance uniformity, the far left and right areas of the display screen were not used to display "fixation stimuli" or "test stimuli" in the SVOP system. Once these screen areas were excluded, the level of variability and error in the eye tracker data and screen luminance were considered more tolerable for the suprathreshold test developed. However, since the development and evaluation of SVOP, there have been ideas about how it may be possible to reduce these errors which would be of use for future versions of SVOP. A newer model of eye tracker (Tobii IS-OEM) was taken on a short term loan from Tobii Technology. One of the main improvements in relation to this research was the improved camera-to-eye distance data. Figure 7.1 shows the distance data variation with different screen fixation points for the X50 and IS-OEM eye trackers (upper and lower charts respectively). The upper chart uses the same data from figure 5.27 in section 5.2.2.2 on page 100. Comparison of the two charts, which have the same y-axis range, clearly demonstrates the improvement in the amount of distance data variation provided by the newer model of eye tracker.

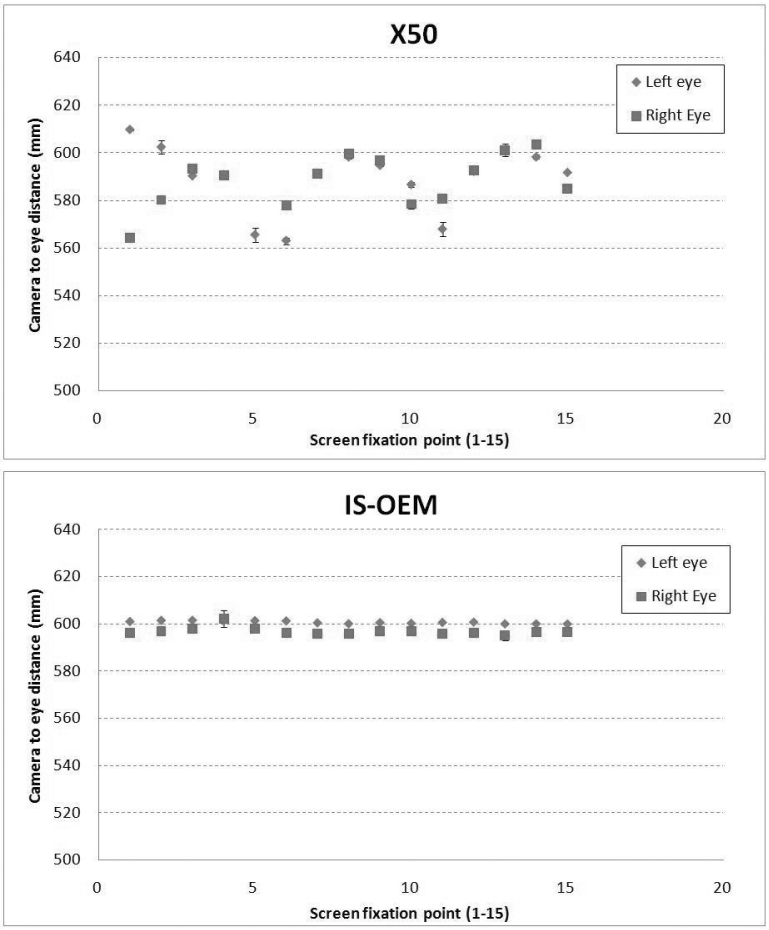

Figure 7.1: Comparison of Tobii Technology X50 and IS-OEM eye trackers in relation to distance data.

The display screen used in the developed SVOP system was a standard 20" LCD monitor. Other flat panel display technologies exist which may overcome many of the display screen issues relevant to developing this research in the future. For example radiology imaging display screens are designed to have higher maximum luminance levels (which would allow the displaying of brighter "test stimuli"), increased colour bit depth (allowing a greater number of displayable grey levels and hence luminance levels), improved screen luminance uniformity and less viewing angle luminance degradation. All these factors would improve on many of the limitations of the LCD screen used in the current SVOP system.

The software algorithm developed to determine if "test stimuli" have been "seen" based on three characteristics of a subject's gaze response (the direction, amplitude and latency), was developed by measuring gaze response characteristics recorded from 38 subjects viewing over 100 "test stimuli" under conditions comparable to that of SVOP testing and the feasibility of the developed SVOP technique was assessed with 29 subjects comprising 4 groups: (i) healthy adults, (ii) healthy children, (iii) adults with visual field defects, and (iv) children with visual

field defects. Subjects performed SVOP tests which were designed to replicate the Humphrey Field Analyser (HFA) C-40 screening test with a stimulus size of Goldmann III and intensity of 14 decibels (dB), and subjects able to do so also performed the equivalent HFA C-40 tests for comparison. In this initial feasibility study SVOP was found to have good agreement with an equivalent HFA test, so a larger clinical trial involving over 120 subjects was devised to more fully assess the SVOP technique. In this larger trial, the sensitivity and specificity of SVOP tests were computed using a direct comparison with reliable HFA tests (as determined using the manufacturers test reliability guidelines). Repeatability of both the SVOP tests and HFA tests were also assessed by means of Cohen's kappa coefficient. In child patients unable to provide a reliable HFA test, their clinical history, other clinical findings and the repeatability of their SVOP tests were used to assess the SVOP results.

Children had a reduced ability to perform the HFA test reliably with a significant increase in reliability indices as compared to the adult subjects, in particular due to "fixation losses". Including all subjects the sensitivity and specificity of the SVOP testing was 72.7% and 96.8% respectively. The sensitivity had a greater variation than the specificity amongst the different subject groups, decreasing to 69.0% and 66.7% for the adult patient and healthy child groups respectively, but increasing to 96.4% and 73.2% for the healthy adult and child patient groups respectively. The repeatability of SVOP tests were slightly reduced as compared to the HFA tests across all groups with an overall kappa statistic for SVOP and HFA tests of 0.65 and 0.74 respectively. In child patients without reliable HFA equivalent tests the SVOP defects picked up could commonly be associated with their clinical history and repeatable testing added to the confidence in the reliability of these tests.

The validation trial study has produced results similar to that of the smaller scale feasibility study, but has provided more detail regarding the variability of comparative results and the reasons why this variability occurs, particularly with the sensitivity values within different subject groups. The reason behind variability in the comparative results is due to several sources of variability present in both HFA tests and SVOP tests. The reason for SVOP being slightly less repeatable than HFA is most likely due to some additional factors which do not affect the HFA. These sources of test-retest variability are described in the following paragraphs.

As discussed, SVOP has a reliance on (i) accuracy of distance data, and (ii) accuracy of the display screen to reproduce specific luminance levels. The errors in these factors were minimised in the developed SVOP system. However, the HFA uses a fixed head position and so does not suffer as much from a variability in eye location data (the value is assumed constant). The HFA has the ability to display specific luminance levels more accurately than a standard LCD display as it uses a uniformly lit bowl. However, despite these differences between SVOP and HFA in relation to eye distance data and display luminance. There are other factors which will more largely contribute to a reduction in perfect comparison and reproducibility. Clearly the

HFA test was not 100% repeatable itself. This fact alone means that it is not an ideal "gold standard" comparison for SVOP. Despite this, SVOP tests shows a slightly lower reproducibility than did the HFA tests. The lower repeatability in the SVOP tests will have also contributed to the reducing sensitivity values. One main contributor to this is due to some failings in the SVOP software decision algorithm which have become apparent during this validation trial. Throughout all subject groups there can be points labelled as "unseen" in SVOP testing when in fact, on post test review of gaze data, there has been a clear gaze movement in the direction of the presented stimuli. The main reason that points are occasionally being falsely labelled as "unseen" is due to the fixation change "end point" not being correctly identified. At present the algorithm looks for the very first change in fixation following the presentation of a "test stimulus". If, for any reason the patient moves their fixation in a different initial direction before readjusting to look towards the correct area, or if they happen to momentarily fixate while on the way to the correct area, this is the end point of the gaze change vector which is measured, and which could easily be incorrect or outside the defined "decision algorithm" limits.

Repeatability in SVOP may also be larger because of potential head tilt. Although errors in visual field "test stimuli" position were calculated as being small based on the eye tracker camera-to-eye distance data accuracy, there could be an additional "test stimuli" location error due to head tilt. Ocular counter-role was expected to counteract this problem to an extent. However, to completely eliminate this problem, a 1:1 ratio (100% gain) between head tilt angle and ocular counter-roll angle would be required. There is debate over the gain of ocular counter-roll, but it is usually reported as a low gain effect of between 10-25% and is dependent on whether vision is binocular or monocular, whether there are visual clues to spatial orientation, and the amount of eye convergence.[44,128,129]. As a result, head tilt has the potential to add variability to SVOP test results. It may be possible to automatically measure head tilt during a test so as to advise an examiner if there are any test points which are likely to have been affected. Additionally, the eye tracker stops tracking at head tilt angles larger than approximately 22° from the horizontal, which prevents more extreme head tilt angles being introduced during a test.

Despite the above described current limitations of SVOP, there are suggested improvements which can reduce or even eliminate many of them. Although discussing all these limitations is important, it should not be forgotten that the results obtained with this "Version 1.0" of SVOP are still highly encouraging. Consistent defects were found in young children where other formal visual field assessment was difficult, or the only other available visual field assessment was the confrontation method which, in some cases proved inaccurate as compared to SVOP. SVOP clearly has the potential to detect more subtle characteristics of visual field defects in these patients than does confrontation and therefore can allow better monitoring of any potential changes to visual field defects. This highlights the lack of detail possible with the confrontation technique which uses a stimulus moving in from the edge of the visual field, and which cannot

analyse specific areas in the central visual field. This is a major advantage of SVOP. The very fact that child SVOP test results obtained during this research have already proved beneficial to the ophthalmologists who have been involved with this study, adds weight to the usefulness of the developed technique. The youngest age child was a surprising 8 months old. Without any alteration the the general SVOP testing procedure or test parameters this infant was able to complete the test easily, and it will be interesting to identify the lower age limit of infants able to perform SVOP testing in future studies.

The way in which SVOP uses the natural saccadic eye movement response to assess the visual field also poses a question about exactly what is being measured. Clearly visual field function is being measured in the vast majority of cases (as the test results have proved). However, it is also possible that SVOP could be making a measurement of a subject's perception of movement. In humans, the lateral geniculate nucleus in the brain receives information from retinal ganglion cells which are not only attributed to dealing with the perception of "seeing" stimuli (the parvocellular system), but also instinctively "reacting" to stimuli (the magnocellular system). The term "blindsight" has been given to a phenomenon where a person who is blind or has visual field defects as a result of damage to the visual cortex, can still "perceive" stimuli presented in their blind field.[130] This has suggested that neural projections from the lateral geniculate body not only travel to the visual cortex, but also to higher cortical areas which are thought to deal with the very quick perception of movement in the visual field. While this presents another potential limitation of SVOP in assessing the visual field of patients with defects as a result of visual cortex damage, it may also mean that SVOP could inadvertently be making an assessment of the retinal ganglion cells which deal with "reacting to" rather than "seeing" stimuli. In glaucoma patients, who potentially have damage to the retinal ganglion cells which deal with "reacting" to stimuli, it may be possible that their initial saccadic reaction to a "test stimulus" is different (perhaps less accurate) to those who are healthy, even though the glaucoma patient still sees the "test stimulus". If this is the case then the current SVOP system which analyses only the first saccadic eye movement could be labelling such a visual stimulus as "unseen" while on the HFA the stimulus would be registered by the patient as "seen". If this is the case it could be a reason for some of the disparities in comparative SVOP and HFA test results for some of the adult glaucoma patients. At this stage, these are simply possible ideas for future work. However, a form of SVOP which assesses the initial saccadic reaction (and compares with normative data) could potentially be a screening test for glaucoma. This of course would require further clinical experimental work. However, it would be reasonably simple to implement using the existing SVOP system.

The young age of many of the child participants in the studies presented here also poses an interesting question for any commercial application of the SVOP screening test. Perimetry guidelines state that suprathreshold screening test stimuli should be presented at a known

brightness level above the "expected" threshold values (unlike the current developed SVOP test which uses a constant luminance level at all locations). These "expected" threshold values will vary with age and the eccentricity of visual field angle being tested. Ordinarily the HFA does do this for its default suprathreshold tests and in order to produce a comparative HFA test to compare with the developed "single intensity" SVOP test in this research, the HFA test had to be forced to present stimuli at a known constant brightness value. This was done because otherwise it was not known at what brightness the HFA would be using during any test (it would be dependent upon the HFA normative database values for different ages) and would be a useless comparison. For the current SVOP technique to satisfy official perimetry guidelines would it need to present stimuli above an expected threshold level, and if so, what would that level be? The question of threshold values in young children (below approximately 7 years) is still largely unanswered.

The developed SVOP technique performs well with accurate eye tracking data and an interested child. The developed system has proved clinically useful in identifying and monitoring visual field defects in several child patients who required regular visual field assessment such as those with visual pathway tumours, and yet there are still improvements which can further enhance the SVOP system described in this thesis.

Future work

Immediate future work includes implementing the improvements which can be made to the current SVOP system. These improvements can be divided into two groups: (i) improvements to hardware, and (ii) improvements to software. Hardware improvements include using a newer model of eye tracker which has demonstrated improved eye location data. Additionally, improved display screen technology has the possibility of reducing the previously described screen luminance uniformity problems and providing the potential for displaying brighter stimuli and an improved ability to display dimmer stimuli approaching normal threshold values. Software improvements are several. The most important of which is improving the "decision algorithm" so that it identifies gaze movements using more than just the first initial fixation change following stimulus presentation. Other software improvements involve introducing a more interactive "game-like" scenario for older children who may quickly become bored of the current strategy, and methods to reduce the test duration.

Future clinical studies will involve visual field testing on a greater number of child patients within specific patient groups. Additionally, more SVOP visual field testing in normal children, in particular in the very young children and infants should be undertaken.

Further development work will include investigating the possibility of extending the current SVOP suprathreshold test so that it can be used to perform threshold testing. This will be

a particular challenge and will require a change in how the "test stimuli" are displayed as the standard LCD screen used is not capable of faithfully reproducing the subtle changes approaching normal threshold brightness values, and may well require different testing strategies.

References

[1] GN Dutton and LK Jacobson. Cerebral visual impairment in children. *Semin Neonatol*, 6(6):477–485, 2001.

[2] E Fazzi, SG Signorini, SM Bova, R La Piana, P Ondei, C Bertone, W Misefari, and PE Bianchi. Spectrum of visual disorders in children with cerebral visual impairment. *J Child Neurol*, 22(3):294–301, 2007.

[3] RS Lowery, D Atkinson, and SR Lambert. Cryptic cerebral visual impairment in children. *Br J Ophthalmol*, 90(8):960–963, 2006.

[4] J Duin, G Cioni, B Bertuccelli, B Fazzi, C Romano, and A Boldrini. Visual outcome at 5 years of newborn infants at risk of cerebral visual impairment. *Dev Med Child Neurol*, 40(5):302–309, 1998.

[5] WC Huang and LS Lee. Visual field defects in patients with pituitary adenomas. *Zhonghua Yi Xue Za Zhi*, 60(5):245–251, 1997.

[6] WV Good, JE Jan, L Desa, AJ Barkovich, M Groenveld, and CS Hoyt. Cortical visual impairment in children. *Surv Ophthalmol*, 38(4):351–364, 1994.

[7] CE Gilbert, L Anderton, L Dandona, and A Foster. Prevalence of visual impairment in children: a review of available data. *Ophthalmic Epidemiol*, 6:73–82, 1999.

[8] T Eke, JF Talbot, and MC Lawden. Severe persistent visual field constriction associated with vigabatrin. *Br Med J*, 314(7075):180–181, 1997.

[9] IM Russell-Eggitt, DA Mackey, DS Taylor, C Timms, and JW Walker. Vigabatrin-associated visual field defects in children. *Eye*, 14:334–339, 2000.

[10] EL Spencer and GFA Harding. Examining visual field defects in the paediatric population exposed to vigabatrin. *Doc Ophthalmol*, 107(3):281–287, 2003.

[11] M Papadopoulos and PT Khaw. Advances in the management of paediatric glaucoma. *Eye*, 21(10):1319–1325, 2007.

[12] EC de Souza, A Berezovsky, PH Morales, PA de Arruda Mello, PP de Oliveira Bonomo, and SR Salomao. Visual field defects in children with congenital glaucoma. *J Pediatr Ophthalmol Strabismus*, 37:266–272, 2000.

[13] RG Ross, AD Radant, DA Young, and DW Hommer. Saccadic eye movements in normal children from 8 to 15 years of age: a developmental study of visuospatial attention. *J Autism Dev Disord*, 24:413–431, 1994.

[14] DP Munoz, JR Broughton, JE Goldring, and IT Armstrong. Age related performance of human subjects on saccadic eye movement tasks. *Exp Brain Res*, 121:391–400, 1998.

[15] E Mutlukan and BE Damato. Computerized perimetry with moving and steady fixation in children. *Eye*, 7(4):554–561, 1993.

[16] SC Johnston, BE Damato, AL Evans, and D Allan. Computerised visual-field test for children using multiple moving fixation targets. *Med Biol Eng Comput*, 27(6):612–616, 1989.

[17] R Lakowski and PA Aspinall. Static perimetry in young children. *Vision Res*, 9(2):305–312, 1969.

[18] C Tschopp, AB Safran, P Viviani, A Bullinger, M Reicherts M, and C Mermoud. Automated visual field examination in children aged 5-8 years. part i: Experimental validation of a testing procedure. *Vision Res*, 38(14):2203–2210, 1998.

[19] EZ Blumenthal, A Haddad, A Horani, and I Anteby. The reliability of frequency doubling perimetry in young children. *Ophthalmology*, 111:435–439, 2004.

[20] J Morales and SM Brown. The feasibility of short automated static perimetry in children. *Ophthalmology*, 108:157–162, 2001.

[21] GE Quinn, AM Fea, and N Minguini. Visual-fields in 4-year-old to 10-year-old children using goldmann and double-arc perimeters. *J Pediatr Ophthalmol Strabismus*, 28(6):314–319, 1991.

[22] M Wilson, G Quinn, V Dobson, and M Breton. Normative values for visual-fields in 4-year-old to 12-year-old children using kinetic perimetry. *J Pediatr Ophthalmol Strabismus*, 28(3):151–153, 1991.

[23] JD Trobe, PC Acosta, JJ Shuster, and JP Krischer. An evaluation of the accuracy of community-based perimetry. *Am J Ophthalmol*, 90:654–660, 1980.

[24] TE Inder, SK Warfield, H Wang, PS Huppi, and JJ Volpe. Abnormal cerebral structure is present at term in premature infants. *Pediatrics*, 115:286–294, 2005.

[25] B Bengtsson and A Heijl. Sita fast, a new rapid perimetric threshold test: Description of methods and evaluation in patients with manifest and suspect glaucoma. *Acta Ophthalmol Scand*, 76:431–437, 1998.

[26] B Bengtsson, A Heijl, and J Olsson. Evaluation of a new threshold visual field strategy, sita, in normal subjects. *Acta Ophthalmol Scand*, 76:165–169, 1998.

[27] J Morales, ML Weitzman, and M Gonsalez de la Rosa. Comparison between tendency-oriented perimetry (top) and octopus threshold perimetry. *Ophthalmology*, 107:134–142, 2000.

[28] SP Donahue and A Porter. Sita visual field testing in children. *J AAPOS*, 5:114–117, 2001.

[29] SM Brown, JC Bradley, MJ Monhart, and DK Baker. Normal values for octopus tendency-oriented perimetry in children 7 through 13 years old. *Graefes Arch Clin Exp Ophthalmol*, 243:886–893, 2005.

[30] AB Safran, GL Laffi, and A Bullinger. Feasibility of automated visual field examination in children between 5 and 8 years of age. *B J Ophthalmol*, 80:515–518, 1996.

[31] IC Murray, BW Fleck, HM Brash, ME MacRae, LL Tan, and RA Minns. Feasibility of saccadic vector optokinetic perimetry - a method of automated static perimetry for children using eye tracking. *Ophthalmology*, 116:2017–2026, 2009.

[32] DB Elliott, I North, and J Flanagan. Confrontation visual field tests. *Opthal Physiol Opt*, 17:S17–S24, 1997.

[33] JP Ranjeet, K Gales, and PG Griffiths. Effectiveness of testing visual fields by confrontation. *Lancet*, 358:1339–1340, 2001.

[34] MD Sheridan. The stycar graded-balls vision test. *Dev Med Child Neurol*, 15:423–432, 1973.

[35] A Heijl and CET Krakau. An automatic perimeter, design and pilot study. *Acta Ophthalmol*, 53:293–310, 1975.

[36] A Heijl and CET Krakau. A note on fixation during perimetry. *Acta Ophthalmol*, 55:854–861, 1977.

[37] RHS Carpenter. *Movements of the eyes*. Pion, London, 2nd edition, 1988.

[38] JE Hyde. Some characteristics of voluntary human ocular movements in the horizontal plane. *Am J Ophthalmol*, 48(1):85–94, 1959.

[39] DA Robinson. The mechanics of human saccadic eye movements. *J Physiol*, 174:245–264, 1964.

[40] LL Wheeless, GH Cohen, and RM Boynton. Luminance as a parameter of the eye-movement control system. *J Opt Soc Am*, (57):394–400, 1967.

[41] S de Brouwer, D Yuksel, G Blohm, M Missal, and P Lefèvre. What triggers catch-up saccades during visual tracking? *J Neurophysiol*, 87(3):1646–1650, 2002.

[42] L R Young. Measuring eye movements. *Am J Med Electron*, 2:300–307, 1963.

[43] SJ Belcher. Ocular torsion. *Br J Physiol Opt*, 21:1–20, 1964.

[44] AP Petrov and GM Zenkin. Torsional eye movements and consistency of the visual field. *Vision Res*, 13:2465–2477, 1973.

[45] EB Delabarre. A method of recording eye movements. *Am J Psychol*, 9:572, 1898.

[46] CH Judd, CN McAllister, and WM Steele. General introduction to a series of eye movements by means of kinetoscope photographs. *Psychol Monogr*, 7:1, 1905.

[47] R Dodge. An experimental study of visual fixation. *Psychol Monogr*, 8(4):1, 1907.

[48] E Totten. Eye-spots for photographic records of eye-movments. *J Comp Psychol*, 6(3):287, 1926.

[49] GH Byford. A sensitive contact lens photoelectric eye movement recorder. *Trans Bio-Med Electron*, 9:236–243, 1962.

[50] DA Robinson. A method of measuring eye movement using a scleral search coil in a magnetic field. *Trans Bio-Med Electron*, 10:137–145, 1963.

[51] L Martin. Measurement of eye movements by contact lens techniques: Analysis of measuring systems and some new methodology. *J Opt Soc Am*, 54(8):1008–1018, 1964.

[52] J Fukushima, T Hatta, and K Fukushima. Development of voluntary control of saccadic eye movements - age related changes in normal children. *Brain Dev*, 22:173–180, 2000.

[53] U Schiefer, J Pätzold, and B Wabbels F Dannheim. Conventional techniques of visual field examination: part 4 static perimetry: interpretation–perimetric indices–follow-up–perimetry in childhood. *Ophthalmologe*, 103(3):235–254, 2006.

[54] U Schiefer, J Pätzold, and F Dannheim. Conventional techniques of visual field examination part 2: confrontation visual field testing – kinetic perimetry. *Ophthalmologe*, 102(8):821–827, 2005.

[55] C Tschopp, AB Safran, JL Laffi, C Mermoud, A Bullinger, and P Viviani. Automated static perimetry in children - methodological and practical issues. *Klin Monatsbl Augenheilkd*, 206(5):416–419, 1995.

[56] C Tschopp, AB Safran, P Viviani, M Reicherts, A Bullinger, and C Mermoud. Automated visual field examination in children aged 5-8 years. part ii: Normative values. *Vision Res*, 38(14):2211–2218, 1998.

[57] B Bengtsson and A Heijl. Evaluation of a new perimetric threshold strategy, sita, in patients with manifest and suspect glaucoma. *Acta Ophthalmol Scand*, 76(3):268–272, 1998.

[58] H Stiebel-Kalish, M Lusky, Y Yassur, Y Kalish, A Shuper, R Erlich, S Lubman, and M Snir. Swedish interactive thresholding algorithm fast for following visual fields in prepubertal idiopathic intracranial hypertension. *Ophthalmology*, 111(9):1673–1675, 2004.

[59] BK Wabbels and S Wilscher. Feasibility and outcome of automated static perimetry in children using continuous light increment perimetry (clip) and fast threshold strategy. *Acta Ophthalmol Scand*, 83:664–669, 2005.

[60] Y Akar, A Yilmaz A, and I Yucel. Assessment of an effective visual field testing strategy for a normal pediatric population. *Ophthalmologica*, 222(5):329–333, 2008.

[61] GE Quinn, DL Miller, JA Evans, WE Tasman, JA McNamara, and DB Schaffer. Measurement of goldmann visual fields in older children who received cryotherapy as infants for threshold retinopathy of prematurity. *Arch Ophthalmol*, 114(4):425–428, 1996.

[62] L Jacobson, A Rydberg, AC Eliasson, A Kits, and C Flodmark. Visual field function in school-aged children with spastic unilateral cerebral palsy related to different patterns of brain damage. *Dev Med Child Neurol*, 52(8):184–187, 2010.

[63] S Agrawal, DL Mayer, RM Hansen, and AB Fulton. Visual fields in young children treated with vigabatrin. *Optom Vis Sci*, 86(6):767–773, 2009.

[64] E Gaily, H Jonsson, and M Lappi. Visual fields at school-age in children treated with vigabatrin in infancy. *Epilepsia*, 50(2):206–16, 2009.

[65] TL Schwartz, V Dobson, DJ Sandstrom, and J van Hof-van Duin. Kinetic perimetry assessment of binocular visual field shape and size in young infants. *Vision Res*, 27(12):2163–2175, 1987.

[66] MF Cummings, J van Hof-van Duin, DL Mayer, RM Hansen, and AB Fulton. Visual fields of young children. *Behav Brain Res*, 29(1-2):7–16, 1988.

[67] J van Hof-van Duin, DJ Heersema, F Groenendaal, W Baerts, and WP Fetter. Visual field and grating acuity development in low-risk preterm infants during the first 2 1/2 years after term. *Behav Brain Res*, 49(1):115–122, 1992.

[68] GE Quinn, V Dobson, RJ Hardy, B Tung, DL Phelps, and EA Palmer. Visual fields measured with double-arc perimetry in eyes with threshold retinopathy of prematurity from the cryotherapy for retinopathy of prematurity trial. the cryo-retinopathy of prematurity cooperative group. *Ophthalmology*, 103(9):1432–1437, 1996.

[69] V Dobson, AM Brown, EM Harvey, and DB Narter. Visual field extent in children 3.5-30 months of age tested with a double-arc led perimeter. *Vision Res*, 38(18):2743–2760, 1998.

[70] A Guzzetta, B Fazzi, E Mercuri, B Bertuccelli, R Canapicchi, J van Hof-van Duin, and G Cioni. Visual function in children with hemiplegia in the first years of life. *Dev Med Child Neurol*, 43(5):321–329, 2001.

[71] S Wilscher, B Wabbels, and B Lorenz. Feasibility and outcome of automated kinetic perimetry in children. *Graefes Arch Clin Exp Ophthalmol*, 248(10):1493–1500, 2010.

[72] RS Harwerth, L Carter-Dawson, EL Smith 3rd, G Barnes, WF Holt, and ML Crawford. Neural losses correlated with visual field losses in clinical perimetry. *Invest Ophthalmol Vis Sci*, 45:3152–3160, 2004.

[73] RS Harwerth, L Carter-Dawson, F Shen, Smith 3rd, and ML Crawford. Ganglion cell losses underlying visual field defects from experimental gloucoma. *Invest Ophthalmol Vis Sci*, 40:2242–2250, 1999.

[74] L Frisen. New, sensitive window on abnormal spatial vision: rarebit probing. *Vision Res*, 42:1931–1939, 2002.

[75] LM Martin. Rarebit and frequency-doubling technology perimetry in children and young adults. *Acta Ophthalmol Scand*, 83:670–677, 2005.

[76] LM Martin and AL Nilsson. Rarebit perimetry and optic disc in pediatric glaucoma. *J Pediatr Ophthalmol Strabismus*, 44(4):223–231, 2007.

[77] T Maddess and GH Henry. Performance of nonlinear visual units in ocular hypertension and glaucoma. *Clin Vision Sci*, 7:371–383, 1992.

[78] KE Cello, JM Nelson-Quigg, and CA Johnson. Frequency doubling technology perimetry for detection of glaucomatous visual field loss. *Am J Ophthalmol*, 129:314–322, 2000.

[79] AJ Anderson and CA Johnson. Frequency-doubling technology perimetry. *Ophthalmol Clin North Am*, 16:213–225, 2003.

[80] DH Kelly. Frequency doubling in visual responses. *J Opt Soc Am*, 56:1628–1633, 1966.

[81] DH Kelly. Nonlinear visual responses to flickering sinusoidal gratings. *J Opt Soc Am*, a71:1051–1055, 1981.

[82] CA Johnson and SJ Samuels. Screening for glaucomatous visual field loss with frequency-doubling perimetry. *Invest Ophthalmol Vis Sci*, 38:413–425, 1997.

[83] K Becker and L Semes. The reliability of frequency doubling technology (fdt) perimetry in a pediatric population. *Optometry*, 74(3):173–179, 2003.

[84] R Nesher, G Norman, Y Stern, L Gorck, E Epstein, Y Raz, and E Assia. Frequency doubling technology threshold testing in the pediatric age group. *J Glaucoma*, 13(4):278–282, 2004.

[85] LM Quinn, SK Gardiner, DT Wheeler, M Newkirk, and CA Johnson. Frequency doubling technology perimetry in normal children. *Am J Ophthalmol*, 142(6):983–989, 2006.

[86] L Frisen. A computer graphics visual field screener using high-pass spatial frequency resolution targets and multiple feedback devices. *Doc Ophthalmol Proc Ser*, 49:441–446, 1987.

[87] L Frisen. High-pass resolution targets in peripheral vision. *Ophthalmology*, 94:1104–1108, 1987.

[88] BC Chauhan. The value of high-pass resolution perimetry in glaucoma. *Curr Opin Ophthalmol*, 11:85–89, 2000.

[89] M Marraffa, V Pucci, G Marchini, S Morselli, R Bellucci, and L Bonomi. Hpr perimetry and humphrey perimetry in glaucomatous children. *Doc Ophthalmol*, 89:383–386, 1995.

[90] HA Baseler, EE Sutter, and SA Klein. The topography of visual evoked response properties across the visual field. *Electroenceph Clin Neurophysiol*, 90:65–81, 1994.

[91] AI Klistorner, SL Graham, JR Grigg, and FA Billson. Multifocal topographic visual evoked potential: improving objective detection of local visual field defects. *Invest Ophthalmol Vis Sci*, 39:937–950, 1998.

[92] GFA Harding, EL Spencer, JM Wild, and RL Bohn. Field-specific visual-evoked potentials - identifying field defects in vigabatrin-treated children. *Neurology*, 58(8):1261–1265, 2002.

[93] E Yukawa, YJ Kim, K Kawasaki, F Taketani, and Y Hara. A child with epilepsy in whom multifocal veps facilitated the objective measurement of the visual field. *Epilepsia*, 46(4):577–579, 2005.

[94] C Balachandran, AI Klistorner, and F Billson F. Multifocal vep in children: its maturation and clinical application. *Br J Ophthalmol*, 88(2):226–232, 2004.

[95] JP Kelly and AH Weiss. Comparison of pattern visual-evoked potentials to perimetry in the detection of visual loss in children with optic pathway gliomas. *J AAPOS*, 10(4):298–306, 2006.

[96] YJ Kim, E Yukawa, K Kawasaki, H Nakase, and T Sakaki. Use of multifocal visual evoked potential tests in the objective evaluation of the visual field in pediatric epilepsy surgery. *J Neurosurg*, 104(3):160–165, 2006.

[97] BE Damato. Oculokinetic perimetry: a simple visual field test for use in the community. *Br J Ophthalmol*, 69:927–931, 1985.

[98] A Hermann, J Paetzold, R Vonthein, E Krapp, S Rauscher, and U Schiefer. Age-dependent normative values for differential luminance sensitivity in automated static perimetry using the octopus 101. *Acta Ophthalmol*, 86(4):446–455, 2008.

[99] BJ Katz and HD Pomeranz. Visual field defects and retinal nerve fiber layer defects in eyes with buried optic nerve drusen. *Am J Ophthalmol*, 141(2):248–253, 2006.

[100] N Calixto, RM Santos, and S Cronemberger. Visual field (octopus 1-2-3) in normal subjects divided into homogeneous age-groups. *Arq Bras Oftalmol*, 69(5):637–643, 2006.

[101] E Larsson, L Martin, and G Holmström. Peripheral and central visual fields in 11-year-old children who had been born prematurely and at term. *J Pediatr Ophthalmol Strabismus*, 41(1):39–45, 2004.

[102] L Lobefalo, A Verrotti, L Mastropasqua, G Della Loggia, V Cherubini, G Morgese, PE Gallenga, and F Chiarelli. Blue-on-yellow and acromatic perimetry in diabetic children without retinopathy. *Diabetes Care*, 21(11):2003–2006, 1998.

[103] L Lobefalo, A Verrotti, L Mastropasqua, F Chiarelli, G Morgese, and PE Gallenga. Flicker perimetry in diabetic children without retinopathy. *Can J Ophthalmol*, 32(5):324–328, 1997.

[104] AI Klistorner and SL Graham. Multifocal pattern vep perimetry: analysis of sectoral waveforms. *Doc Ophthalmol*, 98(2):183–196, 1999.

[105] DC Hood, x Zhang, and BJ Winn. Detecting glaucomatous damage with multifocal visual evoked potentials: how can a monocular test work? *J Glaucoma*, 12(1):3–15, 2003.

[106] E Alvarez, BE Damato, JL Jay, and E McClure. Comparative evaluation of oculokinetic perimetry and conventional perimetry in glaucoma. *Br J Ophthalmol*, 72(4):258–262, 1988.

[107] N Ideguchi, Y Nakano, and K Nunokawa. Development of an objective automatic perimetry using saccadic eye movement. *Proceedings of Vision*, 2005.

[108] K Nunokawa, N Ideguchi N, and Y Nakano. The influence of fixation on new visual field measurement using saccadic eye movement. *Proceedings of Vision*, 2005.

[109] LJ Alexander, DA Corliss, C Vinson, L Casser J Williams, M Fingeret, V Malinovsky, and JC Townsend. Clinical implications of intra- and inter-reader agreement in four different automated visual fields. *J Am Optom Assoc*, 66(11):681–692, 1995.

[110] A Hard-Boberg and JD Wirtschafter. Evaluating the usefulness in neuro-ophthalmology of visual field examination peripheral to 30 degrees. *Doc Ophthal Proceedings Series*, 42:197–206, 1985.

[111] JL Keltner, CA Johnson, JO Spurr, and RW Beck. Comparison of central and peripheral visual field properties in the optic neuritis treatment of trial. *Am J Ophthalmol*, 128(5):543–553, 1999.

[112] FH Raab, EB Blood, TO Steiner, and HR Jones. Magnetic position and orientation tracking system. *IEEE Transactions on Aerospace and Electronic Systems*, 15(5):709–717, 1979.

[113] MA Nixon, BC McCallum, and NB Price. The effects of metals and interfering fields on electromagnetic trackers. *Presence: Teleoperators and Virtual Environments*, 7(2):204–218, 1998.

[114] J Elvesjo, M Skogo, and G Elvers. Tobii technology. method and intallation for detecting and following an eye and the gaze direction thereof. *Patent WO 2004/045399 A1*, 3 June 2004.

[115] A Heijl, A Lindgren, and G Lindgren G. Test-retest variability in glaucomatous visual fields. *Am J Ophthalmol*, 108:130–135, 1989.

[116] YH Kwon, HJ Park, A Jap, S Ugurlu, and J Caprioli J. Test-retest variability of blue-on-yellow perimetry is greater than white-on-white perimetry in normal subjects. *Am J Ophthalmol*, 126:29–36, 1998.

[117] DB Henson, S Chaudry, PH Artes, EB Faragher, and A Ansons. Response variability in the visual field: comparison of optic neuritis, glaucoma, ocular hypertension, and normal eyes. *Invest Ophthalmol Vis Sci*, 41:417–421, 2000.

[118] M Wall, KR Woodward, CK Doyle, and PH Artes. Repeatability of automated perimetry: a comparison between standard automated perimetry with stimulus size iii and v, matrix, and motion perimetry. *Invest Ophthalmol Vis Sci*, 50:974–979, 2009.

[119] AT Duchowski. *Eye tracking methodology: theory and practice*. Springer-Verlag, London, 2nd edition, 2007.

[120] DB Granet and S Khayali. Amblyopia and strabismus. *Pediatr Ann*, 40(2):89–94, 2011.

[121] *Humphrey Field Analyzer II-i series User Manual*. 2005.

[122] TW Loong. Understanding sensitivity and specificity with the right side of the brain. *BMJ*, 327:716–719, 2003.

[123] J Cohen. A coefficient of agreement for nominal scales. *Educ Psychol Meas*, 20:37–46, 1960.

[124] DG Altman. *Practical Statistics for Medical Research*. Chapman and Hall, London, 1991.

[125] A Heijl and VM Patella. *Essential Perimetry*. Carl Zeiss Meditec AG, Gena, Germany, 3rd edition edition, 2002.

[126] AJ Viera and JM Garrett. Understanding interobserver agreement: the kappa statistic. *Fam Med*, 37(5):360–363, 2005.

[127] M Fingeret, E Smith, L Reminick, and C Johnson. Frequency doubling technology perimetry as a screening tool in the general ophthalmic elderly population. in perimetry update 2000/2001. *Ed. M Wall and RP Mills*, pages 271–275, 2001.

[128] D Ooi, ED Cornell, IS Curthoys, AM Burgess, and HG MacDougall. Convergence reduces ocular counterroll (ocr) during static roll-tilt. *Vision Res*, 44:2825–2833, 2004.

[129] HD Schworm, J Ygge, T Pansell, and G Lennerstrand. Assessment of ocular counterroll during head tilt using binocular video oculography. *Invest Ophthalmol Vis Sci*, 43(3):662–667, 2002.

[130] Blindsight: a case study and implications. L weiskrantz. *Oxford Psychology Series No 12*, 50(5):658, 1987.

Appendix A

The table below details the ethical applications relevant to this research. Both of these applications were approved by the Lothian research ethics committee, and were also granted NHS research and development approval.

Application title (short version)	Submission date	Ethics application number
Automated ocular tracking optokinetic perimetry in children	19/09/06	06/S1102/41
An eye tracking system for visual field assessment in children	14/10/08	08/S1102/60

Appendix B

Tobii x50 eye tracker data fields

All data fields supplied by the Tobii x50 eye tracker (at a frequency of 50Hz).

Data Field	Description (units)
Time stamp (Second)	Time stamp when data was sampled
Time stamp (Microsecond)	Microsecond fraction of time stamp when data was sampled
Left eye horizontal gaze point	X screen location of left eye gaze point (0-1, where 0 is left edge of screen)
Left eye vertical gaze point	Y screen location of left eye gaze point (0-1, where 0 is top edge of screen)
Left eye horizontal position as seen by eye tracker	X position of left eye in eye tracker camera field of view (0-1, where 0 is left)
Left eye vertical position as seen by eye tracker	Y position of left eye in eye tracker camera field of view (0-1, where 0 is top)
Left eye distance (mm)	Distance of the left eye from the eye tracker (mm)
Left eye validity code	An estimate of how valid data for this sample is (0-4, see "Validity Codes" below)
Left eye pupil size (mm)	The length of the longest chord of the left pupil ellipse
Right eye horizontal gaze point	X screen location of right eye gaze point (0-1, where 0 is left edge of screen)
Right eye vertical gaze point	Y screen location of right eye gaze point (0-1, where 0 is top edge of screen)
Right eye horizontal position as seen by eye tracker	X position of right eye in eye tracker camera field of view (0-1, where 0 is left)
Right eye vertical position as seen by eye tracker	Y position of right eye in eye tracker camera field of view (0-1, where 0 is top)
Right eye distance (mm)	Distance of the right eye from the eye tracker (mm)
Right eye validity code	An estimate of how valid data for this sample is (0-4, see "Validity Codes" below)
Right eye pupil size (mm)	The length of the longest chord of the right pupil ellipse

Validity Codes

The validity codes are an estimate of how certain the eye tracker is that the data given for an eye really belongs to that eye. The validity code takes one of five values for each each eye ranging from 0 to 4, with the following interpretations:

0 - The eye tracker is certain that the data for this eye is correct. There is no risk of confusing data from the other eye.

1 - The eye tracker has only detected one eye, and has made some assumptions and estimations regarding which is the left and which is the right eye (primarily based on the location of the eye within the camera field of view). The validity code for the other eye in this case is always set to 3.

2 - The eye tracker has only detected one eye, and has no way of determining which one is the left and which one is the right eye. The validity code for both eyes is set to 2.

3 - The eye tracker is fairly confident that the actual gaze data belongs to the other eye. The other eye will always have a validity code of 1.

4 - The data is missing or definitely belongs to the other eye.

Hence there are a limited number of possible combinations of validity codes for the two eyes which are described in the table below:

Validity codes (left eye - right eye)	Description
0 - 0	Both eyes found. Data is valid for both eyes.
0 - 4 or 4 - 0	One eye found. Gaze data is the same for both eyes.
1 - 3 or 3 - 1	One eye found. Gaze data is the same for both eyes.
2 - 2	One eye found. Gaze data is the same for both eyes.
4 - 4	No eyes found. Gaze data for both eyes is invalid.